DESIGN AND ANALYSIS OF A SET OF DISCRETE VARIABLE PROTOCOLS FOR SECURE QUANTUM COMMUNICATION

Thesis submitted in fulfillment of the requirements for the Degree of

DOCTOR OF PHILOSOPHY

by

ARINDAM DUTTA ENROLLMENT NO. 20410009



Department of Physics and Materials Science and Engineering

JAYPEE INSTITUTE OF INFORMATION TECHNOLOGY (Declared Deemed to be University U/S 3 of UGC Act)
A-10, SECTOR-62, NOIDA, INDIA

March, 2025

© Copyright JAYPEE INSTITUTE OF INFORMATION TECHNOLOGY, NOIDA (Declared Deemed to be University U/S 3 of UGC Act)

March, 2025

ALL RIGHTS RESERVED

With deepest love and gratitude,

This thesis is dedicated to the cherished memories of my grandparents,

Bimal Krishna Dutta and Gouri Bala Dutta,

and my mother,

Sulata Dutta.

TABLE OF CONTENTS

		Page Nu	mber
INN	ER FIR	ST PAGE	i
TAB	LE OF	CONTENTS	iii
DEC	LARAT	TION BY SCHOLAR	vii
SUP	ERVIS(DR'S CERTIFICATE	viii
ACK	NOWL	EDGEMENT	ix
ABS	TRACT		xi
LIST	T OF AC	CRONYMS & ABBREVIATIONS	xiii
LIST	OF FI	GURES	xv
LIST	T OF TA	ABLES	xix
CH	APTE	R 1	
INT	RODU	JCTION	1
1.1	INTR	ODUCTORY OVERVIEW	1
	1.1.1	THE BIRTH OF QUANTUM PHYSICS	2
	1.1.2	BRIEF INTRODUCTION QUANTUM TECHNOLOGIES AND MO-	
		TIVATION OF THIS THESIS	4
1.2	BASI	C IDEA OF QUANTUM MECHANICS AND QUANTUM COMMU-	
	NICA	TION	7
	1.2.1	POSTULATES OF QUANTUM MECHANICS	7
	1.2.2	PRELIMINARIES OF QUANTUM COMMUNICATION	8
1.3	WHY	IS QUANTUM IDENTITY AUTHENTICATION NECESSARY?	15
1.4	A SH	ORT CHRONOLOGICAL HISTORY OF THE PROTOCOLS FOR	
	QUA	NTUM IDENTITY AUTHENTICATION	18

1.5	CLAS	SSIFICATION OF THE PROTOCOLS FOR QUANTUM IDENTITY	
	AUTI	HENTICATION	32
	1.5.1	CLASSIFICATION BASED ON THE QUANTUM RESOURCES USED	32
	1.5.2	CLASSIFICATION OF THE PROTOCOLS BASED ON THE COM-	
		PUTATIONAL OR COMMUNICATION TASKS USED TO DESIGN	
		THE SCHEMES	33
1.6	QUA	NTUM KEY DISTRIBUTION FOLLOWING QUANTUM IDENTITY	
	AUTI	HENTICATION	40
1.7	INTR	ODUCTORY DISCUSSION ON QUANTUM KEY AGREEMENT	44
1.8	DISC	USSION ON QUANTUM GAME AND NASH EQUILIBRIUM	46
1.9	OVE	RVIEW OF THIS CHAPTER AND OUTLINE OF THE REMAINING	
	THES	SIS	49
CH	APTEI	R 2	
QU A	ANTU]	M IDENTITY AUTHENTICATION SCHEMES WITH DIF-	
FEF	RENT	QUANTUM RESOURCES	52
2.1	INTR	ODUCTION	52
2.2	NEW	PROTOCOLS FOR QIA BASED ON QSDC	54
	2.2.1	PROTOCOL 2.1	54
	2.2.2	PROTOCOL 2.2	56
	2.2.3	COMPARISON OF THE EXISTING AND THE PROPOSED PRO-	
		TOCOLS	57
	2.2.4	SECURITY ANALYSIS	58
2.3	CON	TROLLED QUANTUM IDENTITY AUTHENTICATION PROTOCOL	
	USIN	G BELL PAIRS (PROTOCOL 2.3)	63
	2.3.1	PRINCIPAL CONCEPT OF PROTOCOL 2.3	64
	2.3.2	DESCRIPTION OF PROTOCOL 2.3	67
	2.3.3	ASSESSMENT OF THE SECURITY ASPECTS IN PROTOCOL 2.3	69
	2.3.4	COLLECTIVE NOISE ANALYSIS OF PROTOCOL 2.3	76
	2.3.5	COMPARISON WITH THE EXISTING PROTOCOLS	80
2.4	NEW	PROTOCOL FOR QUANTUM IDENTITY AUTHENTICATION (PRO-	
	TOC	OL 2.4)	83

	2.4.1	CORE CONCEPT	83
	2.4.2	DESCRIPTION OF PROTOCOL 2.4	86
	2.4.3	SECURITY ANALYSIS OF PROTOCOL 2.4	90
	2.4.4	COMPARISON OF PROTOCOL 2.4 WITH A SET OF EXISTING	j
		PROTOCOLS	94
2.5	CON	CLUSIONS	95
CH	APTE]	R 3	
QU A	ANTU	M KEY DISTRIBUTION WITH TIGHT SECURITY BOU	INDS
3.1	INTE	RODUCTION	98
3.2	PRO	POSED QUANTUM KEY DISTRIBUTION PROTOCOLS (PROTO)_
	COL	3.1 AND 3.2)	100
3.3	SECU	URITY EVALUATION OF THE PROPOSED PROTOCOLS	106
3.4	ANA	LYSIS OF PHOTON NUMBER SPLITTING ATTACK	123
3.5	CON	CLUSION	127
CH	APTE]	R 4	
CO	NTRO	LLED QUANTUM KEY AGREEMENT WITHOUT US	-
ING	QUA	NTUM MEMORY	131
4.1	INTE	RODUCTION	131
4.2	NEW	PROTOCOL FOR CQKA (PROTOCOL 4.1)	133
4.3	SECU	URITY ANALYSIS OF THE PROPOSED PROTOCOLS	140
	4.3.1	SECURITY ANALYSIS AGAINST IMPERSONATION FRAUDULE	ENT
		ATTACK	140
	4.3.2	SECURITY ANALYSIS AGAINST COLLECTIVE ATTACK STRAT	ГЕ-
		GIES IN TWO-WAY CHANNEL	143
4.4	INFL	UENCE OF NOISE ON THE PROPOSED CQKA PROTOCOL	153
4.5	COM	PARISON OF THE PROPOSED CQKA PROTOCOL WITH EXIST	1
	ING I	PROTOCOLS	156
4.6	DISC	USSION	158
4.7	CON	CLUSION	161

CHAPTER 5 "GAMING THE QUANTUM" TO GET SECURE BOUND FOR A **QUANTUM COMMUNICATION PROTOCOL** 163 5.1 **INTRODUCTION** 163 5.2 FUNDAMENTALS OF GAME THEORY 165 5.3 INFORMATION-THEORETIC PARAMETERS IN DIFFERENT ATTACK **SCENARIOS** 177 5.3.1 E_1 ATTACK STRATEGY 177 5.3.2 E_2 ATTACK STRATEGY 184 5.3.3 E_3 ATTACK STRATEGY 190 5.3.4 E_4 ATTACK STRATEGY 197 **5.4** ANALYZING THE QBER THRESHOLD BOUND OF USING NASH EQUI-199 **LIBRIUM** 5.5 **DISCUSSION** 206 **CHAPTER 6** CONCLUSION AND SCOPE OF FUTURE WORKS 210 6.1 **SUMMARY OF THE THESIS** 211 6.2 LIMITATIONS AND FUTURE SCOPE 218 REFERENCES 220 LIST OF AUTHOR'S PUBLICATIONS 256 **SYNOPSIS** Synopsis-1

DECLARATION BY THE SCHOLAR

I hereby declare that the work reported in the Ph.D. thesis entitled "Design and

Analysis of a Set of Discrete Variable Protocols for Secure Quan-

tum Communication" submitted at Jaypee Institute of Information

Technology, Noida, India, is an authentic record of my work carried out un-

der the supervision of Prof. (Dr.) Anirban Pathak. I have not submitted

this work elsewhere for any other degree or diploma. I am fully responsible for the

contents of my Ph.D. thesis.

(Signature of the Scholar)

(Arindam Dutta)

Department of Physics and Materials Science and Engineering

Jaypee Institute of Information Technology, Noida, India

Date:

June, 2025

vii

SUPERVISOR'S CERTIFICATE

This is to certify that the work reported in the Ph.D. thesis entitled "Design and

Analysis of a Set of Discrete Variable Protocols for Secure Quan-

tum Communication", submitted by Arindam Dutta at Jaypee Insti-

tute of Information Technology, Noida, India, is a bonafide record of his

original work carried out under my supervision. This work has not been submitted

elsewhere for any other degree or diploma.

(Signature of Supervisor)

(Prof. (Dr.) Anirban Pathak)

Professor and HOD

Department of Physics and Materials Science and Engineering

Jaypee Institute of Information Technology, Noida, India

Date: June, 2025

viii

ACKNOWLEDGEMENT

Throughout my thesis journey, I have received invaluable support and guidance from many individuals, and I would like to take this opportunity to express my heartfelt gratitude to them.

First and foremost, I extend my deepest appreciation to my supervisor, Prof. (Dr.) Anirban Pathak, for giving me the opportunity to conduct research under his guidance. His mentorship has been instrumental not only in shaping my research but also in teaching me how science should be learned and effectively communicated. His unwavering focus and dedication have been a source of inspiration, motivating me to approach my work with diligence and enthusiasm. One of his memorable Bengali phrases, "Sob korte hobe" (which translates to "Everything has to be done together"), has encouraged me to multitask and persevere through challenges. I sincerely hope that his guidance will continue to inspire me beyond these years.

In addition, I extend my heartfelt thanks to Prof. (Dr.) Subhashish Banerjee, Dr. V. Narayanan, Dr. R. Srikanth, Dr. Anindita Banerjee, and Dr. Sandeep Mishra for their insightful discussions and valuable suggestions that helped shape my work. I am also deeply grateful to my senior group members, Dr. Kishore Thapliyal and Dr. Priya Malpani, for their continuous support and motivation throughout this journey. My sincere appreciation goes to my colleague and friend, Mr. Satish Kumar. Furthermore, I would like to thank Dr. Sukhamoy Bhattacharyya (Sukhamoy Sir), Surajit Sir, Sumit Da, and Didhiti for their encouragement and for imparting valuable life lessons during this period. I extend my sincere gratitude to my DP-MAC members, Prof. (Dr.) Bhagwati Prasad Chamola and Dr. Anuraj Panwar, for their continuous guidance, constructive feedback, and keen observation of my work, which have been instrumental in my academic growth. I am also grateful to all the faculty members and departmental staff for fostering a supportive and enriching research environment. A special note of appreciation goes to the housekeeping staff, whose dedication ensures the smooth functioning of the department. I firmly

believe that knowledge should be freely accessible to all, and scientific journals should be open to readers worldwide. In this regard, I sincerely acknowledge Sci-Hub and arXiv for its open-access initiative, without which the completion of this thesis would not have been possible.

I express my heartfelt gratitude to the memory of my beloved mother (Maa), Mrs. Sulata Dutta, whose unwavering desire for my progress in education and science continues to inspire me. Her absence and cherished memories shape my growth in various aspects of life. I also extend my sincere thanks to my father (Baba), Mr. Asit Baran Dutta, for his constant support and motivation at every stage of my life. His encouragement has been instrumental in shaping my journey in research and beyond. Words are insufficient to express my gratitude to my best friend, Monika. Her incredible and enthusiastic support, from the very beginning of my research to the completion of this thesis, has been invaluable. I sincerely hope that not only her support but also her presence remains a lifelong companion to both me and my work. I would also like to extend my heartfelt appreciation to my dear friend and cousin, Mr. Avishek Audhya (Damu Da). Our conversations, often unpredictable in direction, always bring a sense of healing and inner peace, for which I am truly grateful.

Lastly, I find it difficult to determine whether it is appropriate to express gratitude to Nature—the all-encompassing force of the Universe—but I feel compelled to acknowledge its ever-changing attributes. Nature continuously transforms forms and energies, shaping existence through cycles of destruction and creation. If destruction can be perceived as "death" and creation as "birth", then I, too, am a manifestation of Nature's constant transformation. In essence, Nature evolves within my consciousness just as I change within it. I would find true peace and fulfillment in wholeheartedly dedicating myself to the wisdom and harmony of Nature.

(Arindam Dutta)

ABSTRACT

The advent of quantum key distribution (QKD) has revolutionized secure communication by providing unconditional security, unlike classical cryptographic methods. However, its effectiveness relies on robust identity authentication, as vulnerabilities in the authentication process can cause a compromise with the security of the entire communication system. Over the past three decades, numerous quantum identity authentication (QIA) protocols have been proposed. This thesis first presents a chronological review of these protocols, categorizing them based on quantum resources and computational tasks involved while analyzing their strengths and limitations. Subsequently, by recognizing inherent symmetries present in the existing protocols, we design novel QIA schemes based on secure computational and communication tasks. Specifically, this work introduces a set of new QIA protocols that utilize controlled secure direct quantum communication. The proposed scheme facilitates mutual authentication between two users, Alice and Bob, with assistance from a third party, Charlie, using Bell states. A comprehensive security analysis demonstrates its robustness against impersonation, intercept-resend, and fraudulent authentication attacks. The comparative evaluation highlights its advantages over existing schemes. Additionally, this thesis presents two novel QKD protocols that eliminate the need for entanglement or ideal single-photon sources, making them feasible with commercially available photon sources. These protocols are rigorously proven to be secure against various attacks, including intercept-resend and certain collective attacks. Key rate bounds are established, demonstrating that specific classical pre-processing enhances the tolerable error threshold. A trade-off between quantum resource utilization and information leakage to an eavesdropper (Eve) is identified, with greater efficiency achieved through increased use of quantum resources. Notably, these protocols outperform the SARG04 protocol in efficiency, albeit at the cost of additional quantum resources. Furthermore, their critical distances under photon number splitting (PNS) attacks surpass those for

BB84 and SARG04 protocols under similar conditions. Moreover, this thesis introduces a controlled quantum key agreement protocol and another key agreement scheme with a strong focus on security. Rigorous security analysis establishes their resilience against impersonation and collective attacks while ensuring fairness and correctness. Comparative analysis reveals that, unlike existing schemes, the proposed approach does not require quantum memory. Additionally, the controlled quantum key agreement protocol leverages Bell and single-photon states, which are easier to generate and maintain than the GHZ states used in Tang et al.'s protocol, offering a more practical and efficient alternative. Furthermore, Nash equilibrium is employed to establish a game-theoretic security bound on the quantum bit error rate (QBER) for the DL04 protocol, which is a protocol for quantum secure direct communication that has been experimentally realized recently. The sender, receiver, and eavesdropper are modeled as quantum players, with Eve capable of executing quantum attacks (e.g., Wójcik's original and symmetrized attacks, and Pavičić's attack) and classical intercept-resend attacks. A game-theoretic security analysis reveals the absence of a Pareto optimal Nash equilibrium, leading to the identification of mixed-strategy Nash equilibrium points that define upper and lower bounds for QBER. Additionally, the DL04 protocol's vulnerability to Pavičić's attack in message mode is established, and it is observed that quantum attacks are more effective than classical ones, as they result in lower QBER values and a reduced probability of Eve's detection. Overall, this thesis contributes to the advancement of quantum cryptographic protocols by addressing some of the existing issues with identity authentication, key distribution, key agreement, and security analysis through novel schemes and rigorous theoretical frameworks.

Keywords: Quantum Communication; Quantum Cryptography; Discrete Variable Protocols for Quantum Cryptography; Bell State; Nash Equilibrium; Quantum Game; Security Analysis

LIST OF ACRONYMS & ABBREVIATIONS

AD Amplitude Damping

BQC Blind Quantum Computing

CA Certification Authority

CDSQC Controlled Deterministic Secure Quantum Communication

CNOT Controlled-NOT

CPBS Controlled Polarizing Beam Splitter

CQKA Controlled Quantum Key Agreement

CQSDC Controlled Quantum Secure Direct Communication

CV Continuous Variable

DBS Dichroic Beam Splitter

DFS Decoherence-Free Subspace

DH Diffie-Hellman

DSQC Deterministic Secure Quantum Communication

DV Discrete Variable

EPR Einstein-Podolsky-Rosen

GHZ Greenberger-Horne-Zeilinger

GV Goldenberg Vaidman

HWP Half-Wave Plate

IoT Internet of Things

IR Intercept Resend

IRUD Intercept-Resend Unambiguous Discrimination

KA Key Agreement

MAC Message Authentication Code

MDI Measurement Device Independent

MQKA Multiparty Quantum Key Agreement

OT Oblivious Transfer

PBS Polarizing Beam Splitter

PD Phase Damping

PNS Photon Number Splitting

POVM Positive Operator-Valued Measure

PUF Physical Unclonable Function

QBER Quantum Bit Error Rate

QD Quantum Dialogue

QECC Quantum Error-Correcting Code

QFT Quantum Fourier Transform

QIA Quantum Identity Authentication

QKA Quantum Key Agreement

QKD Quantum Key Distributione

QND Quantum Non-Demolition

QSDC Quantum Secure Direct Communication

QSS Quantum Secret Sharing

RSA Rivest-Shamir-Adleman

SFG Sum-Frequency Generation

SPDC Spontaneous Parametric Down-Conversion

TFQKD Twin-Field Quantum Key Distribution

WCP Weak Coherent Pulse

LIST OF FIGURES

Figure	Caption	Page
Number		Number
1.1	Eve may attempt to mimic Alice (or Bob) while interacting with Bob	17
	(or Alice) by substituting the direct communication channel between	
	Alice and Bob with two separate channels: one connecting Alice to	
	Eve and the other linking Eve to Bob.	
1.2	Categorization of QIA schemes.	41
2.1	The graph presents the correlation between the probability of detecting	59
	Eve's presence, $P(n)$, and the number of classical bits used, n .	
2.2	Flowchart depicting the operational workflow of the proposed QIA	70
	protocol.	
2.3	The probability $P(n)$ of detecting Eve's presence is correlated with the	72
	number of classical authentication keys n that are pre-shared.	
2.4	The IR attack strategy utilized by Eve is structured such that qubits	74
	labeled 1, 2, 3, and 4 correspond to sequences S_{A1} , S_{A2} , S_{B3} and S_{B4} ,	
	respectively.	
2.5	The collective error probability associated with the noise parameter	78
	can be classified into: (a) Collective dephasing error probability,	
	characterized by the noise parameter ϕ , and (b) Collective rotation	
	error probability, defined by the noise parameter θ .	
2.6	A flowchart visually represents the operational framework of the	89
	proposed QIA protocol.	
2.7	The probability of detecting Eve's interference denoted as $P(n)$, is	91
	correlated with the number of classical bits, n , utilized as the	
	pre-shared authentication key.	
2.8	Eve employs an intercept-and-resend strategy. In this context, the	93
	qubits labeled as 1, 2, 3, 4, and 5 correspond to the sequences S_1 , S_2 ,	
	S_3 , S_4 , and S_5 , respectively.	

3.1	The secret key rate is plotted as a function of the quantum bit error rate	117
	(\mathcal{E}): (a) a plot assessing the maximum tolerable error threshold	
	(security limit) for sequence S_{B1} , where the solid (black) line and	
	dashed (blue) line represent scenarios with and without the	
	incorporation of the new variable \mathcal{Y} , respectively; (b) a plot evaluating	
	the maximum tolerable error threshold (security limit) for sequence	
	S_{B2} without introducing the new variable X ; and (c) a plot assessing	
	the maximum tolerable error threshold (security limit) for sequence	
	S_{B2} with the inclusion of the new variable \mathcal{X} .	
3.2	The variation of the secret key rate with respect to bit-flip probability	124
	(q) and QBER (\mathcal{E}) is illustrated: (a) the lower bound on the secret key	
	rate as a function of bit-flip probability and QBER, (b) a contour plot	
	depicting the lower bound error limit, correlating QBER with bit-flip	
	probability, (c) the upper bound on the secret key rate as a function of	
	bit-flip probability and QBER, and (d) a contour plot illustrating the	
	upper bound error limit with respect to QBER and bit-flip probability.	
3.3	The variation in Eve's information as a function of distance is analyzed	128
	to determine the critical distance (l_c) : (a) Eve's information plotted	
	against distance to estimate the critical threshold where the attacker	
	extracts maximum key information via a PNS attack on Protocol 3.1,	
	and (b) Eve's information plotted against distance to estimate the	
	critical threshold where the attacker gains maximum key information	
	using an IRUD attack on Protocol 3.2.	
4.1	The flowchart illustrates the operational framework of the proposed	139
	CQKA protocol.	
4.2	The correlation between Eve's detection probability (d) and the	146
	parameter α , which characterizes non-orthogonality.	
4.3	The dependence of Eve's accessible information (I) on the angle α ,	148
	representing non-orthogonality.	

4.4	The interrelation between Pr, d and n is depicted as follows. (a) The	149
	dependence of Pr on n is examined for varying values of d. In	
	particular, the "circle" line corresponds to $d=0\%$, the "continuous"	
	line represents $d=12.5\%$, the "plus sign" line denotes $d=25\%$, and	
	the "asterisk" line signifies $d=50\%$. (b) A histogram illustrates Eve's	
	probability of success for $n = 6$ across different values of d.	
4.5	The plot illustrates the relationship between tolerable QBER (ε) and	153
	the angle characterizing non-orthogonality (α) .	
4.6	A sketch to visualize the QB scheme of Yan Yu et alThe variation of	155
	average fidelity under a noisy quantum channel is analyzed. (a)	
	Depicts the dependence of average fidelity on the channel parameter η_j	
	for the CQKA scheme within the Markovian framework for AD and	
	PD channels, as described by Equations (4.39) and (4.40). (b) and (c)	
	illustrate the variation in average fidelity for NMDPH and NMDPO	
	channels within the non-Markovian regime, plotted against the	
	time-like parameter p for various values of α , respectively (refer to	
	Equations (4.41) and (4.42)).	
4.7	The optical design of the CQKA scheme integrates entangled photons,	160
	a CNOT operation, and a full Bell state measurement. The entangled	
	photon pairs (Bell states) are generated using two thick β -barium	
	borate (BBO) nonlinear crystals arranged in a cross-configuration	
	[340]. Bell state measurement is performed via nonlinear interactions,	
	specifically sum-frequency generation (SFG) of type-I and type-II. A	
	dichroic beam splitter (DBS) is incorporated, along with two 45°	
	projectors (PP1 and PP2) [341]. The system further utilizes polarizing	
	beam splitter(s) (PBS $_1$ and PBS $_2$), each configured at a 45 $^\circ$ orientation	
	with half-wave plate (HWP) integrated at the input and output [342].	
5.1	The circuit representation of DL04 quantum game.	174

The figure illustrates the Nash equilibrium points where the optimal 206 response functions of the three participants intersect in our mixed-strategy game framework. The response functions are represented as follows: the low-density layer for Alice, the medium-density layer for Bob, and the high-density layer for Eve. The subfigures depict different game scenarios: (a) E_1 - E_2 , (b) E_1 - E_3 , (c) E_2 - E_3 , and (d) E_1 - E_4 .

LIST OF TABLES

Table	Caption	Page
Number		Number
1.1	The classification of existing schemes for QIA is presented. When the	31
	use of a pre-shared key is referred to as "By QKD", as indicated by the	
	authors of the respective studies, it can be interpreted that a classical	
	identity sequence was initially exchanged as a prerequisite for	
	performing QKD for the first time. The following abbreviations are	
	employed in this table: C=classical, B=Bell state, FC=five-particle	
	cluster state, CS=classical identity sequence, N=no, HF=single	
	one-way hash function, QPKC=quantum public key cryptography,	
	Q=quantum, T=trusted, SP=single photon, ST=semi-trusted, Y=yes,	
	UT=un-trusted.	
2.1	The preparation method for the decoy sequence (Protocol 2.1).	54
2.2	The preparation method of the authentication sequence (Protocol 2.1).	55
2.3	Bob employs a predetermined measurement basis to extract results	55
	from the authentication sequence (Protocol 2.1).	
2.4	The preparation method of the authentication sequence (Protocol 2.2).	56
2.5	The measurement basis employed by Bob to extract results for the	56
	authentication sequence (Protocol 2.2).	
2.6	This outlines the possible measurement results for the legitimate	66
	participants within the proposed QIA scheme.	
2.7	A comprehensive comparison of Protocol 2.3 is conducted with various	82
	existing QIA protocols. The column labeled "Minimum secret key	
	required" presents multiple values corresponding to different protocols	
	discussed within the same reference. The following abbreviations are	
	employed in this table: TC=two-way channel, IR=intercept-resend,	
	IF=impersonated fraudulent, EM=entangled measure.	
2.8	This outlines the potential measurement results observed by all	84
	participants within Protocol 2.4 for QIA.	
2.9	Possible results of measurements.	91

2.10	Detailed comparison of Protocol 2.4 with previous protocols.	96
3.1	This table outlines the encoding and decoding principles for both	102
	Protocol 3.1 and Protocol 3.2, while also presenting the measurement	
	results obtained after the classical sifting subprotocol.	
3.2	Table mapping between measurement outcomes and Alice's	105
	determined results in Protocol 3.1.	
3.3	Table mapping between measurement results and Alice's determined	107
	outcomes in Protocol 3.2.	
4.1	The table below illustrates the relationship between the announcements	137
	made by Charlie, Alice, and Bob, and the final key.	
4.2	The table below illustrates the relationship between the announcements	140
	made by Alice, Bob, and the final key.	
4.3	Explicit comparison with earlier protocols. Y - required, N - not	159
	required, QC - quantum channel, QR - quantum resources, TR - third	
	party, QM - quantum memory, NoP - number of parties, QE - quantum	
	efficiency.	
5.1	The payoff matrix corresponding to the $\ensuremath{\mathfrak{M}}$ game is presented, where	176
	the three values within parentheses signify the payoffs of Alice, Bob,	
	and Eve, respectively. Here, the probabilities assigned to an	
	eavesdropper Eve's choice of attack strategies E_i and E_j are denoted by	
	r and $1 - r$, respectively.	
5.2	The table presents Nash equilibrium points for different strategic	209
	interactions and provides qualitative payoff assessments for all	
	involved entities.	

CHAPTER 1

INTRODUCTION

1.1 INTRODUCTORY OVERVIEW

Quantum physics, quantum mechanics, and quantum technologies constitute some of the most transformative advancements in modern science. Collectively, they have redefined our understanding of the natural world and driven significant technological innovations. This section provides a concise historical overview of these fields, highlighting key discoveries, theoretical advancements, and the development of technological applications. Before delving into these topics to establish the background of this thesis, it is important to note that quantum technologies have been in existence for several decades. However, the quantum principles that explain early technologies such as lasers and transistors are relatively intuitive. In contrast, recent advancements leverage more counterintuitive—often described as "weird"—quantum phenomena. For instance, the measurement-induced wavefunction collapse has been utilized in the development of quantum random number generators. Technologies based on such phenomena are often classified under the so-called second quantum revolution. This new generation of quantum technologies can be broadly categorized into three domains: quantum sensing, quantum computing, and quantum communication. The present thesis focuses on secure quantum communication, an area of particular interest for multiple reasons. First, quantum cryptography offers unconditional security, a feature unattainable by classical cryptographic methods. Second, the field has witnessed significant advancements in recent years. Notably, China and Austria have demonstrated satellite-assisted secure quantum communication over a distance of 7,600 km [1]. Additionally, Liu et al. have implemented twin-field quantum key distribution (TFQKD) over a 1,000 km fiber link [2], and several commercial quantum cryptography solutions have emerged [3, 4, 5]. These developments will be discussed in detail in the subsequent sections of this chapter and throughout this thesis. However, this section provides a brief overview of key aspects and advancements in quantum communication to establish the focus and context for the following discussions.

1.1.1 THE BIRTH OF QUANTUM PHYSICS

By the late 19th century, physics was arguably composed of three core areas: classical mechanics, electromagnetism, and thermodynamics. Classical mechanics provided the tools to predict the motion of material bodies, while Maxwell's theory of electromagnetism served as the foundation for studying radiation. Matter and radiation were understood in terms of particles and waves, respectively. Interactions between matter and radiation were effectively explained using the Lorentz force or thermodynamic principles. It appeared that all known physical phenomena could be accounted for within this framework of matter and radiation. However, the beginning of the 20th century brought significant challenges to traditional physics in two key areas: the "relativistic" and "microscopic" domains. In the relativistic domain, Einstein's 1905 work on the special theory of relativity demonstrated that Newtonian mechanics breaks down at velocities approaching the speed of light. In the microscopic domain, advances in experimental techniques that allowed investigation of atomic and subatomic structures revealed that classical physics was inadequate for explaining newly observed phenomena. This inadequacy made it clear that classical physics was not valid at the microscopic scale, necessitating the development of new concepts to describe atomic and molecular structures and their interactions with light. The inability of classical physics to explain phenomena such as blackbody radiation, the photoelectric effect, atomic stability, and atomic spectra highlighted its limitations and paved the way for the emergence of new theories beyond its scope.

The foundations of quantum physics were laid with Max Planck's pioneering concept of energy quantization, introduced in 1901 to resolve the "ultraviolet catastrophe" in black-body radiation [6]. Planck suggested that energy transferred from oscillators in a cavity wall to the radiation field occurs in discrete packets or quanta ($\Delta E = hv$, where h is Plank's constant). Albert Einstein extended this idea in 1905 to explain the photoelectric effect [7], proposing that energy is not only transferred in quantized packets but also traverses in this discrete form (for a detailed overview, see [8]). Niels Bohr's 1913 model of the atom introduced quantized orbits for electrons, explaining atomic spectra. While the model had limitations, it incorporated Planck's quantum ideas into atomic structure [9]. In 1924, Louis de Broglie extended "wave-particle

duality" to matter, proposing that particles such as electrons have an associated wavelength $(\lambda = \frac{h}{p})$, where p is momentum). This hypothesis was later confirmed experimentally by electron diffraction [10]. Quantum mechanics took mathematical shape with Erwin Schrödinger's wave equation (1926) and Werner Heisenberg's matrix mechanics (1925). Schrödinger's approach modeled particles as wavefunctions, while Heisenberg's formalism relied on observable quantities [11, 12]. In 1927, Heisenberg formulated the uncertainty principle, stating that certain pairs of observables, like position and momentum, cannot be simultaneously measured with arbitrary precision. This principle underscored the probabilistic nature of quantum mechanics [13]. This foundation paved the way for major developments, such as the Bohr model, Einstein's work on stimulated emission, de Broglie's matter waves, Heisenberg's uncertainty principle, Dirac's theory of radiation, matrix mechanics, and Schrödinger equation; each transforming our understanding of the microscopic world and establishing quantum mechanics as an advanced model of natural phenomena.

Quantum mechanics introduced numerous counterintuitive concepts that were initially met with skepticism, even by some of its founding figures. For instance, while Einstein's work on the photoelectric effect [7] was instrumental in the development of quantum mechanics, he remained critical of the Copenhagen interpretation. Notably, his objections, as articulated in the Einstein-Podolsky-Rosen (EPR) paper [14], contributed significantly to the evolution of the field and the advancement of future technologies central to this thesis. It is worth emphasizing that initially, several foundational principles of quantum mechanics—such as nonlocality and various no-go theorems (including Heisenberg's uncertainty principle, the no-cloning theorem, and the no-broadcasting theorem)—were perceived as intrinsic limitations of the theory. However, over the past four decades, it has become evident that these so-called limitations can be harnessed to develop quantum technologies that either surpasses classical efficiency and performance constraints or enable entirely novel paradigms with no classical analog. Given that schemes for unconditionally secure quantum communication are central to this thesis, the following section provides a brief introduction to quantum technologies, highlighting the key motivations behind the research presented herein.

1.1.2 BRIEF INTRODUCTION QUANTUM TECHNOLOGIES AND MOTIVATION OF THIS THESIS

From foundational experiments to revolutionary technologies, quantum physics and mechanics have profoundly shaped our understanding of the universe and practical capabilities. As the second quantum revolution accelerates, quantum technologies hold promise for transformative applications across computing, communication, and sensing, ensuring their place at the forefront of scientific and technological innovation. With recent advancements in quantum computation, communication, and foundational studies, the inherent limitations of quantum mechanics—long regarded as constraints—are increasingly recognized as valuable resources for diverse applications. These limitations, first connected through seminal no-go theorems such as Heisenberg's uncertainty principle, and later expanded to include concepts like the nocloning, no-broadcasting, and no-deletion theorems are central to the unique capabilities of quantum systems. For example, Heisenberg's uncertainty principle and the no-cloning theorem plays a key role in quantum key distribution (QKD). The uncertainty principle asserts that measurements of non-commuting operators (e.g., position and momentum) cannot achieve arbitrary precision simultaneously, while the no-cloning theorem prohibits the creation of identical copies of an arbitrary unknown quantum state. Together, these principles underpin the security of QKD protocols based on conjugate coding, such as the BB84 and B92 protocols [15, 16]. These protocols leverage quantum mechanics to ensure that any eavesdropping attempt introduces detectable disturbances. In addition, to secure communication, other important quantum properties like entanglement and nonlocality enable groundbreaking tasks such as quantum teleportation [17], dense coding [18], and measurement device-independent QKD [19, 20]. These capabilities transcend classical limitations, opening new frontiers in information transfer and processing. Moreover, the principles underlying quantum mechanics are crucial to quantum computing. Quantum entanglement and superposition empower algorithms, such as Shor's algorithm and Grover's search, to outperform their classical counterparts in specific computational tasks. These advancements are not confined to computing and communication; they also extend to quantum sensing, where quantum-enhanced precision measurements redefine the limits of sensitivity and accuracy. In summary, the unique, nonclassical properties of quantum systems, along with the constraints defined by quantum no-go theorems, have become indispensable tools across three major domains: (i) quantum communication, (ii) quantum computing,

and (iii) quantum sensing. These advancements underscore the duality of quantum mechanics, where what were once considered limitations now serve as the foundation for transformative technologies.

Cryptography has been a critical tool for protecting information since the beginning of human civilization. Historically, cryptographic methods were developed to disguise secret information, yet cryptanalysts frequently devised more advanced techniques to reveal these secrets. A major advancement occurred in the 1970s with the development of public key cryptography, exemplified by the Rivest-Shamir-Adleman (RSA) scheme [21] and the Diffie-Hellman (DH) scheme [22]. The security of these, along with other classical key distribution schemes, rests on the computational difficulty of the problems they employ. For example, the RSA scheme's security relies on the complexity of factoring a large bi-prime number, while DH security is grounded in the discrete logarithm problem [23]. In a groundbreaking development in 1994, Peter W. Shor demonstrated that quantum computers could efficiently solve both problems in polynomial time [24]. This discovery revealed that many classical cryptographic methods would be vulnerable if scalable quantum computing became feasible, presenting a profound challenge to conventional cryptography. QKD offers a promising solution to this issue, as it secures key distribution using the principles of quantum mechanics rather than computational complexity. The first QKD protocol (BB84) was proposed a decade before Shor's findings highlighted the vulnerability of classical cryptography [15]. This protocol leverages fundamental quantum properties, such as the no-cloning theorem [25], the measurement postulate, and Heisenberg's uncertainty principle, to ensure security, allowing it to be implemented with polarization-encoded single photons or other forms of photonic qubits. In an ideal setting, any eavesdropping attempt on a QKD channel leaves detectable traces. Beyond QKD, the principles of quantum mechanics enable other secure communication methods, including quantum key agreement (QKA), quantum digital signatures, quantum secure direct communication (QSDC), quantum secret sharing (QSS), and so on. Moreover, before initiating any secure communication, it is essential to authenticate the identities of legitimate participants, a process called identity authentication. When quantum techniques provide unconditional security in this verification, the process is termed quantum identity authentication (QIA). This expanding suite of quantum-based protocols thus addresses a variety of cryptographic needs, leveraging the unique properties of quantum physics to offer security resilient to quantum computational threats.

The security of communication critically depends on the security of the key used. Quantum

technology enables the distribution of keys with unconditional security through QKD. However, initiating a QKD protocol requires verifying the authenticity of the communicating parties. In many cases, classical methods are used for authentication, which is vulnerable to attacks where an eavesdropper (Eve) could impersonate a legitimate party, creating a significant loophole in achieving unconditional security. To address this issue, we analyze existing QIA schemes and propose new QIA protocols to enhance security. These QIA schemes utilize various quantum resources, making them feasible for implementation with current technology. Once legitimate user identities are verified, quantum communication protocols like QKD can be performed to distribute symmetric keys. Our analysis of previous QKD schemes reveals that the process involves splitting information into quantum and classical components. We hypothesize that increasing the quantum component while reducing the classical component could enhance both efficiency and security bounds. To test this, we propose new QKD protocols and analyze their security under different scenarios, determining their tolerable security bounds. In QKD schemes, one party may introduce bias in the distributed symmetric key. Furthermore, extending QKD schemes to multiparty scenarios presents significant challenges. To address this, we propose a new QKA scheme that operates without requiring quantum memory. We also conceptualize quantum communication protocols as games, where legitimate parties aim to conceal secure information from Eve and increase her detection probability, while Eve seeks to maximize her information gain and minimize her detection probability. Using game-theoretic principles, we develop a technique to determine the tolerable quantum bit error rate (QBER) based on Nash equilibrium. This approach, referred to as "gaming the quantum", provides a novel perspective on quantum protocol analysis.

This thesis focuses on advancing quantum communication and cryptography, addressing key challenges, and proposing innovative solutions. The security of the proposed protocols is rigorously analyzed and that forms the central contribution. To ensure the thesis is comprehensive and self-contained, foundational concepts of quantum mechanics and quantum communication are discussed in Section 1.2, with a focus on those concepts that are directly relevant to the presented research. A significant portion of this chapter focuses on QIA schemes. An initial discussion on QIA, along with the motivation for exploring QIA schemes are presented in detail in Section 1.3. Subsequently, in Section 1.4, a chronological analysis of previously proposed QIA schemes is conducted, highlighting their evolution in terms of security considerations, quantum resources utilization, and application perspectives. Following this historical overview,

the structural symmetry among these schemes is analyzed, enabling their classification based on the quantum resources utilized and their corresponding communication and computational tasks. This classification is presented in Section 1.5, which also serves as the foundation for introducing novel QIA schemes in Chapter 2. An introductory description and motivation for the research presented in Chapters 3, 4, and 5—focusing on QKA, QKD, and quantum game theory for securing quantum communication protocols—are provided in Sections 1.6, 1.7, and 1.8, respectively. Finally, the chapter concludes with a summary and an overview of the thesis in Section 1.9.

1.2 BASIC IDEA OF QUANTUM MECHANICS AND QUANTUM COM-MUNICATION

1.2.1 POSTULATES OF QUANTUM MECHANICS

In classical mechanics, the state of a particle at any given time t is characterized by two primary dynamical variables: its position r(t) and momentum p(t). These variables provide the foundation for deriving any other physical quantity relevant to the system. Furthermore, if these variables are known at a specific time t, their values for that specific time can be determined using equations such as Hamilton's equations:

$$\frac{dx}{dt} = \frac{\partial H}{\partial p}, \ \frac{dp}{dt} = -\frac{\partial H}{\partial x}.$$

In quantum mechanics, analogous principles are established through postulates that describe the following:

State of a Quantum System: The state of a quantum system at time t is represented by a state vector $|\psi(t)\rangle$ in a Hilbert space \mathcal{H} . This state vector contains all the information required to describe the system. Additionally, any linear superposition of state vectors also represents a valid state vector.

Quantum Operators: For each measurable physical quantity (A) (referred to as an observable or dynamical variable), there exists a corresponding linear Hermitian operator \hat{A} . The eigenvectors of \hat{A} form a complete basis in the Hilbert space.

Eigenvalue of Operator: The measurement of an observable A is mathematically represented by the action of its corresponding operator \hat{A} on the state vector $|\psi(t)\rangle$. The possible outcomes

of the measurement are limited to the eigenvalues a_n of \hat{A} , which are real. Following a measurement that yields the result a_n , the state of the system collapses to the corresponding eigenvector $|\psi_n\rangle$.

$$\hat{A}|\psi(t)\rangle = a_n|\psi_n\rangle,$$

here, $a_n = \langle \psi_n | \psi(t) \rangle$, which represents the component of $| \psi(t) \rangle$ when projected onto the eigenvector $| \psi_n \rangle$.

Collapse on measurement: When measuring an observable A for a system in the state $|\psi\rangle$, the probability of obtaining one of the nondegenerate eigenvalues a_n of the associated operator \hat{A} is expressed as:

$$P_n(a_n) = \frac{|\langle \psi_n | \psi \rangle|^2}{\langle \psi | \psi \rangle} = \frac{|a_n|^2}{\langle \psi | \psi \rangle},$$

where $|\psi_n\rangle$ denotes the eigenstate of \hat{A} corresponding to the eigenvalue a_n . For cases where a_n has m-fold degeneracy, the probability P_n is generalized as:

$$P_n(a_n) = rac{\sum_{j=1}^m \left|\left\langle \psi_n^j | \psi
ight
angle
ight|^2}{\left\langle \psi | \psi
ight
angle} = rac{\sum_{j=1}^m \left|a_n^{(j)}
ight|^2}{\left\langle \psi | \psi
ight
angle}.$$

The measurement process alters the system's state from $|\psi\rangle$ to $|\psi_n\rangle$. If the system is initially in the eigenstate $|\psi_n\rangle$ of \hat{A} , a measurement of A will always yield the eigenvalue a_n with certainty, satisfying: $a_n : \hat{A} |\psi_n\rangle = a_n |\psi_n\rangle$.

1.2.2 PRELIMINARIES OF QUANTUM COMMUNICATION

1.2.2.1 QUBIT AND MEASUREMENT BASIS

The "qubit" serves as the quantum analogue of the "classical bit", fundamental to quantum computation and information. Unlike a classical bit, which exists exclusively in states 0 or 1, a qubit can simultaneously occupy a superposition of these states. These basis states are denoted in Dirac notation as $|0\rangle = \begin{pmatrix} 1 \\ 0 \end{pmatrix}$ and $|1\rangle = \begin{pmatrix} 0 \\ 1 \end{pmatrix}$, referred to as "ket-zero" and "ket-one". The conjugate transpose of a state vector $|\psi\rangle$ is written as $\langle\psi|$, termed "bra- ψ ". State vectors are represented as column matrices $(|\psi\rangle)$, while their conjugates are row matrices $(\langle\psi|)$. A qubit

state is typically represented as $|\psi\rangle = \alpha|0\rangle + \beta|1\rangle$, where α and β are complex probability

amplitudes satisfying $|\alpha|^2 + |\beta|^2 = 1$. The terms $|\alpha|^2$ and $|\beta|^2$ correspond to the probabilities of finding the qubit in states $|0\rangle$ and $|1\rangle$, respectively, when measured in the computational basis. Measurement causes the quantum state to collapse into one of the basis states, depending on the measurement outcome.

Basis Sets: A set of vectors $\{|v_1\rangle, |v_2\rangle, |v_3\rangle, \dots, |v_n\rangle\}$ is a basis if the vectors are linearly independent $(\sum_{i=1}^n a_i |v_i\rangle = 0$ implies $a_i = 0$ for all i), orthogonal $\langle v_i | v_j \rangle = \delta_{ij}$), and satisfy the completeness relation $\sum_{i=1}^n |v_i\rangle \langle v_i| = 1$. This thesis work primarily employs the computational, diagonal, and Bell basis sets, are defined as follows:

Computational basis $\{|0\rangle, |1\rangle\}$: In quantum communication, $|0\rangle$ and $|0\rangle$ are interpreted as horizontal and vertical polarization states of photons, respectively. For multi-qubit systems, the computational basis extends to combinations like $\{|00\rangle, |01\rangle, |10\rangle, |11\rangle\}$, constructed as tensor products of individual qubit states.

Diagonal basis $\{|+\rangle, |-\rangle\}$: Here, $|+\rangle = \frac{|0\rangle + |1\rangle}{\sqrt{2}}$ and $|-\rangle = \frac{|0\rangle - |1\rangle}{\sqrt{2}}$ correspond to photons polarized at 45° and 135° relative to the horizontal direction. This basis is used to exploit superposition principles and complements the computational basis, ensuring the security of quantum protocols through measurements in both bases.

Bell basis $\{|\phi^{+}\rangle, |\phi^{-}\rangle, |\psi^{+}\rangle, |\psi^{-}\rangle\}$: The Bell basis comprises maximally entangled two-qubit states, central to quantum communication protocols involving entanglement. The Bell states are:

$$\begin{array}{rcl} |\phi^{+}\rangle & = & \frac{1}{\sqrt{2}} \left(|00\rangle + |11\rangle \right), & |\phi^{-}\rangle & = & \frac{1}{\sqrt{2}} \left(|00\rangle - |11\rangle \right), \\ |\psi^{+}\rangle & = & \frac{1}{\sqrt{2}} \left(|01\rangle + |10\rangle \right), & |\psi^{-}\rangle & = & \frac{1}{\sqrt{2}} \left(|01\rangle - |10\rangle \right). \end{array}$$

These states are crucial for quantum teleportation and superdense coding. For instance, in quantum teleportation, an entangled Bell pair shared between two parties allows the transmission of an unknown quantum state using classical communication and quantum operations.

1.2.2.2 PURE STATE

If the quantum system's state can be expressed as a linear combination of the basis states $|n\rangle$:

$$|\psi\rangle = \sum_{n} c_{n} |n\rangle$$
,

the state is described as "pure". The density operator ρ for a pure state is defined as:

$$\rho = |\psi\rangle\langle\psi|.$$

By substituting the relevant expressions, we arrive at:

$$ho = \sum_{n} \sum_{m} c_{n} c_{m}^{*} |n\rangle\langle m| = \sum_{n,m}
ho_{nm} |n\rangle\langle m|.$$

The matrix elements of the density operator for a pure quantum state are defined as $\rho_{nm} = \langle n|\rho|m\rangle$. For a measurement performed on the state $|\psi\rangle$, the probability of observing the system in the state $|n\rangle$ is given by $|c_n|^2$. This interpretation connects the diagonal elements of the density matrix to physical probabilities, where $\rho_{nn} = |c_n|^2$. Since the diagonal elements are nonnegative, the density operator is inherently positive. The density operator for a pure state possesses specific mathematical properties.

$$Tr(\rho) = \sum_{n} \rho_{nn} = \sum_{n} |c_n|^2 = 1.$$

Since $\rho^2 = |\psi\rangle\langle\psi|\psi\rangle\langle\psi| = |\psi\rangle\langle\psi| = \rho$ so $Tr(\rho^2) = 1$ as for a normalized state $|\psi\rangle\langle\psi| = 1$.

1.2.2.3 MIXED STATE

A quantum system, however, may not always exist in a pure state. Instead, it might be represented as a mixture of states $|\psi_i\rangle$, which are not necessarily orthogonal. Each state $|\psi_i\rangle$ has its unique expansion in terms of the eigenvector basis $|n\rangle$, with a probability $p_i \geq 0$ associated with finding the system in the pure state $|\psi_i\rangle$. For such mixed states, the density operator is expressed as

$$\rho = \sum_{i} p_{i} |\psi_{i}\rangle \langle \psi_{i}|.$$

This operator satisfies the conditions of positivity and a unit trace. A quantum state is classified as pure if it satisfies the condition $Tr(\rho^2) = 1$, whereas for a mixed state, $Tr(\rho^2) < 1$. Both the state vector representation and the density operator representation are equivalent, with the choice of representation dictated by convenience.

1.2.2.4 QUANTUM GATE

Except for the NOT and Identity gates, all other standard "classical gates"—such as AND, OR, NOR, and NAND—are irreversible (\longrightarrow) . This means that the input state cannot be uniquely reconstructed from the output state. The operation of these irreversible gates results in the erasure of one bit of information since they consistently map a 2-bit input to a 1-bit output. Landauer's groundbreaking work [26] highlighted that erasing a bit of information leads to a minimum energy dissipation of $kT \log 2$. However, this energy loss can be avoided by utilizing reversible logic gates. Although it is technically feasible to construct classical reversible gates, they are less significant because they do not perform tasks that cannot already be achieved by irreversible circuits. In contrast, quantum gates are inherently reversible (\longleftrightarrow) , enabling the unique reconstruction of input states from output states (a bijective mapping). It is essential to note that while all quantum gates are reversible, not all reversible gates qualify as quantum gates. Typically, the term "quantum gates" refers specifically to quantum logic gates, while "reversible gates" pertains to classical reversible gates. This convention will be adhered to here as well. Fundamentally, a "quantum gate" or "quantum logic gate" represents a unitary operation that uniquely maps one quantum state to another. The mapping is inherently bijective. Mathematically, an N-qubit quantum gate is represented as a $2^N \times 2^N$ matrix. In the following sections, important single-qubit and two-qubit quantum gates relevant to this thesis will be discussed. Additionally, certain quantum gates not directly used in this thesis will be briefly summarized.

A single-qubit state is represented as a vector $\begin{pmatrix} \alpha \\ \beta \end{pmatrix}$, while a "single-qubit quantum gate" is described by a 2×2 unitary matrix. Such a gate, denoted as a unitary operator U, transforms an input single-qubit state $|\Psi\rangle_{\rm inp}$ into an output single-qubit state $|\Psi\rangle_{\rm out} = U|\Psi\rangle_{\rm inp}$. The unitarity of U ensures the existence of its inverse U^{-1} , which enables the inverse operation $U^{-1}|\Psi\rangle_{\rm out} = |\Psi\rangle_{\rm imp}$.

Pauli-X gate or NOT gate: The Pauli-X gate, represented as the unitary operator X, has the matrix form:

$$X = \left(\begin{array}{cc} 0 & 1 \\ 1 & 0 \end{array}\right) .$$

Alternatively, it can be expressed as $X = |0\rangle\langle 1| + |1\rangle\langle 0|$. The action of the X gate on a single-

qubit state is described as follows:

$$X(\alpha|0\rangle + \beta|1\rangle) = \alpha|1\rangle + \beta|0\rangle$$
.

Pauli-Z gate: The Pauli-Z gate, represented as the unitary operator Z, has the matrix form:

$$Z = \left(\begin{array}{cc} 1 & 0 \\ 0 & -1 \end{array}\right).$$

It can also be expressed as $Z = |0\rangle\langle 0| - |1\rangle\langle 1|$. The action of the Z gate on a single-qubit state is given by:

$$Z(\alpha|0\rangle + \beta|1\rangle) = \alpha|0\rangle - \beta|1\rangle$$
.

Pauli-Y gate: The matrix form of the unitary operator for the Y-gate is:

$$iY = \left(\begin{array}{cc} 0 & 1 \\ -1 & 0 \end{array}\right) .$$

It can also be expressed as $Y = |0\rangle\langle 1| - |1\rangle\langle 0|$. The action of the *Y*-gate on a single-qubit system can be described as follows. The *Y*-gate is a combination of the *X*-gate and the *Z*-gate, functioning as both a bit-flip and phase-flip operator:

$$Y(\alpha|0\rangle + \beta|1\rangle) = -\alpha|1\rangle + \beta|0\rangle$$
.

Hadamard gate: The matrix representation of the unitary operator for the H-gate is:

$$H = \frac{1}{\sqrt{2}} \left(\begin{array}{cc} 1 & 1 \\ 1 & -1 \end{array} \right) .$$

It can also be represented as $H=|+\rangle\langle 0|-|-\rangle\langle 1|$. The Hadamard transformation is defined as:

$$H|0\rangle = \frac{1}{\sqrt{2}}(|0\rangle + |1\rangle),$$

$$H|1\rangle = \frac{1}{\sqrt{2}}(|0\rangle - |1\rangle).$$

Phase gate: The matrix representation of the phase gate is given by:

$$P(\theta) = \begin{pmatrix} 1 & 0 \\ 0 & \exp(i\theta) \end{pmatrix}.$$

Since θ can take infinitely many values, specific cases are often considered. For $\theta = \frac{\pi}{2}$, the phase gate corresponds to the S-gate:

$$S = P\left(\frac{\pi}{2}\right) = \begin{pmatrix} 1 & 0 \\ 0 & i \end{pmatrix}.$$

The action of the *S*-gate is:

$$S|0\rangle = |0\rangle, S|1\rangle = i|1\rangle.$$

For $\theta = \frac{\pi}{4}$, the phase gate becomes the *T*-gate, represented as:

$$T = P\left(\frac{\pi}{4}\right) = \left(\begin{array}{cc} 1 & 0 \\ 0 & \frac{1}{\sqrt{2}}(1+i) \end{array}\right).$$

It is important to note that the *P*-gate is generally not self-inverse.

A two-qubit quantum state is represented as a column vector: $\begin{pmatrix} \alpha \\ \beta \\ \gamma \\ \delta \end{pmatrix}$, while a two-qubit

quantum gate is expressed as a 4×4 matrix, since $2^2 \times 2^2 = 4 \times 4$. When a "two-qubit gate" acts on a two-qubit state, it transforms the input state into another two-qubit state, with the mapping uniquely defined by the specific gate's properties.

Controlled-NOT gate: The Controlled-NOT (CNOT) gate is a two-qubit gate. Its matrix representation is:

$$\text{CNOT} = \begin{pmatrix} 1 & 0 & 0 & 0 \\ 0 & 1 & 0 & 0 \\ 0 & 0 & 0 & 1 \\ 0 & 0 & 1 & 0 \end{pmatrix},$$

In the bra-ket notation, the CNOT gate can be written as:

$$CNOT = |00\rangle\langle00| + |01\rangle\langle01| + |11\rangle\langle10| + |10\rangle\langle11|.$$

In this gate, the first qubit serves as the control, and the second as the target. If the control qubit is $|0\rangle$, the target qubit remains unchanged. Conversely, if the control qubit is $|1\rangle$, the target qubit is flipped. The CNOT gate performs the following mappings:

$$\begin{array}{ccc} |00\rangle & \longrightarrow & |00\rangle \\ |01\rangle & \longrightarrow & |01\rangle \\ |10\rangle & \longrightarrow & |11\rangle \\ |11\rangle & \longrightarrow & |10\rangle \end{array}.$$

SWAP gate: The SWAP gate is another two-qubit gate. Its matrix representation is:

$$SWAP = \begin{pmatrix} 1 & 0 & 0 & 0 \\ 0 & 0 & 1 & 0 \\ 0 & 1 & 0 & 0 \\ 0 & 0 & 0 & 1 \end{pmatrix}.$$

In bra-ket notation, the SWAP gate is expressed as:

SWAP =
$$|00\rangle\langle00| + |10\rangle\langle01| + |01\rangle\langle10| + |11\rangle\langle11|$$
.

The SWAP gate exchanges the states of the two qubits, performing the following mappings:

$$\begin{array}{ccc}
00\rangle & \longrightarrow & |00\rangle \\
01\rangle & \longrightarrow & |10\rangle \\
10\rangle & \longrightarrow & |01\rangle \\
11\rangle & \longrightarrow & |10\rangle
\end{array}$$

The fundamental concepts introduced thus far are crucial for understanding quantum technologies such as quantum sensing [27], quantum computing [28], and quantum communication. However, this thesis specifically focuses on secure quantum communication—an area where quantum cryptographic schemes provide unconditional security, a feature unattainable by classical counterparts. Notably, current implementations of quantum cryptography, particularly QKD, are not entirely quantum mechanical. A critical pre-QKD phase requires the sender and

receiver to authenticate each other, a process that is typically conducted classically. In the next section, we introduce the core topic of this thesis by addressing a key question: Why is quantum identity authentication necessary? The subsequent sections of this chapter systematically explore foundational concepts related to this work, covering QIA, QKD, QKA, and game theory in the context of quantum communication in Sections 1.3–1.5, 1.6, 1.7, and 1.8, respectively.

1.3 WHY IS QUANTUM IDENTITY AUTHENTICATION NECESSARY?

Identity authentication, often referred to as authentication, is a structured process aimed at verifying the identities of authorized users or devices/components. This procedure is critical in mitigating various types of attacks targeting secure computation and communication frameworks. The significance of identity authentication protocols has grown substantially in recent years, driven by the increased adoption of e-commerce, online banking, the Internet of Things (IoT), online voting, and similar applications. These use cases fundamentally rely on robust identity verification mechanisms. For instance, IoT primarily focuses on authenticating devices or components, while online voting emphasizes verifying the identities of users (voters). From a cryptographic standpoint, the distinction between a user and a device/component is minimal, and thus, they will be treated equivalently in subsequent discussions.

In a two-party framework, authentication can be conceptualized as a process enabling a legitimate sender, Alice, to convey a message X (or a key in the context of key distribution schemes) to a receiver, Bob, ensuring that Bob can verify the message's integrity and confirm it was not altered during transmission through the channel [29]. Essentially, this process serves to authenticate the origin of message X and guarantee its integrity upon reception by Bob. This concept is closely associated with digital signatures, which additionally permit a third party, Charlie, to later verify that the message X received by Bob from Alice has not been tampered with [29]. Although authentication and digital signatures are related, they are distinct tasks. This discussion is confined to authentication schemes, specifically those utilizing quantum resources, referred to as QIA. To understand the significance of QIA schemes, it is helpful to briefly examine the evolution of quantum cryptography, which has historically redefined the concept of security. In 1984, Bennett and Brassard introduced the first QKD protocol [15], now referred to as the BB84 protocol 1 . This groundbreaking proposal asserted the potential for unconditional

¹The origins of quantum cryptography are significantly attributed to Wiesner's pioneering work [30]. For an insightful account of the historical developments in this field, see [31].

security—a feature unattainable through classical key distribution methods, which rely on the computational complexity of specific mathematical problems for security. This assertion captured significant attention within the cryptographic community, leading to the development of several notable QKD protocols, such as the E91 protocol by Ekert (1991) [32] and the B92 protocol by Bennett (1992) [16]. The importance of authenticating the identities of legitimate participants was acknowledged even in the foundational BB84 paper. Bennett and Brassard highlighted, "The need for the public (non-quantum) channel in this scheme to be immune to active eavesdropping can be relaxed if Alice and Bob have agreed beforehand on a small secret key, which they use to create Wegman-Carter authentication tags [33] for their messages over the public channel". Prior to the development of quantum identity authentication protocols in 1995, classical methods like the Wegman-Carter authentication scheme were inherently incorporated into early QKD protocols [34], though this was not always explicitly stated. Across these protocols, as well as in subsequent authentication schemes, the "pre-shared small key" mentioned above remains a fundamental and indispensable component ¹. This concept will be elaborated further in this chapter. The inclusion of the Wegman-Carter scheme, or similar classical methods, in early QKD protocols arose from the practical consideration that no communication channel could be assumed entirely trustworthy. An adversary (Eve) could potentially intercept and replace the communication channel between the sender (Alice) and receiver (Bob) with two separate channels—one connecting Alice to Eve and the other connecting Eve to Bob. In such a case, Eve could generate separate keys with both Alice and Bob, effectively isolating them. To prevent such scenarios, employing identity authentication protocols became a critical necessity.

Since the security of classical authentication methods relies on the computational complexity of certain tasks, they cannot guarantee unconditional security. This limitation introduces potential vulnerabilities in so-called unconditionally secure QKD schemes. Achieving true unconditional security in QKD necessitates unconditionally secure authentication methods, which in turn require the use of quantum resources. Authentication schemes leveraging quantum principles are commonly referred to as QIA schemes. The first such scheme was introduced by Crépeau and Salvail in 1995 [35]. Subsequent advancements followed. For instance, in 1998, Zeng et al. proposed a QKD protocol that simultaneously enabled key distribution and identity verification

¹All QKD protocols can be interpreted as key amplification mechanisms. Each QKD session begins with a small pre-shared key for authentication, generates an extended key, and subsequently uses a portion of the extended key as the pre-shared key for the next session.

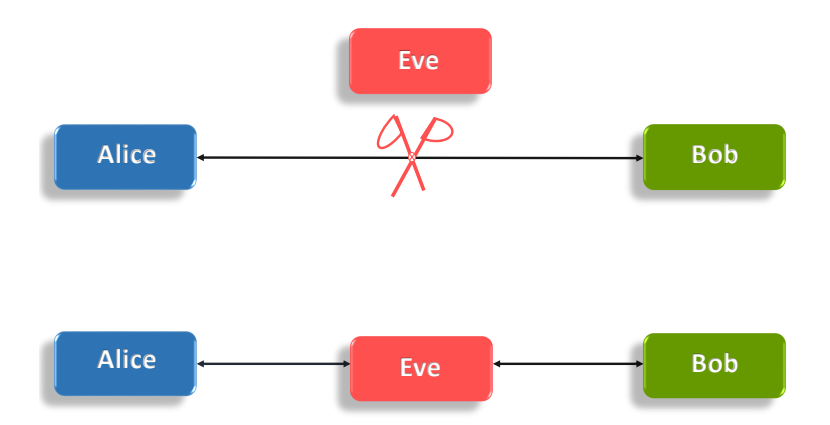


Figure 1.1: Eve may attempt to mimic Alice (or Bob) while interacting with Bob (or Alice) by substituting the direct communication channel between Alice and Bob with two separate channels: one connecting Alice to Eve and the other linking Eve to Bob.

[36]. Shortly after, in 1999, Dušek et al. presented two hybrid QIA protocols [37]. These protocols combined classical authentication methods with QKD, often emphasizing the one-time pad. Over time, numerous QIA schemes emerged, each with distinct advantages and limitations [38, 39, 40, 41, 42, 43, 44, 45]. Given the critical role of authentication in secure quantum communication and computation protocols, this chapter aims to systematically review the existing QIA schemes.

Before delving into a formal chronological review of schemes for QIA, it is essential to briefly introduce the concept of quantum communication complexity in the context of quantum authentication protocols. This is because quantum communication complexity serves as a measure for assessing the amount of communication necessary between two parties, Alice and Bob, to complete a distributed communication task [46]. Consider a scenario where Alice and Bob aim to jointly compute a function f(a,b) using an error-free quantum channel, where Alice possesses input a and Bob holds input b. To accomplish this task, they exchange information according to a specific protocol derived from distributed algorithms. The communication required to execute the task using such a protocol defines the communication complexity for the given scenario. There are three primary models of quantum communication complexity relevant to this discussion. The first is Yao's model, wherein the parties communicate through a quantum channel that facilitates qubit exchange [47]. Both Alice and Bob perform unitary operations and interact by placing qubits into a shared channel that each can access via further unitary operations. The protocol concludes when they successfully compute the precise value of f(a,b). The quantum communication complexity, O(f), in this model, is determined by the number of communi-

cations required to complete the task. The second model, introduced by Cleve and Buhrman, involves parties sharing entangled pairs and exchanging classical information over a classical channel [48]. In this framework, the communication required for pre-sharing entangled states is excluded from the computation of quantum communication complexity. Instead, only the number of classical bits exchanged contributes to the complexity. This model is particularly suitable for analyzing protocols utilizing teleportation and superdense coding, with the quantum communication complexity denoted as $C^*(f)$. The third model, known as the hybrid model, incorporates features of the previous two approaches. It employs a quantum channel, a classical channel, and pre-shared entangled pairs for communication. In this model, the entangled pairs used are not counted again during the evaluation of communication complexity; only the classical bits exchanged are considered. The quantum communication complexity in this case is represented as $Q^*(f)$. The relevance of these models to QIA becomes evident in subsequent sections. The suitability of a particular quantum communication complexity model depends on how a specific QIA scheme is implemented. Recent studies, such as those by Guedes and de Assis (in 2011) and Ghilen et al. (in 2014) [49, 50], have examined quantum communication complexity for various authentication protocols, providing systematic methodologies for analyzing the complexity of such protocols.

1.4 A SHORT CHRONOLOGICAL HISTORY OF THE PROTOCOLS FOR QUANTUM IDENTITY AUTHENTICATION

Classical authentication schemes, such as the Wegman-Carter scheme, were highlighted in Section 1.3 as having been employed in the early protocols of QKD. These message authentication schemes can be effectively conceptualized as operating in two distinct phases. In the initial phase, specific functions are utilized to generate identity authentication, while in the subsequent phase, these functions are used to verify the authenticity of a message. Classical methods like message encryption, message authentication codes (MACs), and hash functions are widely employed for such purposes. Although the primary focus here is not on classical authentication schemes, it is worthwhile to briefly touch upon these concepts before delving into the chronological development of QIA. This brief discussion is pertinent, as hybrid schemes and purely classical methods remain integral to secure quantum communication and computation. Additionally, many classical authentication techniques can be adapted to design schemes for QIA.

To illustrate how classical methods can be used for QIA scheme design, consider a pre-shared key x_1, x_2, \dots, x_n between Alice and Bob, where $x_i \in \{0, 1\}$. Alice can divide this key into two parts, using one half (e.g., all odd-indexed bits) as the message and the other half (e.g., all evenindexed bits) as the key. She can then construct a new sequence of length $\left|\frac{n}{2}\right|$ where the *i*-th bit of the sequence is $x_{2i-1} \oplus x_{2i}$. This sequence can function as a tag or cryptographic element. Alice transmits it using a conventional method, and Bob, employing the same key subset $\{x_{2i}\}\$, can decode it. The ability to convey a message inherently includes the ability to transmit a Tag. As a result, every protocol for QSDC [51, 52], quantum dialogue (QD) [53], and deterministic secure quantum communication (DSQC) [54] can accomplish this function. In other words, the classical method described can be seamlessly adapted to create straightforward schemes for QIA using various QSDC, DSQC, and QD protocols. Furthermore, in the MAC approach, both participants share a common secret key, K. When Alice intends to send a message to Bob, she computes the MAC as a function of the message and the shared key, then transmits the message along with the MAC to Bob. Bob subsequently calculates the MAC for the received message using the same procedure and compares it with the received MAC. A match verifies the message's authenticity and integrity. A hash function, as a variant of MAC, processes input messages of variable lengths to produce a fixed-size output known as a hash code. With its oneway property, the hash function is particularly effective for generating a message fingerprint. The no-cloning theorem, which asserts that it is impossible to duplicate an unknown quantum state with perfect fidelity, alongside the "collapse on measurement" attribute of quantum states, plays a pivotal role in demonstrating the advantages of QIA schemes over their classical counterparts. To illustrate this, imagine a scenario where Eve breaks into Alice's house and secretly replicates her authentication key without leaving any evidence. In the classical domain, such an act would enable Eve to impersonate Alice and communicate with Bob undetected. In contrast, within the quantum realm, such a situation is prevented if the authentication key is encoded and stored in a quantum state, as the no-cloning theorem prohibits perfect copying. Furthermore, the "collapse-on-measurement" principle ensures that any eavesdropping attempt would leave detectable traces, thereby enhancing the security of quantum cryptographic protocols. This serves as the foundation for developing QIA protocols.

In the prior section, it was noted that the first protocol for QIA was introduced by Crépeau et al. [35]. This protocol was grounded in the concept of oblivious transfer (OT), a fundamental cryptographic primitive. However, a pivotal result by Lo and Chau[55] demonstrated the im-

possibility of achieving unconditionally secure two-party OT. The groundbreaking contribution by Crépeau et al. was succeeded by early explorations into QIA, including those by Zeng and Wang (1998), Dušek et al. (1999), and Barnum (1999) [36, 37, 56], as briefly discussed earlier. Despite these initial efforts, progress in quantum or hybrid identity authentication during the 20th century was limited. The landscape has evolved significantly in the 21st century. This section aims to trace the chronological development of QIA protocols. Given the extensive literature, this effort does not strive to cover all contributions but instead highlights representative works that illustrate the progression of quantum and hybrid identity authentication ¹. It also emphasizes that different types of QKD protocols—such as continuous variable QKD (CV-QKD), discrete variable QKD (DV-QKD), counterfactual QKD, and semi-QKD—necessitate tailored QIA schemes to enable the use of shared resources and devices for both communication and authentication tasks. While early QIA protocols were predominantly tied to conventional "conjugate-coding-based" DV cryptographic schemes, their applicability has since expanded significantly.

2000: The year was notably productive, with the introduction of numerous new protocols for QIA, numbering at least ten. The majority of these protocols, with the exception of three proposed by Ljunggren et al. [58] were based on Bell states. In early 2000, Zeng and Guo introduced a Bell state-based approach for QIA [59]. Shortly thereafter, Zhang et al. presented another Bell state-based protocol [40], utilizing a pre-shared Bell state as either a pre-shared secret or an authentication key. Between these developments, Jensen and Schack [60] proposed a protocol founded on bipartite entangled states ², asserting its security even under conditions where Eve has full control over both classical and quantum channels. Their work built upon Barnum's study, providing a generalization while also raising several open research questions [56].

In 2000, Ljunggren et al. introduced a set of five protocols for authenticated QKD between two parties, Alice and Bob [58]. Their approach incorporated a third party, Trent, serving as an arbitrator. Of these protocols, three utilized single-photon techniques [57], while the remaining two were based on Bell states. Notably, one of the entangled

¹For readers seeking a comprehensive list of publications on quantum authentication from 2009 to 2019, Ref. [57] provide an extensive review. Notably, the classification of QIA schemes presented in [57] aligns with the framework established in this chapter, even though their study was encountered after completing this review.

²Although it is not explicitly stated that the particles are maximally entangled, we can, without any loss of generality, interpret this as a Bell-state-based approach for QIA.

state-based protocols exhibited similarities to the B92 protocol. The symmetry identified between QKD and QIA schemes in this protocol suggests the potential for transforming other QKD schemes into frameworks for QIA or authenticated QKD. Furthermore, Trent's role parallels that of a controller in a cryptographic switch, as discussed in Ref. [61, 62]. Leveraging the findings of these studies, the three-party protocols proposed by Ljunggren et al. can be generalized to derive novel protocols for QIA.

2001: Curty et al. introduced an optimal protocol for quantum authentication of classical messages, referred to as the CS01 protocol [63]. This protocol was optimal in that it enabled the authenticated transmission of a two-bit classical message using a single qubit as the authentication key, effectively serving as an optimal pre-shared secret. Notably, they categorized potential attacks on authentication schemes into two types: (i) no-message attacks and (ii) message attacks. In the CS01 protocol and several other message authentication schemes, perfect deterministic decoding of the classical message is achieved. This means that the protocol fails only if Bob erroneously accepts an unauthenticated message as legitimate. Curty et al. observed that this failure can occur through two distinct mechanisms, corresponding to the two categories of attacks. In a no-message attack, an adversary (Eve) prepares a quantum state before Alice transmits any message, intending to trick Bob's decoding algorithm with a certain success probability p_f . This attack is termed "no-message" because it operates in the absence of any transmitted message from Alice. Conversely, in a message attack, Eve intercepts the message sent by Alice to extract information. Using this intercepted data, she constructs a counterfeit message and attempts to bypass Bob's decoding algorithm. This classification of attack strategies significantly facilitated the security analysis of later protocols. However, the security analysis in [63] and many subsequent works relied on the assumption of an idealized noiseless quantum channel, which does not accurately reflect real-world conditions.

2002: In the CS01 protocol, a classical message was authenticated using an optimal amount of quantum resources. This naturally raised intriguing questions, such as: How can a quantum message be authenticated using a quantum key? Is it possible to authenticate a qubit—a minimal-sized quantum message—using another qubit as a minimal-sized pre-shared quantum secret? These questions were explored by Curty et al. [64]), who presented a no-go theorem stating that a single qubit cannot be authenticated using only

another qubit. T. Mihara proposed protocols for QIA and message authentication [45] that utilized pre-shared entanglement. Their QIA scheme involved a trusted third party, while their message authentication protocol combined quantum resources with a hash function, making it a hybrid approach. Notably, the methodology adopted in their message authentication scheme can be generalized, allowing all existing QSDC protocols to design analogous frameworks. However, it was later demonstrated that this scheme while employing quantum correlations, does not leverage them effectively, and the same task can be achieved using classically correlated states [65]. Additionally, the quantum component of Mihara's QIA protocol [45] was found to be susceptible to vulnerabilities. Specifically, during the entanglement distribution phase (see Steps 2–3 in the section "Identifying Alice to Bob" in [45]), neither the BB84 subroutine nor the Goldenberg Vaidman (GV) subroutine [66] was utilized. Instead, all subsequent measurements were performed in the computational basis, making the protocol vulnerable to a "man-in-the-middle attack". This issue could be mitigated by incorporating decoy qubits and implementing one of the aforementioned subroutines, as is commonly done in QSDC protocols [67, 68, 69]. For example, one might refer to the ping-pong protocol described in Ref. [23].

2004: Li et al. introduced a QIA protocol utilizing Bell states [38]. In their approach, a preshared Bell state serves as an identification token between Alice and Bob. During the authentication process, Alice generates an auxiliary Bell state to interact with the identification token and transmits the resulting auxiliary information to Bob. Bob then performs specific operations and concludes the process with a Bell state measurement to authenticate. Notably, this Bell state-based protocol does not leverage the *non-local* properties of Bell states, as the violation of Bell inequalities is not employed as a quantum resource in the QIA design.

2005: Zhou et al. introduced a QIA framework based on quantum teleportation and entanglement swapping [70]. Their approach aimed to address the limitations of straightforward point-to-point QIA systems, leveraging entanglement swapping to increase the range over which authentication could occur. This method, widely recognized and often employed in QKD, helps overcome distance restrictions imposed by noise and the absence of quantum repeaters. However, it also introduces a new security challenge, as the intermediary device facilitating entanglement swapping must be trusted.

One way to assess the efficiency of an authentication protocol is by evaluating the amount of pre-shared information it requires during the authentication process—schemes that use less information are considered more efficient. Using this metric, Peev et al. proposed an efficient QIA scheme [70].

2006: Lee et al. introduced a pair of quantum direct communication protocols incorporating user authentication [71]. In their approach, Alice transmits a confidential message to Bob without relying on a "pre-shared secret". The protocols are structured into two distinct components: one designated for authentication and the other for direct message transmission. A trusted third party, Trent, possessing greater authority than the communicating parties, is responsible for authenticating participants by distributing tripartite "Greenberger-Horne-Zeilinger" (GHZ) states.

Wang et al. introduced an authentication protocol that enables a trusted third party to authenticate multiple users simultaneously by utilizing entanglement swapping and GHZ states [41]. In a separate approach, Zhang et al. presented a one-way QIA scheme [41] based on the ping-pong protocol of QSDC as proposed by Boström and Felbinger [72]. Their scheme qualifies as one-way QIA because it designates Alice as a trusted certification authority (CA), responsible for verifying Bob's identity when he attempts communication with her (Alice). Many existing authentication frameworks share this one-way nature, although it is not always explicitly stated, since one-way authentication inherently allows for two-way verification through repeated application of the process. The authors demonstrated that their protocol effectively resists specific attacks, including impersonation attacks—where an adversary, Eve, without knowledge of the authentication key, attempts to impersonate Bob by forging qubits—and substitution attacks, in which Eve endeavors to obtain the authentication key by leveraging a newly established quantum channel and intercepting qubits transmitted from Bob to Alice. It is important to highlight that while attacks such as message and no-message attacks are not consistently categorized under these labels, the majority of attacks examined can be classified into one of these two categories.

2007: Zhang et al. identified vulnerabilities in the protocol introduced by Lee et al. in 2006 [73], highlighting that Trent could exploit it through two distinct types of attacks. To address these security flaws, Zhang et al. proposed an enhanced version of Lee et al.'s

protocol, effectively mitigating the identified weaknesses. In the domain of cryptography, such analyses—wherein a scheme's vulnerabilities are uncovered, followed by the development of a more robust version—are a common practice. This scenario serves as a representative instance within the context of QIA.

2009: Guang et al. introduced a multiparty QIA protocol utilizing GHZ states [74], which closely resembled the approach previously proposed by Wang et al. [39]. However, their scheme demonstrated greater efficiency as it required fewer quantum resources and operations compared to the protocol by Wang et al.
In another development, Rass et al. proposed a novel approach by shifting the authentication phase to the conclusion of the QKD process [75], diverging from the conventional practice of performing it at the outset. Their scheme integrated concepts from both QKD and quantum coin-flipping, and they successfully derived tight bounds on the amount of

pre-shared secret information necessary for QIA.

- 2010: Dan et al. proposed a straightforward QSDC protocol incorporating authentication, utilizing Bell states with qubits encoded through polarization [76]. Although authentication schemes do not always explicitly specify this detail, it is inherently presumed that the qubits involved are photonic. This assumption arises because other forms of qubits, such as "transmon qubits" used in superconducting quantum computing and other qubit implementations, are not readily transferable over long distances. Furthermore, Dan et al. demonstrated the security of their protocol against common attacks, including interceptand-resend attacks, Trojan horse attacks, and entanglement-based attacks.
- 2011: In a subsequent development, Huang et al. introduced a CV-QIA protocol based on Gaussian-modulated squeezed states [77]. This protocol, along with similar approaches, enables CV-QKD schemes to authenticate using CV states. This advancement is crucial, as employing DV quantum authentication within CV quantum protocols can lead to decreased efficiency and increased operational complexity. The reason for this is that handling both CV and DV states requires additional devices and resources for performing respective operations and measurements.
- **2012:** Gong et al. explored the application of quantum one-way functions to formulate a QIA protocol that incorporated a trusted third party, which they referred to as a trusted server

in their study [78].

Additionally, a hybrid QIA scheme within a quantum cryptographic network was patented by MagiQ Technologies under US Patent number US 8,340,298 B2 [79].

Skoric introduced an intriguing concept that integrates quantum challenges with classical physical unclonable functions (PUFs). The core idea involved utilizing a quantum state to challenge a classical PUF. Due to the no-cloning theorem and the principle of "collapse on measurement", any interception attempt would leave detectable traces. Consequently, the verifier, who issues the challenge through a quantum state, could reliably confirm the prover's identity if the expected quantum state is received in response. It is important to highlight that the concept of PUFs was initially proposed by Pappu et al. at the beginning of the 21st century [80]. A PUF is characterized as a physical entity embedded in a specific structure that is straightforward to evaluate but challenging to characterize comprehensively. It is also considered an entity that is inherently resistant to duplication due to its complex, uncontrollable physical parameters (degrees of freedom) [81]. Notably, PUFs can be implemented using various devices such as FPGAs, RFIDs, and other hardware components, enabling their application in classical authentication protocols [82]. However, the focus here is on PUF-based schemes specifically designed for QIA. The growing interest in such schemes will be examined in the subsequent discussion.

- **2013:** Yang et al. introduced two authenticated direct secure quantum communication protocols utilizing Bell states [83]. These protocols incorporated a third party, Trent, and employed a hybrid approach by integrating Hash functions. The scheme enabled mutual authentication between Alice and Bob through Trent, leveraging Bell states combined with their secret identity sequences and one-way Hash functions h_A and h_B .
- 2014: In the context of controlled quantum teleportation, an intermediary, Charlie, controls the process, allowing Alice to transmit a quantum state to Bob [23, 84]. To resolve the challenge of identity verification in controlled teleportation, Tan et al. proposed identity authentication protocols utilizing entanglement swapping [85]. However, the efficiency of this approach is limited, as it necessitates two (three) entanglement swapping operations for Alice to verify the identity of Charlie (Bob).

Goorden et al. experimentally demonstrated a quantum authentication method for a physical unclonable key [81]. In this approach, the key, which is inherently classical in nature,

was verified by exposing it to a light pulse with fewer photons than the available spatial degrees of freedom. Authentication was achieved by analyzing the spatial characteristics of the reflected light.

Shi et al. introduced a "quantum deniable" authentication protocol leveraging the characteristics of unitary transformations and quantum one-way functions, utilizing the GHZ state [86]. Their protocol ensures both authentication completeness and deniability. Authentication completeness refers to the principle that, provided both the sender and receiver adhere to the protocol, the intended recipient can always verify the origin of the message. In contrast to traditional authentication schemes, deniable authentication guarantees that only the intended recipient can verify the message's source, while preventing the recipient from proving its origin to a third party.

Yuan et al. proposed a practical QIA scheme [87] based on a single-particle ping-pong protocol, similar to the LM05 protocol of QSDC [88]. This approach requires minimal quantum resources and utilizes simple devices.

Fountain codes, also known as "rateless erasure codes", possess a unique feature: starting with n source symbols, they can produce m > n encoded symbols, where m can be arbitrarily large. In a distributed setting, distributed fountain codes exploit this property. Using such codes, [89] devised a QIA scheme within the framework of quantum secret sharing.

- **2015:** Shi et al. enhanced their earlier research [86] by utilizing a single-photon source in place of a GHZ state [90]. This revised protocol demonstrated greater efficiency and required fewer quantum resources. This improvement is intuitive since generating and maintaining single-photon states is significantly simpler compared to photonic GHZ states.
- **2016:** Ma et al. introduced a CV-QIA protocol based on teleportation, employing a two-mode squeezed vacuum state and a coherent state. Notably, CV-QKD protocols outperform their discrete-variable counterparts over short distances [91, 92, 93]. Thus, for urban networks, integrating CV-QKD with CV-QIA is anticipated to provide a more efficient solution.

Rass et al. proposed a quantum information authentication scheme linked to the BB84 protocol [94]. The innovative aspect of this scheme lies in the use of a secondary public channel, distinct from the channel employed for the primary BB84 protocol.

The security of PUF-based authentication schemes, as explored by Goorden et al. and Škorić [81, 95], was challenged in [96]. It was demonstrated that earlier analyses, such as those by Ref. [97] and related works, were incomplete, as they only addressed security against challenge-estimation attacks. However, it was shown that cloning attacks could surpass the effectiveness of challenge-estimation strategies.

Composable security for QIA schemes was introduced by Hayden et al. [98], marking a significant advancement in enabling secure quantum communication across networks. Notably, composable security ensures that a real-world implementation of a protocol remains ε -indistinguishable from an ideal protocol designed for the same purpose. This framework allows for the derivation of information-theoretic security for composite schemes, such that $\varepsilon \leq \varepsilon_p + \varepsilon_a$, where ε_p -secure cryptographic protocols are combined with ε_a -secure applications, as discussed by Renner in [99].

2017: Hong et al. proposed a QIA protocol utilizing single-photon states [100]. This approach was both resource-efficient and practical, as it required fewer resources and facilitated the authentication of two bits of a key sequence using a single qubit.

Abulkasim et al. introduced an authenticated QSS protocol that leveraged Bell states as its foundational mechanism [101]. To enhance security, the protocol incorporated a widely employed technique in secure quantum communication, where the pre-shared key was encrypted prior to usage—a method frequently adopted in quantum communication frameworks.

Nikolopoulos and Diamanti proposed a CV authentication scheme utilizing coherent light states, wavefront shaping, and homodyne detection methods [102].

Portmann presented a quantum authentication scheme featuring key recycling, demonstrating its resilience against noisy channels and shared secret key vulnerabilities [103]. Additionally, the study established that the number of recycled key bits is optimal for certain authentication protocols.

2018: Kang et al. introduced a mutual authentication protocol enabling Alice and Bob to verify each other's identities despite the involvement of an untrusted third party, Trent [43]. This protocol relies on entanglement correlation verification, utilizing GHZ-like states to confirm that the state distributed by Trent is genuinely entangled. To prevent Trent from deducing the key, Alice and Bob incorporate random numbers in their process. This ap-

proach can be extended to other QIA protocols involving a trusted third party, potentially leading to the development of new QIA protocols.

Additionally, a US patent (Patent Number US 9,887,976 B2) was granted for a multi-factor authentication method employing quantum communication. This patent describes a two-stage process, encompassing enrollment and identification, implemented through a computer system acting as a trusted authority [104].

2019: Semi-quantum protocols represent a category of cryptographic protocols designed to extend quantum-level security to certain classical users. The first semi-quantum protocol for QKD was introduced by Boyer et al. in 2007 [105]. Since then, semi-quantum schemes have been developed for a variety of purposes [106, 107, 108, 109]. However, until 2019, no semi-quantum authentication protocol had been proposed, despite its fundamental importance for semi-quantum QKD and other semi-quantum cryptographic applications. This gap was addressed by Wen et al. in 2019 when they introduced a semi-quantum authentication protocol [110] that does not require all users to possess quantum capabilities. Specifically, this protocol enables a quantum-capable Alice (or Bob) to authenticate a classical Bob (or Alice).

In the same year, another significant development in quantum cryptography emerged when Liu et al. proposed a QIA protocol [111], which can be integrated into counterfactual QKD schemes.

Zheng et al. introduced a controlled QSDC (CQSDC) protocol with authentication in 2019, utilizing a five-qubit cluster state [112]. While the protocol was demonstrated to be secure even in noisy environments, the preparation and maintenance of the five-qubit cluster state pose significant challenges. Although it is conceptually straightforward to extend Bell state or GHZ state-based protocols to those employing n-partite entangled states for n > 3, such extensions often lack practical advantages. Notably, this was not the first instance where a five-qubit cluster state was utilized for quantum information applications. For instance, a QIA scheme employing a five-qubit cluster state and one-time pad was proposed in 2014 [44] and later subjected to cryptanalysis in 2016 [113]. Moreover, an entanglement swapping-based protocol using a six-qubit cluster state was proposed in 2012, and in 2015, a scheme for authenticated CQSDC was designed with a six-qubit entangled state [114]. However, none of these approaches relying on multi-

partite entangled states are currently practical for real-world applications.

2020: Many of the QIA protocols referenced above have not accounted for the impact of noise, an inevitable factor in practical scenarios. To address this limitation, Qu et al. introduced a QIA protocol utilizing a "three-photon error-avoidance code" [115]. This approach effectively mitigates the influence of noise on the information transmission through a quantum channels.

Zhang et al. proposed a QIA protocol based on Bell states and entanglement swapping [42], which offers security against the strategies of a semi-honest third party. It is important to note that a semi-honest party adheres to the protocol's rules while attempting to exploit the system within those bounds. As a result, semi-honest attacks are generally weaker than those of a dishonest third party. Therefore, when designing quantum cryptographic protocols, it is preferable to account for the potential threats posed by dishonest adversaries.

- 2021: Existing protocols are either subjected to cryptanalysis or modified to propose enhanced versions of QIA schemes tailored to specific applications. For instance, [116] and [117] examine QIA schemes in the contexts of quantum private query and QSDC, respectively. Additionally, a previously proposed hybrid authentication scheme by Zawadzki [118], which improved upon a single-photon-based protocol introduced by Ho Hong et al. [100], underwent systematic cryptanalysis by González-Guillén et al. [119]. In their analysis [119], they designed two attacks, demonstrating vulnerabilities not only in the protocols from Ho Hong et al. and Zawadzki [100, 118] but also in several other existing QIA protocols. Furthermore, significant interest has been observed in PUF-based quantum authentication schemes [120, 121], and closely related applications explored by [122].
- 2022-2024 Li et al. introduced a multiparty simultaneous identity authentication protocol utilizing the GHZ state [123]. This protocol assumes that the third-party Trent is both honest and a classical participant, which presents a limitation for communication security. In the same year, Das et al. [124] proposed a measurement-device-independent (MDI) QSDC protocol incorporating user authentication [124], wherein authentication is conducted prior to a secure message exchange between authenticated parties. Similarly, He et al. [125] developed a QKA protocol in which quantum authentication is performed first. Leveraging the structural symmetry of these two protocols, Li et al. introduced an

MDI-QKA scheme with integrated identity authentication [126, 127].

In 2023, Chen et al. proposed a QIA scheme employing quantum rotation and public-key cryptography [128]. In subsequent work, the same researchers designed a QIA protocol using quantum homomorphic encryption [129]. Additionally, Zhang et al. introduced a three-party QSDC scheme with user authentication, utilizing a single-photon source and implementing hyper-encoding techniques across different degrees of freedom [130].

Most recently, Mawlia et al. proposed a QSS scheme incorporating user identity authentication via mutually unbiased bases, where each participant performs quantum Fourier transform (QFT) and unitary transformations. This methodology ensures that during the secret recovery phase, the confidential information remains undisclosed and is never directly transmitted [131].

Before concluding this section, it is important to highlight that authentication protocols come in several variations. One notable variant is deniable authentication, which prevents a receiver from proving the message's origin to a third party. For instance, Shi et al. introduced a quantum protocol for deniable authentication [86]. Additionally, most QIA protocols focus on two-party interactions, typically involving a sender (Alice) and a receiver (Bob). However, some schemes incorporate a third party, often called an authenticator (Trent). For example, Lee et al. proposed two three-party QIA schemes using GHZ states [71]. Later, Zhang et al. identified that Trent could eavesdrop on both protocols but also provided a solution to mitigate these vulnerabilities [73]. In [58], a scenario involving three parties was analyzed, where an arbitrator named Trent handled the authentication process. Additionally, it is worth noting that the QIA protocols outlined here in chronological order differ significantly in various technical aspects, such as the inclusion or exclusion of a third party and the use of entangled versus separable states. These differences provide a basis for categorizing the protocols according to such criteria. In fact, the next section focuses on classifying the existing schemes. However, prior to this classification, we presented a chronological summary of the technical features of several representative QIA protocols in Table 1.1. This table not only highlights the uniqueness and progression of these protocols but also suggests the potential for classification-based on the characteristics listed in the third column and those to its right. The following section will expand on this idea, systematically categorizing the QIA protocols.

Table 1.1: The classification of existing schemes for QIA is presented. When the use of a pre-shared key is referred to as "By QKD", as indicated by the authors of the respective studies, it can be interpreted that a classical identity sequence was initially exchanged as a prerequisite for performing QKD for the first time. The following abbreviations are employed in this table: C=classical, B=Bell state, FC=five-particle cluster state, CS=classical identity sequence, N=no, HF=single one-way hash function, QPKC=quantum public key cryptography, Q=quantum, T=trusted, SP=single photon, ST=semi-trusted, Y=yes, UT=un-trusted.

Protocol	Year	Quantum	Pre-	Was	Channel	Is quan-	Computation
pro-	1001	resources	shared	there a	used	tum	or communi-
posed		used	key used	third		mem-	cation task
in		3 5 3		party?		ory	used
				Pully.		used?	0.500
[37]	1999	SP	CS	N	C, Q	N	QKD
[59]	2000	B, SP	CS	N	C, Q	N	QSDC/DSQC
[40]	2000	B, SP	В	N	Q	Y	QSDC/DSQC
[58]	2000	B, SP	By QKD	T	C, Q	Y	QKD
[63][64]	2001	B, SP	В	N	Q	Y	QSDC/DSQC
[45]	2002	В	В	T	C, Q	Y	QSS
[38]	2004	В	В	N	Q	Y	QSDC/DSQC
[70]	2005	В	В	T	C, Q	Y	Teleportation
[41]	2006	B, SP	By QKD	N	Q	Y	QSDC/DSQC
[39]	2006	GHZ	CS, HF	T	C, Q	Y	QSDC/DSQC
[71]	2006	GHZ	CS, HF	UT	C, Q	Y	QSDC/DSQC
[74]	2009	GHZ	CS, HF	T	C, Q	N	QSS
[76]	2010	B, SP	CS	N	C, Q	Y	QSDC/DSQC
[83]	2013	В	CS, HF	T	C, Q	Y	QSDC/DSQC
[44]	2014	FC	CS	UT	Q	N	QSDC/DSQC
[86]	2014	GHZ	By QKD	T	C, Q	N	QSS & MAC
[87]	2014	SP	CS	N	Q	N	QSDC/DSQC
[90]	2015	SP	By QKD	T	Q	N	QSS & MAC
[100]	2017	SP	CS	N	C, Q	N	QSDC/DSQC
[43]	2018	GHZ-like	CS	UT	C, Q	Y	QSDC/DSQC
[111]	2019	SP	CS	N	Q	N	QKD
[110]	2019	GHZ-like,	CS, HF	N	C, Q	Y	Teleportation
		W					
[112]	2019	FC	By QKD	T	C, Q	N	QSS
[42]	2020	В	CS	ST	C, Q	N	QSDC/DSQC
[115]	2020	GHZ-like	CS	N	C, Q	N	QECC
[132]	2020	SP	CS	N	C, Q	N	QSDC/DSQC
[125]	2022	В	CS	N	C, Q	Y	QSDC/DSQC
[128]	2023	SP	CS	N	Q	N	QPKC
[130]	2024	SP	By QKD	N	C, Q	Y	QSDC

1.5 CLASSIFICATION OF THE PROTOCOLS FOR QUANTUM IDENTITY AUTHENTICATION

The classification of any concept depends on the selected criteria. In this context, the existing schemes for QIA are categorized based on two specific criteria: (i) the quantum resources utilized in the design of the schemes (as detailed in the third column of Table 1.1 and (ii) the computational or communication tasks inherently employed in their design (as described in the final column of Table 1.1). It is important to note that this classification is neither exhaustive nor exclusive. Alternative criteria, such as a technical feature highlighted in another column of Table 1.1, could be chosen for classification. The primary motivation for using these two criteria is to uncover the underlying symmetry among existing QIA protocols and to establish a foundation for developing new protocols.

1.5.1 CLASSIFICATION BASED ON THE QUANTUM RESOURCES USED

When classified by quantum resources, the existing QIA schemes can be divided into two main categories: (a) those utilizing entangled states (e.g., [38, 39, 40, 41, 42, 43, 44, 45]) and (b) those not relying on entangled states (e.g., [118, 100, 90, 87, 37, 132]).

1.5.1.1 ENTANGLED STATE BASED SCHEMES OF QIA

Bell states represent the simplest form of entangled states and are straightforward to generate and preserve. Consequently, numerous QIA schemes have been developed based on Bell states. Protocols utilizing solely Bell states are outlined in several studies, including [40, 59, 58, 63, 64, 45, 38, 70, 41, 76, 83, 101, 42]. These protocols vary significantly, with some employing Bell states for entanglement swapping (e.g., [85, 39]) and others leveraging Bell states to design authentication schemes analogous to the ping-pong protocol for QSDC [72]. Despite their versatility, the full potential of Bell states, particularly their non-local properties, remains underexplored. For instance, the inherent symmetry discussed in this review could inspire the development of device-independent or semi-device-independent QIA schemes. Additionally, QIA protocols exploiting violations of Bell inequalities could be proposed, though their implementation would likely be more challenging than existing schemes while offering distinct advantages. Some QIA schemes also rely on multipartite entangled states. For example,

three-qubit GHZ states are employed for authentication in studies such as [39, 71, 74, 85, 86]. Similarly, GHZ-like states have been used for QIA in [43, 110], while five-qubit cluster states are utilized in [44]. However, the creation and stabilization of such multipartite entangled states remain technically demanding. Furthermore, many entanglement-based QIA schemes necessitate quantum memory, a technology that is currently unavailable.

1.5.1.2 SCHEMES OF QIA WHICH DON'T USE ENTANGLEMENT

Several QIA schemes utilize separable states, specifically single-photon states. Examples include the protocols proposed in [118, 100, 90, 87, 37, 132], among others. These approaches hold an advantage over entangled-state-based schemes due to the relative simplicity of preparing single-qubit states. Furthermore, most entangled-state-based protocols require quantum memory for storing home qubits, a technology that remains unavailable, whereas single-qubit-based schemes generally do not depend on quantum memory. This characteristic makes single-qubitbased protocols more practical for implementation. Such schemes often employ BB84-style encoding, where travel qubits are prepared in the $Z = \{|0\rangle, |1\rangle\}$ basis or the $X = \{|+\rangle, |-\rangle\}$ basis. The selection of the basis is determined by a pre-shared authentication key and a predefined rule linking the key's bit values to the corresponding basis for travel qubit preparation. A notable example of this type is Zawadzki's QIA protocol [118]. However, González-Guillén et al. [119] recently demonstrated that Zawadzki's scheme is fundamentally insecure. They showed that the logarithmic security claimed for the protocol is compromised under a key space reduction attack, as explicitly described in their work. Many such schemes incorporate hash functions to secure the authentication process. While relying on hash functions moves away from strictly quantum-based security, current cryptographic confidence in specific hash functions remains high. In Chapter 2, we propose two novel QIA protocols based on single qubits. These protocols address vulnerabilities, including key space reduction attacks and other known strategies, thereby enhancing their robustness.

1.5.2 CLASSIFICATION OF THE PROTOCOLS BASED ON THE COMPUTATIONAL OR COMMUNICATION TASKS USED TO DESIGN THE SCHEMES

Here, we categorize existing protocols for QIA based on the computational or communication tasks required for their implementation. To begin, we will outline QIA schemes that rely on

specific quantum communication tasks.

1.5.2.1 PROTOCOLS BASED ON THE SCHEMES FOR QKD

Numerous authentication protocols are fundamentally rooted in QKD schemes. In principle, any QKD scheme can be adapted into a QIA scheme, provided a pre-shared secret key is available. However, slight modifications to the original QKD protocol may be necessary to achieve this adaptation. For instance, Sobota et al. [133] demonstrated how the BB84 QKD protocol could be modified to establish a QIA scheme. More recently, Liu et al. [111] proposed a QIA scheme by altering a counterfactual QKD protocol. In earlier research by Dušek et al., a hybrid classical-quantum authentication scheme was introduced, where the quantum component was derived from QKD. Specifically, this approach leveraged the fact that QKD schemes are inherently designed for key amplification. In this method, Alice and Bob begin with a "pre-shared sequence" for identity authentication, which is used only once to authenticate their identities and generate a secure key through QKD. In subsequent rounds of identity authentication, a portion of the key generated by QKD is employed. While this method primarily uses QKD to refresh the authentication sequence, it does not fully qualify as a QIA scheme. Nonetheless, this early work was significantly influenced by QKD. Today, the integration of QKD in authentication processes is widely observed.

1.5.2.2 PROTOCOLS BASED ON THE SCHEMES FOR QSDC AND DSQC

Secure quantum direct communication protocols are categorized into two types: QSDC and DSQC. Numerous QSDC and DSQC protocols have been proposed (see [134, 106, 51, 135, 54], among others), all enabling the direct transmission of information from a sender (Alice) to a receiver (Bob) with unconditional security. When Alice and Bob share a "pre-shared secret", Alice can transmit part or all of this secret using a QSDC or DSQC protocol. Bob, in turn, can decode the message and compare it with his own secret to authenticate Alice's identity. Consequently, any QSDC or DSQC protocol can, in principle, be adapted for QIA. An example of an early QSDC protocol is the ping-pong protocol, which Zhang et al. (in 2006) extended to develop a QIA scheme [41]. It is noteworthy that even "secure direct quantum communication" protocols unsuitable for long-distance communication due to noise can still serve as the foundation for QIA. In the case of CV-secure direct quantum communication, this adaptability

was highlighted in [136]. CV-QIA schemes, whether derived from CV-QSDC or CV-DSQC protocols, leverage existing infrastructure for their implementation, making them particularly advantageous as indicated in [136].

LM05, introduced by Lucamarini and Mancini in 2005 [88], is a single-photon-based protocol for QSDC, conceptually similar to the ping-pong protocol. Building upon LM05, Yuan et al. (2014) proposed another QIA scheme [87], describing it as a non-entangled ping-pong protocol. However, it is essentially a modified version of the LM05 protocol. Notably, neither Zhang et al., Yuan et al., nor subsequent authors have acknowledged the fundamental symmetry that enables the transformation of existing QSDC and DSQC protocols into QIA schemes.

The transformation of QSDC or DSQC protocols into schemes tailored for QIA often necessitates certain modifications that move the resulting protocol beyond the conventional definitions of QSDC or DSQC. Consequently, what we achieve are QSDC- or DSQC-inspired protocols for QIA. For instance, the structure of Zhang et al.'s scheme [40] resembles the original ping-pong protocol but differs in that the travel qubit sent by Bob to Alice is not subsequently returned by Alice. Specifically, in Zhang et al.'s scheme, a Bell state $\psi_{AB}^+ (= \frac{1}{\sqrt{2}} (|0\rangle_A |1\rangle_B + |1\rangle_A |0\rangle_B))$ is preshared between Alice and Bob, where the subscripts A and B denote the qubits held by Alice and Bob, respectively. In the original ping-pong protocol, Bob generates the Bell state and transmits one of its qubits (the travel qubit) to Alice, which may be considered an analogous step. In Zhang et al.'s scheme, however, Bob makes any single-qubit pure state $|\psi_1\rangle = \alpha |0\rangle + \beta |1\rangle$ and sends it to Alice. Alice then performs a CNOT operation, using her portion of the Bell state as the control qubit and $|\psi_1\rangle$ as the target qubit. Alice subsequently returns the qubit labeled as qubit 1 (establishing the analogy with the ping-pong protocol). Upon receiving qubit 1, Bob applies a CNOT operation, with his share of the Bell state (qubit B) serving as the control qubit and qubit 1 as the target qubit. Bob then measures qubit 1 in a basis where $|\psi_1\rangle=\alpha|0\rangle+\beta|1\rangle$ is a basis element. If the measurement yields $|\psi_1\rangle$, the authentication is deemed successful. This type of QSDC-inspired protocol garners additional attention for two specific reasons. Firstly, this work introduces novel QSDC/DSQC-based protocols. Secondly, several QSDC/DSQCbased protocols for QIA have recently been developed, many of which can be classified within the ping-pong protocol framework. For instance, Li et al. proposed a QIA protocol in 2004 [38] that shares similarities with Zhang et al.'s scheme, but with a key difference: instead of Bob preparing and sharing a single-qubit state $|\psi_1\rangle$, Alice prepares an auxiliary Bell state and executes a CNOT operation. In this operation, the first qubit of the auxiliary Bell state acts as

the control qubit, while Alice's qubit (qubit *A*) from the pre-shared Bell state serves as the target qubit. Alice then transmits the auxiliary Bell pair to Bob, who subsequently performs a CNOT operation, using the second qubit of the auxiliary pair as the control qubit and his qubit (qubit *B*) as the target. Authentication is deemed successful if Bob's Bell measurement on the auxiliary Bell state yields the same state initially prepared by Alice. Both protocols necessitate quantum memory; however, commercial quantum memory devices are not yet available, and the current laboratory-grade quantum memory technologies require significant advancement before they can be deployed in practical applications.

Moreover, Zhang et al. [41] introduced a one-way QIA protocol, which bears similarities to the protocol proposed by Zhang et al. [40]. This was followed by Li et al.'s protocol [137], which can be regarded as a modified version of their earlier work [38]. In this updated version, the auxiliary state is independently prepared by Alice and Bob in single-qubit states instead of Bell states. From the overview of these protocols, it is evident that they all belong to the "ping-pong" family of QIA protocols. This family also includes Yuan et al.'s single-qubit-based protocol [87].

1.5.2.3 PROTOCOLS BASED ON TELEPORTATION

Teleportation is recognized as a method for enabling secure communication, provided an ideal (noise-free) quantum channel is available, as noted by Lo and Chau [138]. This particular challenge, along with related concerns, will be explored in further detail in Section 1.5.2.7. Despite these challenges, including issues associated with entanglement concentration [139, 140] and purification, numerous researchers have proposed QIA schemes leveraging teleportation. Examples include the works of Tan and Jiang (2014), Ma et al. (2016), Zhou et al. (2005) [85, 141, 70], among others cited therein. Notably, a teleportation-based approach has also been suggested for CV-QIA by Ma et al. [141]. However, the effectiveness of these schemes is constrained by the susceptibility of shared entanglement to noise, which necessitates entanglement purification or concentration to restore the desired entangled state. This process requires interaction between Alice and Bob prior to authentication. It should be emphasized that this issue also affects a wide range of QIA protocols that rely on shared entanglement but do not explicitly involve teleportation, such as those discussed in [40] and similar approaches. The need for such interaction is a notable limitation of QIA protocols that rely directly on teleportation

or shared entanglement. Nevertheless, innovative techniques, like the approach presented by Barnum et al. [142], offer potential solutions to address this limitation. A brief discussion of these techniques can be found in Section 1.5.2.7.

1.5.2.4 PROTOCOLS BASED ON QUANTUM SECRET SHARING

Quantum secret sharing (QSS) protocols [143] have been adapted to develop schemes for QIA, allowing for the authentication of legitimate users either individually or collectively by a group of users or a trusted third party [144]. Furthermore, various QSS schemes incorporating identity authentication to enhance security have been introduced [145, 101, 146, 147]. These schemes employ a range of quantum resources and operations, such as Bell states, phase-shift operations, and GHZ states. Notably, Abulkasim et al. explored the simultaneous integration of QSS and QD concepts to develop protocols for mutual QIA [145], as also discussed in Banerjee et al. (2017) and Shukla et al. (2013) [148, 53]. In the multiparty version of the protocol by Abulkasim et al., Alice was designated as the boss, with Bob and Charlie acting as her agents. However, Gao et al. identified a security vulnerability in this scheme [149], demonstrating that collusion between agents (Bob and Charlie) compromised its security. In response to this issue, Abulkasim et al. introduced an improved QSS-based protocol in 2018, designed to withstand collusion attacks by agents [150].

The protocols reviewed and categorized in this section are primarily derived from those developed for various quantum communication applications, such as quantum teleportation, QKD, QSDC, and DSQC. Subsequently, it will be shown that similar derivations can also be made from protocols intended for quantum computing tasks.

PROTOCOLS BASED ON QUANTUM COMPUTATION TASKS

As discussed earlier, existing protocols for various quantum computing tasks can be adapted to develop schemes for QIA, and this approach has been employed since the inception of QIA. Notably, the foundational effort by Crépeau et al. [35] in designing QIA utilized OT. We begin by acknowledging this contribution and proceed to examine schemes that have been developed—or could potentially be developed—by leveraging protocols designed for other quantum computing tasks, such as "blind quantum computing" and "quantum private comparison".

1.5.2.5 PROTOCOLS UTILIZING OBLIVIOUS TRANSFER

As outlined in Section 1.3, the first QIA protocol, proposed by Crépeau and Salvail (in 1995) [35], was based on OT. This protocol aimed to verify the identities of legitimate participants by comparing their mutual knowledge of pre-shared common information. This pioneering work introduced a QIA scheme whose security relied on the fundamental principles of quantum mechanics, a foundation that has since been expanded upon by many subsequent efforts. Indeed, the security of all QIA protocols reviewed here stems from quantum mechanical properties. However, OT has been infrequently employed as a resource in designing QIA schemes.

1.5.2.6 PROTOCOLS BASED ON BLIND QUANTUM COMPUTING

Blind quantum computing (BQC), introduced by Childs in 2005 [151], allows a client with limited quantum resources to delegate computational tasks to a quantum server or user with greater quantum capabilities. Crucially, this delegation ensures the privacy of the client's input, output, and computational process, such that the more powerful quantum server remains unaware of these details. Various BQC schemes incorporating identity authentication have been proposed, including works by Li et al. (2018), Quan et al. (2021), and Shan et al. (2021) [152, 153, 154]. However, the potential of BQC in designing QIA schemes remains underutilized. A closely related concept, blind quantum signatures, was explored in Li et al. (in 20127) [155]) using BQC principles. By mapping this approach to QIA, there is significant potential to develop QIA schemes by leveraging both existing and novel BQC frameworks. This represents a promising area for further investigation.

1.5.2.7 PROTOCOLS BASED ON QUANTUM ERROR DETECTION OR CORREC-TION CODE

Authentication can be achieved by employing a shared entangled state and a private quantum key, which Alice teleports to Bob using the shared entanglement to verify her identity. However, the entangled state may degrade due to noise, necessitating a purity-testing protocol to confirm whether the shared entangled state remains in the intended configuration. Unlike entanglement concentration and purification schemes, such protocols focus on verification rather than correction. Barnum et al. in 2002 observed that purity testing protocols are typically interactive [142], a feature undesirable in QIA and quantum message authentication when one-way authen-

tication is preferred. To address this, Barnum et al. demonstrated that purity-testing could be implemented using a family of quantum error-correcting codes (QECCs) characterized by their ability to detect any Pauli error in most codes within the family. They further established that secure non-interactive quantum authentication schemes could be derived from purity-testing protocols constructed from QECCs. This marked a significant milestone in using QECCs for quantum authentication. Building on this foundation, Qu et al. later introduced a QIA protocol leveraging a three-photon "error-avoidance code" [115, 156].

1.5.2.8 PROTOCOLS BASED ON QUANTUM PRIVATE COMPARISON

In 2017, Hong et al. introduced a highly efficient single-qubit protocol for QIA, incorporating decoy qubits to ensure security against eavesdropping [100]. The efficiency of the protocol stemmed from its ability to verify two bits of authentication information using just a single qubit. Subsequently, Zawadzki conducted a cryptanalysis of this protocol and proposed enhancements [118]. Zawadzki's primary critique was that each execution of Hong et al.'s protocol resulted in information leakage, allowing an eavesdropper to accumulate data over multiple protocol runs. To address this issue, Zawadzki presented an improved protocol that incorporated a hash function for added security. However, recent research by González-Guillén et al. (in 2021) [119] revealed that Zawadzki's protocol is vulnerable to key space reduction attacks. While a detailed examination of this vulnerability is beyond the scope of this discussion, it is worth noting that in Zawadzki's protocol, as well as many other QIA protocols, the core objective is to perform quantum private comparison. This involves computing a function f(A, B), where f(A,B) = 0 if $A \neq B$ and f(A,B) = 1 if A = B, using quantum resources without revealing the actual values of A and B to the party performing the computation. Naturally, some logical information can be inferred from the computed value of f(A,B). This issue is a well-established challenge in secure multiparty computation, as discussed in [157, 134, 158]. The task is also strongly connected to the socialist millionaire problem, as noted by Shukla et al. [53]. To better understand this, we examine Zawadzki's protocol in greater detail. In Zawadzki's protocol, as well as in many other similar protocols, Alice and Bob share a secret authentication key k. Alice begins by generating a random number r_A and computes a session secret $s_A = H(k, r_A)$ using the shared secret key k and a hash function H. Alice then sends r_A to Bob, who may receive a different value r_B . Bob uses r_B to compute his own session secret $s_B = H(k, r_B)$. The task subsequently reduces to leveraging quantum resources to determine whether $s_A = s_B$, effectively performing a quantum private comparison by evaluating $f(s_A, s_B)$.. If s_A and s_B are equal, successful authentication is achieved. Recognizing the connection between quantum private comparison and QIA allows us to infer that existing protocols for quantum private comparison and the socialist millionaire problem can be transformed into QIA protocols. Protocols proposed by some of the recent authors and detailed in Shukla et al. (2013), Shukla et al. (2017), Banerjee et al. (2017), Saxena et al. (2020), and Thapliyal et al. (2018) can be straightforwardly adapted into schemes for QIA [53, 106, 148, 157, 107]. Notably, several of these adapted QIA schemes remain functional within the semi-quantum framework [106, 107], wherein not all participants require access to quantum resources. Additionally, it is worth highlighting that the ability to perform QD, enabling simultaneous two-way communication between Alice and Bob, or quantum conferencing [159], inherently enables QSDC or DSQC, which can be leveraged for QIA (as elaborated in Section 1.5.2.2). Consequently, without converting QD or quantum conference protocols into quantum private comparison schemes, one can adopt a more direct approach by designing novel QSDC/DSQC-based schemes for QIA.

The classification of schemes for QIA discussed in this section is concisely depicted in Fig. (1.2). This figure demonstrates the diverse methodologies and resources available for implementing QIA. The selection of a specific scheme is influenced by the task's requirements and the resources at hand. For example, existing schemes can be categorized based on factors such as the necessity of classical communication channels, quantum memory, the involvement of a third party, the type of pre-shared key (classical or quantum), and whether one-way or two-way authentication is desired.

It is important to highlight that Table 1.1 serves as a complement to Figure 1.2, detailing the placement of representative schemes within the classification framework depicted in the figure. Each row of Table 1.1 provides comprehensive information about a specific scheme, thereby encapsulating the discussion of this section and substantiating the proposed classification.

1.6 QUANTUM KEY DISTRIBUTION FOLLOWING QUANTUM IDEN-TITY AUTHENTICATION

Cryptography has been a critical and invaluable tool for humanity since the dawn of civilization. Historically, cryptographic techniques have been employed to conceal confidential information,

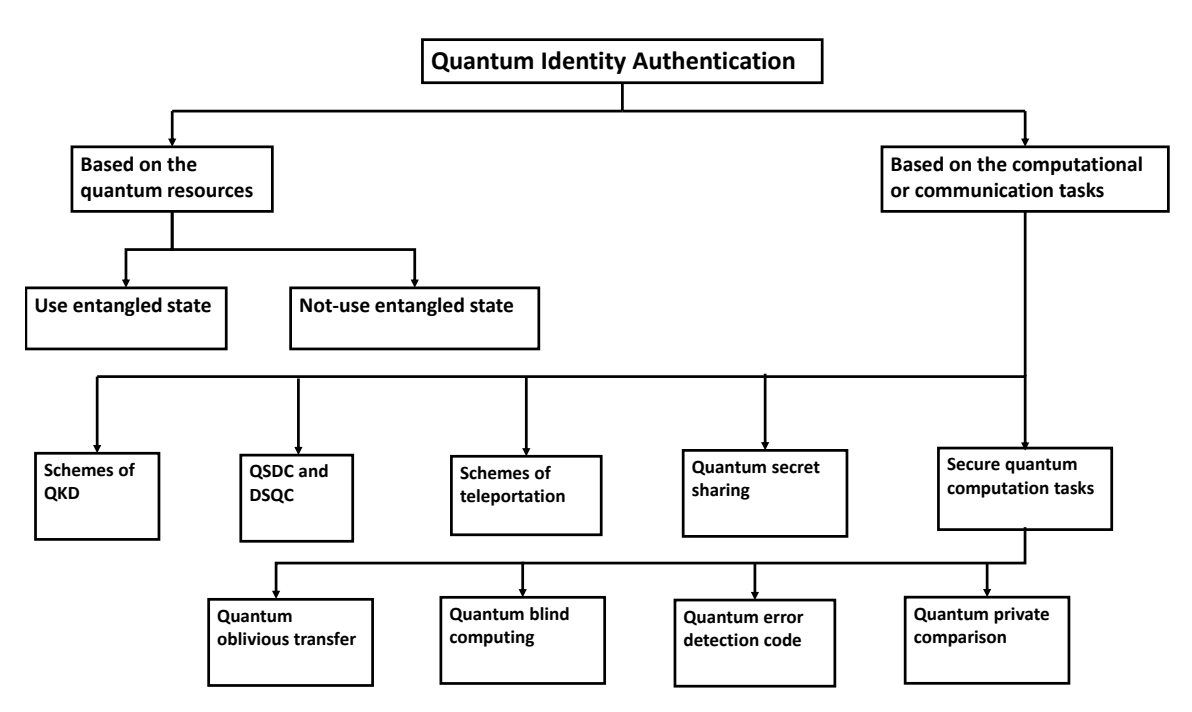


Figure 1.2: Categorization of QIA schemes.

though cryptanalysts have frequently developed more advanced methods to decrypt such messages. A significant transformation in cryptography occurred in the 1970s with the advent of public-key cryptography, exemplified by schemes such as RSA [21] and the DH protocol [22]. The security of these and similar classical key distribution methods is fundamentally based on the computational difficulty of specific mathematical problems integral to their design. For instance, the RSA scheme derives its security from the complexity of factoring large semi-prime numbers, while the DH protocol relies on the computational challenge of solving the discrete logarithm problem [23]. In a groundbreaking study published in 1994, Peter W. Shor [24] demonstrated that both the factorization of large semi-prime numbers and the discrete logarithm problem could be efficiently addressed using quantum computers, specifically in polynomial time. This revelation highlights the potential vulnerabilities in many classical key distribution methods should scalable quantum computers become a reality. Consequently, cryptography is significantly challenged by the advent of quantum computers, or more precisely, by quantum algorithms that outperform classical algorithms in solving various computational problems. Notably, a resolution to this challenge has long existed in the form of QKD. Unlike classical methods, QKD leverages quantum resources for key distribution, ensuring security that relies on the fundamental principles of quantum mechanics rather than the computational intractability of certain problems. The earliest QKD protocol was introduced a decade prior to Shor's groundbreaking work, which challenged the security of classical cryptography. Specifically, Bennett and Brassard [15] developed the first QKD scheme, leveraging fundamental physical principles such as the no-cloning theorem [25], the "collapse on measurement", and Heisenberg's uncertainty principle. These principles underpin the security of the protocol, which is based on single qubits and can be implemented using polarization-encoded single photons or other forms of photonic qubits. Notably, under ideal conditions, any eavesdropping attempt in a QKD protocol leaves a detectable trace. However, in practical scenarios, device imperfections may enable undetected eavesdropping.

Following the introduction of the BB84 protocol, numerous QKD protocols were proposed, including those by [16, 32, 160, 134], along with protocols addressing related cryptographic applications (e.g., [51, 53, 161, 148, 106, 107, 62, 134, 162]). For comprehensive reviews, refer to Refs. [163, 164]. These protocols present various benefits and limitations. While most are theoretically unconditionally secure, practical implementations often encounter imperfections in devices, which introduce vulnerabilities exploitable via quantum hacking techniques ¹. For instance, the BB84 protocol, along with similar protocols like B92 [16], theoretically necessitates the use of a single-photon source, as Alice needs to transmit single-photon states to Bob. Significant experimental progress has been made in developing reliable single-photon sources (refer to [167, 168]), but commercially available systems typically rely on weak coherent pulses (WCPs), produced by attenuating laser outputs [169], as approximate single-photon sources. The quantum state of such WCPs is represented as follows:

$$|\alpha\rangle = |\sqrt{\mu} \exp(i\theta)\rangle = \sum_{n=0}^{\infty} \left(\frac{e^{-\mu}\mu^n}{n!}\right)^{\frac{1}{2}} \exp(in\theta)|n\rangle,$$
 (1.1)

Alice prepares a quantum state characterized by a superposition of Fock states, where $|n\rangle$ represents an n-photon Fock state, and the mean photon number is $\mu = |\alpha|^2 \ll 1$. The photon number follows a Poissonian distribution, given by $p(n,\mu) = \frac{e^{-\mu}\mu^n}{n!}$. Consequently, the probability of generating a single-photon state is $p(1,\mu)$, while the probability of emitting multi-photon pulses is $1 - p(0,\mu) - p(1,\mu)$. The presence of multi-photon states introduces a vulnerability, as an adversary, Eve, could exploit this to execute a photon-number-splitting (PNS) attack, as discussed by Huttner et al. [170]. Furthermore, in long-distance quantum communication, channel

¹Quantum identity authentication, as discussed by Curty and Santos, Dutta and Pathak [63, 165, 166], is a fundamental prerequisite for ensuring secure communication prior to the implementation of a QKD protocol.

loss presents a critical security risk. An eavesdropper with advanced technological capabilities may replace the lossy channel with an ideal, lossless one, facilitating an undetectable interception attack, as demonstrated by Brassard et al. [171]. To mitigate this vulnerability, Scarani et al. [172] introduced the SARG04 QKD protocol, which enhances security against PNS attacks. In Chapter 3, we propose two novel QKD protocols designed to be resilient against PNS attacks, akin to SARG04, while also offering improved resistance to a broader class of adversarial strategies. These protocols provide distinct advantages over SARG04 and similar QKD schemes in terms of security and implementation.

In every QKD protocol, an inherent process of information partitioning occurs. For instance, in the BB84 [15] and B92 [16] protocols, the transmitted information is divided into a classical component (detailing the basis used for qubit preparation) and a quantum component (the transmitted qubits themselves). A similar partitioning mechanism is observed in the SARG04 protocol [172]. However, in certain other protocols, such as the GV protocol [160], the information is distributed across two quantum components. The security of these protocols fundamentally relies on the impossibility of an eavesdropper (Eve) simultaneously accessing multiple information fragments. This observation raises a fundamental question: can the efficiency and/or secret-key rate bounds of a protocol be modified by altering the protocol in a manner that reduces the information present in the classical component? To explore this, we consider the SARG04 protocol as a reference framework. In Chapter 3, we will present two novel QKD protocols that share similarities with the SARG04 protocol but incorporate a reduced amount of classical information compared to SARG04. The SARG04 protocol was originally developed to significantly mitigate the probability of a PNS attack, as discussed by Huttner et al. [170]. However, it exhibited lower efficiency relative to various other single-photon-based QKD schemes. This limitation motivated our investigation into an alternative approach, wherein PNS attacks are countered by employing a greater reliance on quantum resources rather than classical ones, thereby circumventing the current technological constraints such as channel loss and channel noise. Accordingly, Chapter 3 will introduce two new QKD protocols that enhance efficiency beyond SARG04 while maintaining resilience against PNS attacks and a range of other established attack strategies.

¹The efficiency assessment follows Cabello's framework [173], wherein the transmission cost of qubits is equated to that of classical bits. This model assumes a quantum channel with minimal noise, which may not always align with practical scenarios, particularly in long-distance communication with current technological constraints.

1.7 INTRODUCTORY DISCUSSION ON QUANTUM KEY AGREEMENT

Key agreement (KA) constitutes a critical area of research in cryptography and plays a fundamental role in ensuring perfect forward secrecy. A KA protocol enables two or more parties to collaboratively establish a key—essentially generating a shared random number—such that all legitimate participants contribute to the outcome. Moreover, neither a subset of legitimate parties nor an eavesdropper should be capable of imposing a predetermined key. This represents a relatively weaker characterization of KA. A more rigorous definition, frequently adopted in the literature on QKA, requires that all legitimate parties exert equal influence over the final key. The concept of KA was first introduced by Diffie and Hellman in 1976 through a classical two-party protocol [22]. Subsequent advancements extended the Diffie-Hellman framework to multiparty scenarios, enhancing the efficiency of KA protocols [174, 175, 176, 177]. Adhering to the stronger definition of KA necessitates that each legitimate participant contributes equally to the establishment of a common secret key. This characteristic, which ensures that no individual or subset of participants can disproportionately influence the final key, is commonly referred to as "fairness" [178, 179].

The security of classical cryptographic techniques, including KA, primarily relies on the computational complexity of certain mathematical problems. However, the advent of quantum computing poses a significant threat to this security paradigm, as many of these hard problems, which form the foundation of classical cryptographic schemes, could potentially be solved in polynomial time with scalable quantum computers. To address this challenge, various principles of quantum mechanics—such as collapse on measurement, the no-cloning theorem, nonlocality, Heisenberg's uncertainty principle, and contextuality—have been leveraged. It has been demonstrated that numerous cryptographic tasks can achieve unconditional security through the appropriate utilization of quantum resources. One such task is QKA, as introduced by Hahn et al. [180]. In Chapter 4, we propose two novel QKA protocols and present their security proofs. Before delving into QKA and its multipartite extension, it is beneficial to briefly discuss other aspects of quantum cryptography. This discussion will highlight the distinctive nature of QKA while providing a broader perspective on various quantum cryptographic techniques.

In 1984, Bennett and Brassard introduced the renowned BB84 protocol [15], which effectively facilitates key distribution between two distant parties under ideal conditions by leveraging quantum resources. The security of BB84 is fundamentally rooted in the principles of quantum

mechanics. Following this breakthrough, QKD emerged as a rapidly advancing field that garnered significant attention in cryptographic research, progressing swiftly in both theoretical and experimental domains[32, 181, 16, 172, 23, 163, 162, 182, 183, 184]. Moreover, several other essential aspects of quantum cryptography have been explored, including QSDC [72, 185], QSS [186, 187, 188, 189], QIA [37, 165, 166], quantum private comparison [190, 191, 192, 193], and quantum digital signatures [194, 195, 196]. In addition to these advancements, QKA has emerged as a crucial cryptographic primitive, enabling two or more participants to collaboratively establish a shared key by contributing their individual key components through quantum resources. QKA's significance lies in its diverse applications, such as electronic auctions, secure multiparty computation, and access control [176], as well as its role in ensuring forward secrecy. Given its applicability in various domains, QKA has recently been recognized as an integral area within quantum cryptography.

To the best of our understanding, the first QKA protocol was introduced by Zhou et al. in 2004, where two participants utilized quantum teleportation to establish a common key [197]. However, in 2009, Tsai and Hwang identified a critical flaw in Zhou et al.'s protocol, demonstrating that one participant could unilaterally determine the shared key and subsequently distribute it to the other, thereby compromising fairness. Moreover, the security of Zhou et al.'s scheme was later invalidated by Chong et al. in 2011 [198]. Subsequently, Shi and Zhou proposed the first multiparty QKA (MQKA) protocol in 2013, leveraging entanglement swapping [199]. However, this scheme was also proven insecure [200]. In the interim, Chong et al. developed a QKA protocol based on the BB84 framework, incorporating delay measurement techniques along with an authenticated classical channel [201]. Over time, several two-party QKA protocols were extended to multiparty settings [200, 202, 203, 204]. These MQKA protocols are generally classified into three categories [205]: tree-type [203], circle-type ([206], and references therein), and complete-graph-type [200]. Among them, the circle-type structure is considered the most practical for implementation due to its greater efficiency.

A robust QKA protocol must fulfill three essential criteria: *Correctness*, ensuring that all participants obtain the agreed-upon key accurately upon the protocol's successful execution; *Security*, guaranteeing that no unauthorized entity can intercept or extract information about the final agreement key without detection; and *Fairness*, requiring that all legitimate participants contribute equally to the key generation, preventing any subset of them from independently determining the final key. Based on these principles, we introduce, for the first time, a QKA

protocol incorporating a central controller, Charlie, to facilitate key agreement between two legitimate parties without relying on quantum memory. Our proposed scheme in Chapter 4 is specifically designed to meet the demands of quantum cryptographic applications. Such scenarios frequently arise in quantum cryptography, prompting the development of various controlled quantum cryptographic schemes in recent years. In particular, extensive research has been conducted on controlled-QKD [207, 208], controlled-quantum dialogue [209, 210], and controlled-secure direct quantum communication [211, 212, 213, 166]. However, to the best of our knowledge, no existing controlled quantum key agreement (CQKA) scheme has been proposed without relying on quantum memory [214]. This motivates us to introduce a CQKA protocol that leverages Bell states and single-qubit states as quantum resources. Our scheme employs a one-way quantum channel to mitigate unnecessary noise, distinguishing it from several QKA protocols that rely on two-way quantum channels [202, 204, 214], which are more susceptible to channel-induced noise. We rigorously analyze the security of the proposed protocol and demonstrate its feasibility using current quantum technologies. Furthermore, comparative analysis reveals that the proposed CQKA scheme exhibits superior efficiency over many existing approaches in Chapter 4. The inclusion of a controller further enhances its applicability in specific scenarios.

1.8 DISCUSSION ON QUANTUM GAME AND NASH EQUILIBRIUM

Game theory analyzes and models the behavior of individuals in scenarios that require strategic reasoning and interactive decision-making. It plays a fundamental role in optimizing decision-making processes and evaluating potential outcomes across various domains, including business and daily life. Situations demanding strategic analysis are widespread in disciplines such as economics [215], political science [216], biology [217, 218], and military strategy [219, 220]. In such contexts, participants select from a set of possible actions, termed strategies, with their preferences structured within a payoff matrix. Game theory focuses on modeling these interactions and determining optimal strategic choices. Among its fundamental principles, the Nash equilibrium holds particular significance, as it describes a state where no participant can enhance their payoff by unilaterally changing their strategy, given the decisions of others [221, 222].

Quantum mechanics remains one of the most profound and impactful theories in scientific his-

tory. Although its emergence was met with controversy, its theoretical predictions have been consistently validated through precise experimental verification [223]. Quantum game theory facilitates the study of interactive decision-making processes where players employ quantum resources. This framework serves a dual function: acting as a quantum communication protocol while also offering a more effective means of randomizing strategic choices compared to conventional game-theoretic approaches [224]. The formalization of quantum game theory dates back to 1999, with pioneering contributions from David Meyer [225] as well as Jens Eisert, Martin Wilkens, and Maciej Lewenstein [226]. Their work introduced games leveraging quantum information, illustrating instances in which quantum strategies outperformed their classical counterparts. Since then, numerous quantum game variants, primarily based on the foundational studies of Meyer and Eisert et al., have been extensively analyzed. Comprehensive discussions on these advancements can be found in review articles such as in [227]. Experimentally, the quantum version of the Prisoner's Dilemma has been realized using an NMR quantum computer [228]. Vaidman introduced in 1999 a straightforward game where players can secure consistent victories by initially sharing a GHZ state, in contrast to classical counterparts, whose success remains probabilistic [229]. Quantum strategies have been leveraged to incorporate fairness mechanisms in remote gambling scenarios [230] and to develop quantum auction algorithms that offer significant security benefits [231]. Flitney and Abbott investigated quantum variations of Parrondo's games [232]. These studies not only contribute to the design of secure networks and the discovery of novel quantum algorithms but also provide a unique perspective on defining games and protocols [162, 233, 234]. Moreover, concepts such as eavesdropping [32, 235] and optimal cloning [236] can be interpreted as strategic games among participants. Consequently, the intersection of game theory and quantum mechanics has been extensively explored.

There exist two principal frameworks that delineate this interconnection. The first framework involves utilizing quantum resources to execute a conventional game that can also be played in the absence of such resources; however, the incorporation of quantum mechanics introduces certain advantages. Conversely, the second framework employs game-theoretic principles to model and analyze quantum mechanical scenarios. Hereafter, these approaches will be referred to as the "quantized game" and "gaming the quantum", respectively. A quantized game can be formally characterized as a unitary transformation that maps the Cartesian product of quantum superpositions of players' pure strategies onto the Hilbert space governing the game, thereby

preserving the fundamental structure of the classical game under specific constraints. In contrast, the concept of gaming the quantum, as described by Khan and Phoenix [237], pertains to the application of game-theoretic methodologies to quantum mechanics to derive strategic solutions. Our work in Chapter 5 follows the "gaming the quantum" approach by employing non-cooperative game theory within a quantum communication protocol to illustrate how Nash equilibrium can serve as an effective solution framework.

By leveraging the insights discussed earlier, Nash equilibrium points in game theory can be utilized to define secure boundaries for various quantum information parameters. This approach involves reformulating any quantum scheme into a game-theoretic framework and analyzing its Nash equilibrium points. These equilibrium points represent stable configurations or offer rational probability distributions that guide stakeholders' decision-making within a mixed-strategy game. The probabilities derived from these equilibrium points contribute to maintaining a stable strategic environment for all participants. This stability allows for evaluating key cryptographic parameters, such as determining the threshold for the QBER. In realistic scenarios where participants make independent decisions, achieving such stability is less likely, potentially leading to increased uncertainty. Therefore, identifying the minimum QBER value within a stable game-theoretic setting establishes a secure threshold, ensuring the practical feasibility of protocols for secure quantum communication. Chapter 5 focuses on analyzing the secure threshold bound for the QBER within the framework of the DL04 protocol proposed by Deng and Long [238]. It is essential to contextualize this discussion within the realm of "direct secure quantum communication" protocols, as the DL04 scheme is a part of this category. These protocols can be classified into two main types [239]. The first category includes DSQC protocols [240, 241, 165, 166], in which the recipient can only retrieve the encoded message after receiving at least one bit of supplementary classical information per qubit from the sender. The second category comprises QSDC protocols [242, 243, 244, 245, 238, 246, 247, 248, 249], which function without necessitating any classical information exchange. A notable QSDC scheme was proposed by Beige et al. [242], where the message remains inaccessible until additional classical information is transmitted for each qubit. Boström and Felbinger introduced a ping-pong QSDC scheme [244], which ensures security for key distribution and provides quasi-secure direct secret communication under ideal quantum channel conditions. In 2004, Deng and Long proposed the DL04 QSDC protocol [238], which operates without relying on entangled states. A notable discovery was the capability to achieve secure information transmission via the two-photon component, consistent with findings in two-way QKD [250, 88, 251]. This characteristic is particularly relevant to the specific conditions outlined in the DL04 QSDC protocol [238]. In Chapter 5, the primary objective of our work is to determine the secure threshold bound of the QBER within the DL04 protocol. This protocol is chosen due to its extensive adoption in experimental implementations and its practicality for secure deployment [252, 253, 254, 255, 256, 257, 258].

1.9 OVERVIEW OF THIS CHAPTER AND OUTLINE OF THE REMAIN-ING THESIS

This chapter provides a concise overview of the historical development of quantum mechanics, highlighting key inventions in the field. It also presents the fundamental postulates and mathematical formulations relevant to this thesis. A significant portion of the chapter is dedicated to an in-depth discussion of QIA, which is essential for ensuring the unconditional security of quantum protocol implementations by verifying the identities of legitimate users. The discussion on QIA follows a chronological approach, categorizing various schemes based on the quantum resources utilized and the computational or communication tasks inherent in their design. A critical analysis of earlier protocols is conducted, identifying their limitations in terms of security and resource utilization. Additionally, potential criticisms from other researchers are addressed. The initial and core content of this chapter has been published in [165]. Following the discussion on QIA, various quantum protocols, including QKD and QKA, are explored. The motivation for proposing novel quantum communication schemes is also examined. The chapter concludes with an exploration of quantum games, specifically the concept of "gaming the quantum", and introduces the rationale behind establishing a security bound on the QBER using Nash equilibrium principles.

This thesis is structured into six chapters. The current chapter provides fundamental concepts of quantum mechanics along with a systematic review of QIA schemes. Additionally, it outlines the motivation for the research presented in the subsequent chapters. Chapter 2 introduces novel QIA schemes that utilize single photons and Bell states as quantum resources, accompanied by a comprehensive security analysis. The design of these new protocols is informed by the systematic review presented in this chapter. Specifically, two QIA protocols are proposed, inspired by controlled secure direct quantum communication. In the first approach, Alice and

Bob authenticate each other's identities with the assistance of a third party, Charlie, using Bell states. The second set of schemes is designed for a two-party authentication scenario that relies solely on single-photon states. A rigorous security analysis is conducted to demonstrate the resilience of the proposed protocols against various attacks, including impersonation, interceptresend, and fraudulent impersonation attacks. Furthermore, a comparative analysis highlights the advantages of the proposed protocols over existing QIA schemes, emphasizing their security and efficiency. The works in Chapter 2 are published in Refs. [165, 166, 234]. In Chapter 3, we introduce two new QKD protocols that aim to be more efficient than SARG04 while maintaining resilience against PNS attacks and a variety of other well-known attacks. These protocols are compatible with commercially available single-photon sources, making them practical for implementation. We demonstrate that the proposed schemes are secure against several types of attacks, including the intercept-resend attack and certain collective attacks. We derive key rate bounds and show that specific classical pre-processing techniques can increase the tolerable error threshold. Our analysis indicates a trade-off between the quantum resources used and the information that could potentially be accessed by an eavesdropper. By employing slightly more quantum resources, the new protocols achieve higher efficiency compared to similar protocols, such as SARG04. In particular, our schemes outperform SARG04 in efficiency, although at the cost of increased quantum resource usage. Additionally, the proposed protocols exhibit greater critical distances under PNS attacks than both the BB84 and SARG04 protocols in comparable scenarios. The findings presented in this chapter have been reported in Ref. [162]. In Chapter 4, we present, for the first time, a QKA protocol that involves a controller (Charlie) to facilitate key agreement between two legitimate parties without relying on quantum memory. This design meets the growing need for practical quantum cryptographic solutions, as quantum memory is not yet available commercially. We introduce both a controlled quantum key agreement protocol and a standard key agreement protocol, providing a thorough security analysis. Our security proof demonstrates the protocols' resilience against impersonation and collective attacks, confirming their adherence to essential properties such as fairness and correctness. Additionally, we conduct a detailed comparison of our protocols with several existing QKA schemes, including the controlled QKA protocol of Tang et al [214]. Our proposed scheme stands out by not requiring quantum memory, unlike many existing protocols. Furthermore, our controlled QKA protocol uses simpler quantum resources, such as Bell states and single-photon states, instead of the more complex GHZ states employed in Tang et al.'s protocol. The findings presented in this chapter have been published in Ref. [233]. The analysis in Chapter 5 considers the sender, receiver, and eavesdropper (Eve) as quantum players, capable of executing quantum operations. Notably, Eve is assumed to possess the ability to perform various quantum attacks, such as Wójcik's original attack, its symmetrized variant, and Pavičić's attack, as well as a classical intercept-and-resend strategy. A game-theoretic evaluation of the DL04 protocol's security under these conditions is conducted by examining multiple game scenarios. The findings indicate the absence of a Pareto optimal Nash equilibrium in these cases. Therefore, mixed strategy Nash equilibrium points are identified and employed to derive upper and lower bounds for QBER. Additionally, the analysis highlights the susceptibility of the DL04 protocol to Pavičić's attack in the message transmission mode. It is also observed that the quantum attacks by Eve are more effective than the classical attacks, as they result in lower QBER values and a decreased probability of detecting Eve's intrusion. The results reported in this chapter are published in Ref. [259]. This Chapter 6 summarizes the findings of the entire thesis will an emphasis on the newly proposed quantum protocols, highlighting their advantages, and the thesis as a whole—ends with a discussion of potential future work suggested by these findings.

CHAPTER 2

QUANTUM IDENTITY AUTHENTICATION SCHEMES WITH DIFFERENT QUANTUM RESOURCES

2.1 INTRODUCTION

With the proliferation of online banking, e-commerce systems, and IoT devices, users have become familiar with identity verification mechanisms. The frequent utilization of these technologies highlights the critical role of authentication frameworks, which serve as structured approaches to confirming the legitimacy of users or connected devices. These authentication methods are fundamental to various cryptographic operations, ensuring secure communication and computational integrity. Quantum cryptography has fundamentally transformed security by introducing unconditional security, an aspect unattainable in classical systems. The groundbreaking BB84 protocol was the first unconditionally secure QKD scheme [15]. Unlike classical cryptographic methods that depend on computational complexity, BB84 derives its security from quantum mechanical principles. Various other QKD protocols ([32, 16, 260, 261] and additional works [182, 262, 263, 264, 265]) facilitate secure key distribution between a sender (Alice) and a receiver (Bob). However, to prevent impersonation by an adversary (Eve), Alice and Bob must first authenticate each other before initiating any QKD protocol. Identity authentication is thus essential for QKD and broader quantum cryptographic applications. Initially, classical authentication schemes, such as the Wegman–Carter scheme [33], were suggested for QKD authentication, including in the original BB84 protocol. However, these schemes lack unconditional security. Current QKD implementations, both commercial and experimental, still rely on classical or post-quantum authentication schemes, meaning QKD is not yet fully quantum or unconditionally secure. To address this, researchers have proposed various QIA protocols [35, 38, 39, 41, 42, 43, 44, 45, 165, 166, 266, 123] leveraging quantum resources for enhanced security. Some recent efforts focus on device-independent QIA [267] and QIA using homomorphic encryption with qubit rotation [128].

The first QIA scheme, introduced by Crépeau et al. [35] in 1995, OT as its cryptographic foundation. However, Lo and Chau [55] later proved that quantum OT lacks unconditional security in two-party settings, rendering Crépeau et al.'s scheme similarly insecure. Notably, OT is not the only cryptographic primitive applicable to QIA design. Subsequent QIA protocols [38, 39, 41, 42, 43, 44, 45, 36, 37, 165] leveraged diverse cryptographic frameworks. Some were adapted from secure direct quantum communication, which enables message transmission via quantum resources without key generation [243, 88, 23]. For a detailed exploration of QIA schemes and their cryptographic underpinnings, refer to Chapter 1. Before summarizing existing QIA schemes derived from modified secure direct communication methods, it is essential to distinguish between two secure quantum direct communication types: QSDC and DSQC. Various QSDC and DSQC protocols exist [243, 134, 106, 51, 135, 245, 259, 268], with early versions often relying on entangled states [243, 245, 244]. For example, Zhang et al. [41] adapted the entangled-state ping-pong protocol [244] for QSDC to develop a QIA scheme, while Yuan et al. [87] introduced a QIA protocol based on the LM05 protocol [88], a single-photon counterpart of the ping-pong protocol. Other researchers have modified DSQC and QSDC protocols to construct QIA schemes [38, 40, 137]. Additionally, controlled DSQC (CDSQC) schemes have been proposed [106, 269], where Alice, under Charlie's supervision, securely communicates with Bob using quantum resources. The adaptation of CDSQC for QIA remains underexplored. Given the importance of identity authentication, we propose a new QIA protocol incorporating simultaneous authentication of legitimate entities, inspired by CDSQC principles. The following sections introduce two single photon-based and two Bell state-based QIA protocol leveraging CDSQC concepts and analyze its robustness against common attacks. The remainder of this chapter is organized as follows: Section 2.2 presents the proposed QIA protocols utilizing single-qubit states and evaluates their security against various attacks. Section 2.3 introduces a new controlled QIA scheme based on Bell states and permutation operations, providing a comprehensive security analysis. This section also includes a comparison of the proposed protocol with recent relevant QIA schemes. In Section 2.4, another controlled QIA scheme is proposed, employing Bell states and CNOT operations. Its resilience against multiple attacks is demonstrated, along with a comparison to existing protocols within the same category. Finally, Section 2.5 concludes the chapter with a discussion of key insights.

2.2 NEW PROTOCOLS FOR QIA BASED ON QSDC

In Chapter 1, we previously noted that secure direct quantum communication protocols can, in principle, serve as a foundation for constructing QIA schemes. Several QIA protocols have already been developed based on QSDC and DSQC. However, recognizing the inherent symmetry among these protocols enables the formulation of novel schemes. As an illustration, we introduce four new QIA protocols, they derived from QSDC principles. We begin with the first protocol.

2.2.1 **PROTOCOL 2.1**

This QIA protocol, built upon QSDC, exhibits both distinct characteristics and structural similarities to the frameworks proposed in [44, 87]. Hereafter, this QSDC-inspired approach is designated as Protocol 2.1, with its procedural steps indexed as Step 1.j (more generally, Step i.j, where $i, j \in \{1, 2, \dots\}$, denotes the j^{th} step of the i^{th} proposed protocol). The protocol assumes that Alice and Bob share a pre-shared authentication key $K = \{k_1, k_2, k_3, \dots, k_{2n}\}$. Furthermore, the execution of the protocol relies on non-entangled quantum states as the fundamental resource. The procedural steps are outlined as follows.

• Encoding mode

Table 2.1: The preparation method for the decoy sequence (Protocol 2.1).

$(2i)^{th}$ bit value: k_{2i}	0	1
i^{th} qubit of decoy sequence: K_{d_i}	$ 0\rangle$ or $ 1\rangle$	$ +\rangle$ or $ -\rangle$

- **Step 1.1:** Alice constructs a structured sequence of n-qubit decoy states denoted as K_d , which is determined by the bit values of a pre-shared key K. If $k_{2i} = 0$, the i^{th} qubit of K_d is prepared in either $|0\rangle$ or $|1\rangle$. Otherwise, it is initialized in $|+\rangle$ or $|-\rangle$, with Alice being the sole entity aware of the precise quantum states assigned to each qubit in K_d .
- **Step 1.2:** Alice then generates an additional qubit sequence, K_a , designated for authentication purposes. The i^{th} qubit in K_a is assigned the state $|0\rangle$ if $k_{2i-1} \oplus k_{2i} = 0$, otherwise, it is prepared in the state $|-\rangle$. To form an extended sequence K_A , Alice interleaves the authentication qubits from K_a into K_d based on the following rule: if $k_{2i-1} \oplus k_{2i} = 0$, the

 i^{th} qubit of K_a is placed immediately after the corresponding i^{th} qubit in K_d ; otherwise, it is inserted before it. Finally, Alice transmits the augmented quantum sequence K_A to Bob.

Table 2.2: The preparation method of the authentication sequence (Protocol 2.1).

Additional modulo 2: $k_{2i-1} \oplus k_{2i}$	0	1
i^{th} qubit of authentication sequence: K_{a_i}	$ 0\rangle$	$ -\rangle$

Decoding mode

Table 2.3: Bob employs a predetermined measurement basis to extract results from the authentication sequence (Protocol 2.1).

Additional modulo 2: $k_{2i-1} \oplus k_{2i}$	0	1
Measurement basis: $B_i = \{B_z, B_x\}$	$B_z = \{ 0\rangle, 1\rangle\}$	$B_{x}=\{ + angle, - angle\}$
Measurement result:	$ 0\rangle$	$ -\rangle$

Step 1.3: Based on the pre-shared key K, Bob determines the placement and measurement basis for the decoy and authentication qubits that Alice has prepared. He then sequentially measures the decoy qubits K_d and authentication qubits K_a following a predefined rule: if $k_{2i} = 0$, Bob employs the Z-basis $(\{|0\rangle, |1\rangle\})$ for measuring K_d ; otherwise, he utilizes the X-basis $(\{|+\rangle, |-\rangle\})$. The authentication qubits K_a are measured based on the function $k_{2i-1} \oplus k_{2i}$, and the results are compared with the expected values outlined in Table 2.3. To assess the security of the channel, Bob computes the QBER using the decoy qubit measurement results. If the QBER remains within an acceptable threshold, the channel is deemed secure. However, if discrepancies in the authentication sequence K_a exceed the permissible limit, Bob terminates the protocol. Otherwise, he verifies Alice's identity.

Step 1.4: Bob generates a new decoy sequence K'_d using the same procedure described in Step 1.1. Similarly, he encodes the authentication qubit sequence K'_a following the same encoding rules and constructing an extended sequence K_B . He then transmits K_B to Alice.

Step 1.5: Upon receiving the sequence, Alice extracts the decoy and authentication qubits. She then verifies Bob's identity using the same approach outlined in Step 1.3.

2.2.2 **PROTOCOL 2.2**

Similar to the previous protocol, Alice and Bob are assumed to have pre-shared an authentication key denoted as $K = \{k_1, k_2, k_3, \dots, k_{4n}\}$. The primary distinction from the earlier scheme is that the length of the shared key is now 4n, which is twice that of the prior approach.

Encoding mode

Table 2.4: The preparation method of the authentication sequence (Protocol 2.2).

Additional modulo 2: $k_{2i-1} \oplus k_{2i}$	0	1
Bit value: k_{2i}	0 1	0 1
Prepared authentication state: K_{A_i}	$ 0\rangle$ $ 1\rangle$	$ +\rangle$ $ -\rangle$

Step 2.1: Alice constructs an ordered sequence of n particles, K_A , utilizing the first half of the pre-shared key (comprising 2n bits). The particle states are assigned based on the following condition: if $k_{2i-1} \oplus k_{2i} = 0$, then Alice encodes the states as $|0\rangle$ and $|1\rangle$, corresponding to $k_{2i} = 0$ and $k_{2i} = 1$, respectively. Conversely, if $k_{2i-1} \oplus k_{2i} = 1$, Alice prepares the states as $|+\rangle$ and $|-\rangle$, corresponding to $k_{2i} = 0$ and $k_{2i} = 1$, respectively. She then transmits the ordered particle sequence, K_B , to Bob.

Step 2.2: Upon receiving the sequence, Bob measures the i^{th} particle of K_B in the Z-basis $(\{|0\rangle, |1\rangle\})$ if $k_{2i-1} \oplus k_{2i} = 0$. Otherwise, he employs the X-basis $(\{|+\rangle, |-\rangle\})$ for measurement. He then constructs a classical bit sequence, S_B , by assigning a bit value of 0 to the states $|0\rangle$ and $|+\rangle$, and a bit value of 1 to the states $|1\rangle$ and $|-\rangle$. Bob then compares the i^{th} bit of S_B with k_{2i} , which ideally should match $K_B = k_{2i}$. If the observed error rate remains within an acceptable threshold, Bob validates Alice's identity.

• Decoding mode

Table 2.5: The measurement basis employed by Bob to extract results for the authentication sequence (Protocol 2.2).

Additional modulo 2: $k_{2i-1} \oplus k_{2i}$	0	1
Bit value: k_{2i}	0 1	0 1
Measurement basis: $B_i = \{B_z, B_x\}$	$B_z = \{ 0\rangle, 1\rangle\}$	$B_z = \{ +\rangle, -\rangle\}$
Measurement result:	$ 0\rangle$ $ 1\rangle$	$ +\rangle$ $ -\rangle$

Step 2.3: Bob executes a procedure analogous to Step 2.1, utilizing the remaining half of the pre-shared authentication key, similar to Alice's approach.

Step 2.4: Alice replicates the process in Step 2.2 to authenticate Bob's identity.

As outlined earlier, Protocols 1 and 2 serve as illustrative examples of protocols that can be constructed using QSDC-based schemes. In a similar manner, other existing QSDC schemes can be adapted to develop protocols for QIA. A detailed security analysis of these QIA schemes will be presented in Section 2.2.4.

2.2.3 COMPARISON OF THE EXISTING AND THE PROPOSED PROTOCOLS

Many of the existing protocols, including the seminal work of Crépeau et al. [35], have been criticized due to their reliance on two-party secure multiparty computation (two-party SMC), which is not feasible within the framework of non-relativistic quantum mechanics. To comprehend this limitation affecting a subset of protocols, it is essential to highlight key findings by Lo in 1997 [270] and by Lo and Chau in 1998 [271]. These studies demonstrated that fundamental cryptographic primitives such as quantum bit commitment, quantum remote coin tossing¹, and quantum OT cannot achieve unconditional security within a two-party quantum setting. Notably, the groundbreaking QIA protocol by Crépeau et al. [35] was constructed on OT; however, at the time of its publication, the results of Lo and Chau were not yet established. Interestingly, despite the findings of Lo, Chau, and subsequent researchers [272, 273], numerous QIA protocols have continued to emerge, leveraging computational tasks deemed infeasible for unconditional security as per Lo-Chau and related impossibility results. For instance, while the secure quantum private comparison is known to be unachievable in a twoparty setting, several QIA protocols have nonetheless been designed based on this very mechanism. The question at hand is whether the findings of Lo and Chau invalidate all proposed schemes for QIA. The answer remains negative. Here, we present arguments supporting this stance. Furthermore, the security vulnerabilities inherent in Mihara's scheme [45] have been analyzed, along with potential countermeasures. Additionally, numerous theoretical frameworks for QIA necessitate quantum memory, as exemplified by the protocols outlined in Refs. [36, 45, 38, 40, 70, 76, 71, 39, 83, 85, 101, 43, 110]. Given that a fully functional quantum

¹It is important to note that only a weak form of coin tossing can be realized using quantum resources.

memory is yet to be realized, these QIA protocols are currently impractical for real-world implementation. While certain approaches can partially mitigate the requirement for quantum memory through the use of time delays, this remains a constrained solution. Another critical limitation affecting the feasibility of QIA over long distances is the absence of quantum repeaters. Some protocols, such as the QIA scheme proposed by Zhou et al. [70], attempt to overcome this challenge via entanglement swapping. However, this method relies on a trusted intermediary for entanglement swapping, which introduces potential security vulnerabilities.

2.2.4 SECURITY ANALYSIS

Here, we evaluate the security of the proposed protocols against common external attacks, specifically those by an adversary (Eve). Insider attacks are outside the scope of identity authentication and are therefore not considered in this analysis. We begin by examining impersonation attacks and systematically assessing the security of each proposed protocol against this threat.

IMPERSONATION ATTACK

In this category of attacks, an external adversary, Eve, attempts to impersonate a legitimate user, either Alice or Bob, to successfully complete the authentication process. The following analysis demonstrates that the proposed protocols remain secure against such impersonation attempts by Eve.

2.2.4.1 SECURITY ANALYSIS OF PROTOCOL 2.1 AGAINST IMPERSONATION ATTACK BY EVE

Consider the scenario where Eve attempts to impersonate Alice. According to the protocol, n authentication particles are embedded within an n-particle decoy sequence. The probability of Eve correctly identifying the authentication state of a particle is $\frac{1}{2}$. Additionally, she must accurately determine the position of the decoy particle, which also occurs with a probability of $\frac{1}{2}$. Consequently, the overall probability of Eve successfully impersonating Alice is $(\frac{1}{4})^n$. Thus, the probability of detecting Eve's presence is given by $P_1 = 1 - (\frac{1}{4})^n$, which approaches 1 for sufficiently large n (see Figure 2.1). A similar analysis applies when Eve attempts to impersonate Bob.

2.2.4.2 SECURITY ANALYSIS OF PROTOCOL 2.2 AGAINST IMPERSONATION ATTACK BY EVE

Assume Eve generates a sequence of 2n random classical bits in an attempt to impersonate Alice. She then computes $k_{2i-1} \oplus k_{2i}$. The probability that Eve's result matches Alice's is $\frac{1}{2}$. Furthermore, the probability that Eve correctly prepares and transmits the expected quantum states to Bob is also $\frac{1}{2}$. Consequently, the probability of detecting Eve's intrusion is given by $P_2 = 1 - (\frac{1}{4})^n$. As n increases, P_2 approaches 1, ensuring that an impersonation attempt is effectively identified. Therefore, Protocol 2.2 maintains the same level of security against this attack as Protocol 2.1. It follows that $P_1 = P_2 = P(n) = 1 - (\frac{1}{4})^n$, where the dependence of P(n) on n is depicted in Figure 2.1. This figure illustrates that, to reliably detect Eve's presence, Protocol 2.1 requires a minimum of 6 pre-shared classical bits, whereas Protocol 2.2 necessitates at least 10.

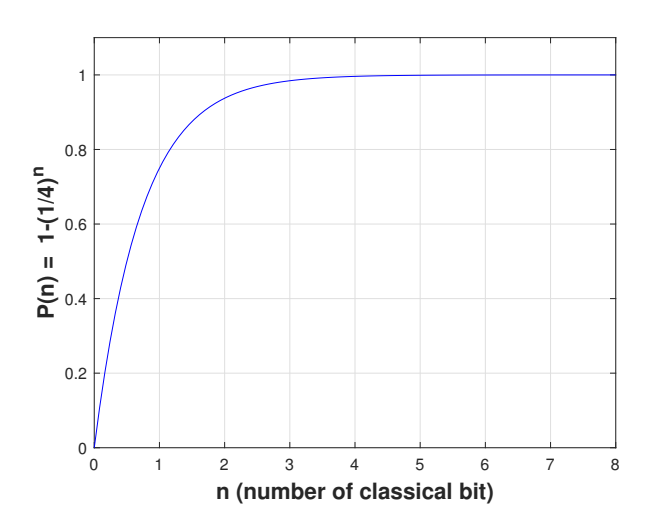


Figure 2.1: The graph presents the correlation between the probability of detecting Eve's presence, P(n), and the number of classical bits used, n.

MEASUREMENT AND RESEND ATTACK

2.2.4.3 SECURITY ANALYSIS OF PROTOCOL 2.1 AGAINST THE MEASUREMENT-RESEND ATTACK

In this attack scenario, Eve intercepts and measures the qubits transmitted from Alice to Bob, then forwards newly prepared states to Bob based on her measurement outcomes. To successfully impersonate Alice, Eve would need to distinguish between decoy qubits and authentication

qubits. However, since she lacks prior knowledge of the positions of the decoy states, any attempt to execute the measure-resend attack inevitably affects the information qubits as well, thereby leaving detectable traces of her interference. To illustrate this, consider the case where Eve measures all qubits traveling through the channel (a similar analysis holds even if she intercepts only a fraction f of them). She performs measurements on each qubit randomly in either the $\{|0\rangle, |1\rangle\}$ basis or the $\{|+\rangle, |-\rangle\}$ basis, with an equal probability of $\frac{1}{2}$ for each basis selection. To further analyze this scenario, we compute the mutual information between Alice and Bob in the presence of Eve, specifically focusing on authentication particles. Let P(B,A) denote the joint probability of Bob obtaining measurement result B when Alice initially prepares the state A, and let P(B) represent the total probability of Bob measuring the state B. when measurements of A and B are performed in an identical basis, yet yield distinct outcomes.

 $P(B,A) = \begin{cases} \frac{1}{8} & \text{measurement of } A \text{ and } B \text{ is performed with identical basis, with distinct outcomes} \\ \frac{3}{8} & \text{measurement of } A \text{ and } B \text{ is performed with identical basis, with distinct outcomes} \\ 0 & \text{when } B \text{ and } A \text{ are meassured in the different basis} \end{cases}$

and

$$P(B = |0\rangle) = P(B = |-\rangle) = \frac{3}{8}$$

$$P(B = |1\rangle) = P(B = |+\rangle) = \frac{1}{8}$$

where $A \in \{|0\rangle, |-\rangle\}$ and $B \in \{|0\rangle, |1\rangle, |+\rangle, |-\rangle\}$.

The conditional entropy is given by 1 , $H(B|A) = \left[2 \times \frac{1}{2} \left(-\frac{3}{4} \log_2 \frac{3}{4} - \frac{1}{4} \log_2 \frac{1}{4}\right)\right] = 0.811278$ bit, where H(A) = 1 and H(B) is computed as $H(B) = 2 \times \left(-\frac{3}{8} \log_2 \frac{3}{8} - \frac{1}{8} \log_2 \frac{1}{8}\right) = 1.811278$ bit. The mutual information shared between Alice and Bob is determined by, I(A:B) = H(B) - H(B|A) = 1.0 bit 2 .

Similarly, the probability relations for Alice and Eve follow the same structure.

The conditional probability is expressed as, $P(B = |i\rangle|A = |j\rangle) = \frac{P(B = |i\rangle,A = |j\rangle)}{P(A = |j\rangle)}$ and the conditional entropy is formulated as $H(B|A) = -\sum_{j} P(A = |j\rangle) \sum_{i} P(B = |i\rangle|A = |j\rangle) \log_2 P(B = |i\rangle|A = |j\rangle)$.

²The mutual information shared between two parties is constrained by the Shannon entropy of the probability distributions associated with a single particle. Mathematically, this is expressed as $0 \le I(A:B) \le min[H(A), H(B)]$, where the joint entropy is defined as H(A,B) := [max[H(A),H(B)],H(A)+H(B)]. Consequently, the mutual information is given by I(A:B) := H(A) + H(B) - [max[H(A),H(B)],H(A)+H(B)] which simplifies to I(A:B) := [0,min[H(A),H(B)]].

 $P(E,A) = \begin{cases} 0 & \text{measurement of } E \text{ and } A \text{ is performed with identical basis, with distinct outcomes} \\ \frac{1}{4} & \text{measurement of } E \text{ and } A \text{ is performed with identical basis, with distinct outcomes} \\ \frac{1}{8} & \text{when } E \text{ and } A \text{ are meassured in the different basis} \end{cases}$

and

$$P(E = |0\rangle) = P(E = |-\rangle) = \frac{3}{8},$$

$$P(E = |1\rangle) = P(E = |+\rangle) = \frac{1}{8},$$

where $A \in \{|0\rangle, |-\rangle\}$ and $E \in \{|0\rangle, |1\rangle, |+\rangle, |-\rangle\}$.

The conditional entropy is computed as $H(E|A) = \left[2 \times \frac{1}{2}(-\frac{1}{2}\log_2\frac{1}{2} - \frac{1}{4}\log_2\frac{1}{4} - \frac{1}{4}\log_2\frac{1}{4}\right] = 1.5$ bit. Similarly, the entropy of E is given by: $H(E) = 2 \times \left(-\frac{3}{8}\log_2\frac{3}{8} - \frac{1}{8}\log_2\frac{1}{8}\right) = 1.811278$. The mutual information between Eve and Alice is determined as I(A:E) = H(E) - H(E|A) = 0.311278 bit. Furthermore, it is established that the mutual information I(A:E) is constrained by the Holevo bound [274], which in this case is 0.600876. Clearly, $I(A:E) \le 0.600876$ and I(A:B) > I(A:E), indicating that Eve's accessible information is significantly lower than Bob's.

For Eve to successfully impersonate Bob, she must target the expanded particle sequence K_B that Bob returns. This requirement mirrors the conditions necessary for her to impersonate Alice.

2.2.4.4 SECURITY ANALYSIS OF PROTOCOL 2.2 AGAINST MEASUREMENT-RESEND ATTACK

Eve conducts arbitrary measurements on the quantum particles transmitted by Alice, obtaining certain outcomes. Analogous to Protocol 2.1, the mutual information shared between Alice and Bob can be determined as follows:

$$P(B,A) = \frac{1}{16} + \frac{1}{8}\delta_{A,B} \text{ and } P(B = |0\rangle) = P(B = |+\rangle) = (B = |1\rangle) = P(B = |-\rangle) = \frac{1}{4},$$

where $\delta_{A,B} = 1$ if Alice's and Bob's measurement results match when using the same basis, and $\delta_{A,B} = 0$ otherwise.

The conditional entropy is calculated as $H(B|A) = \frac{1}{4} \left[4 \times \left(-\frac{3}{4} \log_2 \frac{3}{4} \right) + 4 \times \left(-\frac{1}{4} \log_2 \frac{1}{4} \right) \right] = 0.81127$ bit. Additionally, the entropy values for Alice and Bob are, $H(A) = H(B) = 4 \times \left[-\frac{1}{4} \log_2 \frac{1}{4} \right] = 2$ bits. Consequently, the mutual information between Alice and Bob is derived as, I(A:B) = H(B) - H(B|A) = 1.18872 bit which exceeds 1, as they already share identical classical information established via a pre-shared key.

To get mutual information between Alice and Eve,

$$P(E,A) = \begin{cases} 0 & \text{measurement of } E \text{ and } A \text{ is performed with identical basis, with distinct outcomes} \\ \frac{1}{8} & \text{measurement of } E \text{ and } A \text{ is performed with identical basis, with distinct outcomes} \\ \frac{1}{16} & \text{when } E \text{ and } A \text{ are meassured in the different basis} \end{cases}$$

and

$$P(E=|0\rangle)=P(E=|1\rangle)=P(E=|+\rangle)=P(E=|-\rangle)=\frac{1}{4}.$$

The conditional entropy is given by $H(E|A) = \frac{1}{4} \times [8 \times (-\frac{1}{4}\log_2\frac{1}{4}) - 4 \times (-\frac{1}{2}\log_2\frac{1}{2})] = 1.5$ bits, while the entropy H(E) is calculated as $H(E) = 4 \times [-\frac{1}{4}\log_2\frac{1}{4}] = 2$ bits. The mutual information shared between Eve and Alice is then determined as I(A:E) = H(E) - H(E|A) = 0.5. Additionally, it is established that the mutual information I(A:E) is constrained by the Holevo bound [274], which, in this scenario, equals 1. Consequently, it follows that $I(A:E) \le 1$ and I(A:B) > I(A:E), fulfilling the security condition that ensures Alice's communication remains confidential without leaking significant information to Eve. A similar outcome holds in cases where Eve attempts to impersonate Bob.

IMPERSONATED FRAUDULENT ATTACK

2.2.4.5 SECURITY EVALUATION OF PROTOCOL 2.1 AGAINST IMPERSONATED FRAUDULENT ATTACK VIA FORGED NEW QUBITS

In this scenario, Eve attempts to assume Alice's identity by employing a unitary transformation U_E to establish a correlation between Alice's qubit and an ancillary qubit. Once the unitary operation is applied, the resulting quantum state can be represented as

$$U_E|0\chi\rangle_{Ae}=|\psi\rangle_0=a_0|00\rangle+b_0|01\rangle+c_0|0+\rangle+d_0|0-\rangle,$$

$$U_E|1\chi\rangle_{Ae} = |\psi\rangle_1 = a_1|10\rangle + b_1|11\rangle + c_1|1+\rangle + d_1|1-\rangle,$$

$$U_E |+\chi\rangle_{Ae} = |\psi\rangle_{+} = a_{+}|+0\rangle + b_{+}|+1\rangle + c_{+}|++\rangle + d_{+}|+-\rangle,$$

$$U_E|-\chi\rangle_{Ae}=|\psi\rangle_-=a_-|-0\rangle+b_-|-1\rangle+c_-|-+\rangle+d_-|--\rangle.$$

Now, we get the entire state as,

$$|\rho\rangle = \frac{1}{4} (|\psi\rangle_{00} \langle \psi| + |\psi\rangle_{11} \langle \psi| + |\psi\rangle_{++} \langle \psi| + |\psi\rangle_{--} \langle \psi|). \tag{2.1}$$

The probability of Bob obtaining the correct measurement outcome for each authentication state and the decoy sequence is $\frac{1}{2}$. Assuming the correct state is $|0\rangle$, the probability of detecting Eve is given by $P_0 = \frac{1}{2}$. Similarly, the probabilities for other states are $P_1 = P_+ = P_- = \frac{1}{2}$. The overall detection probability for each qubit is computed as $P_d = \frac{1}{4}(P_0 + P_1 + P_+ + P_-) = \frac{1}{2}$. Based on Simmons theory [275], the protocol ensures unconditional security against impersonation attacks using (2.1).

2.2.4.6 SECURITY EVALUATION OF PROTOCOL 2.2 AGAINST IMPERSONATED FRAUDULENT ATTACK VIA FORGED QUBITS

In this protocol, Alice selects authentication states within the computational and Hadamard bases with equal probability, and Bob's expected measurement results are also evenly distributed. Consequently, the attack scenario is the same with of Protocol 2.1. Under these conditions, Protocol 2.2 remains secure against impersonation-based fraudulent attacks.

2.3 CONTROLLED QUANTUM IDENTITY AUTHENTICATION PROTOCOL USING BELL PAIRS (PROTOCOL 2.3)

In this section, we propose a novel framework for QIA, modeled similarly to approaches derived from QSDC. Since our protocol incorporates Bell states, it can be categorized as an entanglement-based method for QIA. Within this framework, two authorized participants authenticate each other with the assistance of an untrusted intermediary, utilizing unitary transfor-

mations. Before presenting the detailed structure of our protocol, it is essential to outline the foundational principles that inform its design.

2.3.1 PRINCIPAL CONCEPT OF PROTOCOL 2.3

This protocol is fundamentally based on Bell-state entanglement swapping and the application of Pauli operations. The correlation between the Bell state and the pre-shared authentication key can be articulated as follows:

$$00: |\phi^{+}\rangle = \frac{1}{\sqrt{2}} (|00\rangle + |11\rangle),$$

$$01: |\phi^{-}\rangle = \frac{1}{\sqrt{2}} (|00\rangle - |11\rangle),$$

$$10: |\psi^{+}\rangle = \frac{1}{\sqrt{2}} (|01\rangle + |10\rangle),$$

$$11: |\psi^{-}\rangle = \frac{1}{\sqrt{2}} (|01\rangle - |10\rangle).$$
(2.2)

The Equations (2.2) and (2.3) define the relationship between the pre-shared key, the Bell state initialized by Alice and Bob, and the Pauli operations they execute. The connection between the corresponding Pauli operations and the pre-shared authentication key can be expressed as follows:

$$00: \mathbb{1}_{2} = |0\rangle\langle 0| + |1\rangle\langle 1|,$$

$$01: \sigma_{x} = |0\rangle\langle 1| + |1\rangle\langle 0|,$$

$$10: i\sigma_{y} = |0\rangle\langle 1| - |1\rangle\langle 0|,$$

$$11: \sigma_{z} = |0\rangle\langle 0| - |1\rangle\langle 1|.$$

$$(2.3)$$

We present a succinct summary of the described protocol. Alice and Bob shares a pre-established authentication key sequence comprising n+1 pairs of bits, where each pair encodes two bits of information. To illustrate, consider a specific case where the first two secret keys in the sequence are represented as 11 and 00. Alice selects the second key (00), typically denoted as the $(m+1)^{th}$ key in the sequence, while Bob chooses the XOR operation between the second and first keys, computed as $00 \oplus 11 = 11$. More generally, this corresponds to the XOR of the $(m+1)^{th}$ and m^{th} keys, where $m=1,2,\cdots,n$. Subsequently, Alice and Bob utilize their respective keys to generate Bell states according to Equation (2.2). In this process, they prepare the quantum states $|\phi^+\rangle_{12}$ and $|\psi^-\rangle_{34}$, where subscripts 1,2 correspond to Alice's particles and 3,4 to Bob's particles. By leveraging the pre-shared authentication key sequence, they generate

multiple Bell states in a similar manner. Alice retains the sequence of particle 1 from these Bell states and transmits the sequence associated with particle 2 to an untrusted third party, Charlie. Charlie then applies a permutation operator Π_n [51, 62, 276, 269] on the sequence of particle 2 while keeping the original sequence undisclosed. After performing the permutation, Charlie forwards the modified sequence to Bob. Meanwhile, Bob independently prepares two sequences corresponding to particles 3 and 4, sending the sequence associated with particle 4 directly to Alice. As a result, Alice and Bob respectively obtain sequences comprising particles (1,4) and (2,3). Given these specific secret keys, the resulting composite system is characterized by:

$$|\phi^{+}\rangle_{12}|\psi^{-}\rangle_{34} = \frac{1}{2}(|\psi^{+}\rangle_{14}|\phi^{-}\rangle_{23} + |\psi^{-}\rangle_{14}|\phi^{+}\rangle_{23} - |\phi^{+}\rangle_{14}|\psi^{-}\rangle_{23} - |\phi^{-}\rangle_{14}|\psi^{+}\rangle_{23}).$$

Alice (Bob) implements a Pauli σ_z operation on qubit 1 (qubit 3) based on the initial key, which is designated as 11. This¹ operation follows the mapping defined in Equation (2.3). After executing their respective operations, Alice and Bob publicly confirm their completion. Subsequently, Charlie announces the permutation operation Π_n . In response, Bob applies the inverse permutation to his sequence of particle 2, thereby restoring the original ordering. Following this step, Alice and Bob proceed with a Bell-state measurement on their respective qubits (Alice on qubits 1 and 4, and Bob on qubits 2 and 3). The resultant quantum system is given by:

$$\begin{aligned} |\Psi^{11}\rangle &= \sigma_{z1} \otimes \sigma_{z3} (|\phi^{+}\rangle_{12} |\psi^{-}\rangle_{34}) \\ &= \frac{1}{2} (|\psi^{-}\rangle_{14} |\phi^{+}\rangle_{23} + |\psi^{+}\rangle_{14} |\phi^{-}\rangle_{23} - |\phi^{-}\rangle_{14} |\psi^{+}\rangle_{23} - |\phi^{+}\rangle_{14} |\psi^{-}\rangle_{23}). \end{aligned} (2.4)$$

Alice (or Bob) encodes the result of her (his) Bell-state measurement into classical bits following Equation (2.2), while keeping the measurement outcome undisclosed. In this framework, Alice's measurement outcomes, each occurring with a probability of $\frac{1}{4}$, correspond to the Bell states $|\psi^-\rangle$, $|\psi^+\rangle$, $|\phi^-\rangle$ and $|\phi^+\rangle$, which are mapped to classical bit values 11, 10, 01, and 00, respectively. Conversely, Bob's measurement outcomes align with $|\phi^+\rangle$, $|\phi^-\rangle$, $|\psi^+\rangle$ and $|\psi^-\rangle$, associated with classical bit values 00, 01, 10, and 11, respectively. Within this setting, Alice assumes the verifier role, given that two secret keys are involved in the scheme. If Bob announces his bit value as 00 via an unjammable classical communication channel, Alice per-

¹For an extended pre-shared key sequence, the Pauli operation is dictated by the *m*th key.

forms an XOR operation between Bob's transmitted bit and her classical bit value (11) derived from her measurement. In an ideal scenario with no quantum channel disturbances such as noise or eavesdropping, the computed XOR value should correspond to the first key from the pre-shared sequence, which is 11. More generally, this XOR result would match the m^{th} key within the pre-established key sequence. The complete set of potential measurement outcomes and their correlations is presented in Table 2.6, assuming the initial pre-shared keys are 11 and 00.

Table 2.6: This outlines the possible measurement results for the legitimate participants within the proposed QIA scheme.

Alice and Bob's possible measurement	Additional modulo 2	
outcomes		
$ \psi^{-}\rangle_{14}\otimes \phi^{+}\rangle_{23}$	$11 \oplus 00 = 11$	
$ \psi^{+}\rangle_{14}\otimes \phi^{-}\rangle_{23}$	$10 \oplus 01 = 11$	
$ \phi^{-}\rangle_{14}\otimes \psi^{+}\rangle_{23}$	$01 \oplus 10 = 11$	
$ \phi^{+}\rangle_{14}\otimes \psi^{-}\rangle_{23}$	$00 \oplus 11 = 11$	

We examine three additional cases to validate the robustness of our conclusion across the remaining possible secret keys positioned at the m^{th} place in the pre-shared key sequence, specifically $\{00\}$, $\{01\}$ and $\{10\}$. This allows us to illustrate the final quantum state shared between Alice and Bob. The resultant composite systems, where the secret keys at the m^{th} and $(m+1)^{th}$ positions in the sequence take values $\{00,01\}$, $\{01,10\}$ and $\{10,11\}$, respectively, are formulated as follows:

$$\begin{aligned} |\Psi^{00}\rangle &= \mathbb{1}_{1} \otimes \mathbb{1}_{3} (|\phi^{-}\rangle_{12} |\phi^{-}\rangle_{34}) \\ &= \frac{1}{2} (|\phi^{+}\rangle_{14} |\phi^{+}\rangle_{23} + |\phi^{-}\rangle_{14} |\phi^{-}\rangle_{23} - |\psi^{+}\rangle_{14} |\psi^{+}\rangle_{23} - |\psi^{-}\rangle_{14} |\psi^{-}\rangle_{23}) \end{aligned}, (2.5)$$

$$\begin{aligned} |\Psi^{01}\rangle &= \sigma_{x1} \otimes \sigma_{x3} (|\psi^{+}\rangle_{12} |\psi^{-}\rangle_{34}) \\ &= \frac{1}{2} (-|\phi^{+}\rangle_{14} |\phi^{-}\rangle_{23} - |\phi^{-}\rangle_{14} |\phi^{+}\rangle_{23} + |\psi^{+}\rangle_{14} |\psi^{-}\rangle_{23} + |\psi^{-}\rangle_{14} |\psi^{+}\rangle_{23}) \end{aligned}, (2.6)$$

and

$$\begin{aligned}
|\Psi^{10}\rangle &= i\sigma_{y1} \otimes i\sigma_{y3} (|\psi^{-}\rangle_{12}|\phi^{-}\rangle_{34}) \\
&= \frac{1}{2} (|\psi^{+}\rangle_{14}|\phi^{+}\rangle_{23} + |\psi^{-}\rangle_{14}|\phi^{-}\rangle_{23} + |\phi^{+}\rangle_{14}|\psi^{+}\rangle_{23} + |\phi^{-}\rangle_{14}|\psi^{-}\rangle_{23})
\end{aligned}, (2.7)$$

respectively. In Equations (2.4 - 2.7), we evaluate four distinct pairwise combinations of the m^{th} and $(m+1)^{th}$ keys. However, there are twelve additional key pairings that yield identical measurement outcomes, thereby reinforcing authentication between legitimate users.

2.3.2 DESCRIPTION OF PROTOCOL 2.3

In the scenario examined in this part, two legitimate parties, Alice and Bob, aim to authenticate themselves with assistance from an untrusted intermediary, Charlie. Within this authentication framework, Alice and Bob share a pre-established classical secret key, denoted as $K_{AB} = \{k_1^1 k_2^1, k_1^2 k_2^2, k_1^3 k_2^3, \cdots, k_1^m k_2^m, \cdots k_1^{n+1} k_2^{n+1}\}$. This secret key sequence, K_{AB} , consists of two-bit key elements distributed uniformly, represented as $k_1^m k_2^m$, where $k_1^m k_2^m \in \{00,01,10,11\}$. Before detailing the authentication protocol's execution, it is essential to outline the role of the decoy states in establishing secure communication between two entities [277]. In this approach, one party randomly integrates decoy qubits—ideally matching the original information sequence in quantity—into the transmitted qubit sequence. This expanded sequence is then forwarded to the receiving party. Upon reception, the receiving party requests information regarding the positions and encoding of the decoy qubits via a secure public channel. The sender publicly discloses this data, enabling the recipient to validate it by measuring the decoy qubits. If the detected error rate surpasses an acceptable threshold, both parties discard the entire qubit sequence. The implementation of decoy states strengthens channel security, ensuring reliable information exchange between communicating entities.

The subsequent part elaborates on the stepwise procedure involved in the authentication process.

Step 3.1 Alice and Bob construct Bell state sequences A_{12} and B_{34} by utilizing the $(m+1)^{th}$ key and performing an XOR operation on the m^{th} and $(m+1)^{th}$ keys from the entire sequence K_{AB} , as prescribed by the protocol described in Equation (2.2), where $m=1,2,\cdots,n$.

$$A = \{|A\rangle_{12}^{1}, |A\rangle_{12}^{2}, |A\rangle_{12}^{3}, \cdots, |A\rangle_{12}^{m}, \cdots, |A\rangle_{12}^{n}\},$$

$$B = \{|B\rangle_{34}^{1}, |B\rangle_{34}^{2}, |B\rangle_{34}^{3}, \cdots, |B\rangle_{34}^{m}, \cdots, |B\rangle_{34}^{n}\}.$$

Here, the subscripts 1,2 and 3,4 denote the respective particles assigned to Alice and Bob. Ideally, both sets of states should be identical.

Step 3.2 Alice and Bob divide the states of their Bell pairs into two separate sequences, each containing n particles. Within these sequences, the first particle of each Bell pair forms one sequence, while the second particle constitutes the other. Consequently, Alice and Bob hold the sequences S_{A1} , S_{A2} and S_{B3} , S_{B4} , respectively.

$$S_{A1} = \{s_1^1, s_1^2, s_1^3, \cdots, s_1^m, \cdots, s_1^n\},$$

$$S_{A2} = \{s_2^1, s_2^2, s_2^3, \cdots, s_2^m, \cdots, s_2^n\},$$

$$S_{B3} = \{s_3^1, s_3^2, s_3^3, \cdots, s_3^m, \cdots, s_3^n\},$$

$$S_{B4} = \{s_4^1, s_4^2, s_4^3, \cdots, s_4^m, \cdots, s_4^n\}.$$

Specifically, S_{A1} (S_{A2}) consists of the first (second) particles of all Bell pairs in sequence A, while S_{B3} (S_{B4}) contains the first (second) particles of all Bell pairs in sequence B. Alice and Bob retain the sequences S_{A1} and S_{B3} with themselves, respectively. Additionally, Alice (Bob) embeds decoy particles D_A (D_B) into S_{A2} (S_{B4}), generating the modified sequence S'_{A2} (S'_{B4}). Alice (Bob) then transmits S'_{A2} (S'_{B4}) through a quantum channel to Charlie (Alice).

- Step 3.3 Upon receiving S'_{A2} , Charlie performs security verification using the decoy particles. Once the security tests are completed, Charlie discards D_A to reconstruct the original sequence S_{A2} . After obtaining S_{A2} , Charlie applies a permutation operation Π_n and introduces additional decoy states, forming a new sequence S^*_{A2} . Finally, Charlie forwards S^*_{A2} to Bob.
- **Step 3.4** Alice and Bob execute a security validation using decoy particles. Once the security test is completed, Alice discards the decoy states, labeled as D_B , from the expanded sequence S'_{B4} , thereby reverting it to the original sequence S_{B4} as initially prepared by Bob. Following this, Charlie publicly announces the exact arrangement of the sequence S^*_{A2} ,

which corresponds to the inverse operation of the Π_n operator. Bob then reorders his sequence accordingly to reconstruct its initial configuration, denoted as S_{A2} .

- Step 3.5 Alice (Bob) applies Pauli operations to each m^{th} particle in the sequence S_{A1} (S_{B3}) based on the corresponding m^{th} key from their pre-shared key sequence, in accordance with Equation 2.3). Afterward, Alice (Bob) retains the sequences S_{A1} , S_{B4} (S_{A2} , S_{B3}) and proceeds to perform Bell measurements on the paired particles within these sequences¹. The results from these Bell state measurements are then recorded by Alice and Bob as classical key sequences, denoted as $R_{14} = \{r_{14}^1, r_{14}^2, r_{14}^3, \cdots, r_{14}^m, \cdots, r_{14}^n\}$ and $R_{23} = \{r_{23}^1, r_{23}^2, r_{23}^3, \cdots, r_{23}^m, \cdots, r_{23}^m, \cdots, r_{23}^n\}$, following Equation (2.2).
- **Step 3.6** Alice publicly reveals the positions and values of $\frac{n}{2}$ keys from the sequence R_{14} , while Bob discloses $\frac{n}{2}$ keys from the sequence R_{23} at the corresponding remaining positions within R_{14} . Alice (Bob) performs XOR operations between the key announced by Bob (Alice) and the corresponding key from her (his) sequence R_{14} (R_{23}), thereby generating a new two-bit key sequence r_A (r_B) of length n.
- **Step 3.7** In the absence of errors, the elements of r_A and r_B should correspond to the respective key elements of the initial sequence K_{AB}^2 . If this condition is satisfied, mutual authentication between Alice and Bob is successfully established. This authentication procedure is conducted simultaneously by both legitimate parties.

The proposed QIA protocol is visually represented in the flowchart shown in Figure 2.2.

2.3.3 ASSESSMENT OF THE SECURITY ASPECTS IN PROTOCOL 2.3

This section assesses the security resilience of the proposed protocol against several well-established attacks that an eavesdropper, commonly referred to as Eve, might attempt. Notably, insider threats originating from Alice and Bob are excluded from this discussion, as they fall outside the scope of QIA. The evaluation begins with the impersonation attack, where an untrusted entity, Charlie, seeks unauthorized access to sensitive information while adhering to all

¹A Bell measurement is conducted on the m^{th} particle of sequence $S_{A1}(S_{A2})$ along with the corresponding m^{th} particle of sequence $S_{B4}(S_{B3})$.

²In this process, the *n* elements of the sequences r_A and r_B must align with the corresponding *n* elements of K_{AB} . It is important to note that K_{AB} consists of n+1 pre-shared keys.

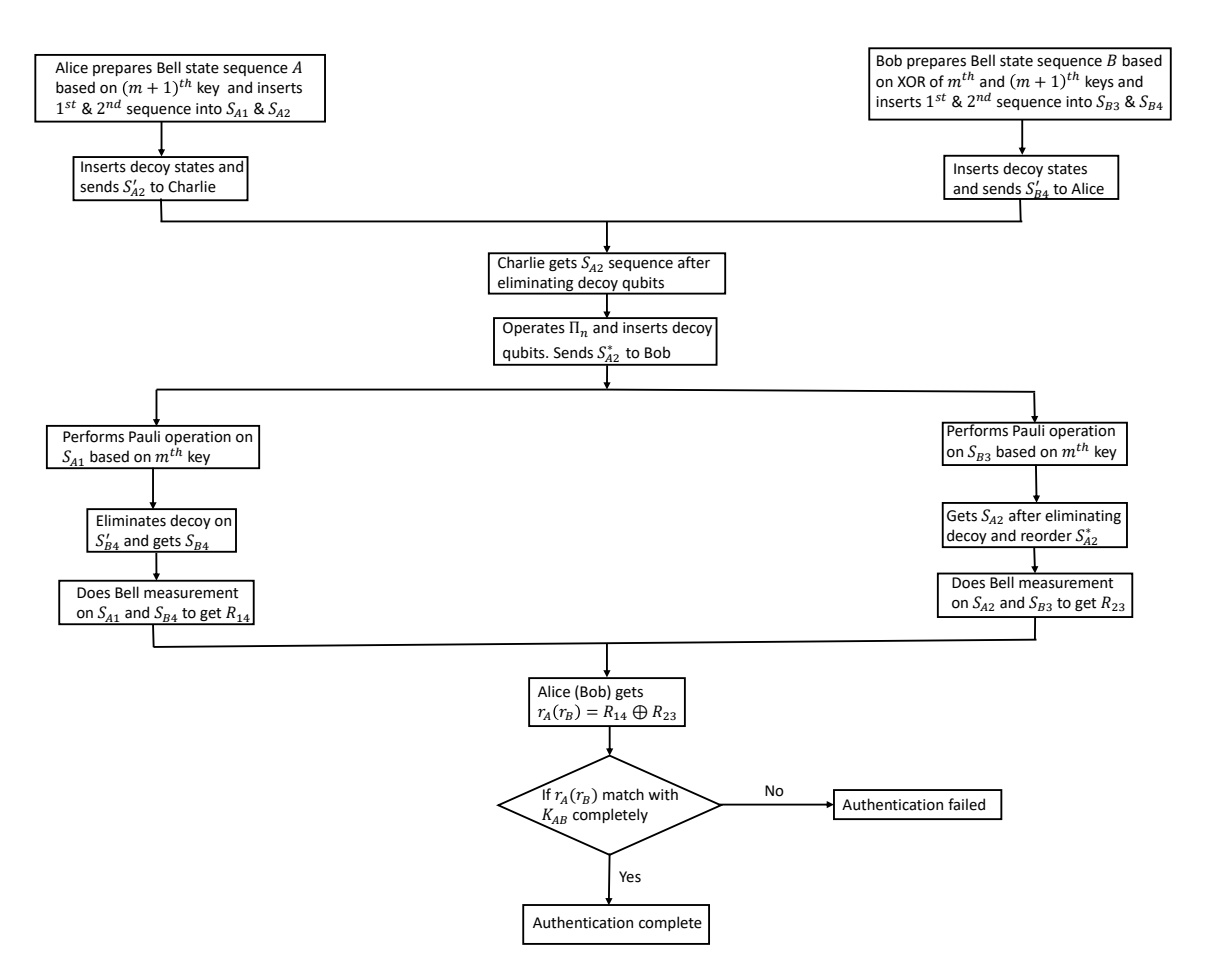


Figure 2.2: Flowchart depicting the operational workflow of the proposed QIA protocol.

protocol steps. Additionally, an impersonation-based fraudulent attack involves an external adversary, such as Eve, attempting to masquerade as a legitimate participant—Alice or Bob—to successfully navigates the authentication mechanism. Among the various threats analyzed in this section, the intercept-resend attack and impersonation-based fraudulent attack specifically exploit vulnerabilities within the quantum channel.

2.3.3.1 SECURITY EVALUATION OF PROTOCOL 2.3 AGAINST AN IMPERSONATION ATTACK BY EVE

To analyze the security of the protocol, consider the impersonation scenario discussed in Section 2.3.1. In this case, Eve assumes Alice's identity and selects the state $|\phi^+\rangle_{12}$, subsequently transmitting the particle sequence S_{e2} (corresponding to particle 2) to Charlie¹. Charlie proceeds according to the protocol, performing the designated permutation operation before forwarding the modified sequence S'_{e2} to Bob. Once Charlie publicly discloses the correct ordering of S'_{e2} , Bob reconstructs the original sequence S_{e2} . Additionally, Bob transmits the particle sequence S_{B4} directly to Eve. Eve, impersonating Alice, executes all protocol steps as required, applying the Pauli operation (σ_{z1}) on Particle 1. In parallel, Bob applies the Pauli operation (σ_{z3}) on his own Particle 3. Following this, both Bob and Eve conduct Bell-state measurements. The outcomes of these measurements, as detailed in Table 2.6, expose Eve's attempt at impersonation. Since Eve lacks access to the legitimate key pair K_{AB} (e.g., 11 and 00) and the permutation operation Π_n performed by Charlie, her probability of correctly determining the Bell state is $\frac{1}{4}$. For Eve to remain undetected, she must correctly guess all n Bell states. Consequently, the probability of a successful impersonation attempt is $\left(\frac{1}{4}\right)^n$. As *n* increases, this probability approaches zero, making successful impersonation virtually impossible. Therefore, the probability P(n)of detecting Eve's presence is given by $1 - \left(\frac{1}{4}\right)^n$. For sufficiently large n, P(n) approaches 1, ensuring the detection of an impersonation attack with near certainty. The dependence of P(n)on n is depicted in Figure 2.3, demonstrating that a minimum of six pre-shared keys is required to reliably identify Eve's intrusion.

¹The term "sequence" is used here for generalization purposes, though the security assessment follows a specific example from Section 2.3.1.

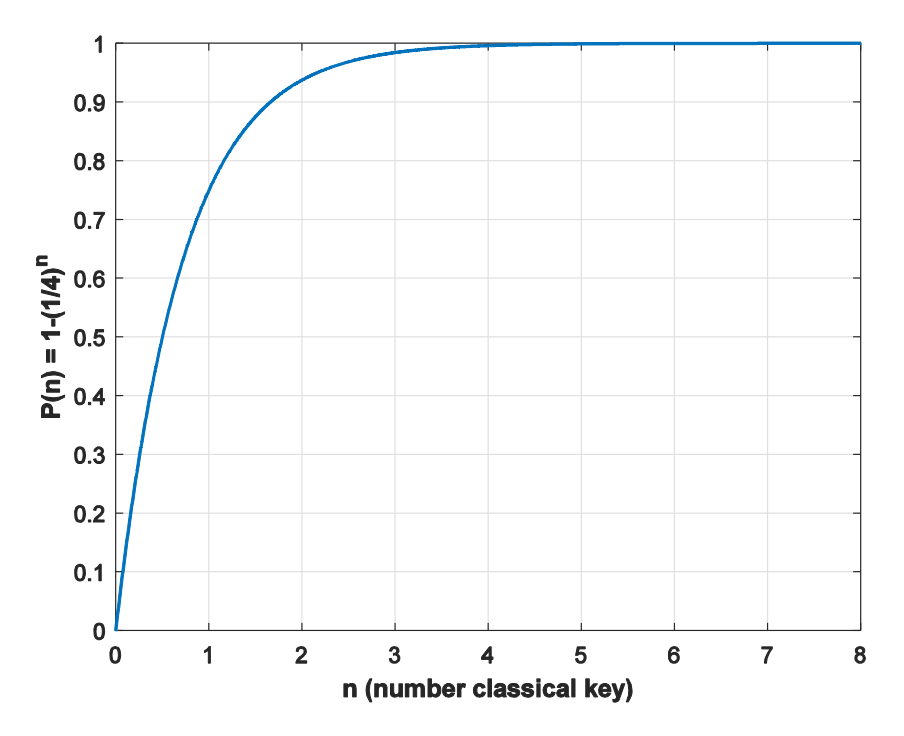


Figure 2.3: The probability P(n) of detecting Eve's presence is correlated with the number of classical authentication keys n that are pre-shared.

2.3.3.2 SECURITY EVALUATION OF PROTOCOL 2.3 AGAINST INTERCEPT AND RESEND ATTACK

In this quantum protocol, Alice and Bob utilize their pre-shared secret key to generate Bell states. Rather than transmitting their complete quantum states, they selectively send Particle 2 and Particle 4 via the quantum channel. This method confines Eve's attack opportunities to these specific particles at any given time. For clarity, we assume that Eve attempts to intercept Particle 2 during its transmission from Alice to Charlie and Particle 4 when sent from Bob to Alice. The amount of information Eve can extract from the quantum channel is fundamentally restricted by the Holevo bound or Holevo quantity [274], given by

$$\chi(\rho) = S(\rho) - \sum_{i} p_{i} S(\rho_{i}),$$
 (2.8)

which defines the upper limit of accessible information. Here, $S(\rho) = -\text{Tr}(\rho \log_2 \rho)$ represents the von Neumann entropy, where ρ_i denotes an individual component of the mixed state ρ with

probability p_i . The density matrix ρ is formulated as

$$\rho = \frac{1}{4} \left[\left| \Psi^{00} \right\rangle + \left| \Psi^{01} \right\rangle + \left| \Psi^{10} \right\rangle + \left| \Psi^{11} \right\rangle \right]_{1234} = \sum_{i} p_{i} \rho_{i},$$

where ρ_i represents the density matrix of the states defined in Equations (2.4), (2.5), (2.6) and (2.7). As previously established, Eve's objective is to target Particles 2 and 4. We aim to demonstrate a scenario where she can simultaneously intercept both. However, in such a case, the amount of useful information Eve can acquire remains constrained by the Holevo quantity. To ensure consistency with this constraint, we modify Equation (2.8) accordingly.

$$\chi\left(\rho^{24}\right) = S\left(\rho^{24}\right) - \sum_{i} p_{i} S\left(\rho_{i}^{24}\right), \qquad (2.9)$$

In this context, ρ^{24} and ρ_i^{24} denote the reduced density matrices derived from ρ and ρ_i , respectively, by executing a partial trace over particles 1 and 3. Through direct computation, we find that $\rho^{24} = \text{Tr}_{13}(\rho) = \frac{1}{4}(|11\rangle\langle11| + |10\rangle\langle10| + |01\rangle\langle01| + |00\rangle\langle00|) = \frac{1}{4}\mathbb{1}_4$, where $\mathbb{1}_4$ represents the 4×4 identity matrix. Likewise, the von Neumann entropy for each component of the mixed state ρ after the partial trace, expressed as $\rho_i^{24} = \text{Tr}_{13}(\rho_i) = \frac{1}{4}\mathbb{1}_4$, follows the same structure. By substituting ρ^{24} and ρ_i^{24} into Equation (2.9), it follows that $\chi(\rho^{24}) = 0$. This result implies that Eve is unable to extract any key information through direct interception of the transmitted particles. The intercept-resend (IR) attack strategy adopted by Eve is illustrated in Figure 2.4. To mitigate or nullify Eve's information gain from the communication channel in an IR attack, the maximally mixed state is formulated with an equal probability distribution among the Bell states, as described in Equation (2.9). However, if these probabilities are asymmetric, the system's security against IR attacks will depend on the specific probability values of the Bell states within the mixed state. The protocol remains secure against the IR attack as long as the mutual information between Alice and Bob exceeds the Holevo bound, i.e., $I(A|B) > \chi(\rho)$ [278].

2.3.3.3 SECURITY EVALUATION OF PROTOCOL 2.3 AGAINST IMPERSONATED FRAUDULENT ATTACK

To analyze the resilience of our protocol against impersonation-based fraudulent attacks, we consider two pre-shared secret keys, namely 11 and 00. Initially, Alice and Bob generate the Bell states $|\phi^{+}\rangle_{12}$ and $|\psi^{-}\rangle_{34}$, respectively. Simultaneously, Eve fabricates two single-qubit

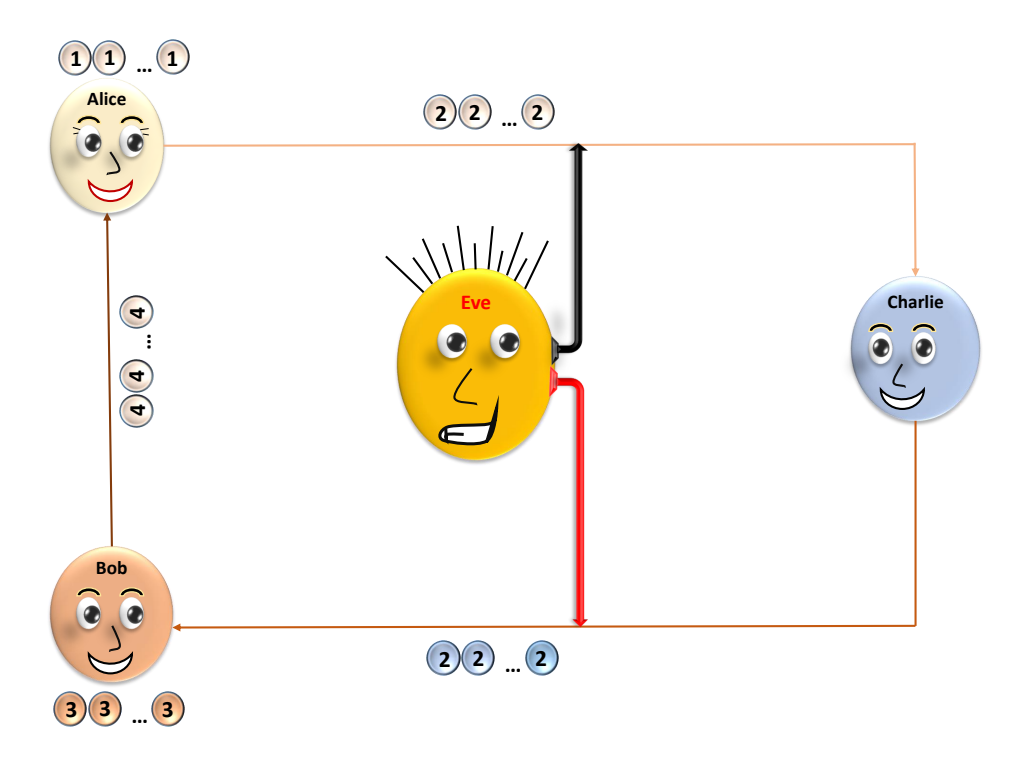


Figure 2.4: The IR attack strategy utilized by Eve is structured such that qubits labeled 1, 2, 3, and 4 correspond to sequences S_{A1} , S_{A2} , S_{B3} and S_{B4} , respectively.

states, $|\chi\rangle_5$ and $|\chi\rangle_6$, which serve as counterfeit (fake) states. These states are defined as $a|0\rangle+b|1\rangle$ and $c|0\rangle+d|1\rangle$, respectively, where the normalization conditions $|a|^2+|b|^2=1$ and $|c|^2+|d|^2=1$ hold. To execute the attack, Eve applies a CNOT gate, using qubit 2 (4) as the control and qubit 5 (6) as the target. She retains qubits 2 and 4 while transmitting qubits 5 and 6 to Bob and Alice, respectively. The resultant composite state after Eve's manipulation through the CNOT operation is given by:

$$\begin{aligned} &\text{CNOT}_{2(4)\to 5(6)} |\phi^{+}\rangle_{12} \otimes |\psi^{-}\rangle_{34} \otimes |\chi\rangle_{5} \otimes |\chi\rangle_{6} \\ &= \frac{1}{2} \left[|0001\rangle \left(a|0\rangle + b|1\rangle \right) \left(c|1\rangle + d|0\rangle \right) - |0010\rangle \left(a|0\rangle + b|1\rangle \right) \left(c|0\rangle + d|1\rangle \right) \\ &+ |1101\rangle \left(a|1\rangle + b|0\rangle \right) \left(c|1\rangle + d|0\rangle \right) - |1110\rangle \left(a|1\rangle + b|0\rangle \right) \left(c|0\rangle + d|1\rangle \right) \right]_{123456} \\ &= \frac{1}{2} \left[ac|000101\rangle + ad|000100\rangle + bc|000111\rangle + bd|000110\rangle \\ &- ac|001000\rangle - ad|001001\rangle - bc|001010\rangle - bd|001011\rangle \\ &+ ac|110111\rangle - ad|110110\rangle - bc|1110101\rangle - bd|110100\rangle \\ &- ac|111010\rangle - ad|111011\rangle - bc|111000\rangle - bd|111001\rangle \right]_{123456} \end{aligned}$$

According to the protocol, Alice and Bob each perform a σ_z operation on their respective qubits 1 and 3. Following this, they conduct Bell-state measurements, with Alice measuring the entan-

gled pair (1,6) and Bob measuring (5,3). Meanwhile, Eve retains qubits 2 and 4. The overall quantum system encompassing Alice, Bob, and Eve, post-Pauli operations and Bell measurements as per Equation (2.10), is represented as:

$$|\Psi\rangle = \frac{1}{2\sqrt{2}} [ac(|\psi^{+}\rangle|\phi^{+}\rangle|\psi^{-}\rangle + |\psi^{+}\rangle|\phi^{-}\rangle|\psi^{+}\rangle + |\psi^{-}\rangle|\phi^{+}\rangle|\psi^{+}\rangle + |\psi^{-}\rangle|\phi^{-}\rangle|\psi^{+}\rangle + |\phi^{+}\rangle|\psi^{+}\rangle|\phi^{-}\rangle + |\phi^{+}\rangle|\psi^{-}\rangle|\phi^{+}\rangle + |\phi^{-}\rangle|\psi^{+}\rangle|\phi^{+}\rangle + |\phi^{-}\rangle|\psi^{-}\rangle|\phi^{-}\rangle) + ad(|\phi^{+}\rangle|\phi^{+}\rangle|\psi^{-}\rangle + |\phi^{+}\rangle|\phi^{-}\rangle|\psi^{+}\rangle + |\phi^{-}\rangle|\phi^{+}\rangle|\psi^{+}\rangle + |\phi^{-}\rangle|\phi^{-}\rangle|\psi^{-}\rangle + |\psi^{+}\rangle|\psi^{+}\rangle|\phi^{-}\rangle + |\psi^{+}\rangle|\psi^{-}\rangle|\phi^{+}\rangle + |\psi^{-}\rangle|\psi^{+}\rangle|\phi^{+}\rangle + |\psi^{-}\rangle|\psi^{-}\rangle|\phi^{-}\rangle) + bc(|\psi^{+}\rangle|\psi^{+}\rangle|\psi^{-}\rangle - |\psi^{+}\rangle|\psi^{+}\rangle + |\psi^{-}\rangle|\psi^{+}\rangle|\psi^{+}\rangle - |\psi^{-}\rangle|\psi^{-}\rangle + |\phi^{+}\rangle|\phi^{+}\rangle|\phi^{-}\rangle - |\phi^{+}\rangle|\phi^{+}\rangle + |\phi^{-}\rangle|\phi^{+}\rangle|\phi^{+}\rangle - |\phi^{-}\rangle|\phi^{-}\rangle) bd(|\phi^{+}\rangle|\psi^{+}\rangle|\psi^{-}\rangle - |\phi^{+}\rangle|\psi^{-}\rangle|\psi^{+}\rangle + |\phi^{-}\rangle|\psi^{+}\rangle|\psi^{+}\rangle - |\phi^{-}\rangle|\psi^{-}\rangle + |\psi^{+}\rangle|\phi^{+}\rangle|\phi^{-}\rangle - |\psi^{+}\rangle|\phi^{-}\rangle|\phi^{+}\rangle|\phi^{+}\rangle + |\psi^{-}\rangle|\phi^{+}\rangle|\phi^{+}\rangle - |\psi^{-}\rangle|\phi^{-}\rangle)]_{165324}$$

$$(2.11)$$

When Alice and Bob receive Bell pairs in the states $|\psi^{+}\rangle_{16}|\phi^{-}\rangle_{53}$, $|\psi^{-}\rangle_{16}|\phi^{+}\rangle_{53}$, $|\phi^{+}\rangle_{16}|\psi^{-}\rangle_{53}$ and $|\phi^{-}\rangle_{16}|\psi^{+}\rangle_{53}$ following measurement, the probability of detecting an eavesdropper becomes zero. By evaluating the density operator of the final composite state, $|\Psi\rangle\langle\Psi|$, as given in Equation (2.11), the probability of Eve remaining undetected, denoted as P_{nd} , is given by $\frac{1}{2}\left(|ac|^2+|bd|^2\right)$. Consequently, the probability of detecting Eve, P_d , is expressed as

$$P_{d} = 1 - \frac{1}{2} (|ac|^{2} + |bd|^{2}).$$

To minimize her detection probability, Eve can choose $|a| = |b| = |c| = |d| = \frac{1}{\sqrt{2}}$, leading to her single-qubit states being $|+\rangle_5 = \frac{1}{\sqrt{2}}(|0\rangle + |1\rangle)_5$ and $|+\rangle_6 = \frac{1}{\sqrt{2}}(|0\rangle + |1\rangle)_6$. Under this condition, the minimum detection probability of Eve's presence is $P_d = \frac{3}{4}$, when she employs a single-qubit fake state.

Next, we examine the same scenario with the only distinction being that Eve uses an entangled fake state to mimic a legitimate participant. Retaining the same pre-shared key pairs, 11 and 00, Eve's fake state is given by $|\chi'\rangle_{56} = (a'|00\rangle + b'|01\rangle + c'|10\rangle + d'|11\rangle_{56}$, where the coefficients satisfy the normalization condition $|a'|^2 + |b'|^2 + |c'|^2 + |d'|^2 = 1$. The rest of the procedure remains unchanged from the previous case. Ultimately, the final composite system of Alice, Bob, and Eve after their Bell measurement is,

$$|\Psi'\rangle = \frac{1}{2\sqrt{2}} [a'(|\psi^{+}\rangle|\phi^{+}\rangle|\psi^{-}\rangle + |\psi^{+}\rangle|\phi^{-}\rangle|\psi^{+}\rangle + |\psi^{-}\rangle|\phi^{+}\rangle|\psi^{+}\rangle + |\psi^{-}\rangle|\phi^{-}\rangle|\psi^{+}\rangle + |\phi^{+}\rangle|\psi^{+}\rangle|\phi^{-}\rangle + |\phi^{+}\rangle|\psi^{-}\rangle|\phi^{+}\rangle + |\phi^{-}\rangle|\psi^{+}\rangle|\phi^{+}\rangle + |\phi^{-}\rangle|\psi^{-}\rangle|\phi^{-}\rangle) + b'(|\phi^{+}\rangle|\phi^{+}\rangle|\psi^{-}\rangle + |\phi^{+}\rangle|\phi^{-}\rangle|\psi^{+}\rangle + |\phi^{-}\rangle|\phi^{+}\rangle|\psi^{+}\rangle + |\phi^{-}\rangle|\phi^{-}\rangle|\psi^{-}\rangle + |\psi^{+}\rangle|\psi^{+}\rangle|\phi^{-}\rangle + |\psi^{+}\rangle|\psi^{-}\rangle|\phi^{+}\rangle + |\psi^{-}\rangle|\psi^{+}\rangle|\phi^{+}\rangle + |\psi^{-}\rangle|\psi^{-}\rangle|\phi^{-}\rangle) + c'(|\psi^{+}\rangle|\psi^{+}\rangle|\psi^{-}\rangle - |\psi^{+}\rangle|\psi^{+}\rangle + |\psi^{-}\rangle|\psi^{+}\rangle|\psi^{+}\rangle - |\psi^{-}\rangle|\psi^{-}\rangle + |\phi^{+}\rangle|\phi^{+}\rangle|\phi^{-}\rangle|\phi^{+}\rangle|\phi^{+}\rangle + |\phi^{-}\rangle|\phi^{+}\rangle|\phi^{+}\rangle - |\phi^{-}\rangle|\phi^{-}\rangle) d'(|\phi^{+}\rangle|\psi^{+}\rangle|\psi^{-}\rangle - |\phi^{+}\rangle|\psi^{-}\rangle|\psi^{+}\rangle + |\phi^{-}\rangle|\psi^{+}\rangle|\psi^{+}\rangle - |\phi^{-}\rangle|\psi^{-}\rangle|\psi^{-}\rangle + |\psi^{+}\rangle|\phi^{+}\rangle|\phi^{-}\rangle - |\psi^{+}\rangle|\phi^{-}\rangle|\phi^{+}\rangle + |\psi^{-}\rangle|\phi^{+}\rangle|\phi^{+}\rangle - |\psi^{-}\rangle|\phi^{-}\rangle)]_{165324} (2.12)$$

In the given scenario, the probability of detecting Eve's presence is zero when Alice and Bob obtain measurement results corresponding to specific Bell pairs: $|\psi^+\rangle_{16}|\phi^-\rangle_{53}$, $|\psi^-\rangle_{16}|\phi^+\rangle_{53}$, $|\phi^+\rangle_{16}|\psi^-\rangle_{53}$ and $|\phi^-\rangle_{16}|\psi^+\rangle_{53}$. The probability of Eve remaining undetected is determined using the density matrix $|\Psi'\rangle\langle\Psi'|$ from Equation (2.12), expressed as $P_{nd}=\frac{1}{2}\left(|a'|^2+|d'|^2\right)$. Consequently, the probability of detecting Eve is given by $P_d=1-\frac{1}{2}\left(|a'|^2+|d'|^2\right)$. To minimize her probability of detection, Eve selects $|a'|=|d'|=\frac{1}{\sqrt{2}}$ and |b'|=|c'|=0. The entangled state utilized by Eve is given by $|\phi^+\rangle_{56}=\frac{1}{\sqrt{2}}\left(|00\rangle+|11\rangle\right)_{56}$, which results in a detection probability of $P_d=\frac{1}{2}$. This indicates that employing an entangled state rather than a single qubit state reduces the probability of Eve's detection. Consequently, the minimal detection probabilities for single qubit and entangled states are $\frac{3}{4}$ and $\frac{1}{2}$, respectively. Based on this analysis, it can be concluded that the protocol remains secure against an impersonation attack by Eve, particularly under her optimal strategy.

2.3.4 COLLECTIVE NOISE ANALYSIS OF PROTOCOL 2.3

The previously discussed QIA protocol was examined under the assumption of an ideal quantum channel. However, in practical scenarios, quantum channels introduce noise, which can perturb the transmitted particles' states. Moreover, an adversary may exploit this noise to conceal an attack, making it challenging to distinguish between errors originating from environmental noise and those introduced by malicious interference. Mitigating the effects of collective noise in quantum communication remains a significant challenge[279, 280, 281]. Walton et al. [282] proposed the concept of a decoherence-free subspace (DFS) [283, 284], which serves

as a means to counteract collective noise by preserving the states of quantum particles within these protected subspaces. Subsequent research has further explored quantum communication under the influence of collective noise [285, 286]. Collective noise generally encompasses both collective-dephasing and collective-rotation noise [287]. The following analysis examines the impact of these noise types on the proposed scheme.

2.3.4.1 COLLECTIVE-DEPHASING NOISE

Collective-dephasing noise can be described as [287, 286]

$$U_{dp}|0\rangle = |0\rangle$$
 , $U_{dp}|1\rangle = e^{i\phi}|1\rangle$.

This type of noise is associated with a time-dependent parameter ϕ . A logical qubit encoded in the product states of two physical qubits, given by

$$|0\rangle_L = |01\rangle$$
 , $|1\rangle_L = |10\rangle$,

is inherently resilient to collective-dephasing noise, as both logical qubit components acquire an identical phase factor $e^{i\phi}$.

Here, the subscript L designates a logical qubit, whereas 0 and 1 correspond to horizontal and vertical polarization states, respectively—these being the eigenstates of the Pauli operator σ_z (Z basis). The logical states $|+_L\rangle$ and $|-_L\rangle$ are defined as follows:

$$\begin{array}{rcl} |+_{L}\rangle & = & \frac{1}{\sqrt{2}} \left(|0_{L}\rangle + |1_{L}\rangle \right) & = & \frac{1}{\sqrt{2}} \left(|01\rangle + |10\rangle \right) \\ |-_{L}\rangle & = & \frac{1}{\sqrt{2}} \left(|0_{L}\rangle - |1_{L}\rangle \right) & = & \frac{1}{\sqrt{2}} \left(|01\rangle + |10\rangle \right) \end{array}.$$

Based on the equations presented in Section 2.3.1, particularly Equations (2.4) and (2.7), it is evident that particles 2 and 4 within the composite states serve as carriers of quantum information through the quantum channel. For instance, considering Equation (2.4):

$$\begin{split} \left| \Psi^{11} \right\rangle &= \sigma_{z1} \otimes \sigma_{z3} \left(\left| \phi^{+} \right\rangle_{12} \left| \psi^{-} \right\rangle_{34} \right) \\ &= \frac{1}{2} \sigma_{z1} \otimes \sigma_{z3} \left(\left| 0001 \right\rangle - \left| 0010 \right\rangle + \left| 1101 \right\rangle - \left| 1110 \right\rangle \right)_{1234} \\ &= \frac{1}{2} \left(\left| 0001 \right\rangle + \left| 0010 \right\rangle - \left| 1101 \right\rangle - \left| 1110 \right\rangle \right)_{1234} \end{split}$$

Upon introducing collective dephasing noise to particles 2 and 4, the system evolves as follows:

$$\begin{split} \left| \Psi^{11} \right\rangle_{dp} &= \frac{1}{2} \left(e^{i\phi} |0001\rangle + |0010\rangle - e^{2i\phi} |1101\rangle - e^{i\phi} |1110\rangle \right)_{1234} \\ &= \frac{1}{2} \left(e^{i\phi} |01\rangle |00\rangle + |00\rangle |01\rangle - e^{2i\phi} |11\rangle |10\rangle - e^{i\phi} |10\rangle |11\rangle \right)_{1423} \\ &= \frac{1}{4} \left[2e^{i\phi} \left(|\psi^{+}\rangle|\phi^{-}\rangle + |\psi^{-}\rangle|\phi^{+}\rangle \right) + \left(1 - e^{2i\phi} \right) \left(|\phi^{+}\rangle|\psi^{+}\rangle + |\phi^{-}\rangle|\psi^{-}\rangle \right)_{1423} \\ &+ \left. \left(1 + e^{2i\phi} \right) \left(|\phi^{+}\rangle|\psi^{-}\rangle + |\phi^{-}\rangle|\psi^{+}\rangle \right) \right]_{1423} \end{split}$$

In an ideal scenario where no errors occur in the channel, the Bell pairs shared between Alice and Bob belong to the set $\{|\psi^-\rangle|\phi^+\rangle, |\psi^+\rangle|\phi^-\rangle, |\phi^-\rangle|\psi^+\rangle, |\phi^+\rangle|\psi^-\rangle\}$. However, the presence of collective dephasing noise can alter the output pairs to $\{|\phi^+\rangle|\psi^+\rangle, |\phi^-\rangle|\psi^-\rangle\}$, thereby introducing errors in the transmission. The probability of such errors occurring due to this noise is given by $\frac{1}{4}(1-\cosh(2i\phi))$, where ϕ denotes the noise parameter. Figure 2.5 illustrates how this probability varies with respect to the noise parameter. As shown in Figure 2.5.(a), the error probability follows a characteristic curve, reaching a peak value of 0.5 at $\phi=90^\circ$ and approaching zero at $\phi=0^\circ$ and 180° . To mitigate or eliminate errors induced by this noise, the quantum channel must be chosen such that the error remains within an acceptable threshold. Given a tolerable error limit p, the solutions to $p=\frac{1}{4}(1-\cosh(2i\phi))$ within the range $0^\circ < \phi < 180^\circ$ must be determined. If two solutions, ϕ_1 and ϕ_2 , are found such that $\phi_1 < \phi_2$, the protocol remains secure when operating in a channel where $\phi < \phi_1$ or $\phi > \phi_2$. To verify this condition in practical implementations, it is essential to conduct channel characterization prior to executing the protocol.

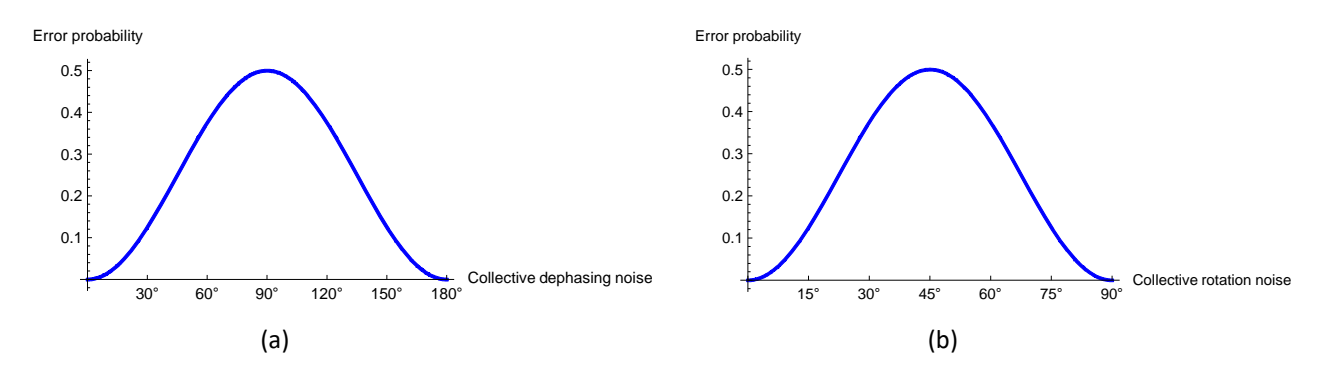


Figure 2.5: The collective error probability associated with the noise parameter can be classified into: (a) Collective dephasing error probability, characterized by the noise parameter ϕ , and (b) Collective rotation error probability, defined by the noise parameter θ .

2.3.4.2 COLLECTIVE-ROTATION NOISE

The collective rotation noise is mathematically expressed as:

$$U_r|0\rangle = \cos\theta|0\rangle + \sin\theta|1\rangle$$
 , $U_r|1\rangle = -\sin\theta|0\rangle + \cos\theta|1\rangle$,

Here, the parameter θ represents the collective rotation noise, which varies dynamically within the quantum channel. For instance, when this noise affects particles 2 and 4 as per Equation (2.4), the resulting expression is obtained after extensive calculations,

$$\begin{array}{ll} U_{r2}\otimes U_{r4}\left|\Psi^{11}\right\rangle &=& \frac{1}{2}\left[-\sin\theta\cos\theta|0000\rangle-\sin^2\theta|0010\rangle+\cos^2\theta|0100\rangle+\sin\theta\cos\theta|0110\rangle\\ &+& \sin\theta\cos\theta|1001\rangle-\cos^2\theta|1011\rangle+\sin^2\theta|1101\rangle-\sin\theta\cos\theta|1111\rangle\\ &-& \left(\cos^2\theta|0001\rangle+\sin\theta\cos\theta|0011\rangle+\sin\theta\cos\theta|0101\rangle+\sin^2\theta|0111\rangle\\ &-& \sin^2\theta|1000\rangle+\sin\theta\cos\theta|1010\rangle+\sin\theta\cos\theta|1100\rangle-\cos^2\theta|1110\rangle\right)\right]_{1423}.\\ &=& \frac{1}{2}\left[2\sin\theta\cos\theta\left(-|\phi^+\rangle|\phi^+\rangle-|\psi^-\rangle|\psi^-\rangle\right)\\ &+& \sin^2\theta\left(|\phi^+\rangle|\psi^-\rangle-|\phi^-\rangle|\psi^+\rangle+|\psi^+\rangle|\phi^-\rangle-|\psi^-\rangle|\phi^+\rangle\right)\\ &+& \cos^2\theta\left(|\psi^+\rangle|\phi^-\rangle+|\psi^-\rangle|\phi^+\rangle-|\phi^+\rangle|\psi^-\rangle-|\phi^-\rangle|\psi^+\rangle\right)\right]_{1423}. \end{array}$$

From this configuration, the probability of an error induced by collective rotation noise is determined as $2\sin^2\theta\cos^2\theta$, which is contingent on the noise parameter θ . Likewise, when collective rotation noise is applied to particles 2 and 4 as referenced in Equation (2.5), the corresponding expression follows,

$$\begin{array}{ll} U_{r2}\otimes U_{r4}\left|\Psi^{00}\right\rangle &=& \frac{1}{2}\left[\cos^{2}\theta\left|0000\right\rangle+\sin\theta\cos\theta\left|0010\right\rangle+\sin\theta\cos\theta\left|0100\right\rangle+\sin^{2}\theta\left|0110\right\rangle\right.\\ &+& \sin^{2}\theta\left|1001\right\rangle-\sin\theta\cos\theta\left|1011\right\rangle-\sin\theta\cos\theta\left|1101\right\rangle+\cos^{2}\theta\left|1111\right\rangle\\ &-& \left(-\sin\theta\cos\theta\left|0001\right\rangle-\sin^{2}\theta\left|0011\right\rangle+\cos^{2}\theta\left|0101\right\rangle+\sin\theta\cos\theta\left|0111\right\rangle\\ &-& -\sin\theta\cos\theta\left|1000\right\rangle+\cos^{2}\theta\left|1010\right\rangle-\sin^{2}\theta\left|1100\right\rangle+-\sin\theta\cos\theta\left|1110\right\rangle\right)\right]_{1423}.\\ &=& \frac{1}{2}\left[2\sin\theta\cos\theta\left(|\phi^{-}\rangle|\psi^{+}\rangle+|\psi^{+}\rangle|\phi^{-}\rangle\right)\\ &+& \sin^{2}\theta\left(|\psi^{+}\rangle|\psi^{+}\rangle-|\psi^{-}\rangle|\psi^{-}\rangle+|\phi^{+}\rangle|\phi^{+}\rangle-|\phi^{-}\rangle|\phi^{-}\rangle\right)\\ &+& \cos^{2}\theta\left(|\phi^{+}\rangle|\phi^{+}+|\phi^{-}\rangle|\phi^{-}\rangle+|\psi^{+}\rangle|\psi^{+}\rangle+|\psi^{-}\rangle|\psi^{-}\rangle\right)\right]_{1423}. \end{array}$$

For the state $|\Psi^{00}\rangle$, errors do not occur if the final Bell pairs shared between Alice and Bob are among the set $\{|\phi^{+}\rangle|\phi^{+}\rangle, |\phi^{-}\rangle|\psi^{-}\rangle, |\psi^{+}\rangle|\psi^{+}\rangle, |\psi^{-}\rangle|\psi^{-}\rangle\}$. Analyzing this outcome reveals

that the probability of error due to collective rotation noise exhibits the same functional dependence, $2\sin^2\theta\cos^2\theta$, as observed for $|\Psi^{11}\rangle$. The variation of error probability with respect to θ is illustrated in Figure 2.5.(b). From this figure, it is evident that the probability of a rotation-induced error reaches its peak value of 0.5 when $\theta=45^\circ$ and reduces to zero at $\theta=0^\circ$ and $\theta=90^\circ$. To mitigate or entirely suppress errors arising from this noise, it is crucial to choose a communication channel where the error probability remains within an acceptable threshold. Denoting this threshold as p', one must solve the equation $p'=2\sin^2\theta\cos^2\theta$ for $0^\circ<\theta<90^\circ$. If the solutions to this equation are θ_1 and θ_2 with $\theta_1<\theta_2$, the protocol will operate securely in a channel where $\theta<\theta_1$ or $\theta>\theta_2$. To ensure this condition is met in real-world applications, channel characterization must be performed before implementing the protocol. Recent developments in quantum communication have demonstrated intrinsic robustness against collective noise [288, 289, 290]. Similar approaches can be incorporated into this scheme to further enhance its resilience against collective noise.

2.3.5 COMPARISON WITH THE EXISTING PROTOCOLS

This section presents a concise comparative evaluation of the proposed protocol against a selection of existing QIA schemes. The analysis considers key factors, including the quantum resource requirements, the role of third-party entities (distinguishing between honest, semi-honest, and untrusted models), the minimum number of pre-shared authentication keys, and whether the scheme supports bidirectional mutual authentication or restricts verification to a single legitimate party. Given the extensive range of QIA schemes, a representative subset has been carefully selected, with emphasis on those grounded in secure direct quantum communication protocols, similar to the proposed approach, which is influenced by CDSQC.

We initiate the comparative analysis by evaluating Zhang et al.'s QIA scheme [41], which utilizes the ping-pong protocol for QSDC. Within this framework, Alice functions as the trusted certification authority, while Bob is the general user whose identity must be authenticated by Alice. Similarly, Yuan et al.'s scheme [87], which is based on the LM05 protocol for single-photon QSDC, follows the same structural approach, with Alice serving as the certification authority. Both of these QSDC-driven QIA protocols [41, 87] operate in a unidirectional manner, in contrast to the proposed bidirectional scheme, thereby demonstrating an advantage of the latter. This superiority extends to various unidirectional QIA protocols, including the one

introduced by Hong et al. [100]. However, this bidirectional feature is not exclusive, as similar capabilities are incorporated in Kang et al.'s schemes [43, 291] and Zhang et al.'s 2020 study [42]. Notably, all these protocols [42, 43, 291] require a minimum of six pre-established keys for authentication, whereas the proposed approach necessitates only four, making it more resource-efficient given the high cost of quantum resources. Furthermore, the studies conducted by Kang et al. [43, 291] incorporate GHZ-like states, which are tripartite entangled states. These states present greater challenges in both preparation and stability compared to the Bell states employed in our protocol. Additionally, the 2020 study by Zhang et al. assumes a semi-honest third party, whereas our proposed framework operates under the assumption that the third party is untrusted, thereby improving security. Jiang et al. introduced a semi-quantum QIA protocol analogous to the ping-pong protocol [292], where Bob possesses only classical computational abilities with restricted quantum interaction, whereas Alice has extensive quantum capabilities, enabling her to prepare and measure Bell states along with other quantum operations. However, this approach increases noise probability due to the two-way communication and allows Eve complete access to the Bell state within the quantum channel. In contrast, our proposed scheme employs a one-way quantum channel, effectively preventing Eve from obtaining full access to the Bell state. Another approach integrating QIA with QKA, utilizing Bell and GHZ states under the assumption of a semi-honest third party, was introduced by Wu et al. [293]. However, their protocol necessitates substantial quantum resources and presents maintenance difficulties in comparison to our scheme. Moreover, their reliance on hash functions for authentication may not fully comply with quantum security principles. Similarly, Li et al. proposed a simultaneous QIA scheme based on GHZ states [123], but sustaining these states proves to be more complex than managing Bell states. Thus, our proposed protocol achieves the essential QIA properties while optimizing resource efficiency, particularly when evaluated against other QIA schemes reliant on entangled states. The comparative analysis provided aims to highlight the significance and benefits of our scheme. A summarized comparison is presented in Table 2.7 for enhanced clarity.

Table 2.7: A comprehensive comparison of Protocol 2.3 is conducted with various existing QIA protocols. The column labeled "Minimum secret key required" presents multiple values corresponding to different protocols discussed within the same reference. The following abbreviations are employed in this table: TC=two-way channel, IR=intercept-resend, IF=impersonated fraudulent, EM=entangled measure.

Protocol	Quantum	Minimum	Way of authentication	Nature	Secure against
	re-	secret key	-	of the	attacks
	sources	required		third	
				party	
Zhang et	Bell	3	Unidirectional	No	IF, direct
al. [41]	state				measurement on
					channel particles,
					attack on TC
Yuan et	Single	1	Unidirectional	No	IR, EM on TC
al. [87]	photon				
Hong et	Single	1	Unidirectional	No	IF, IR, EM
al. [100]	photon				
Kang et	GHZ-	6	Bidirectional	Untrusted	_
al. [43,	like				
291]					
Zhang et	Bell	6	Bidirectional	Semi-	IF, EM, IR
al. [42]	state			honest	
Jiang et	Bell	18,35	Bidirectional	No	IF, IR, EM
al. [292]	state				
Wu et	Bell	6	Unidirectional	Semi-	External,
al. [293]	state,			honest	dishonest
	GHZ				participants', IF
	state				
Li et al.	GHZ	10,3	Bidirectional	Trusted	IF, EM, IR
[123]	state				
Our	Bell	4	Bidirectional	Untrusted	IF, IR, EM
protocol	state				

2.4 NEW PROTOCOL FOR QUANTUM IDENTITY AUTHENTICATION (PROTOCOL 2.4)

In this work, we introduce a novel QIA scheme, which can be interpreted as a secure direct quantum communication-inspired approach for QIA. Since the protocol utilizes Bell states, it can also be classified as an entangled-state-based QIA protocol. Prior to detailing the proposed scheme, we outline the fundamental concept underlying its design.

2.4.1 CORE CONCEPT

The protocol leverages the properties of Bell states and entanglement swapping. The relationships between Bell states and the pre-shared authentication key can be considered as Equation (2.2). Additionally, the corresponding mappings between Pauli operations and the pre-shared authentication key can be defined as Equation (2.3). To summarize the underlying mechanism of this protocol, consider that Alice and Bob have pre-established an authentication key represented as a bit string of a specific length. Suppose this bit string is 10; accordingly, Alice and Bob generate Bell states based on Equation (2.2).

$$|\psi^{+}\rangle = \frac{1}{\sqrt{2}}(|01\rangle_{12(34)} + |10\rangle_{12(34)}).$$
 (2.13)

Here, subscripts 1,2 and 3,4 denote the particles associated with Alice and Bob, respectively. Alice (Bob) transmits particle 2 (4) to a semi-honest third party, Charlie, who serves as the authentication verifier. Charlie then prepares one of the following quantum states

$$|\pm\rangle = \frac{1}{\sqrt{2}}(|0\rangle_5 \pm |1\rangle_5). \tag{2.14}$$

Consider the scenario where Charlie selects the $|-\rangle$ state. The collective quantum state of Alice, Bob, and Charlie can be represented as follows:

$$|\psi^{+}\rangle_{12} \otimes |\psi^{+}\rangle_{34} \otimes |-\rangle_{5} = \frac{1}{2\sqrt{2}}[(|01\rangle + |10\rangle)_{12} \otimes (|01\rangle + |10\rangle)_{34} \otimes (|0\rangle - |1\rangle)_{5}].$$

Charlie executes a CNOT operation, where Particle 5 serves as the control qubit, and the target qubit is randomly chosen between Particle 2 or Particle 4. Following this, Charlie transmits

Particle 2 to Bob and Particle 4 to Alice. Concurrently, Alice and Bob apply the $i\sigma_y$ operator to their respective particles (Particles 1 and 3) based on their shared secret key $S_{AB} = \{10\}$, as indicated in (2.3). Assuming Particle 2 is designated as the target qubit for the CNOT operation, the resulting joint quantum state after the application of both the CNOT and Pauli operations can be formulated as follows:

$$|\Psi^{10}\rangle_{12345} = \frac{1}{2\sqrt{2}}[|11110\rangle - |10111\rangle - |11000\rangle + |10001\rangle - |00110\rangle + |01111\rangle + |00000\rangle - |01001\rangle]_{12345}.$$
(2.15)

Rearranging this expression, it can be rewritten in an equivalent form

$$|\Psi^{10}\rangle_{14235} = \frac{1}{2\sqrt{2}} [(|\phi^{+}\rangle_{14} \otimes |\phi^{+}\rangle_{23} + |\phi^{-}\rangle_{14} \otimes |\phi^{-}\rangle_{23} - |\psi^{+}\rangle_{14} \otimes |\psi^{+}\rangle_{23} - |\psi^{-}\rangle_{14} \otimes |\psi^{-}\rangle_{23}) \otimes |0\rangle_{5} + (-|\phi^{+}\rangle_{14} \otimes |\psi^{+}\rangle_{23} + |\phi^{-}\rangle_{14} \otimes |\psi^{-}\rangle_{23} + |\psi^{+}\rangle_{14} \otimes |\phi^{+}\rangle_{23} - |\psi^{-}\rangle_{14} \otimes |\phi^{-}\rangle_{23}) \otimes |1\rangle_{5}].$$

$$(2.16)$$

Subsequently, Alice and Bob each conduct Bell measurements on their respective particles—Alice on Particles 1 and 4, and Bob on Particles 2 and 3. They then communicate their classical measurement outcomes to Charlie, following the procedure detailed in (2.2). Charlie proceeds to measure Particle 5 in the computational basis $(\{|0\rangle, |1\rangle\})$, obtaining either $|0\rangle$ or $|1\rangle$ with equal probability $(\frac{1}{2})$. After receiving the classical bits from Alice and Bob, Charlie applies an XOR operation on their results. The set of possible outcomes corresponding to the measurements performed by Alice, Bob, and Charlie in this specific instance is summarized in Table 2.8.

Table 2.8: This outlines the potential measurement results observed by all participants within Protocol 2.4 for QIA.

Alice and Bob's possible combination result	Charlie's result	Additional modulo 2
$ \phi^{+}\rangle_{14}\oplus \phi^{+}\rangle_{23}$	$ 0\rangle_5$	$00 \oplus 00 = 00$
$ \phi^- angle_{14}\oplus \phi^- angle_{23}$	$ 0\rangle_5$	$01 \oplus 01 = 00$
$ \psi^{+}\rangle_{14}\oplus \psi^{+}\rangle_{23}$	$ 0\rangle_5$	$10 \oplus 10 = 00$
$ \psi^{-}\rangle_{14} \oplus \psi^{-}\rangle_{23}$	$ 0\rangle_5$	$11 \oplus 11 = 00$
$ \phi^{+}\rangle_{14} \oplus \psi^{+}\rangle_{23}$	$ 1\rangle_5$	$00 \oplus 10 = 10$
$ \phi^- angle_{14}\oplus \psi^- angle_{23}$	$ 1\rangle_5$	$01 \oplus 11 = 10$
$ \psi^{+}\rangle_{14} \oplus \phi^{+}\rangle_{23}$	$ 1\rangle_5$	$10 \oplus 00 = 10$
$ \psi^{-}\rangle_{14} \oplus \phi^{-}\rangle_{23}$	$ 1\rangle_5$	$11 \oplus 01 = 10$

From Table 2.8, it is evident that if Charlie receives the state $|0\rangle$, the XOR of the classical

bits transmitted by Alice and Bob consistently results in 00. Conversely, if Charlie obtains the state $|1\rangle$, the XOR operation always yields 10. Any deviation from these expected results would indicate the presence of an eavesdropper. A similar methodology can be applied to derive the same conclusion for alternative secret keys. For instance, consider the secret key $S_{AB} = \{11\}$. In this scenario, both Alice and Bob select the Bell state $|\psi^-\rangle$, with Charlie designating his particle $|+\rangle$ as the control qubit. The collective quantum state of the three parties can be represented as follows:

$$|\psi^{-}\rangle_{12} \otimes |\psi^{-}\rangle_{34} \otimes |+\rangle = \frac{1}{2\sqrt{2}}[(|01\rangle - |10\rangle)_{12} \otimes (|01\rangle - |10\rangle)_{34} \otimes (|0\rangle + |1\rangle)_{5}].$$

Alice and Bob send their respective particles 2 and 4 to Charlie and apply the σ_z operator on their respective particles 1 and 3. Charlie then executes a CNOT operation, using his particle as the control qubit and particle 4 as the target qubit. Following this, he returns particle 2 (4) to Bob (Alice). After completing these operations, the quantum state evolves into

$$\begin{aligned} |\Psi^{11}\rangle_{12345} &= \frac{1}{2\sqrt{2}}[|01010\rangle - |01001\rangle - |01100\rangle + |01111\rangle \\ &- |10010\rangle + |10001\rangle + |10100\rangle - |10111\rangle]_{12345}. \end{aligned}$$
(2.17)

Alice and Bob subsequently perform Bell measurements on their respective particle pairs (1 and 4 for Alice, 2 and 3 for Bob), obtaining outcomes correlated with Charlie's measurement results, as previously discussed. For clarity, the above expression can be further simplified to

$$|\Psi^{11}\rangle_{14235} = \frac{1}{2\sqrt{2}} [(|\phi^{+}\rangle_{14} \otimes |\phi^{+}\rangle_{23} - |\phi^{-}\rangle_{14} \otimes |\phi^{-}\rangle_{23} + |\psi^{+}\rangle_{14} \otimes |\psi^{+}\rangle_{23} - |\psi^{-}\rangle_{14} \otimes |\psi^{-}\rangle_{23}) \otimes |0\rangle_{5} + (|\phi^{+}\rangle_{14} \otimes |\psi^{+}\rangle_{23} - |\phi^{-}\rangle_{14} \otimes |\psi^{-}\rangle_{23} + |\psi^{+}\rangle_{14} \otimes |\phi^{+}\rangle_{23} - |\psi^{-}\rangle_{14} \otimes |\phi^{-}\rangle_{23}) \otimes |1\rangle_{5}].$$

$$(2.18)$$

Analyzing Equation (2.18) confirms the same conclusions outlined in Table 2.8. Furthermore, to establish that this conclusion holds for the remaining secret keys {01} and {10}, the final quantum state shared among Alice, Bob, and Charlie can be expressed as follows:

$$|\Psi^{01}\rangle_{14235} = \frac{1}{2\sqrt{2}}[(|01100\rangle + |00101\rangle + |00110\rangle + |01111\rangle + |11000\rangle + |10001\rangle + |10010\rangle + |11011\rangle]_{14235}$$
$$= \frac{1}{2\sqrt{2}}[(|\psi^{+}\rangle_{14} \otimes |\psi^{+}\rangle_{23} - |\psi^{-}\rangle_{14} \otimes |\psi^{-}\rangle_{23} + |\phi^{+}\rangle_{14} \otimes |\phi^{+}\rangle_{23} - |\phi^{-}\rangle_{14} \otimes |\phi^{-}\rangle_{23}) \otimes |0\rangle_{5} + (|\phi^{+}\rangle_{14} \otimes |\psi^{+}\rangle_{23} - |\phi^{-}\rangle_{14} \otimes |\psi^{-}\rangle_{23} + |\psi^{+}\rangle_{14} \otimes |\phi^{+}\rangle_{23} - |\psi^{-}\rangle_{14} \otimes |\phi^{-}\rangle_{23}) \otimes |1\rangle_{5}],$$
(2.19)

and

$$|\Psi^{00}\rangle_{14235} = \frac{1}{2\sqrt{2}}[(|10010\rangle + |11011\rangle - |11000\rangle - |10001\rangle - |00110\rangle - |01111\rangle + |01100\rangle + |00101\rangle]_{14235}$$
$$= \frac{1}{2\sqrt{2}}[(|\psi^{+}\rangle_{14} \otimes |\psi^{+}\rangle_{23} - |\psi^{-}\rangle_{14} \otimes |\psi^{-}\rangle_{23} - |\phi^{+}\rangle_{14} \otimes |\phi^{+}\rangle_{23} + |\phi^{-}\rangle_{14} \otimes |\phi^{-}\rangle_{23}) \otimes |0\rangle_{5} + (|\phi^{+}\rangle_{14} \otimes |\psi^{+}\rangle_{23} - |\phi^{-}\rangle_{14} \otimes |\psi^{-}\rangle_{23} - |\psi^{+}\rangle_{14} \otimes |\phi^{+}\rangle_{23} + |\psi^{-}\rangle_{14} \otimes |\phi^{-}\rangle_{23}) \otimes |1\rangle_{5}].$$
(2.20)

Equations (2.19) and (2.20) align with the authentication criteria specified in Table 2.8 for the secret keys $S_{AB} = \{01\}$ and $\{00\}$, respectively. In this protocol, the controller does not require any permutation operation to manage authentication; instead, quantum mechanical principles facilitate the process.

2.4.2 DESCRIPTION OF PROTOCOL 2.4

Alice and Bob aim to authenticate themselves as legitimate users with the assistance of a third party, Charlie. Within this protocol, Alice and Bob share a pre-established classical secret key sequence, denoted as $K_{AB} = \{k_1^1 k_2^1, k_1^2 k_2^2, k_1^3 k_2^3, \cdots, k_1^i k_2^i, \cdots, k_1^n k_2^n, \}$. Before detailing the protocol in a stepwise manner, it is essential to briefly discuss the role of decoy states in establishing a secure communication channel between any two entities [277, 294]. In general, one party introduces decoy qubits at random positions within the sequence of information qubits and transmits this extended sequence to the other party. Upon receiving it, the second party requests the positional and encoding details of the decoy qubits via an unjammable public channel. The first party then publicly discloses this information, allowing the second party to verify it by measuring the decoy qubits. If the detected error rate exceeds an acceptable threshold, both

parties discard the entire qubit sequence. This decoy-state mechanism enhances channel security, ensuring the secure transmission of information between parties. The authentication process consists of the following steps:

Step 4.1: Alice and Bob independently generate a series of n Bell states, denoted as A_{12} and B_{34} , respectively. The preparation follows the pre-shared key K_{AB} and adheres to the rule specified in (2.2). The sequences are represented as follows:

$$A = \{|A\rangle_{12}^{1}, |A\rangle_{12}^{2}, |A\rangle_{12}^{3}, \cdots, |A\rangle_{12}^{i}, \cdots, |A\rangle_{12}^{n}\},$$

$$B = \{|B\rangle_{34}^{1}, |B\rangle_{34}^{2}, |B\rangle_{34}^{3}, \cdots, |B\rangle_{34}^{i}, \cdots, |B\rangle_{34}^{n}\}.$$
(2.21)

The subscripts 1, 2, 3, and 4 are used to distinguish the particles in the sequences. Ideally, A = B. Here, the subscripts (1, 2, 3, 4) are used to distinguish individual particles in each sequence. Ideally, the prepared sequences satisfy A = B.

Step 4.2: Each Bell state is then separated into two ordered sequences of *n* particles. The first particle of each Bell state forms one sequence, while the second particle forms another.

$$S_{1} = \{s_{1}^{1}, s_{1}^{2}, s_{1}^{3}, \dots, s_{1}^{i}, \dots, s_{1}^{n}\},$$

$$S_{2} = \{s_{2}^{1}, s_{2}^{2}, s_{2}^{3}, \dots, s_{2}^{i}, \dots, s_{2}^{n}\},$$

$$S_{3} = \{s_{3}^{1}, s_{3}^{2}, s_{3}^{3}, \dots, s_{3}^{i}, \dots, s_{3}^{n}\},$$

$$S_{4} = \{s_{4}^{1}, s_{4}^{2}, s_{4}^{3}, \dots, s_{4}^{i}, \dots, s_{4}^{n}\}.$$

$$(2.22)$$

The sequences S_1 and S_2 consist of the first and second particles of all Bell states in A, respectively. Likewise, S_3 and S_4 are composed of the first and second particles of all Bell states in B. Alice and Bob retain sequences S_1 and S_3 while proceeding with further operations. To enhance security, Alice and Bob each randomly introduce decoy particles, d_a and d_a , into sequences S_2 and S_4 , respectively. This results in expanded sequences S_2' and S_4' . Alice then transmits S_2' to Charlie via a quantum channel, while Bob also sends S_4' to Charlie.

Step 4.3: Upon receiving S'_2 and S'_4 , Charlie performs security verification using the embedded decoy particles. If the security check is successful, Charlie removes the decoy particles to recover the original sequences S_2 and S_4 . Next, Charlie generates a sequence of n qubits:

$$S_5 = \{s_5^1, s_5^2, s_5^3, \cdots, s_5^i, \cdots, s_5^n\}$$

Each qubit in S_5 is prepared in either the $|+\rangle$ or $|-\rangle$ state at random. Charlie then applies a CNOT operation, using the qubits in S_5 as the control qubits and those in S_2 or S_4 as the target qubits, selected randomly.

- **Step 4.4:** Charlie generates decoy particles, denoted as d_c and d_d , and randomly integrates them into the sequences S_2 and S_4 , thereby forming the extended sequences S_2' and S_4' . These modified sequences, S_2' and S_4' , are then transmitted to Bob and Alice, respectively. Following successful security validation using the decoy particles and their subsequent removal, Alice retains the sequences S_1 and S_4 , while Bob holds S_2 and S_3 .
- Step 4.5: Alice (Bob) applies the Pauli operation on the particles in sequence S_1 (S_3) based on a pre-established classical key, as specified in (2.3). This operation transforms the sequences into S_1^* and S_3^* . Alice then conducts a Bell-state measurement on the particles in S_1^* and S_4 , recording the measurement outcomes as a classical sequence $R_{14} = \{r_{14}^1, r_{14}^2, \cdots, r_{14}^i, \cdots, r_{14}^n\}$, following (2.2). Similarly, Bob performs a Bell-state measurement on the particles in S_2 and S_3^* , obtaining the classical sequence $R_{23} = \{r_{23}^1, r_{23}^2, \cdots, r_{23}^i, \cdots, r_{23}^n\}$. Both Alice and Bob forward their respective measurement results, R_{14} and R_{23} , to Charlie. Concurrently, Charlie measures the sequence S_5 using the computational basis $\{|0\rangle, |1\rangle\}$, producing the sequence $R_5 = \{r_5^1, r_5^2, \cdots, r_5^i, \cdots, r_5^n\}$, where each outcome r_5^i takes a value of either 0 or 1, corresponding to the states $|0\rangle$ and $|1\rangle$, respectively.
- **Step 4.6:** At this stage, the third party, Charlie, possesses three classical sequences: $R_{14} = \{r_{14}^1, r_{14}^2, \cdots, r_{14}^i, \cdots, r_{14}^n\}, R_{23} = \{r_{23}^1, r_{23}^2, \cdots, r_{23}^i, \cdots, r_{23}^n\}$ and $R_5 = \{r_5^1, r_5^2, \cdots, r_5^i, \cdots, r_5^n\}$. Charlie executes an XOR operation on the bit strings R_{14} and R_{23} at corresponding positions. If r_5^i is 0 and the XOR result is $r_{14}^i \oplus r_{23}^i = 00$, or if r_5^i is 1 and the XOR result is $r_{14}^i \oplus r_{23}^i = 10$, then Charlie confirms the authentication of Alice and Bob.
- **Step 4.7:** Charlie then publicly verifies and announces the authentication status of Alice and Bob via an unjammable public channel.

The QIA protocol elaborated above is also illustrated through a flowchart, as depicted in Figure 2.6.

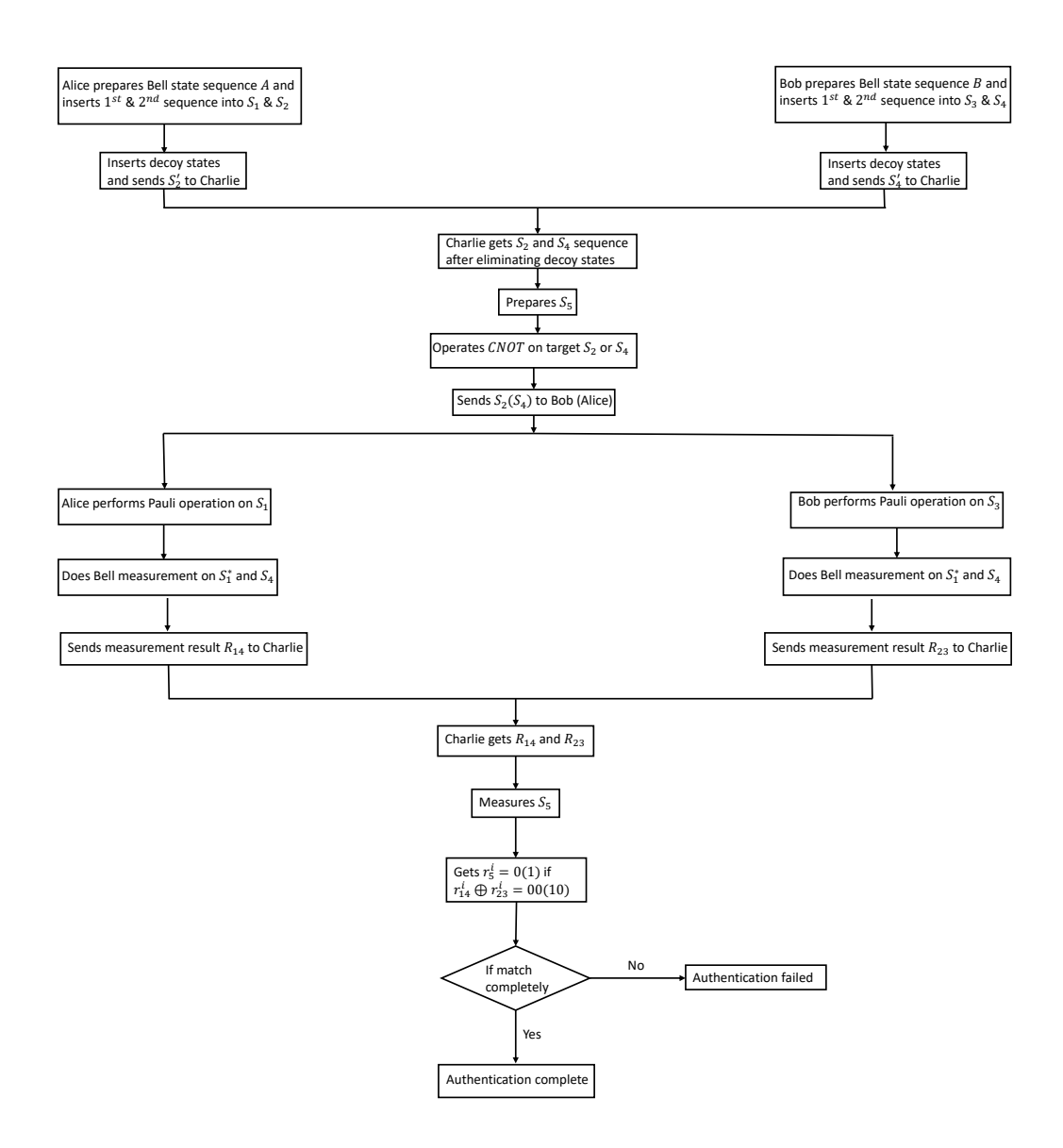


Figure 2.6: A flowchart visually represents the operational framework of the proposed QIA protocol.

2.4.3 SECURITY ANALYSIS OF PROTOCOL 2.4

This section aims to evaluate the security of the proposed protocol against several well-known attacks that an eavesdropper (Eve) could potentially execute. It is important to note that insider attacks are not considered in this analysis, as they are irrelevant in the context of QIA. The following discussion will demonstrate the security of the protocol against specific attack scenarios. Initially, we assess its resilience against impersonation attacks, where an external adversary, Eve attempts to mimic a legitimate user, Alice or Bob, to bypass the authentication mechanism.

2.4.3.1 SECURITY EVALUATION OF PROTOCOL 2.4 AGAINST IMPERSONATION ATTACK BY EVE

To analyze the security of the protocol, consider the scenario outlined in Section 2.4, where an adversary, Eve, attempts to impersonate Alice. Eve initiates the attack by selecting the Bell state $|\phi^+\rangle_{12}$ and transmits the sequence S_{e2} (comprising particle 2) to Charlie. Following the protocol, Charlie processes the sequence and returns S_{2e} (denoted as S_4) to Bob, who in this case is Eve. Then Eve executes the protocol steps as Alice would, applying the Pauli identity operation (*I*) on Particle 1. Subsequently, Bob and Eve perform Bell state measurements. The results, presented in Table 2.9, indicate scenarios that reveal Eve's presence. Since Eve lacks knowledge of the legitimate key K_{AB} , her probability of selecting the correct Bell state at each step is $\frac{1}{4}$. To bypass detection, she must correctly guess all n Bell states, making the overall probability of a successful impersonation attack $(\frac{1}{4})^n$. As n increases significantly, this probability approaches zero. Therefore, the probability P(n) of detecting Eve is given by, $P(n) = 1 - (\frac{1}{4})^n$. For sufficiently large n, P(n) approaches 1, ensuring the detection of an impersonation attempt. Figure 2.7 illustrates the dependence of P(n) on n, demonstrating that at least six bits of pre-shared classical information are required to reliably detect Eve's presence.

2.4.3.2 SECURITY ANALYSIS OF PROTOCOL 2.4 AGAINST INTERCEPT AND RE-SEND ATTACK

In this protocol, Alice and Bob generate Bell states based on their pre-shared secret key. Neither Alice nor Bob transmits their quantum states in their entirety, forcing Eve to intercept only one

Table 2.9: Possible results of measurements.

Eve and Bob's possible combined result	Charlie's result	Modulo 2 addition
$\overline{ \psi^+ angle_{14}\!\otimes\! \psi^- angle_{23}}$	$ 0\rangle_5$	$10 \oplus 11 = 01$
$ \psi^{-} angle_{14}\!\otimes\! \psi^{+} angle_{23}$	$ 0\rangle_5$	$11 \oplus 10 = 01$
$ \phi^{+} angle_{14}\otimes \phi^{-} angle_{23}$	$ 0\rangle_5$	$00 \oplus 01 = 01$
$ \phi^{-} angle_{14}\otimes \phi^{+} angle_{23}$	$ 0\rangle_5$	$01 \oplus 00 = 01$
$ \psi^{+}\rangle_{14}\otimes \phi^{-}\rangle_{23}$	$ 1\rangle_5$	$10 \oplus 01 = 11$
$ \psi^{-}\rangle_{14}\otimes \phi^{+}\rangle_{23}$	$ 1\rangle_5$	$11 \oplus 00 = 11$
$ \phi^{+} angle_{14}\otimes \psi^{-} angle_{23}$	$ 1\rangle_5$	$00 \oplus 11 = 11$
$ \phi^{-} angle_{14}\otimes \psi^{+} angle_{23}$	$ 1\rangle_5$	$01 \oplus 10 = 11$

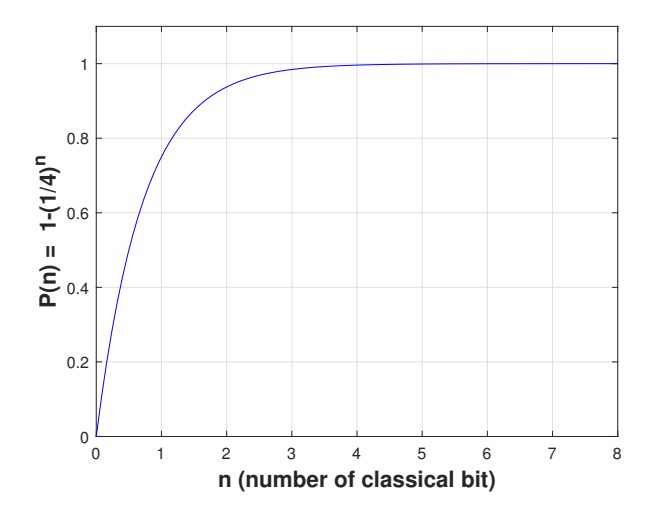


Figure 2.7: The probability of detecting Eve's interference denoted as P(n), is correlated with the number of classical bits, n, utilized as the pre-shared authentication key.

particle at a time. Without loss of generality, we assume Eve targets Particle 2 (Particle 4) when Alice sends it to Charlie (or when Charlie sends it to Alice). The amount of information Eve can extract from the quantum channel is fundamentally constrained by the "Holevo bound or "Holevo quantity" [274].

$$\chi(\rho) = S(\rho) - \sum_{i} p_i S(\rho_i), \qquad (2.23)$$

Considering the von Neumann entropy, defined as $S(\rho) = -Tr(\rho \log_2 \rho)$, where ρ_i represents a component of the mixed state ρ with probability p_i , the density matrix can be expressed as: $\rho = \sum_i p_i \rho_i = \frac{1}{4} \left[|\Psi^{00}\rangle \langle \Psi^{00}| + |\Psi^{01}\rangle \langle \Psi^{01}| + |\Psi^{10}\rangle \langle \Psi^{10}| + |\Psi^{11}\rangle \langle \Psi^{11}| \right]_{14235}$. Here, ρ_i corresponds to the density matrices of the states described in (2.15), (2.17), (2.19), and (2.20). Since Eve targets particle 2 (or 4), Equation (2.23) can be reformulated accordingly.

$$\chi(\rho_{2(4)}) = S(\rho_{2(4)}) - \sum_{i} p_{i} S(\rho_{2(4)_{i}}). \tag{2.24}$$

Here, the reduced density matrices $\rho_{2(4)}$ and $\rho_{2(4)_i}$ correspond to ρ and ρ_i , respectively, after performing a partial trace over particles 1, 4(2), 3, and 5. The resultant reduced density matrix for particle 2 (or 4) consistently takes the form:

$$\rho_{2(4)} = Tr_{14(2)35}(\rho)$$

$$= \frac{1}{8} \times (|0\rangle\langle 0| + |1\rangle\langle 1|) \times 4$$

$$= \frac{1}{2}I_2.$$

Furthermore, it follows that $\rho_{2(4)_i} = \frac{1}{2}I$. By substituting $\rho_{2(4)}$ and $\rho_{2(4)_i}$ into Equation (2.24), we obtain $\chi(\rho_{2(4)}) = 0$. This result indicates that an adversary, Eve would be unable to extract any useful information through a direct measurement attack on particle 2 (or 4). Beyond this scenario, we must also consider an alternative attack strategy where Eve attempts to gain information from both particles 2 and 4 simultaneously. Employing the same reasoning, we determine that the Holevo bound constraints Eve from accessing any meaningful data. To align with our conditions, we reformulate Equation (2.23) in the following manner:

$$\chi(\rho_{24}) = S(\rho_{24}) - \sum_{i} p_i S(\rho_{24_i}). \tag{2.25}$$

Here, ρ_{24} and ρ_{24_i} represent the reduced density matrices of ρ and ρ_i , respectively, after tracing out particles 1, 3, and 5. Since the overall conditions remain unchanged, a straightforward calculation yields:

$$\rho_{24} = Tr_{135}(\rho) = \frac{1}{8} \times (|00\rangle\langle 00| + |01\rangle\langle 01| + |10\rangle\langle 10| + |11\rangle\langle 11|) \times 2 = \frac{1}{4}I_4,$$

where I_4 denotes the 4×4 identity matrix. The von Neumann entropy of each component of the mixed state ρ after partial tracing, specifically ρ_{24_i} , is given by $\rho_{24_i} = \frac{1}{4}I_4$. Substituting ρ_{24} and ρ_{24_i} into Equation (2.25) results in $\chi(\rho_2) = 0$. Consequently, it can be concluded that Eve is unable to acquire any key information through a direct intercept attack on the transmitted particles. A schematic representation of Eve's intercept-resend attack strategy is illustrated in Figure 2.8.

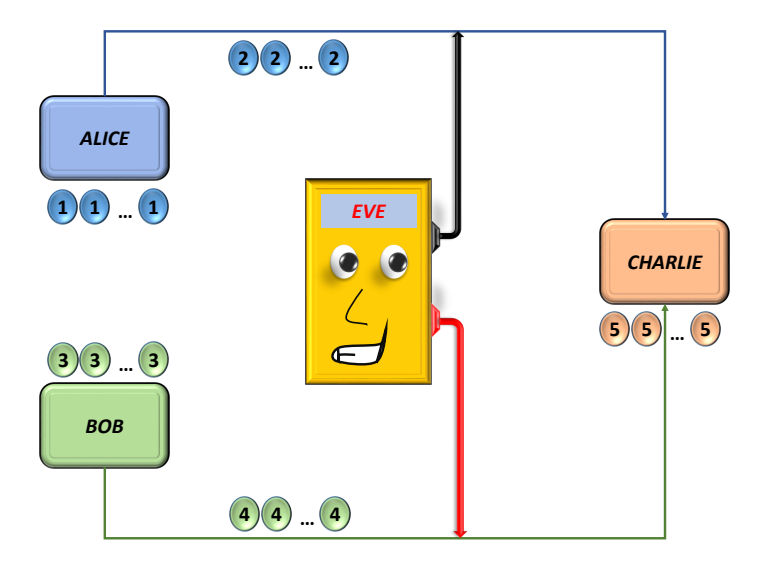


Figure 2.8: Eve employs an intercept-and-resend strategy. In this context, the qubits labeled as 1, 2, 3, 4, and 5 correspond to the sequences S_1 , S_2 , S_3 , S_4 , and S_5 , respectively.

2.4.3.3 SECURITY ANALYSIS OF PROTOCOL 2.4 AGAINST IMPERSONATED FRAUD-ULENT ATTACK

To successfully impersonate Alice, Eve's optimal approach involves interacting with the traveling particle (qubit 2) that Alice transmits, using an ancillary state she prepares. After applying a general operation to the traveling qubit, the resulting state is expressed as follows:

$$U_E|1\chi\rangle_{2e} = (a_0|10\rangle + b_0|11\rangle + c_0|00\rangle + d_0|01\rangle)_{2e},$$
(2.26)

$$U_E|0\chi\rangle_{2e} = (a_1|10\rangle + b_1|11\rangle + c_1|00\rangle + d_1|01\rangle)_{2e}.$$
 (2.27)

Here, $|\chi\rangle_e$ represents Eve's ancillary state, where the subscript e signifies that it is prepared by Eve, and 2 denotes Alice's traveling qubit. The normalization condition is maintained as $|a_1^2| + |b_1^2| + |c_1^2| + |d_1^2| = |a_0^2| + |b_0^2| + |c_0^2| + |d_0^2| = 1$. Through her operation, Eve generates the state:

$$|\Psi'\rangle_{12e} = \frac{1}{\sqrt{2}} \left(a_0 |010\rangle + b_0 |011\rangle + c_0 |000\rangle + d_0 |001\rangle + a_1 |110\rangle + b_1 |111\rangle + c_1 |100\rangle + d_1 |101\rangle \right). \tag{2.28}$$

For simplicity, Eve applies a general operation on the traveling qubit while retaining her own qubit. She then forwards Alice's qubit to Charlie, who processes it according to the prescribed

protocol before returning it. The objective is to determine the final composite state, factoring in Eve's attack within the scenario outlined in Section 2.4.

$$\begin{split} |\Psi''\rangle_{12e345} &= \frac{1}{2\sqrt{2}}[a_0|110110\rangle - a_0|100111\rangle - a_0|110000\rangle + a_0|100001\rangle \\ &+ b_0|111110\rangle - b_0|101111\rangle - b_0|111000\rangle + b_0|101001\rangle \\ &- c_0|100110\rangle - c_0|110111\rangle - c_0|100000\rangle + c_0|110001\rangle \\ &+ d_0|101110\rangle - d_0|111111\rangle - d_0|101000\rangle + d_0|111001\rangle \\ &- a_1|010110\rangle + a_1|000111\rangle + a_1|010000\rangle + a_1|000001\rangle \\ &- b_1|011110\rangle + b_1|001111\rangle + b_1|011000\rangle - b_1|001001\rangle \\ &- c_1|000110\rangle + c_1|010111\rangle + c_1|000000\rangle - c_1|010001\rangle \\ &- d_1|001110\rangle + d_1|011111\rangle + d_1|001000\rangle - d_1|011001\rangle]. \end{split}$$

Upon receiving particle 4 from Charlie, Eve and Bob conduct a Bell measurement on their respective particles and transmit the classical sequence of measurement outcomes to Charlie. By enforcing the authentication condition, the probabilities of Eve successfully passing authentication and failing authentication can be determined as $\frac{1}{4}(|b_0|^2+|c_0|^2)+\frac{1}{8}$ and $\frac{1}{4}(|a_0|^2+|d_0|^2+1)+\frac{3}{8}$, respectively. If Eve prepares the ancillary state to maximize $|b_0|^2+|c_0|^2$ while minimizing $|a_0|^2+|d_0|^2$, she can achieve the highest possible deception probability as an authenticated participant, given by $P_3^2=\frac{3}{8}$. For all other scenarios, the probability satisfies $P_3^2\leq\frac{3}{8}$. This analysis confirms that the protocol remains secure under an acceptable error threshold even in the most favorable conditions for a collective attack by Eve.

2.4.4 COMPARISON OF PROTOCOL 2.4 WITH A SET OF EXISTING PROTOCOLS

In this section, we provide a concise comparison of the proposed protocol with previously introduced QIA schemes. The evaluation considers key aspects such as quantum resource utilization, the nature of the third party (whether it is assumed to be honest, semi-honest, or untrusted), the minimum number of qubits required for authentication (i.e., the total number of qubits needed to execute the protocol when the pre-shared authentication key size is 1 bit), and whether the protocol supports bidirectional authentication (mutual verification) or only allows one party to authenticate the other (unidirectional). Given the extensive range of QIA schemes, a representative subset has been selected for comparison, with a particular focus on those derived

from secure direct quantum communication protocols, as the proposed scheme shares a similar foundation. Specifically, the protocol presented here is inspired by CDSQC.

To initiate the comparison, we analyze Zhang et al.'s QIA scheme [41] from 2006, which employs the ping-pong protocol for QSDC. In this protocol, Alice functions as the trusted "certification authority", while Bob represents a regular user whose identity requires validation by Alice. A similar framework is observed in Yuan et al.'s protocol [87], which is based on the single-photon QSDC protocol known as the LM05 protocol, wherein Alice also serves as the certification authority. Notably, both of these QSDC-based QIA protocols [41, 87] operate in a unidirectional manner, unlike the proposed scheme, which enables bidirectional authentication. This characteristic provides a distinct advantage of the proposed protocol over Zhang et al.'s scheme. Furthermore, this advantage extends beyond Zhang et al.'s protocol to a broader category of unidirectional QIA protocols, such as Hong et al.'s scheme [100]. However, this advantage is not exclusive, as similar bidirectional capabilities are also demonstrated in Kang et al.'s protocols [43, 291] and Zhang et al.'s 2020 work [42]. A key distinction is that these protocols [43, 291, 42] necessitate at least six qubits for authentication, whereas the proposed scheme requires a minimum of only five qubits. Given the high cost of quantum resources, this reduction can be considered beneficial. Additionally, Kang et al.'s protocols [43, 291] utilize GHZ-like states, which are tripartite entangled states that are comparatively more complex to generate and maintain than the Bell states adopted in the proposed scheme. Moreover, in Zhang et al.'s 2020 protocol, the third party is assumed to be semi-honest, whereas in the proposed scheme, the third party is treated as untrusted, thereby enhancing security. Consequently, the proposed scheme efficiently achieves the desired QIA features while optimizing resource utilization. The comparison conducted to establish the significance of the proposed protocol, particularly concerning entangled-state-based QIA schemes, is summarized in Table 2.10.

2.5 CONCLUSIONS

We have examined the existing protocols for QIA in Chapter 1 to discern their inherent symmetry. This analysis has identified symmetries across various protocols, facilitating their classification and enabling the formulation of straightforward strategies to adapt these protocols for different quantum computing and communication applications, ultimately leading to novel QIA schemes. To substantiate this approach, four new QIA protocols have been introduced and

Table 2.10: Detailed comparison of Protocol 2.4 with previous protocols.

Protocol	Quantum	Minimum	Way of	Nature of the
	Resources	number of	authentication	third party
		qubits		
		required		
Zhang et al.	Bell state	3	unidirectional	no
[41]				
Yuan et al.[87]	Single photon	1	unidirectional	no
Hong et al.	Single photon	1	unidirectional	no
[100]				
Kang et al.	GHZ-like	6	bidirectional	untrusted
[43, 291]				
Zhang et al.	Bell state	6	bidirectional	semi-honest
[42]				
Proposed	Bell state	5	bidirectional	untrusted
Protocol 2.4				

demonstrated to be secure against specific potential attacks. Notably, many of the discussed protocols, including several existing ones, are not practically implementable with current technology. For instance, certain protocols require a user to retain a photon until the travel photon(s) return, such as in ping-pong-based QIA schemes [41] or authentication mechanisms outlined in [45, 38, 40, 70, 39, 85, 43, 110]. The feasibility of such QIA protocols is hindered by the necessity of quantum memory, which remains commercially unviable. In particular, most entangledstate-based QSDC protocols for QIA, as well as entangled-state protocols relying on quantum private comparison and those involving a third party (e.g., Trent) responsible for storing a photon, encounter similar limitations. At present, it is preferable to prioritize QIA protocols that do not rely on quantum memory. Notably, the protocols introduced in this work do not require quantum memory, making them feasible with existing technology. While numerous approaches have been proposed for constructing quantum memory, and such memory-dependent schemes may become beneficial in the future, direct teleportation-based QIA schemes (such as those in [70, 85]) are unlikely to have widespread applications, even in the long term. This limitation arises because teleportation can only facilitate secure quantum communication in the absence of noise in the quantum channel. Additionally, any protocol dependent on shared entanglement (e.g., those discussed in [63, 64, 40, 45, 38, 70]) may necessitate entanglement purification or concentration, as shared entanglement degrades due to decoherence. These processes could introduce undesirable and potentially insecure interactions between Alice and Bob. Despite these challenges and technological constraints, research in QIA is advancing rapidly, largely due to

the fact that the purported unconditional security of quantum cryptographic protocols hinges on the robustness of the identity authentication mechanisms employed.

The current chapter, in conjunction with our research references [166, 234], highlights the potential for developing a diverse range of novel QIA schemes. A thorough investigation in this domain could be instrumental in identifying the most effective QIA scheme that can be realized with existing technology. The proposed QIA protocol is an entangled-state-based approach that employs Bell states. Drawing inspiration from secure direct quantum communication, it enables Alice to transmit information securely to Bob, contingent upon authorization from controller Charlie, without requiring pre-shared keys. While the protocol exclusively utilizes Bell states, its implementation demands quantum memory, which is not yet commercially accessible. However, this constraint is not specific to the proposed protocol but is a common challenge across various QIA, QSDC, DSQC, and quantum dialogue protocols. With increasing research efforts and advancements in quantum memory technology, along with recent proposals for its development, commercial availability is expected in the near future [295]. Meanwhile, a delay mechanism can function as an interim solution to replace quantum memory in implementing the proposed QIA protocol, thereby improving the robustness of secure quantum communication protocols. The other two proposed protocols in this chapter utilize a single-photon source as the qubit. These protocols are viable for implementation using current technology to facilitate bi-directional identity authentication.

Furthermore, to provide a comprehensive discussion, it is important to acknowledge the numerous post-quantum authentication schemes introduced in recent years [296, 297]. However, these schemes have not been covered here, as they are fundamentally classical and only conditionally secure. A key underlying assumption of these schemes is that quantum computers will be unable to efficiently solve problems beyond the bounded-error "quantum polynomial time" complexity class. This assumption lacks formal proof and is essentially equivalent to presume that if an efficient algorithm for a given computational problem is not currently known, it will remain undiscoverable in the future.

CHAPTER 3

QUANTUM KEY DISTRIBUTION WITH TIGHT SECURITY BOUNDS

3.1 INTRODUCTION

Cryptography has been a fundamental tool for securing information since ancient times. Traditionally, cryptographic techniques concealed secret data, but advancements in cryptanalysis often led to their decryption. A major breakthrough occurred in the 1970s with the advent of the schemes for public-key cryptography, including RSA [21] and Diffie-Hellman (DH) [22] schemes, whose security relies on the computational complexity of the tasks like factorization of odd square-free bi-primes and discrete logarithm problems [23], respectively. The security of these schemes is essentially obtained from the fact that the computational problems (i.e., factorization of odd square-free bi-primes and discrete logarithm problems) that are used to construct these schemes for cryptography belong to the NP complexity class, and thus these problems cannot be solved efficiently, i.e., in a polynomial number of steps. In contrast to these classical results, in 1994, Peter W. Shor [24] demonstrated that quantum computers can efficiently (i.e., in polynomial time) solve these two problems. This established that classical cryptographic schemes like RSA and DH are vulnerable against attacks using quantum computers. Thus, a challenge arose from quantum algorithms outperforming classical counterparts in solving complex tasks. However, QKD offers a solution by ensuring security through fundamental physical laws rather than computational complexity. Notably, the first QKD protocol was introduced a decade before Shor's breakthrough by Bennett and Brassard in 1984 [15]. Principles such as the no-cloning theorem [25], measurement collapse, and Heisenberg's uncertainty principle underpin QKD security, enabling implementations with polarization-encoded single photons and other photonic qubits. While QKD ideally detects eavesdropping, practical limitations in devices may allow undetected breaches. The BB84 protocol paved the way for various QKD protocols [16, 32, 160, 134] and other cryptographic applications [51, 53, 161, 148, 106, 107, 62, 134, 162] (for a review, see [163, 164]). Each protocol offers distinct advantages and limitations. While most are unconditionally secure in an ideal setting, practical implementations suffer from device imperfections, leading to vulnerabilities via side-channel attacks. Quantum identity authentication [63, 165, 166] is essential before executing a QKD protocol to ensure secure communication. However, real-world QKD implementations face challenges, such as the requirement for a true single-photon source. Protocols like BB84 and B92 [16] ideally depend on single-photon states sent from Alice to Bob. Although significant experimental progress has been made toward reliable single-photon sources [167, 168], most commercial systems use WCP by attenuating laser outputs as an approximation. The quantum state of an attenuated WCP can be described as:

$$|\alpha\rangle = |\sqrt{\mu} \exp(i\theta)\rangle = \sum_{n=0}^{\infty} \left(\frac{e^{-\mu}\mu^n}{n!}\right)^{\frac{1}{2}} \exp(in\theta)|n\rangle.$$
 (3.1)

A Fock state $|n\rangle$ represents an n-photon state, with Alice generating a quantum state as a superposition of Fock states following a Poissonian photon number distribution: $p(n,\mu) = \frac{e^{-\mu}\mu^n}{n!}$, where the mean photon number is $\mu = |\alpha|^2 \ll 1$. Using such a source, Alice emits the desired one-photon state with probability $p(1,\mu)$, while multi-photon pulses occur with probability $1 - p(0,\mu) - p(1,\mu)$. This enables Eve to exploit a PNS attack [170]. In long-distance communication, channel loss further facilitates eavesdropping, as an adversary with advanced technology can replace the lossy channel with a transparent one and intercept signals undetected [171]. To mitigate PNS attacks, Scarani et al. introduced the SARG04 QKD protocol in 2004 [172]. Here, we propose two novel QKD protocols designed to counter not only PNS attacks but also a broader range of attacks while offering specific advantages over SARG04 and similar existing protocols.

Information splitting is a fundamental aspect of every QKD protocol. In BB84 and B92, information is divided into a classical component (basis choice) and a quantum component (transmitted qubits), whereas in SARG04, a similar division occurs. However, protocols like GV protocol [160] split information into two quantum parts. The security of these protocols stems from Eve's inability to access both pieces simultaneously. This raises an important question: Can protocol efficiency and secret-key rate bounds be modified by reducing the classical information content? To explore this, we use SARG04 as a test case and introduce two new QKD

protocols that contain less classical information than SARG04. The SARG04 protocol was designed to mitigate the PNS attack but is less efficient than other single-photon QKD schemes. Efficiency is assessed using Cabello's definition [173], assuming equal costs for qubit and classical bit transmission and a low-noise quantum channel—conditions that are often unrealistic for long-distance communication. Motivated by these limitations, we investigate whether increasing quantum resource utilization can counteract the PNS attack while reducing dependence on classical resources. Our goal is to develop two new QKD protocols that enhance efficiency compared to SARG04 while maintaining resilience against PNS and other standard attacks. The structure of the chapter is outlined as follows. Section 3.2 introduces a novel QKD protocol based on single-photon transmissions, which eliminates the necessity for an ideal single-photon source. This protocol, designated as Protocol 3.1, is initially presented in a generalized framework, followed by a stepwise explanation. A minor modification in the sifting subprotocol of Protocol 3.1 results in an improved protocol (Protocol 3.2) with enhanced efficiency. Section 3.3 provides a comprehensive security analysis, utilizing a depolarizing channel to model errors introduced by either Eve or the communication channel itself. This approach enables the determination of the tolerable error threshold for the initial quantum particle sequence generated by Bob. Additionally, security is evaluated against various collective attack strategies. Section 3.4 examines the PNS attack on both Protocol 3.1 and Protocol 3.2, deriving the critical distance and demonstrating the benefits of employing a relatively higher quantum resource allocation. Finally, Section 3.5 presents the conclusion of the chapter.

3.2 PROPOSED QUANTUM KEY DISTRIBUTION PROTOCOLS (PROTOCOL 3.1 AND 3.2)

As previously discussed, numerous QKD protocols that rely on non-orthogonal state sequences require the partitioning of information into quantum and classical components. This segmentation ensures that any eavesdropping attempt by Eve leaves detectable traces through measurement disturbances. In all such QKD frameworks, Alice and Bob must eventually compare the initial states (or bases) used for encoding with those measured at the receiving end. This comparison helps identify correlations that could indicate the presence of an eavesdropper. After performing this verification, Alice and Bob retain only the states that satisfy predefined conditions, forming the basis for the final key generation. This process constitutes a specific stage

within the protocol, often referred to as the classical key-sifting subprotocol. In this chapter, we employ a bi-directional quantum channel for the secure distribution of quantum information using single-photon states. The objective is to establish a secret key between Alice and Bob after executing the key-sifting subprotocol. Here, Alice possesses prior knowledge of the quantum states in the initial sequence that she prepares for Bob. This prior information facilitates agreement on the positions of the sifted key following the information reconciliation process. To formalize our approach, we define the following notation: When encoding a bit value x, Alice prepares the quantum state ψ_J^x , utilizing mutually unbiased bases (MUBs) in a Hilbert space $\mathcal H$ of dimension $\mathcal H$. The bit value x represents the encoded information, while J specifies the basis used for encoding. Without loss of generality, we define $J := \{Z, X\}$, where the basis sets Z and X correspond to $\{|0\rangle, |1\rangle\}$ and $\{|+\rangle, |-\rangle\}$, respectively. These basis sets are commonly referred to as the computational and diagonal bases. For ease of classical key-sifting, we designate J=0 for the Z-basis and J=1 for the X-basis. Building upon this notation, we now outline the generalized structure of our proposed protocol.

(1) State generation, transmission, and measurement: Alice prepares and transmits a sequence of qubits, denoted as S_A , to Bob. Each qubit is encoded in one of the four quantum states $\psi_J^x := \{\psi_Z^x, \psi_X^x\}$, where the bit value x is randomly selected from $\{0,1\}$. Bob then measures each qubit using either the computational or diagonal basis at random, resulting in a sequence of quantum states $\psi_J^y := \{\psi_Z^x, \psi_X^{x/x^{\perp}}\}$, where $\psi_J^{x^{\perp}}$ represents the state orthogonal to ψ_J^x , and $x, y \in \{0,1\}$. It is assumed that no decoherence occurs during qubit transmission. Additionally, Alice does not disclose her chosen measurement basis to Bob. Up to this stage, the procedure is analogous to the BB84 QKD protocol [15].

Based on his measurement results, Bob constructs a sequence of quantum states, denoted as S_{B1} , and transmits it back to Alice. Upon receiving S_{B1} , Alice measures each qubit using the same basis originally used in S_A and records the results. Given the assumption of a long sequence and a noise-free quantum channel, Alice will observe the state $\psi_J^{\chi^{\perp}}$ with a probability of $\frac{1}{4}$. If this probability falls within the predefined threshold around $\frac{1}{4}$, Alice publicly instructs Bob to send the next sequence of qubits, denoted as S_{B2} .

¹Consider two orthonormal basis sets in a d-dimensional Hilbert space, represented as $\psi_{j_1} := \{\psi_1, \psi_2, \dots, \psi_d\}$ and $\psi_{j_2} := \{\psi'_1, \psi'_2, \dots, \psi'_d\}$, These bases are mutually unbiased if the squared modulus of the inner product between any two different basis vectors equals $\frac{1}{d}$, mathematically expressed as $\left|\langle \psi_a | \psi'_b \rangle\right|^2 = \frac{1}{d}$, $\forall a, b \in \{1, 2, \dots, d\}$. When a quantum system is prepared in one of these mutually unbiased bases (MUBs), measuring it in another basis results in a completely random outcome, maximizing measurement uncertainty.

- (2) Preparation and measurement of the second sequence (S_{B2}) : Upon receiving Alice's request, Bob prepares the sequence S_{B2} using the mutually unbiased basis (MUB) alternative to the one previously used for the *n*th qubit in sequence S_{B1} . Specifically, if the Z (or X) basis was employed for a particular qubit in S_{B1} , then the X (or Z) basis is chosen for the corresponding qubit in S_{B2} , ensuring the same bit values at equivalent positions as in sequence S_{B1} (ψ_J^{γ}). Bob then transmits S_{B2} to Alice. Upon receiving it, Alice performs measurements based on the following rule: If her measurement of S_{B1} yields the state ψ_J^{γ} , she utilizes the alternate MUB (the second basis). However, if she obtains the orthogonal state ψ_J^{γ} (relative to the corresponding elements of her initial sequence S_A), she continues using the same basis.
- (3) Condition for key-sifting: To enhance the retention of raw key bits post-sifting while reducing the amount of disclosed classical information compared to the SARG04 protocol, a classical subprotocol is introduced. Alice reveals only the positions of qubits for which Bob's measurement outcomes of S_A contribute to key generation, based on the following conditions: (i) If Alice's measurement of SB1SB1 results in an orthogonal state ψ_Z^{\perp} with respect to her initial sequence S_A , and the corresponding measurement outcome for S_{B2} is either ψ_Z^x or $\psi_Z^{x^{\perp}}$, Alice infers that Bob's measurement result for S_A was either ψ_X^x or $\psi_X^{x^{\perp}}$. (ii) If Alice measures S_{B1} and obtains ψ_Z^x , and the corresponding measurement outcome of S_{B2} from Bob is ψ_X^x , then Alice deduces that Bob's measurement outcome for S_A was ψ_Z^x . However, this holds only if Bob's announced J value for each measurement matches the corresponding J value for elements in Alice's initial sequence S_A . The J value is disclosed selectively for a subset of qubits—specifically, for those where Alice's measurement of S_{B1} aligns with the respective elements of S_A , given that the corresponding qubits in S_{B2} maintain bitwise consistency in a distinct basis relative to S_{B1} . In the subsequent sections, we provide a comprehensive step-by-step breakdown of our primary protocol, designated as Protocol 3.1. Following this, we illustrate how a minor refinement to the key-sifting subprotocol within Protocol 3.1 can enhance the efficiency of our proposed QKD protocol. The optimized version will be referred to as Protocol 3.2 (see Table 3.1 for further details).

Table 3.1: This table outlines the encoding and decoding principles for both Protocol 3.1 and Protocol 3.2, while also presenting the measurement results obtained after the classical sifting subprotocol.

S_A	S_{B1}	S_{B2}	Measurement	Measurement	Probability	J	Result	M	Result
			result of S_{B1}	result of S_{B2}		value	deter-	value	deter-
			by Alice	by Alice		for	mine	for	mine
						P1	by P1	P2	by P2
	$ 0\rangle$	$ +\rangle$	$ 0\rangle$	$\ket{+}$	1/8	0	$ 0\rangle$	0	$ 0\rangle$
			$ 0\rangle$	$\ket{+}$	1/64	1	_	0	$ 0\rangle$
	$ +\rangle$	$ 0\rangle$	$ 0\rangle$	$ -\rangle$	1/64	_	_	0	$ +\rangle$
$ 0\rangle$			$ 1\rangle$	$ 0\rangle$	1/32	_	$ +\rangle$	_	$ +\rangle$
			$ 0\rangle$	$\ket{+}$	1/64	1	_	1	$ -\rangle$
	$ -\rangle$	$ 1\rangle$	$ 0\rangle$	$ -\rangle$	1/64	_	_	1	$ -\rangle$
			$ 1\rangle$	$ 1\rangle$	1/32	_	$ -\rangle$	_	$ -\rangle$
	1>	$ -\rangle$	$ 1\rangle$	$ -\rangle$	1/8	0	$ 1\rangle$	1	$ 1\rangle$
			$ 1\rangle$	$\ket{+}$	1/64	_	_	0	$ +\rangle$
	$ +\rangle$	$ 0\rangle$	$ 1\rangle$	- angle	1/64	1	_	0	$ +\rangle$
$ 1\rangle$			$ 0\rangle$	$ 0\rangle$	1/32	_	$ +\rangle$	_	$ +\rangle$
			$ 1\rangle$	$\ket{+}$	1/64	_	_	1	$ -\rangle$
	$ - \rangle$	$ 1\rangle$	$ 1\rangle$	$ -\rangle$	1/64	1	_	1	$ 1\rangle$
			$ 0\rangle$	$ 1\rangle$	1/32	_	$ -\rangle$	_	$ -\rangle$
	$ +\rangle$	$ 0\rangle$	$ +\rangle$	$ 0\rangle$	1/8	1	$ +\rangle$	0	$ +\rangle$
			$ +\rangle$	$ 0\rangle$	1/64	0	_	0	$ +\rangle$
	$ 0\rangle$	$ +\rangle$	$ +\rangle$	$ 1\rangle$	1/64	_	_	0	$ 0\rangle$
$ +\rangle$			$ -\rangle$	$\ket{+}$	1/32	_	$ 0\rangle$	_	$ 0\rangle$
			$ +\rangle$	$ 0\rangle$	1/64	0	_	1	$ 1\rangle$
	$ 1\rangle$	$ - \rangle$	$\ket{+}$	$ 1\rangle$	1/64	_	_	1	$ 1\rangle$
			$\ket{-}$	$ -\rangle$	1/32	_	$ 1\rangle$	_	$ 1\rangle$
	$ -\rangle$	$ 1\rangle$	$\ket{-}$	$ 1\rangle$	1/8	1	$ -\rangle$	1	$ -\rangle$
			$\ket{-}$	$ 0\rangle$	1/64	_	_	0	$ 0\rangle$
	$ 0\rangle$	$ +\rangle$	$\ket{-}$	$ 1\rangle$	1/64	0	_	0	$ 0\rangle$
$ -\rangle$			$\ket{+}$	$\ket{+}$	1/32	_	$ 0\rangle$	_	$ 0\rangle$
			$\ket{-}$	$ 0\rangle$	1/64	_	_	1	$ 1\rangle$
	$ 1\rangle$	$ \hspace{.06cm} \hspace{.06cm} - angle$	- angle	$ 1\rangle$	1/64	0	_	1	$ -\rangle$

 $|\hspace{.06cm}|\hspace{.08cm}|+
angle\hspace{.08cm}|angle\hspace{.08cm}|angle\hspace{.08cm}|\hspace{.08cm}1/32\hspace{.1cm}|\hspace{.08cm}-\hspace{.08cm}|\hspace{.08cm}|1
angle\hspace{.08cm}|\hspace{.08cm}-\hspace{.08cm}|\hspace{.08cm}|1
angle$

PROTOCOL 3.1

To define these protocols, we employ elements from the Z and X bases, utilizing a notation where basis states are expressed as $|+z\rangle/|-z\rangle(|+x\rangle/|-x\rangle) := |0\rangle/|1\rangle(|+\rangle/|-\rangle)$.. The Z and X basis elements are further defined as:

$$|+x\rangle = \frac{1}{\sqrt{2}}(|0\rangle + |1\rangle) \qquad , \quad |-x\rangle = \frac{1}{\sqrt{2}}(|0\rangle - |1\rangle) |+z\rangle = \frac{1}{\sqrt{2}}(|+x\rangle + |-x\rangle) \qquad , \quad |-z\rangle = \frac{1}{\sqrt{2}}(|+x\rangle - |-x\rangle).$$
(3.2)

- **Step 1** Alice randomly prepares a sequence of single qubits, S_A , in either the Z or X basis, keeping the basis choice confidential, and transmits the sequence to Bob.
- **Step 2** Bob performs measurements on the qubits in S_A , choosing randomly between the Z and X bases, and records the outcomes. He then generates a new qubit sequence, S_{B1} , with states corresponding to his measurement results and forwards it back to Alice.
- **Step 3** Alice measures each qubit in S_{B1} using the same basis initially chosen to prepare the corresponding qubit in S_A . Specifically, if the i^{th} qubit in S_A was prepared in the Z basis (X basis), Alice measures the i^{th} qubit of S_{B1} using the Z basis (X basis). She records the outcomes and instructs Bob to proceed only if the measurement results remain within an acceptable deviation from the expected probability distribution.
- **Step 4** Bob generates a second qubit sequence, S_{B2} , which mirrors the bit values of S_{B1} but is prepared using the complementary basis. Specifically, if the i^{th} qubit in S_{B1} is in the state $|\pm z\rangle(|\pm x\rangle)$, then the corresponding qubit in S_{B2} is prepared in the state $|\pm x\rangle(|\pm z\rangle)$ before being transmitted to Alice.
- **Step 5** Alice measures each qubit in S_{B2} , choosing the measurement basis based on her results from S_{B1} . If the measurement outcome for a qubit in S_{B1} is $|\pm z\rangle$ or $|\pm x\rangle$, she uses the X or Z basis accordingly. Conversely, if the outcome is the orthogonal state ($|\mp z\rangle$ or $|\mp x\rangle$), she switches the basis for measurement on S_{B2} . The measurement strategy is aligned with the initial sequence S_A .

Step 6 Alice extracts the conclusive measurement results—those that definitively determine Bob's corresponding measurements—by analyzing the outcomes from both S_{B1} and S_{B2} . If she originally prepared the i^{th} qubit of S_A in $|\pm z\rangle(|\pm x\rangle)$ and observes measurement results of $|\mp z\rangle(|\mp x\rangle)$ from S_{B1} and $|\pm z\rangle(|\pm x\rangle)$ or $|\mp z\rangle(|\mp x\rangle)$ from S_{B2} , she deduces Bob's measurement result for S_A as either $|\pm x\rangle(|\pm z\rangle)$ or $|\mp x\rangle(|\mp z\rangle)$. This step directly corresponds to the point (a) of the "condition for key-sifting" and facilitates key generation without publicly revealing the value of J.

Step 7 Alice retains only those bits as part of the sifted key where the J value matches for both parties. For instance, if Alice prepares S_A in $|\pm z\rangle(|\pm x\rangle)$ and obtains measurement results of $|\pm z\rangle(|\pm x\rangle)$ from S_{B1} and $|\pm x\rangle(|\pm z\rangle)$ from S_{B2} , then she determines Bob's corresponding result as $|\pm z\rangle(|\pm x\rangle)$ only if the preparation and measurement bases align (i.e., the same J value is used). This step aligns with point (b) of "condition for key-sifting" and finalizes the sifted key using J (refer to Table 3.2). Notably, the J value is revealed only for qubits where Alice's S_{B1} measurement matches S_A , and the corresponding qubits in S_{B2} maintain the same bit values under an alternate basis relative to S_{B1} .

This process ensures that the key-sifting mechanism is executed efficiently, establishing a shared secret key between Alice and Bob.

Table 3.2: Table mapping between measurement outcomes and Alice's determined results in Protocol 3.1.

S_A	Measurement result of	Result determined	Result determined with
	S_{B1} , S_{B2} by Alice	without J value	same J value
$ \pm z\rangle$	$ \pm z\rangle, \pm x\rangle$	_	$ \pm z\rangle$
	$ \mp z\rangle, \pm z\rangle \text{ or } \mp z\rangle, \pm z\rangle$	$ \pm x\rangle$ or $ \mp x\rangle$	_
$ \pm x\rangle$	$ \pm x\rangle, \pm z\rangle$	_	$ \pm x\rangle$
	$ +x\rangle, \pm x\rangle \text{ or } \mp x\rangle, \mp x\rangle$	$ \pm z\rangle$ or $ \mp z\rangle$	_

PROTOCOL 3.2

To facilitate the interpretation of Bob's measurement results for the sequence S_A , we introduce a new variable $M \in \{0,1\}$. This variable is essential for the classical key-sifting process and is defined as follows: M = 0 corresponds to the states $\{|+z\rangle, |+x\rangle\}$, while M = 1 corresponds to $\{|-z\rangle, |-x\rangle\}$. Protocol 3.2 follows the same steps (1 to 6) as Protocol 3.1, but with certain

modifications in the classical post-processing, specifically in Step 7. By employing this modified sifting process, the resulting sifted key retains a maximum intrinsic error probability of 1/16, yet it enhances efficiency compared to Protocol 3.1. A detailed analysis of this trade-off will be presented later.

Step 7 If Alice prepares the sequence S_A using the states $|+z\rangle/|+x\rangle$ or $|-z\rangle/|-x\rangle$, the following rules apply: If Bob publicly announces M=1(0), Alice assigns Bob's measurement outcome for S_A as $|-x\rangle/|-z\rangle$ (or $|+x\rangle/|+z\rangle$, regardless of the measurement outcomes of S_{B1} and S_{B2} . If Bob announces M=0(1), Alice determines Bob's measurement result as (i) $|+x\rangle/|+z\rangle$ (or $|-x\rangle/|-z\rangle$) if the corresponding measurement outcomes of S_{B1} and S_{B2} are $|+z\rangle/|+x\rangle$ (or $|-z\rangle/|-x\rangle$) and $|-x\rangle/|-z\rangle$ (or $|+x\rangle/|+z\rangle$), respectively. (ii) $|+z\rangle/|+x\rangle$ (or $|-z\rangle/|-x\rangle$) if the measurement outcomes of S_{B1} and S_{B2} are $|+z\rangle/|+x\rangle$ (or $|-z\rangle/|-x\rangle$) and $|+x\rangle/|+z\rangle$ (or $|-x\rangle/|-z\rangle$), respectively (see Table 3.3). The value of M is disclosed only for a subset of qubits where Alice's measurements of S_{B1} match the corresponding elements of S_A , ensuring that the qubits in S_{B1} are measured in a basis distinct from their corresponding qubits in S_{B2} . Once Bob reveals the values of M for specific qubits, the encryption criteria transition from the BB84 protocol to the SARG04 protocol. Specifically, in Protocol 3.2, the encryption rule is defined such that the states $|\pm z\rangle$ encode bit value 0, while $|\pm x\rangle$ encode bit value 1. Consequently, revealing the values of M do not provide sufficient information to reconstruct the final key.

Assuming an inherent error probability of $\frac{1}{16}$, Protocol 3.2 achieves a higher key rate than Protocol 3.1 in an environment free of an eavesdropper. In particular, the efficiencies of Protocol 3.2 and Protocol 3.1 are 0.192 and 0.2069, respectively. However, unlike Protocol 3.2, and Protocol 3.1 do not introduce intrinsic errors. A comprehensive analysis of these results and the related trade-offs is provided in Section 3.5.

3.3 SECURITY EVALUATION OF THE PROPOSED PROTOCOLS

As previously discussed, Bob must await Alice's approval of the sequence S_{B1} before proceeding with the transmission of S_{B2} . Once Alice confirms S_{B1} , Bob transmits the second sequence, S_{B2} . The protocol concludes with Alice and Bob establishing a shared secret key, contingent upon the computed error rate remaining within the acceptable threshold. The primary focus of

Table 3.3: Table mapping between measurement results and Alice's determined outcomes in Protocol 3.2.

S_A	Value of M	Measurement	Measurement	Result determined
		result of S_{B1} by	result of S_{B2} by	
		Alice	Alice	
	1	_	_	$ -x\rangle/ -z\rangle$
$ +z\rangle/ +x\rangle$	0	$ +z\rangle/ +x\rangle$	$ -x\rangle/ -z\rangle$	$ +x\rangle/ +z\rangle$
	0	$ +z\rangle/ +x\rangle$	$ +x\rangle/ +z\rangle$	$ +z\rangle/ +x\rangle$
	0	_	_	$ +x\rangle/ +z\rangle$
$ -z\rangle/ -x\rangle$	1	$ -z\rangle/ -x\rangle$	$ +x\rangle/ +z\rangle$	$ -x\rangle/ -z\rangle$
	1	$ -z\rangle/ -x\rangle$	$ -x\rangle/ -z\rangle$	$ -z\rangle/ -x\rangle$

our security analysis is to determine the maximum tolerable error rate in the presence of collective attacks. To assess Eve's potential attack strategies, we adopt an approach inspired by Ref. [298], which utilizes a depolarizing map to transform any arbitrary two-qubit state into a Bell-diagonal state. In order to rigorously analyze the security of the proposed QKD protocols in accordance with the principles outlined in Ref. [298], we must reformulate them into equivalent entanglement-based versions. A corresponding entanglement-based representation of Protocol 3.1/2 can be conceptualized as follows: Alice generates a set of n entangled twoqubit states (such as Bell states) and applies her encoding operation to the first qubit of each pair, while the second qubit is transmitted to Bob. Specifically, if Alice initially prepares the state $|\Phi^+\rangle$, she applies the transformation $A_j \otimes I_2 |\Phi^+\rangle$ and sends the second qubit to Bob. Here, $|\Phi^{\pm}\rangle = \frac{1}{\sqrt{2}}(|00\rangle \pm |11\rangle)$, where A_j represents Alice's encoding operation, and I_2 denotes the identity operator in a two-dimensional Hilbert space. Upon receiving the qubits, Bob independently and randomly applies one of his encoding operations, B_i , to each qubit he receives. The 2n-qubit state shared between Alice and Bob can be represented as $\tilde{\rho}_{AB}^n$. Subsequently, Alice and Bob perform measurements on their respective qubits of $\tilde{
ho}_{AB}^n$ using randomly chosen Xand Z bases, assigning the outcomes to binary values (0 or 1). To formalize this process, two completely positive maps (CPMs), denoted as \mathcal{O}_1 and \mathcal{O}_2 , are introduced. The first map, \mathcal{O}_1 , is entirely dictated by the protocol, while O2 remains independent of it. Specifically, these maps are defined as:

$$\mathcal{O}_1(\boldsymbol{\rho}) = \frac{1}{N} \sum_j p_j A_j \otimes B_j(\boldsymbol{\rho}) A_j^{\dagger} \otimes B_j^{\dagger}$$

$$\mathcal{O}_2(\boldsymbol{\rho}) = \sum_l M_l \otimes M_l(\boldsymbol{\rho}) M_l^{\dagger} \otimes M_l^{\dagger}$$

Here, $p_j \ge 0$ represents the probability that Alice and Bob retain a bit value in the sifting subprotocol, and N is a normalization constant. The operator M_l characterizes a quantum operation, where $M_l \in I_2$, σ_x , σ_y , σ_z , with

$$I_2 = |0\rangle\langle 0| + |1\rangle\langle 1|, \qquad \sigma_x = |0\rangle\langle 1| + |1\rangle\langle 0|,$$

$$i\sigma_y = |0\rangle\langle 1| + |1\rangle\langle 0|, \qquad \sigma_z = |0\rangle\langle 0| - |1\rangle\langle 1|.$$

Since $\mathcal{O}_2(\rho)$ applies identical operators to both qubits, the possible two-qubit operations are given by $M_l \otimes M_l \in \{I \otimes I, \sigma_x \otimes \sigma_x, \sigma_y \otimes \sigma_y, \sigma_z \otimes \sigma_z\}$. These transformations occur randomly with uniform probability. Interestingly, this random application effectively simulates the behavior of a depolarizing channel, which maps any two-qubit state to a Bell-diagonal state. If Alice and Bob implement a unitary transformation $A_j \otimes B_j$, upon completing the sifting phase, Alice and Bob obtain their sifted key, with the normalization constraint $\sum_j p_j = 1$. The normalized two-qubit density operator from Equation (1) of Ref. [299] is employed for n = 1 (see [298] for further details). Finally, the notation $P_{|\Phi\rangle} = |\Phi\rangle\langle\Phi|$ represents a state projection operator, which projects a quantum state of the corresponding dimension onto $|\Phi\rangle$. Now,

$$\rho^{1}[\mu] = \mu_{1} P_{|\Phi^{+}\rangle} + \mu_{2} P_{|\Phi^{-}\rangle} + \mu_{3} P_{|\Psi^{+}\rangle} + \mu_{4} P_{|\Psi^{-}\rangle}. \tag{3.3}$$

The operators $P_{|\Phi^{\pm}\rangle}$ and $P_{|\Psi^{\pm}\rangle}$ represent the state projections onto the Bell states $|\Phi^{\pm}\rangle = \frac{1}{\sqrt{2}}(|00\rangle \pm |11\rangle)$ and $|\Psi^{\pm}\rangle = \frac{1}{\sqrt{2}}(|01\rangle \pm |10\rangle)$. The parameters $\mu_{1/2}$ and $\mu_{3/4}$ denote the corresponding probabilities of obtaining these Bell states when a system undergoes depolarization. To evaluate the security of the sequence S_{B1} , the following key rate equation is employed:

$$r := I(A:B) - \max_{\rho \in \mathcal{R}} S(\rho), \tag{3.4}$$

where A and B represent the quantum states acquired by Alice and Bob after measurement. Here, I(A:B) quantifies the mutual information between Alice and Bob, while $S(\rho)$ denotes

The encoding and decoding operations can be expressed as $A_j = |0\rangle\langle(\phi_j^0)^*| + |1\rangle\langle(\phi_j^1)^*|$ and $B_j = |0\rangle\langle(\phi_j^1)^\perp| + |1\rangle\langle(\phi_j^0)^\perp|$ where $|(\phi_j^i)^*\rangle$ denotes the complex conjugate of $|\phi_j^i\rangle$ and $|(\phi_j^i)^\perp\rangle$ represents its orthogonal complement in the computational basis. The index $j \in \{1, \dots, m\}$ corresponds to the states encoding the bit values i = 0, 1 [299, 298].

the von Neumann entropy of the joint quantum state ρ . The set \mathcal{R} represents the density range¹ of ρ , as formally defined in Definition 3.16 of [278]. This equation, initially introduced in Ref. [278], Equation (3.4) does not directly determine the key rate for the protocols under consideration. Instead, it establishes the threshold for secure errors in S_{B1} . Since S_{B1} is transmitted through a one-way quantum channel from Bob to Alice, this key rate equation is applicable. Bob discloses partial information about his measurement results for sequence S_A (or the states prepared for S_{B1}), enabling both parties to validate security through correlation checks following this classical disclosure. Given that Alice possesses knowledge of her initial sequence S_A , she can utilize the key rate Equation (3.4) to determine the tolerable error threshold for S_{B1} . Assume that the QBER is $\mathcal{E} \in [0,1]$ for measurements conducted in both the X and Z bases. The outcome of projective measurements on the quantum state ρ can be described by a random variable V. Since measurements in the Z and X bases yield four possible outcomes, we associate four distinct probabilities with these outcomes. Specifically, the probabilities of obtaining each measurement outcome in the respective bases can be expressed as μ_i for $i \in \{1,2,3,4\}$, corresponding to different values of V. The entropy associated with the variable V is given by $H(V) = -\sum_{V \in \mu_i} V \log_2 V \ge S(\rho)$. The probabilities μ_i can be efficiently determined by computing the expectation values of ρ with respect to the relevant states. Specifically, in this scenario, we have $\mu_1 = \langle \Phi^+ | \rho | \Phi^+ \rangle$, $\mu_2 = \langle \Phi^- | \rho | \Phi^- \rangle$, $\mu_3 = \langle | \Psi^+ | \rho | \Psi^+ \rangle$ and $\mu_4 = \langle | \Psi^- | \rho | \Psi^- \rangle$. A systematic yet lengthy derivation establishes relationships among these probabilities for the system described in Equation (3.3), yielding the following equations: $\mu_3 + \mu_4 = \mathcal{E}$, $\mu_2 + \mu_4 = \mathcal{E}$, $\mu_1 + \mu_2 = 1 - \mathcal{E}$, and $\mu_1 + \mu_3 = 1 - \mathcal{E}$. However, these four equations are not linearly independent. Instead, only three of them form an independent set, which can be chosen in different ways—for instance, by selecting (i) the first three equations or (ii) the first two along with the last one. Due to this dependence, direct resolution of the system is not feasible. Instead, one probability can be treated as a free parameter, with the remaining ones expressed in terms of it. Here, μ_4 is selected as the free parameter, leading to the expressions $\mu_1 = 1 - 2\mathcal{E} + \mu_4$ and $\mu_2 = \mu_3 = \mathcal{E} - \mu_4$. The range of μ_4 is constrained by $0 \le \mu_4 \le \mathcal{E}$, as probability values must lie within [0, 1], and the condition $\mu_2 + \mu_4 = \mathcal{E}$ holds (see the mathematical analysis in the next

¹Let $S(\mathcal{H})$ represent the collection of density operators on the Hilbert space $\mathcal{H} \equiv H_A \otimes \mathcal{H}_B$. Consider a density operator ρ' defined on $\mathcal{H}^{\otimes n}$, meaning $\rho' \in S(\mathcal{H}^{\otimes n})$, with an associated density range $\mathcal{R} \subseteq S(\mathcal{H})$. The set \mathcal{R} , known as the density range, consists of reduced density operators corresponding to individual subsystems obtained from ρ' . More specifically, $\mathcal{R} := \mathcal{R}(a,b)$ defines the set of density operators on $\mathcal{H}_A \otimes \mathcal{H}_B$, ensuring that the measurement statistics for any $\rho \in \mathcal{R}$ align with the measurement operations performed by Alice and Bob [278].

part). The proposed framework prioritizes maximizing the quantum component while minimizing the classical contribution. Our analysis primarily explores the information-theoretic security limits of each quantum sequence. If the QBER remains within the acceptable secure threshold, both parties continue with the next steps of the protocol. This security assessment applies to both newly introduced protocols since all operations before the classical sub-protocol (i.e., the quantum phase) are identical in both cases. For simplicity, the security evaluation is confined to the quantum aspect of the proposed approach.

As discussed in the previous text, the Bell states are defined as: $|\Phi^{\pm}\rangle = \frac{1}{\sqrt{2}}(|00\rangle \pm |11\rangle)$ and $|\Psi^{\pm}\rangle = \frac{1}{\sqrt{2}}(|01\rangle \pm |10\rangle)$. These Bell states can also be represented in the diagonal basis as $|\Phi^{+}\rangle = \frac{1}{\sqrt{2}}(|++\rangle + |--\rangle), |\Phi^{-}\rangle = \frac{1}{\sqrt{2}}(|+-\rangle + |-+\rangle), |\Psi^{+}\rangle = \frac{1}{\sqrt{2}}(|++\rangle - |--\rangle), |\Psi^{-}\rangle = \frac{1}{\sqrt{2}}(|-+\rangle - |+-\rangle)$. From Equation (3.3),

$$\mu_{2} = \langle \Phi^{-}|\rho|\Phi^{-}\rangle$$

$$= \frac{1}{2}(\langle +-|\rho|+-\rangle + \langle +-|\rho|-+\rangle + \langle -+|\rho|+-\rangle + \langle -+|\rho|-+\rangle),$$
(3.5)

$$\mu_{4} = \langle \Psi^{-}|\rho|\Psi^{-}\rangle
= \frac{1}{2}(\langle +-|\rho|+-\rangle - \langle +-|\rho|-+\rangle - \langle -+|\rho|+-\rangle + \langle -+|\rho|-+\rangle),$$
(3.6)

$$\mu_{3} = \langle \Psi^{+} | \rho | \Psi^{+} \rangle$$

$$= \frac{1}{2} (\langle 01 | \rho | 01 \rangle + \langle 01 | \rho | 10 \rangle + \langle 10 | \rho | 01 \rangle + \langle 10 | \rho | 10 \rangle),$$
(3.7)

and

$$\mu_{4} = \langle \Psi^{-}|\rho|\Psi^{-}\rangle
= \frac{1}{2} (\langle 01|\rho|01\rangle - \langle 01|\rho|10\rangle - \langle 10|\rho|01\rangle + \langle 10|\rho|10\rangle).$$
(3.8)

We define \mathcal{E} as a symmetric error, ensuring that the following conditions hold:

$$\langle 00|\rho|00\rangle + \langle 11|\rho|11\rangle = 1 - \mathcal{E},$$

$$\langle + + |\rho| + + \rangle + \langle - - |\rho| - - \rangle = 1 - \mathcal{E},$$

$$\langle 01|\rho|01\rangle + \langle 10|\rho|10\rangle = \mathcal{E},$$

$$\langle + - |\rho| + - \rangle + \langle - + |\rho| - + \rangle = \mathcal{E}.$$
(3.9)

Using these Equations (3.5), (3.6), (3.7), and (3.8) in Equation (3.9), we obtain

$$\mu_2 + \mu_4 = (\langle + -|\rho| + - \rangle + \langle - +|\rho| - + \rangle) = \mathcal{E}$$

 $\mu_2 = \mathcal{E} - \mu_4$

and

$$\mu_3 + \mu_4 = (\langle 01|\rho|01\rangle + \langle 10|\rho|10\rangle) = \mathcal{E}$$

$$\mu_3 = \mathcal{E} - \mu_4.$$

The total probability must adhere to the condition $\mu_1 + \mu_2 + \mu_3 + \mu_4 = 1$. Leveraging the established relationship with preceding results, we derive $\mu_1 = 1 - 2\mathcal{E} + \mu_4$ and $\mu_2 = \mu_3 = \mathcal{E} - \mu_4$. This analysis establishes the secure error threshold for the sequence S_{B1} both with and without classical pre-processing [278]. To optimize the entropy of the random variable V, we solve the equation $\frac{d(H(V))}{d\mu_4} = 0$, which results in $\mu_4 = \mathcal{E}^2$. Consequently, the entropy H(V) is given by $2h(\mathcal{E})$, where $h(\mathcal{E}) = -\mathcal{E}\log_2\mathcal{E} - (1-\mathcal{E})\log_2(1-\mathcal{E})$ represents the binary entropy function. Bob's measurement results yield an entropy of H(B) = 2, while the conditional entropy of B given A is expressed as $H(B|A) = 1 - \frac{1-\mathcal{E}}{2}\log_2\frac{1-\mathcal{E}}{2} - \frac{\mathcal{E}}{2}\log_2\frac{\mathcal{E}}{2}$. The security threshold, or the highest permissible error rate, corresponds to the maximum value of \mathcal{E} for which Equation (3.4) remains positive for S_{B1} . Under these constraints, solving $1 + \frac{1-\mathcal{E}}{2}\log_2\frac{1-\mathcal{E}}{2} + \frac{\mathcal{E}}{2}\log_2\frac{\mathcal{E}}{2} - 2h(\mathcal{E}) = 0$ yields $\mathcal{E} \approx 0.0314$ (i.e., a QBER of 3.14%). Further details can be found in this analysis, These expressions are utilized to determine the key rate. The conditional probability is given by, $Pr(B = |i\rangle|A = |j\rangle) = \frac{Pr(B=|i\rangle,A=|j\rangle)}{Pr(A=|j\rangle)}$ and alongside the corresponding conditional entropy,

$$H(B|A) = -\sum_{j} Pr(A = |j\rangle) \sum_{i} Pr(B = |i\rangle|A = |j\rangle) \log_{2} Pr(B = |i\rangle|A = |j\rangle), \qquad (3.10)$$

$$Pr(B = |0\rangle|A = |0\rangle) = Pr(B = |1\rangle|A = |1\rangle) = \frac{\mu_{1} + \mu_{2}}{2},$$

$$Pr(B = |1\rangle|A = |0\rangle) = Pr(B = |0\rangle|A = |1\rangle) = \frac{\mu_{3} + \mu_{4}}{2},$$

$$Pr(B = |+\rangle|A = |+\rangle) = Pr(B = |-\rangle|A = |-\rangle) = \frac{\mu_{1} + \mu_{3}}{2},$$

$$Pr(B = |-\rangle|A = |+\rangle) = Pr(B = |+\rangle|A = |-\rangle) = \frac{\mu_{2} + \mu_{4}}{2},$$

$$Pr(B = |0\rangle|A = |0\rangle) = Pr(B = |1\rangle|A = |1\rangle) = \frac{\mu_{1} + \mu_{2}}{2},$$

$$Pr(B = |1\rangle|A = |0\rangle) = Pr(B = |0\rangle|A = |1\rangle) = \frac{\mu_{3} + \mu_{4}}{2},$$

$$Pr(B = |+\rangle|A = |+\rangle) = Pr(B = |-\rangle|A = |-\rangle) = \frac{\mu_{1} + \mu_{3}}{2},$$

$$Pr(B = |-\rangle|A = |+\rangle) = Pr(B = |+\rangle|A = |-\rangle) = \frac{\mu_{2} + \mu_{4}}{2},$$

$$Pr(B = |m\rangle|A = |n\rangle) = Pr(B = |n\rangle|A = |m\rangle) = \frac{1}{4},$$

$$Pr(B=|m\rangle) = Pr(B=|n\rangle) = \frac{1}{4},$$

$$Pr(A = |m\rangle) = Pr(A = |n\rangle) = \frac{1}{4}.$$

For indices $m \neq n$, where $m \in \{|0\rangle, |1\rangle\}$ and $n \in \{|+\rangle, |-\rangle, \}$, we can derive relevant expressions using Equation (3.10),

$$H(B|A) = -\frac{\mu_1 + \mu_2}{4} \log_2 \frac{\mu_1 + \mu_2}{2} - \frac{\mu_3 + \mu_4}{4} \log_2 \frac{\mu_3 + \mu_4}{2}$$
$$- \frac{\mu_1 + \mu_3}{4} \log_2 \frac{\mu_1 + \mu_3}{2} - \frac{\mu_2 + \mu_4}{4} \log_2 \frac{\mu_2 + \mu_4}{2} - \frac{1}{2} \log_2 \frac{1}{4}$$
$$= -\frac{1 - \mathcal{E}}{2} \log_2 \frac{1 - \mathcal{E}}{2} - \frac{\mathcal{E}}{2} \log_2 \frac{\mathcal{E}}{2} + 1,$$

and

$$H(B) = -4 \times \frac{1}{4} \log_2 \frac{1}{4}$$

= 2

Therefore,

$$I(A:B) = H(B) - H(B|A)$$
$$= 1 + \frac{1-\mathcal{E}}{2} \log_2 \frac{1-\mathcal{E}}{2} + \frac{\mathcal{E}}{2} \log_2 \frac{\mathcal{E}}{2},$$

utilizing the secret key rate we have,

$$\begin{array}{rcl} r & = & I(A:B) - H(V) \\ & = & 1 + \frac{1 - \mathcal{E}}{2} \log_2 \frac{1 - \mathcal{E}}{2} + \frac{\mathcal{E}}{2} \log_2 \frac{\mathcal{E}}{2} - 2h(\mathcal{E}). \end{array}$$

This result indicates that, in the absence of classical pre-processing, the maximum theoretical error tolerance for S_{B1} is 3.14% following Bob's classical announcement and correlation evaluation for security verification. To enhance this security threshold, we define a new variable $\mathcal{Y} = j_A \oplus j_B$, where j_A and j_B denote the basis choices made by Alice and Bob when measuring particles within S_{B1} and S_A , respectively. Here, the basis indices satisfy $j_A, j_B \in \{0, 1\}$. Solving the equation:

¹This framework can be interpreted as a classical pre-processing approach aimed at enhancing the key rate while simultaneously increasing the maximum permissible error threshold [278]. Additionally, \mathcal{X} serves a similar role in the context of the sequence S_{B2} .

$$1 + \frac{1-\varepsilon}{2}\log_2\frac{1-\varepsilon}{2} + \frac{\varepsilon}{2}\log_2\frac{\varepsilon}{2} - h(\varepsilon) = 0 ,$$

yields $\mathcal{E} \approx 0.0617$ (equivalent to a 6.17% bit error rate; refer to Figure 3.1. a. This outcome indicates that when \mathcal{Y} is disclosed, the highest permissible error threshold for the measurement of S_A and S_{B1} rises to 6.17%. Consequently, under classical pre-processing, the theoretical maximum tolerable error rate for S_{B1} is established at 6.17%. As discussed in Section 3.2, the probability of obtaining the expected outcomes from S_A is $\frac{1}{2}$ (ψ_X^x) when using the same basis and $\frac{1}{4}$ ($\psi_X^{x/x^{\perp}}$) when different bases are employed. For S_{B1} , the probability is given by $\frac{1}{4}$ ($\psi_J^{x^{\perp}}$). The maximum allowable deviations from these probability values correspond to an error margin of 3.14% when \mathcal{Y} is not announced, increasing to 6.17% upon its disclosure. The introduction of new variables \mathcal{Y} (alongside \mathcal{X} , introduced subsequently) follows the approach proposed by Christandl et al. [278]. The methodology for determining these variables is rooted in the concepts of information reconciliation and privacy amplification against quantum adversaries. Within information reconciliation, hash and guessing functions are employed to establish these variables. Privacy amplification, on the other hand, involves the use of hash functions and a transformation based on the measurement outcomes of quantum states relative to an arbitrary POVM, which is also influenced by the hash function (refer to Sections 4.2, 4.3, and 5.1 in [278]).

Alice begins by verifying that the security threshold for the sequence S_{B1} remains within the designated limits. She then measures the second sequence, S_{B2} , which is sent by Bob, thereby completing the sifting subprotocol. Following this, both Alice and Bob assess whether the QBER is below the established security threshold. The method used to determine this threshold value is identical to the previously described approach. The entropy associated with Bob's final bit string, b, after executing the sifting subprotocol is given by H(b) = 1, while the conditional entropy of b given Alice's bit string, a, is expressed as $H(b|a) = h(\frac{1}{6} + \frac{2\mathcal{E}}{3})$, where $a, b \in \{0, 1\}$. The detailed mathematical derivation, along with the key rate equation, is subsequently determined by analyzing the key-sifting subprotocol performed by both parties, ensuring that only probabilities meeting the necessary conditions are considered.

$$\begin{split} \Pr(b=0|a=0) &= \Pr(b=1|a=1) &= \frac{1}{6} + \frac{2\mu_1 + \mu_2 + \mu_3}{3}, \\ \Pr(b=0|a=1) &= \Pr(b=1|a=0) &= \frac{1}{6} + \frac{\mu_2 + \mu_3 + 2\mu_4}{3}, \end{split}$$

$$Pr(b=0) = Pr(b=1) = \frac{1}{2}.$$

Applying a similar methodology as in Equation (3.10), we obtain the final expression for the secret key rate.

$$\begin{array}{lll} H(b|a) & = & -\frac{1+4\mu_1+2\mu_2+2\mu_3}{6}\log_2\frac{1+4\mu_1+2\mu_2+2\mu_3}{6} - \frac{1+2\mu_2+2\mu_3+4\mu_4}{6}\log_2\frac{1+2\mu_2+2\mu_3+4\mu_4}{6} \\ & = & -\frac{5-4\mathcal{E}}{6}\log_2\frac{5-4\mathcal{E}}{6} - \frac{1+4\mathcal{E}}{6}\log_2\frac{1+4\mathcal{E}}{6} \\ & = & h\left(\frac{1}{6} + \frac{2\mathcal{E}}{3}\right), \end{array}$$

$$\begin{split} I(a|b) &= H(b) - H(b|a) \\ &= -\frac{1}{2} \log_2 \frac{1}{2} - h(b|a) \\ &= 1 - h\left(\frac{1}{6} + \frac{2\mathcal{E}}{3}\right), \end{split}$$

the secret key rate,

$$\begin{array}{rcl} r & = & I(a|b) - H(V) \\ & = & 1 - h\left(\frac{1}{6} + \frac{2\mathcal{E}}{3}\right) - 2h(\mathcal{E}). \end{array}$$

Using a similar approach, the equation governing the positive key rate for a one-way quantum channel is derived to determine the tolerable QBER for S_{B2} . By solving the equation

$$1 - h(\frac{1}{6} + \frac{2\mathcal{E}}{3}) - 2h(\mathcal{E}) = 0. \tag{3.11}$$

Under the condition r=0, the security threshold is calculated as $\mathcal{E}\approx 0.0316$, corresponding to a 3.16% QBER (see Figure 3.1. b). Enhancing the security threshold can be achieved by introducing a random variable $\mathcal{X}=a\oplus b$, which carries information regarding error positions. This inclusion reduces the quantum contribution (final term) in Equation (3.4), while preserving the minimum entropy of b (refer to Sec. 5.1 of Ref. [278] for more details). To check the effect of this variable mathematically, we formulate it as follows,

Alice and Bob assess the security threshold of particle sequences, denoted as S_A and S_{B1} , under the condition that they use the same basis for state preparation or measurement. The presence or absence of errors is determined based on their measurement of the states $|\Phi^{\pm}\rangle$ (or $|\Psi^{\pm}\rangle$) within the computational basis. Likewise, error-free or erroneous outcomes arise when both parties measure $|\Phi^{+}\rangle$ and $|\Psi^{+}\rangle$ (or $|\Phi^{-}\rangle$ and $|\Psi^{-}\rangle$) using the diagonal basis. This results in

four distinct scenarios to analyze. Furthermore, it follows that the quantum state ρ can be measured with equal probability by both Alice and Bob, regardless of whether they employ the computational or diagonal basis. To illustrate, consider a case where both parties measure the Bell states $|\Phi^+\rangle$ and $|\Psi^+\rangle$ using the computational basis. The corresponding probabilities of obtaining an error-free outcome and an erroneous outcome are $\frac{\mu_1}{2}$ and $\frac{\mu_3}{2}$, respectively¹. Consequently, the probabilities of obtaining an error-free result and an error when measuring $|\Phi^+\rangle$ and $|\Psi^+\rangle$ are given by $\frac{1-\mathcal{E}}{2}$ and $\frac{\mathcal{E}}{2}$, respectively². Considering the total number of qubits, the probabilities of encountering an error-free or erroneous outcome when measuring $|\Phi^+\rangle$ and $|\Psi^+\rangle$ in the computational basis are given by $\frac{\mu_1}{1-\mathcal{E}}$ and $\frac{\mu_3}{2}$, which simplify to $\frac{\mu_1}{1-\mathcal{E}}$ and $\frac{\mu_3}{2}$, respectively. Similarly, when measuring $|\Phi^-\rangle$ and $|\Psi^-\rangle$ within the computational basis, the corresponding probabilities are $\frac{\mu_2}{1-\mathcal{E}}$ and $\frac{\mu_4}{\mathcal{E}}$. For measurements in the diagonal basis, the probabilities of obtaining an error-free outcome and an error when measuring $|\Phi^+\rangle$ and $|\Psi^+\rangle$ are given by $\frac{\mu_1}{1-\mathcal{E}}$ and $\frac{\mu_3}{1-\mathcal{E}}$, respectively. Likewise, for the states $|\Phi^-\rangle$ and $|\Psi^-\rangle$, the probabilities are $\frac{\mu_2}{\mathcal{E}}$ and $\frac{\mu_4}{\mathcal{E}}$, respectively. Finally, in a scenario where no errors are present, the entropy can be computed as follows:

$$\begin{array}{lll} H_{\text{no-error}} & = & -\frac{1}{2} \left[\frac{\mu_1}{1-\mathcal{E}} \log_2 \frac{\mu_1}{1-\mathcal{E}} + \frac{\mu_2}{1-\mathcal{E}} \log_2 \frac{\mu_2}{1-\mathcal{E}} + \frac{\mu_1}{1-\mathcal{E}} \log_2 \frac{\mu_1}{1-\mathcal{E}} + \frac{\mu_3}{1-\mathcal{E}} \log_2 \frac{\mu_3}{1-\mathcal{E}} \right] \\ & = & -\frac{1}{2} \left[\frac{2\mu_1}{1-\mathcal{E}} \log_2 \frac{\mu_1}{1-\mathcal{E}} + \frac{2\mu_2}{1-\mathcal{E}} \log_2 \frac{\mu_2}{1-\mathcal{E}} \right] \text{ as } \mu_2 = \mu_3 \\ & = & -\left[\frac{(1-2\mathcal{E}+\mu_4)}{1-\mathcal{E}} \log_2 \frac{(1-2\mathcal{E}+\mu_4)}{1-\mathcal{E}} + \frac{(\mathcal{E}-\mu_4)}{1-\mathcal{E}} \log_2 \frac{(\mathcal{E}-\mu_4)}{1-\mathcal{E}} \right] \text{ (using Eqs (3.5)} - (3.9)) \\ & = & h\left(\frac{1-2\mathcal{E}+\mu_4}{1-\mathcal{E}}\right). \end{array}$$

In the presence of errors, entropy can be determined as follows:

$$\begin{aligned} \mathbf{H}_{\text{error}} &= -\frac{1}{2} \left[\frac{\mu_{3}}{\mathcal{E}} \log_{2} \frac{\mu_{3}}{\mathcal{E}} + \frac{\mu_{4}}{\mathcal{E}} \log_{2} \frac{\mu_{4}}{\mathcal{E}} + \frac{\mu_{2}}{\mathcal{E}} \log_{2} \frac{\mu_{2}}{\mathcal{E}} + \frac{\mu_{4}}{\mathcal{E}} \log_{2} \frac{\mu_{4}}{\mathcal{E}} \right] \\ &= -\frac{1}{2} \left[\frac{2\mu_{2}}{\mathcal{E}} \log_{2} \frac{2\mu_{2}}{\mathcal{E}} + \frac{2\mu_{4}}{\mathcal{E}} \log_{2} \frac{2\mu_{4}}{\mathcal{E}} \right] \text{ as } \mu_{2} = \mu_{3} \\ &= -\left[\frac{(\mathcal{E} - \mu_{4})}{\mathcal{E}} \log_{2} \frac{(\mathcal{E} - \mu_{4})}{\mathcal{E}} + \frac{\mu_{4}}{\mathcal{E}} \log_{2} \frac{\mu_{4}}{\mathcal{E}} \right] \text{ (using Eqs (3.5)} - (3.9)) \\ &= h\left(\frac{\mathcal{E} - \mu_{4}}{\mathcal{E}} \right). \end{aligned}$$

By performing statistical averaging over both error-free and erroneous cases, we derive:

¹For simplicity, we assume that both participants measure all qubits in the same basis—either both using the computational basis or both using the diagonal basis—during the error verification stage.

²In this framework, the factor of 2 arises due to the equal distribution of the total error-checking qubits between computational and diagonal basis measurements.

$$\begin{split} &(1-\mathcal{E})\, H_{\text{no-error}} + \mathcal{E} H_{error} \\ &= (1-\mathcal{E})\, h\left(\frac{1-2\mathcal{E} + \mu_4}{1-\mathcal{E}}\right) + \mathcal{E} h\left(\frac{\mathcal{E} - \mu_4}{\mathcal{E}}\right) \\ &= - (1-\mathcal{E})\left[\frac{(1-2\mathcal{E} + \mu_4)}{1-\mathcal{E}}\log_2\frac{(1-2\mathcal{E} + \mu_4)}{1-\mathcal{E}} + \frac{(\mathcal{E} - \mu_4)}{1-\mathcal{E}}\log_2\frac{(\mathcal{E} - \mu_4)}{1-\mathcal{E}}\right] \\ &- \mathcal{E}\left[\frac{(\mathcal{E} - \mu_4)}{\mathcal{E}}\log_2\frac{(\mathcal{E} - \mu_4)}{\mathcal{E}} + \frac{\mu_4}{\mathcal{E}}\log_2\frac{\mu_4}{\mathcal{E}}\right] \\ &= - \left[(1-2\mathcal{E} + \mu_4)\log_2\left(1-2\mathcal{E} + \mu_4\right) + (\mathcal{E} - \mu_4)\log_2\left(\mathcal{E} - \mu_4\right) \\ &- (1-2\mathcal{E} + \mu_4)\log_2\left(1-\mathcal{E}\right) - (\mathcal{E} - \mu_4)\log_2\left(1-\mathcal{E}\right)\right] \\ &- \left[(\mathcal{E} - \mu_4)\log_2\left(\mathcal{E} - \mu_4\right) + \mu_4\log_2\mu_4 - (\mathcal{E} - \mu_4)\log_2\mathcal{E} - \mu_4\log_2\mathcal{E}\right] \\ &= - \left[(1-2\mathcal{E} + \mu_4)\log_2\left(1-2\mathcal{E} + \mu_4\right) + 2\left(\mathcal{E} - \mu_4\right)\log_2\left(\mathcal{E} - \mu_4\right) + \mu_4\log_2\mu_4\right] \\ &+ (1-2\mathcal{E} + \mu_4 + \mathcal{E} - \mu_4)\log_2\left(1-\mathcal{E}\right) + (\mathcal{E} - \mu_4 + \mu_4)\log_2\mathcal{E} \\ &= H(V) + (1-\mathcal{E})\log_2\left(1-\mathcal{E}\right) + \mathcal{E}\log_2\mathcal{E} \\ &= H(V) - h(\mathcal{E}). \end{split}$$

To elucidate this further, the quantum system can be decomposed into four distinct subsystems, where two correspond to error states and the other two to error-free states for each basis. Within the Z(X) basis, errors and non-errors account for fractions of $\frac{\mathcal{E}}{2}$ and $\frac{1-\mathcal{E}}{2}$, respectively, of the total qubits. By computing the entropy for these four subsystems in both error and no-error cases, one derives $h\left(\frac{\mathcal{E}-\mu_4}{\mathcal{E}}\right)$ and $h\left(\frac{1-2\mathcal{E}+\mu_4}{1-\mathcal{E}}\right)$ as the respective entropy values. Subsequently, performing statistical averaging over all four subsystems yields the final result.

$$(1-\mathcal{E})h\left(\frac{1-2\mathcal{E}+\mu_4}{1-\mathcal{E}}\right) + \mathcal{E}h\left(\frac{\mathcal{E}-\mu_4}{\mathcal{E}}\right) = H(V) - h(\mathcal{E})$$
(3.12)

By substituting the reconditioned entropy for variable V in Equation (3.11), we derive a modified key rate equation for a one-way quantum channel, establishing the tolerable QBER as S_{B2} .

$$r = 1 - h(\frac{1}{6} + \frac{2\mathcal{E}}{3}) - h(\mathcal{E}). \tag{3.13}$$

In this context, the equation's solution for a positive r determines the security threshold, yielding $\mathcal{E} \approx 0.15$. Consequently, the corresponding bit error rate is approximately 15% (see Figure 3.1 c).

Next, we evaluate the secret-key rate under the assumption that the protocol remains secure against collective attacks by Eve. To begin, we characterize the initial quantum state ρ_{AB}^n , which depends on the threshold QBER beyond which the protocol prematurely terminates. Ideally, ρ_{AB}^n

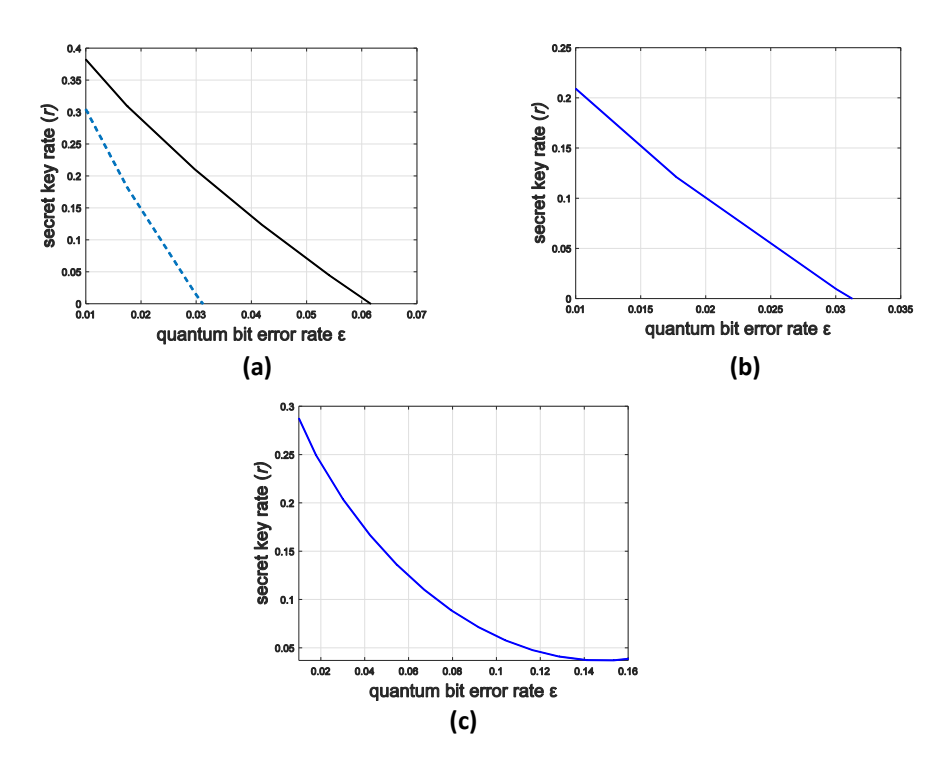


Figure 3.1: The secret key rate is plotted as a function of the quantum bit error rate (\mathcal{E}): (a) a plot assessing the maximum tolerable error threshold (security limit) for sequence S_{B1} , where the solid (black) line and dashed (blue) line represent scenarios with and without the incorporation of the new variable \mathcal{Y} , respectively; (b) a plot evaluating the maximum tolerable error threshold (security limit) for sequence S_{B2} without introducing the new variable \mathcal{X} ; and (c) a plot assessing the maximum tolerable error threshold (security limit) for sequence S_{B2} with the inclusion of the new variable \mathcal{X} .

represents a quantum state shared exclusively between Alice and Bob, though Eve may access it and potentially launch collective attacks. Let Γ denote the set of all two-qubit states σ_{AB} that could arise from Eve's collective attack on ρ_{AB}^n . The effectiveness of Eve's attack is determined by whether it remains undetectable. If the attack leaves no observable traces, the resulting state satisfies $\sigma_{AB}^{\otimes n} = \rho_{AB}^n$. However, unsuccessful attacks introduce detectable disturbances, leading to protocol termination. Our focus is on scenarios where the protocol continues to operate. To account for such cases, we assume the existence of an operation that allows Eve to construct the state $\sigma_{AB}^{\otimes n} = \rho_{AB}^n$ using ancillary qubits and the portion of the initial state accessible via the quantum channel. Following the framework established in Ref. [299], we define Γ_{QBER} as a subset of Γ containing all states σ_{AB} for which the protocol does not terminate. That is, if $\sigma_{AB} \in \Gamma_{QBER}$, then the protocol is capable of generating a secure key. As demonstrated by Renner et al. in [299], under these conditions, both lower and upper bounds on the secret-key rate can be rigorously determined for any one-way post-processing protocol.

$$r \ge \sup_{c \leftarrow a\sigma_{AB} \in \Gamma_{QBER}} inf \left(S(c|E) - H(c|b) \right). \tag{3.14}$$

In this context, $r_{c \leftarrow a}$ represents the achievable rate when the channel $c \leftarrow a$ is employed for preprocessing¹. The quantity S(c|E) corresponds to the von Neumann entropy of c, conditioned on Eve's initial state, mathematically defined as $S(c|E) = S(\sigma_{cE}) - S(\sigma_{E})$. The bipartite state σ_{cE} is derived from the two-qubit state σ_{AB} by considering a purification σ_{ABE} of its Bell diagonal form, denoted as $\sigma_{AB}^{diag} := \mathcal{O}_2(\sigma_{AB})$, where σ_{AB}^{diag} retains the same diagonal elements as σ_{AB} in the Bell basis. The symbols a, b and e represent the measurement outcomes corresponding to Alice, Bob, and Eve, respectively, following the application of measurements to the first, second, and third subsystems of σ_{ABE} .

To determine an upper bound on the achievable rate, it is sufficient to restrict our consideration to collective attacks. The joint quantum system involving Alice, Bob, and Eve adheres to a product structure, represented as $\rho_{ABE}^n := \sigma_{ABE}^{\otimes n}$, where σ_{ABE} denotes a tripartite quantum state. The *n*-fold tensor product state σ_{abE}^n describes the scenario in which the single-copy state σ_{abE} arises from Alice and Bob's measurements performed on σ_{ABE} (for a rigorous proof, refer to Section IV of Ref. [299]). Consequently, the upper bound on the secret key rate is given by:

 $^{^1}$ The channel $c \leftarrow a$ can be interpreted as a probabilistic mixture of quantum transitions, formally described as $q(|1\rangle_{ca}\langle 0|+|0\rangle_{ca}\langle 1|)+(1-q)(|0\rangle_{ca}\langle 0|+|1\rangle_{ca}\langle 1|)$. Here, a denotes Alice's register containing the classical measurement outcomes, while c represents the register storing the noisy counterpart of a.

$$r(a,b,e) = \sup_{c \leftarrow a} (H(c|e) - H(c|b)).$$
 (3.15)

This result indicates that when the supremum is taken over all possible channels—including both quantum and classical, $c \leftarrow a$ establishes an upper limit on the secret key rate. Next, we analyze the protocol in terms of both lower and upper bounds on the secret key rate. As before, we set n = 1 and define $\sigma_{AB} = \rho^1[\mu]$. It is necessary to consider a purification $|\Psi\rangle_{ABE}$ of the Bell diagonal state $\mathcal{O}_2(\sigma_{AB})$, which originates from σ_{AB} and is expressed as:

$$|\Psi\rangle_{ABE} := \sum_{i=1}^{4} \sqrt{\mu_i} |\varphi_i\rangle_{AB} \otimes |\varepsilon_i\rangle_{E}. \tag{3.16}$$

In this context, $|\varphi_i\rangle_{AB}$ represents the Bell states associated with the joint quantum system shared between Alice and Bob¹. Meanwhile, $|\varepsilon_i\rangle_E$ corresponds to a set of mutually orthogonal states forming a basis in Eve's system, denoted as $\varepsilon_E \in \{|\varepsilon_1\rangle_E, \dots, |\varepsilon_4\rangle_E\}$. It is straightforward to verify that when Alice measures her qubit in the Z (or X) basis and Bob performs measurements in either the Z or X basis with equal probability, their respective measurement outcomes are represented as $|A\rangle$ and $|B\rangle$. For illustration, we assume $|A\rangle \in \{|0\rangle, |1\rangle\}$ and $|B\rangle \in \{|0\rangle, |1\rangle, |+\rangle, |-\rangle\}$. Under this framework, Eve's quantum state is denoted as $|\phi^{A,B}\rangle$. We have,

$$|\phi^{0,0}\rangle = \frac{1}{\sqrt{2}} \left(\sqrt{\mu_{1}} |\varepsilon_{1}\rangle_{E} + \sqrt{\mu_{2}} |\varepsilon_{2}\rangle_{E} \right),$$

$$|\phi^{1,1}\rangle = \frac{1}{\sqrt{2}} \left(\sqrt{\mu_{1}} |\varepsilon_{1}\rangle_{E} - \sqrt{\mu_{2}} |\varepsilon_{2}\rangle_{E} \right),$$

$$|\phi^{0,1}\rangle = \frac{1}{\sqrt{2}} \left(\sqrt{\mu_{3}} |\varepsilon_{3}\rangle_{E} + \sqrt{\mu_{4}} |\varepsilon_{4}\rangle_{E} \right),$$

$$|\phi^{1,0}\rangle = \frac{1}{\sqrt{2}} \left(\sqrt{\mu_{3}} |\varepsilon_{3}\rangle_{E} - \sqrt{\mu_{4}} |\varepsilon_{4}\rangle_{E} \right),$$

$$|\phi^{0,+}\rangle = \frac{1}{2} \left(\sqrt{\mu_{1}} |\varepsilon_{1}\rangle_{E} + \sqrt{\mu_{2}} |\varepsilon_{2}\rangle_{E} + \sqrt{\mu_{3}} |\varepsilon_{3}\rangle_{E} + \sqrt{\mu_{4}} |\varepsilon_{4}\rangle_{E} \right),$$

$$|\phi^{0,-}\rangle = \frac{1}{2} \left(\sqrt{\mu_{1}} |\varepsilon_{1}\rangle_{E} + \sqrt{\mu_{2}} |\varepsilon_{2}\rangle_{E} - \sqrt{\mu_{3}} |\varepsilon_{3}\rangle_{E} - \sqrt{\mu_{4}} |\varepsilon_{4}\rangle_{E} \right),$$

$$|\phi^{1,+}\rangle = \frac{1}{2} \left(\sqrt{\mu_{1}} |\varepsilon_{1}\rangle_{E} - \sqrt{\mu_{2}} |\varepsilon_{2}\rangle_{E} + \sqrt{\mu_{3}} |\varepsilon_{3}\rangle_{E} - \sqrt{\mu_{4}} |\varepsilon_{4}\rangle_{E} \right),$$

$$|\phi^{1,-}\rangle = \frac{1}{2} \left(-\sqrt{\mu_{1}} |\varepsilon_{1}\rangle_{E} + \sqrt{\mu_{2}} |\varepsilon_{2}\rangle_{E} + \sqrt{\mu_{3}} |\varepsilon_{3}\rangle_{E} - \sqrt{\mu_{4}} |\varepsilon_{4}\rangle_{E} \right).$$

A comprehensive explanation of the mathematical procedures leading from Equation (3.16) to Equation (3.18) is provided here. Initially, we analyze a scenario where both Alice and Bob measure their qubits in the Z basis (a similar result holds when employing the X basis).

¹Alice performs a measurement on her qubit using the *Z* basis, whereas Bob measures his qubit using either the *Z* or *X* basis with equal probability $(\frac{1}{2})$.

$$\begin{split} |\Psi\rangle_{ABE} &:= \sum_{i=1}^{4} \sqrt{\mu_{i}} |\varphi_{i}\rangle_{AB} \otimes |\varepsilon_{i}\rangle_{E} \\ &= \frac{1}{2\sqrt{2}} \left[\sqrt{\mu_{1}} \left(|00\rangle + |11\rangle \right) \otimes |\varepsilon_{1}\rangle + \sqrt{\mu_{2}} \left(|00\rangle - |11\rangle \right) \otimes |\varepsilon_{2}\rangle \\ &+ \sqrt{\mu_{3}} \left(|01\rangle + |10\rangle \right) \otimes |\varepsilon_{3}\rangle + \sqrt{\mu_{4}} \left(|01\rangle - |10\rangle \right) \otimes |\varepsilon_{4}\rangle \right]_{ABE} \\ &= \frac{1}{2\sqrt{2}} \left[|00\rangle \left(\sqrt{\mu_{1}} |\varepsilon_{1}\rangle + \sqrt{\mu_{2}} |\varepsilon_{2}\rangle \right) + |11\rangle \left(\sqrt{\mu_{1}} |\varepsilon_{1}\rangle - \sqrt{\mu_{2}} |\varepsilon_{2}\rangle \right) \\ &+ |01\rangle \left(\sqrt{\mu_{3}} |\varepsilon_{3}\rangle + \sqrt{\mu_{4}} |\varepsilon_{4}\rangle \right) + |10\rangle \left(\sqrt{\mu_{3}} |\varepsilon_{3}\rangle - \sqrt{\mu_{4}} |\varepsilon_{4}\rangle \right) \right]_{ABE} \\ &= \frac{1}{2} \left[|00\rangle \otimes |\phi^{0,0}\rangle + |11\rangle \otimes |\phi^{1,1}\rangle + |01\rangle \otimes |\phi^{0,1}\rangle + |10\rangle \otimes |\phi^{1,0}\rangle \right]_{ABE} \end{split}$$

Next, we examine the case where Alice and Bob perform measurements using the Z and X bases, respectively¹,

$$\begin{split} |\Psi\rangle_{ABE} &:= \sum_{i=1}^{4} \sqrt{\mu_{i}} |\varphi_{i}\rangle_{AB} \otimes |\varepsilon_{i}\rangle_{E} \\ &= \frac{1}{2\sqrt{2}} \left[\sqrt{\mu_{1}} (|00\rangle + |11\rangle) \otimes |\varepsilon_{1}\rangle + \sqrt{\mu_{2}} (|00\rangle - |11\rangle) \otimes |\varepsilon_{2}\rangle \\ &+ \sqrt{\mu_{3}} (|01\rangle + |10\rangle) \otimes |\varepsilon_{3}\rangle + \sqrt{\mu_{4}} (|01\rangle - |10\rangle) \otimes |\varepsilon_{4}\rangle \right]_{ABE} \\ &= \frac{1}{4} \left[\sqrt{\mu_{1}} \left\{ |0\rangle (|+\rangle + |-\rangle) + |1\rangle (|+\rangle - |-\rangle) \right\} |\varepsilon_{1}\rangle \\ &+ \sqrt{\mu_{2}} \left\{ |0\rangle (|+\rangle + |-\rangle) - |1\rangle (|+\rangle - |-\rangle) \right\} |\varepsilon_{2}\rangle \\ &+ \sqrt{\mu_{3}} \left\{ |0\rangle (|+\rangle - |-\rangle) + |1\rangle (|+\rangle + |-\rangle) \right\} |\varepsilon_{3}\rangle \\ &+ \sqrt{\mu_{4}} \left\{ |0\rangle (|+\rangle - |-\rangle) - |1\rangle (|+\rangle + |-\rangle) \right\} |\varepsilon_{4}\rangle \right]_{ABE} \\ &= \frac{1}{4} \left[|0+\rangle \left\{ \sqrt{\mu_{1}} |\varepsilon_{1}\rangle + \sqrt{\mu_{2}} |\varepsilon_{2}\rangle + \sqrt{\mu_{3}} |\varepsilon_{3}\rangle + \sqrt{\mu_{4}} |\varepsilon_{4}\rangle \right\} \\ &+ |0-\rangle \left\{ \sqrt{\mu_{1}} |\varepsilon_{1}\rangle + \sqrt{\mu_{2}} |\varepsilon_{2}\rangle - \sqrt{\mu_{3}} |\varepsilon_{3}\rangle - \sqrt{\mu_{4}} |\varepsilon_{4}\rangle \right\} \\ &+ |1+\rangle \left\{ \sqrt{\mu_{1}} |\varepsilon_{1}\rangle - \sqrt{\mu_{2}} |\varepsilon_{2}\rangle + \sqrt{\mu_{3}} |\varepsilon_{3}\rangle - \sqrt{\mu_{4}} |\varepsilon_{4}\rangle \right\} \\ &+ |1-\rangle \left\{ -\sqrt{\mu_{1}} |\varepsilon_{1}\rangle + \sqrt{\mu_{2}} |\varepsilon_{2}\rangle + \sqrt{\mu_{3}} |\varepsilon_{3}\rangle - \sqrt{\mu_{4}} |\varepsilon_{4}\rangle \right\} \right]_{ABE} \\ &= \frac{1}{2} \left[|0+\rangle |\phi^{0,+}\rangle + |0-\rangle |\phi^{0,-}\rangle + |1+\rangle |\phi^{1,+}\rangle + |1-\rangle |\phi^{1,-}\rangle \right]_{ABE} \end{split}$$

In the primary text, we have outlined the details of Eve's initial state, represented as ε_E , along with Eve's state $|\phi^{\mathcal{A},\mathbb{B}}\rangle$ after Alice and Bob's measurement process. Our focus remains exclusively on the instances accepted by Alice and Bob following classical pre-processing. After normalization, we analyze the density operator of Eve's system under the condition that Alice's measurement yields an outcome of 0,

$$\begin{array}{ll} \pmb{\sigma}_{E}^{0} & = & \frac{1}{2} \left[|\pmb{\phi}^{0,0}\rangle \langle \pmb{\phi}^{0,0}| + |\pmb{\phi}^{0,1}\rangle \langle \pmb{\phi}^{0,1}| \right] + \frac{1}{2} \left[|\pmb{\phi}^{0,+}\rangle \langle \pmb{\phi}^{0,+}| + |\pmb{\phi}^{0,-}\rangle \langle \pmb{\phi}^{0,-}| \right] \\ & = & \frac{1}{2} \left(P_{|\pmb{\phi}^{0,0}\rangle} + P_{|\pmb{\phi}^{0,1}\rangle} \right) + \frac{1}{2} \left(P_{|\pmb{\phi}^{0,+}\rangle} + P_{|\pmb{\phi}^{0,-}\rangle} \right) \end{array}$$

 $^{^{-1}}$ It is crucial to highlight that the same results arise when Alice and Bob interchange their measurement bases to X and Z.

and similarly, when Alice's measurement results in an outcome of 1,

$$\begin{array}{lcl} \sigma_E^1 & = & \frac{1}{2} \left[|\phi^{1,0}\rangle \langle \phi^{1,0}| + |\phi^{1,1}\rangle \langle \phi^{1,1}| \right] + \frac{1}{2} \left[|\phi^{1,+}\rangle \langle \phi^{1,+}| + |\phi^{1,-}\rangle \langle \phi^{1,-}| \right] \\ & = & \frac{1}{2} \left(P_{|\phi^{1,0}\rangle} + P_{|\phi^{1,1}\rangle} \right) + \frac{1}{2} \left(P_{|\phi^{1,+}\rangle} + P_{|\phi^{1,-}\rangle} \right) \end{array}.$$

Subsequently, we express Eve's state in terms of the orthonormal basis $|\varepsilon_i\rangle_E$, where $i \in \{1, \dots, 4\}$.

$$\sigma_E^k = \begin{pmatrix} \mu_1 & (-1)^k \sqrt{\mu_1 \mu_2} & 0 & 0\\ (-1)^k \sqrt{\mu_1 \mu_2} & \mu_2 & 0 & 0\\ 0 & 0 & \mu_3 & (-1)^k \sqrt{\mu_1 \mu_2}\\ 0 & 0 & (-1)^k \sqrt{\mu_1 \mu_2} & \mu_4 \end{pmatrix}, \quad (3.18)$$

where $k \in \{0, 1\}$.

Additionally, we consider a communication channel where c is a noisy version of a, represented by the transition $c \leftarrow a$. In this model, Alice applies a bit-flip operation with probability q, leading to the conditional probabilities $p_{c|a=0}(1) = p_{c|a=1}(0) = q$. Using standard information-theoretic relations, we simplify the right-hand side of Equation (3.14),

$$S(c|E) = S(cE) - S(E)$$

= $[H(c) + S(E|c) - S(E)],$ (3.19)

and

$$H(c|b) = H(cb) - H(b)$$

= $[H(c) + H(b|c) - H(b)].$ (3.20)

By substituting Equation (3.19) and Equation (3.20) into Equation (3.14), we express the entropy difference in the following form:

$$S(c|E) - H(c|b) = S(E|c) - S(E) - (H(b|c) - H(b)).$$
(3.21)

The aforementioned substitution alters Equation (3.14) in a way that facilitates the computation of the lower bound for the secret key rate in our protocol.

If entropy is computed solely based on Eve's system, there exist only two possible scenarios where Alice's bit value can be either 0 or 1. Furthermore, determining the entropy of Eve's system, conditioned on the value c (announced by Alice), depends on the bit flip probability. This leads to the expression:

$$S(E|c) = \frac{1}{2}S\left((1-q)\sigma_E^0 + q\sigma_E^1\right) + \frac{1}{2}S\left(q\sigma_E^0 + (1-q)\sigma_E^1\right),$$

and

$$S(E) = S\left(\frac{1}{2}\sigma_E^0 + \frac{1}{2}\sigma_E^1\right).$$

Next, we examine Bob's bit string, which is derived from the measurement outcome of his particle (system B) in the state $|\Psi_{ABE}\rangle$. Conceptually, if only Bob's bit string is taken into account, there should be an equal probability of obtaining bit values 0 and 1. Moreover, when evaluating the conditional entropy of Bob's bit string given Alice's noisy bit string (value c), both error and no-error probabilities must be incorporated. Consequently, we obtain:

$$H(b) = 1$$

and

$$H(b|c) = h[q(1-\mathcal{E}) + (1-q)\mathcal{E}].$$

By utilizing these relations and optimizing the parameter q, a positive secret key can be established if $\mathcal{E} \leq 0.124$ (refer to Figure 3.2. a). This threshold represents the maximum tolerable error rate under classical pre-processing, which accounts for the noise introduced by Alice. Now, let us determine the upper bound of the secret key rate using Equation (3.15). In this scenario, the states of Eve, corresponding to Alice and Bob obtaining the results (0,0),(0,0),(1,1), and (1,1), are given by $|\phi^{0,0}\rangle, |\phi^{0,+}\rangle, |\phi^{1,1}\rangle$, and $|\phi^{1,-}\rangle$, respectively. To analyze the worst-case scenario for an adversary, we assume Eve performs a von Neumann measurement using the projectors: $\frac{1}{\sqrt{2}}(|\phi^{0,0}\rangle+|\phi^{1,1}\rangle), \frac{1}{\sqrt{2}}(|\phi^{0,0}\rangle-|\phi^{1,1}\rangle), \frac{1}{\sqrt{2}}(|\phi^{0,+}\rangle+|\phi^{0,-}\rangle),$ and $\frac{1}{\sqrt{2}}(|\phi^{0,+}\rangle-|\phi^{0,-}\rangle)^1$ to obtain an outcome e. Applying this condition appropriately modifies Equation (3.15) as follows:

$$r(a,b,e) = H(c|e) - H(c|b)$$

$$= H(e|c) - H(e) - [H(b|c) - H(b)]$$

$$\leq -\chi(E) - [H(b|c) - H(b)],$$
(3.22)

¹The probabilities of executing the last two projector operations are half of those for the first two. Specifically, the probability of applying the last two projectors is $\frac{1}{6}$, while for the first two, it is $\frac{1}{3}$ each.

here

$$\begin{split} \chi(E) &= S\left[\frac{1}{3}\left(P_{|\phi^{0,0}\rangle} + P_{|\phi^{1,1}\rangle}\right) + \frac{1}{6}\left(P_{|\phi^{0,+}\rangle} + P_{|\phi^{1,-}\rangle}\right)\right] \\ &- \frac{1}{2}S\left[\left(1 - q\right)\left(\frac{2}{3}P_{|\phi^{0,0}\rangle} + \frac{1}{3}P_{|\phi^{0,+}\rangle}\right) + q\left(\frac{2}{3}P_{|\phi^{1,1}\rangle} + \frac{1}{3}P_{|\phi^{1,-}\rangle}\right)\right] \\ &- \frac{1}{2}S\left[q\left(\frac{2}{3}P_{|\phi^{0,0}\rangle} + \frac{1}{3}P_{|\phi^{0,+}\rangle}\right) + \left(1 - q\right)\left(\frac{2}{3}P_{|\phi^{1,1}\rangle} + \frac{1}{3}P_{|\phi^{1,-}\rangle}\right)\right] \end{aligned}$$

The above expression is the Holevo quantity [274] establishes the upper limit of mutual information between e and c across all conceivable measurement strategies that Eve might employ. This enables the computation of an upper bound on the key rate by solving r(a,b,e)=0. The resulting solution provides an upper bound of $\varepsilon \geq 0.114$, assuming the optimal selection of q (refer to Figure 3.2. c). In the BB84 protocol, a single transmission of the qubit sequence occurs over a one-way quantum channel. Conversely, the proposed scheme necessitates three quantum channel transmissions, prioritizing a more substantial quantum component while reducing reliance on the classical component. These three transmissions correspond to distinct sequences generated by Alice and Bob. Although the BB84 protocol incorporates one-way classical post-processing, the proposed scheme retains this feature. Given the three separate quantum transmissions, security validation for each sequence is imperative through information reconciliation. Since the sequences differ, their security is assessed independently. Our approach employs an information-theoretic framework, utilizing two-qubit density operators to establish the upper and lower bounds of the secret key rate based on the QBER, following a methodology similar to that used in BB84. For the BB84 protocol, the lower bound on the tolerable QBER with classical pre-processing is $\xi \le 0.124$, while the upper bound for the key rate is $\varepsilon \ge 0.146$. In contrast, the proposed scheme maintains the same lower bound at $\varepsilon \le 0.124$ but exhibits a reduced upper bound at $\mathcal{E} \geq 0.114$.

3.4 ANALYSIS OF PHOTON NUMBER SPLITTING ATTACK

As previously discussed, our proposed schemes can be implemented using sources emitting WCPs (refer to Equation (3.1)). However, cryptographic protocols relying on WCP may encounter security vulnerabilities due to the potential exploitation of PNS and related attacks by an adversary. Therefore, it is essential to analyze and ensure the robustness of our schemes against various forms of PNS attacks that an eavesdropper could execute under the assumption of a vanishing QBER (i.e., QBER = 0). The sub-protocols incorporated in our framework ne-

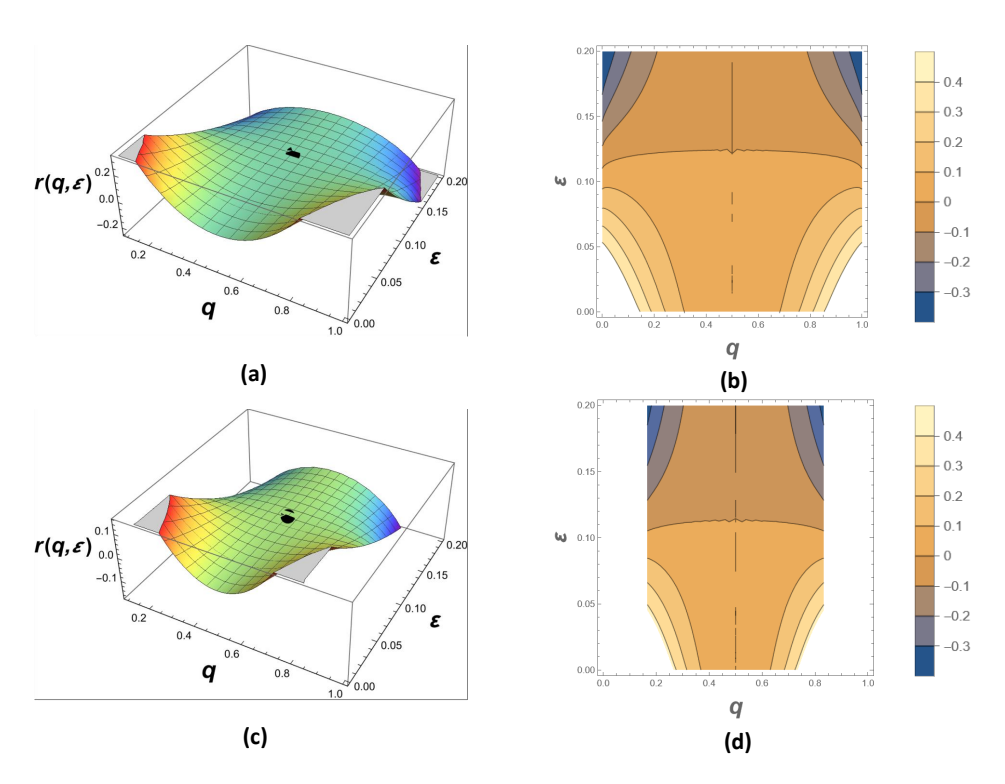


Figure 3.2: The variation of the secret key rate with respect to bit-flip probability (q) and QBER (\mathcal{E}) is illustrated: (a) the lower bound on the secret key rate as a function of bit-flip probability and QBER, (b) a contour plot depicting the lower bound error limit, correlating QBER with bit-flip probability, (c) the upper bound on the secret key rate as a function of bit-flip probability and QBER, and (d) a contour plot illustrating the upper bound error limit with respect to QBER and bit-flip probability.

cessitate Bob to disclose basis information or a specific set of non-orthogonal state parameters. With this in mind, the following observations are noteworthy:

1. In Protocol 3.1 for QKD, Eve carries out a PNS attack under the assumption of having unlimited technological resources, constrained only by the fundamental principles of physics. The PNS attack, inherently dependent on quantum memory, is also referred to as a quantum storage attack. Here, we consider an optimal scenario for Eve's strategy. The probability of an *n*-photon state occurring follows the distribution p(n, μ) = e^{-μμ¹}/n!, where μ represents the mean photon number. Both Alice and Bob possess knowledge of the channel transmittance (η) and the mean photon number (μ). In an ideal case without eavesdropping, the expected probability of detecting at least one photon is given by ∑ p(n, μη), commonly referred to as the raw detection rate per pulse. Within this framework, sequence S_{B2} is generated independently but encodes the same bit information as sequence S_{B1}, albeit in a distinct basis. Eve strategically targets only S_{B1} to maximize her probability of extracting information. Specifically, we consider a scenario where Eve initially performs a photon-number QND measurement on S_{B1} to determine the number of

photons present. She subsequently discards single-photon pulses while selectively retaining one photon from multi-photon pulses. The remaining photons are then transmitted to Alice through an ideal lossless channel¹ ($\eta = 1$). However, Eve cannot arbitrarily discard multi-photon pulses, as maintaining a QBER of zero imposes constraints on such actions. The extent to which Eve can filter multi-photon pulses is fundamentally dependent on the channel transmittance η between Alice and Bob. For this attack to be feasible, the following condition must hold [300]:

$$\sum_{n\geq 1} p(n, \mu \eta) = t_1 p(1, \mu) + \sum_{n\geq 2} p(n, \mu).$$

In this context, t_1 represents the proportion of single-photon pulses that successfully reach Bob. When faced with a highly capable eavesdropper, losses can be so significant that $t_1 = 0$. Under these circumstances, Eve exclusively intercepts multi-photon pulses, occurring with a probability given by $\sum_{n \geq 2} p(n, \mu)$. The amount of information Eve acquires is expressed as:

$$I_{\text{Evel}} = \frac{0.5 \times \sum\limits_{n \ge 2} p(n, \mu)}{0.75 \times \sum\limits_{n \ge 1} p(n, \mu \eta)},$$

The factor of 0.5 in the numerator originates from the classical information disclosed by Bob during the generation of the sifted key², while the factor of 0.75 in the denominator arises from Alice's information related to non-empty pulses. Specifically, 0.5 accounts for Bob's revealed classical information, and the remaining 0.25 corresponds to Alice's information gain in the absence of Bob's announcement. Figure 3.3. a depicts the variation of I_{Eve1} with distance l for an attenuation of $\alpha = 0.25$ dB/km and a mean photon number $\mu = 0.1$, ensuring a fair comparison with the BB84 protocol ($\mu = 0.1$). The estimated critical attenuation is $\delta_c = 15.05$ dB, corresponding to a critical distance of $l_c = 60.2$ km,

¹The transmission efficiency in an optical fiber of length II is given by $\eta = 10^{-\frac{\delta}{10}}$, where δ is defined as $\delta = \alpha l [\mathrm{dB}]$. Here, α represents the fiber loss in dB/km. Since both α and l are non-negative, δ also remains non-negative. The boundary conditions for δ, specifically $\delta = 0$ and $\delta \to \infty$, yield $\eta = 1$ and $\eta = 0$, respectively. Consequently, the range $0 \le \eta \le 1$ characterizes the attenuation in the transmission channel, where $\eta = 1$ corresponds to an ideal, lossless channel allowing full transmission, and $\eta = 0$ represents a completely opaque channel with no transmission.

²For Protocol 3.1, a total of 0.625 bits of information is revealed to Eve, out of which only 0.5 bits are useful for generating the sifted key.

beyond which the attacker acquires full bit information under the PNS attack. Comparatively, the critical distance for the BB84 protocol under similar conditions is 52 km [300], which is shorter than that of our protocol. Additionally, the figure indicates that Eve gains almost no information up to a distance of 30 km. This advantage stems from the utilization of a higher amount of quantum signal or equivalently a higher amount of quantum resources in the communication process. Furthermore, as this protocol reveals less classical information than BB84, Eve's ability to extract information after the classical announcement in a collective attack scenario is reduced, thereby enhancing the security of the final key.

2. In Protocol 3.2 for QKD, Bob discloses information about the non-orthogonal states. Given this setup, Eve can employ a PNS attack variant known as the intercept-resend unambiguous discrimination (IRUD) attack. This strategy begins with Eve conducting a quantum non-demolition (QND) measurement to ascertain the photon number within each pulse. She discards all pulses containing fewer than three photons and proceeds to measure the remaining ones (those with at least three photons) using a specific measurement process¹, denoted as \mathcal{M} . Upon obtaining a definite outcome from \mathcal{M} , she reconstructs a new photon state and transmits it to Bob. This attack assumes that Eve operates in a lossless channel ($\eta = 1$) and possesses quantum memory. The attack is exclusively executed on sequence S_{B1} , following the same principle as the PNS attack in Protocol 3.1 for QKD. However, unlike the standard PNS attack, Eve cannot indiscriminately discard pulses with fewer than three photons, as maintaining a QBER of zero is essential. For the attack to be effective, the following condition must be met:

$$\sum_{n\geq 1} p(n,\mu\eta) = t_1 p(1,\mu) + t_2 p(2,\mu) + \sum_{n\geq 3} p(n,\mu),$$

where t_1 and t_2 represent the proportions of single-photon and two-photon pulses, respectively, that reach Bob. Since the probability of pulses containing more than three photons is negligible, it can be approximated as $\sum_{n\geq 3} p(n,\mu) \approx p(3,\mu)$. For an adversary with maximal capabilities, channel losses ensure that $t_1=0$ and $t_2=0$, meaning Eve exclusively

The measurement \mathfrak{M} represents a von Neumann measurement capable of distinguishing the following four quantum states: $|\Phi_1\rangle = \frac{1}{\sqrt{2}}\left(|000\rangle - |011\rangle\right), |\Phi_2\rangle = \frac{1}{2}\left(|101\rangle + |010\rangle + |100\rangle + |110\rangle\right), |\Phi_3\rangle = \frac{1}{\sqrt{2}}\left(|111\rangle - |001\rangle\right),$ and $|\Phi_4\rangle = \frac{1}{2}\left(|101\rangle - |010\rangle - |100\rangle + |110\rangle\right)$ [172].

targets three-photon pulses, which occur with a probability of $p(3,\mu)$. The amount of information Eve extracts in this scenario is given by:

$$I_{\text{Eve2}} = \frac{I(3, \chi)p(3, \mu)}{\sum\limits_{n \ge 1} p(n, \mu \eta)},$$

where $I(n,\chi)$ represents the maximum information Eve can extract using n photons in a single pulse. χ is the overlap of two states within each set of non-orthogonal states announced by Bob¹. The denominator represents the raw detection rate per pulse in the absence of an eavesdropper, given a channel transmittance η between Alice and Bob. For a fair comparison with the SARG04 protocol ($\mu=0.2$), we also set $\mu=0.2$. Assuming an attenuation factor of $\alpha=0.25$ dB/km and $\mu=0.2$, we analyze the variation of Eve's information (I_{Eve2}) with distance to determine the critical attenuation (see Figure 3.3. b). From Figure 3.3. b, the critical attenuation is found to be $\delta_c=23.75$ dB, corresponding to a critical distance of $I_c=95$ km. In comparison, under similar conditions, the critical distance for the SARG04 protocol ranges from approximately 50 km to 100 km [172], which is comparable to the critical distance achieved with our protocol. For this attack, Eve gains almost no information up to 60 km. Additionally, our protocol reveals less classical information, thereby offering better protection against Eve's collective attack, which relies on the information disclosed in the classical subprotocol.

3.5 CONCLUSION

This chapter introduces a novel protocol for QKD along with a variant of the same. While the proposed protocols require greater quantum resources compared to SARG04 and similar schemes, they minimize the amount of classical information transmitted over the public channel, thereby reducing the probability of certain side-channel attacks. A comprehensive security analysis has been conducted for the proposed protocols. Additionally, the tolerable error thresholds for the upper and lower bounds of the secret key rate under collective attacks have been determined. The findings indicate that the implementation of specific classical pre-processing techniques enhances the tolerable error limit, a result that is further illustrated through graph-

 $I(n,\chi) = 1 - h(P, 1-P)$ with h(P, 1-P) being the binary entropy function and $P = \frac{1}{2} \left(1 + \sqrt{1 - \chi^{2n}} \right)$ [301]. In our case, the overlap, $\chi = \frac{1}{\sqrt{2}}$.

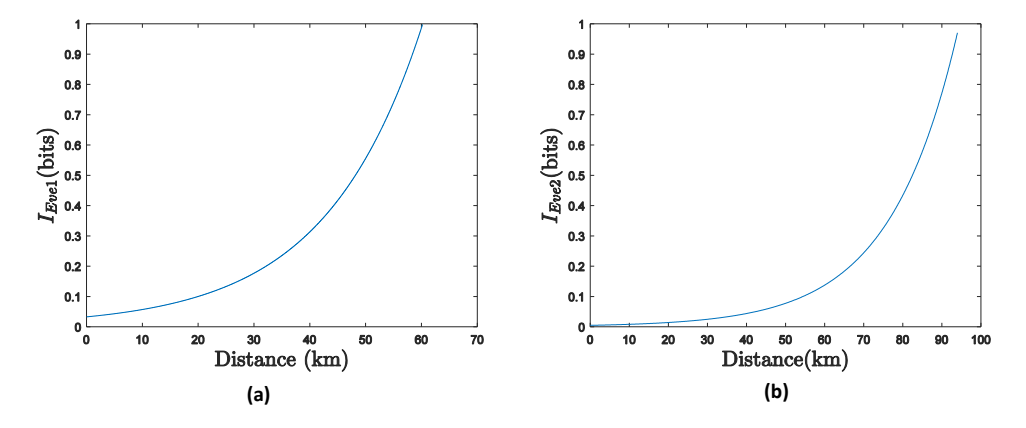


Figure 3.3: The variation in Eve's information as a function of distance is analyzed to determine the critical distance (l_c) : (a) Eve's information plotted against distance to estimate the critical threshold where the attacker extracts maximum key information via a PNS attack on Protocol 3.1, and (b) Eve's information plotted against distance to estimate the critical threshold where the attacker gains maximum key information using an IRUD attack on Protocol 3.2.

ical representations. Before concluding, it is important to highlight key observations from the analysis. In [299], the density operators of Eve's final state were derived for the six-state QKD protocol. Interestingly, despite structural differences, the density operators characterizing Eve's final system in the proposed protocols are found to be identical to those in [299]. Notably, in Protocol 3.2 (Protocol 3.1), Alice and Bob (Alice) do not disclose their (her) measurement outcomes when different bases are used for state preparation and measurement. The reason behind the equivalence of density operators lies in the cancellation of terms in the density matrix in cases of basis mismatch. Furthermore, it is explicitly shown that for the proposed protocols, the tolerable QBER is constrained within $\mathcal{E} \leq 0.124$ for the lower bound and $\mathcal{E} \geq 0.114$ for the upper bound of the secret key rate when classical pre-processing is applied. In the absence of such pre-processing, a reduction in these tolerable error limits is expected.

In practical cryptographic implementations, various types of errors can arise during qubit transmission. When the QBER exceeds zero, an eavesdropper may attempt to exploit partial cloning machines [302, 303, 304]. Acín et al. demonstrated that legitimate users of the SARG04 protocol can tolerate an error rate of up to 15% when Eve employs the most effective known partial cloning strategy [300]. Additionally, they established that this tolerable error threshold surpasses that of the BB84 protocol. In our analysis, for QBER > 0, we similarly determine the tolerable error limit to be 15% (refer to Section 3.3), which exceeds the performance of BB84 and its variants. Furthermore, we conduct a security-efficiency trade-off evaluation for the proposed schemes, benchmarking their efficiency against the SARG04 protocol.

Security-efficiency trade-off for our protocol: In 2000, Cabello [173] introduced a measure of the efficiency of quantum communication protocols as $\eta = \frac{b_s}{q_t + b_t}$, where b_s is the number of secret bits exchanged by the protocol, q_t is the number of qubits interchanged via the quantum channel in each step of the protocol, and b_t is the classical bit information exchanged between Alice and Bob via the classical channel¹. As far as Protocol 3.2 is concerned, an inherent error arises during its execution. If Alice's initial state is $|0\rangle$, and Bob's measurement outcomes are $|0\rangle$ or $|-\rangle$, no error occurs. However, if Bob's outcome is $|+\rangle$, an inherent error is introduced. The probabilities of Bob obtaining $|0\rangle$, $|-\rangle$, and $|+\rangle$ are $\frac{1}{8}$, $\frac{1}{16}$, and $\frac{1}{16}$, respectively (see Table 3.1). In this case, when the measurement result is determined as $|0\rangle$, the error probability corresponding to Bob's measurement outcomes $|0\rangle$ and $|+\rangle$ is calculated as $(\frac{1}{64})/(\frac{1}{64}+\frac{1}{8})=\frac{1}{9}$. A similar scenario applies when Alice's initial state is $|1\rangle$, $|+\rangle$ or $|-\rangle$. For instance, if Alice's initial state is $|1\rangle$, no error occurs when Bob's measurement results are $\{|1\rangle, |+\rangle\}$, whereas an error arises when the outcome is $|-\rangle$. The same probability calculations hold for the remaining cases of Alice's initial states. Finally, the secret key bits (b_3) are transformed as follows:

$$b_s = \left[\left(\frac{1}{16} + \frac{1}{32} + \frac{1}{64} \right) + \left(\frac{1}{8} + \frac{1}{64} \right) \left(1 - h(\frac{1}{9}) \right) \right] \times 4$$

$$= 0.72$$

For the sifting subprotocol of the second QKD protocol (Protocol 3.2), the values of the essential parameters are $b_s = 0.72$, $q_t = 3$ and $b_t = 0.75$, resulting in an efficiency of $\eta = 0.192$. For the sifting subprotocol of our Protocol 3.1, the values of the essential parameter are $b_s = 0.75$, $q_t = 3$ and $b_t = 0.625$, giving an efficiency of $\eta = 0.2069$ with no inherent error. In this specific sifting condition, the basis information will be revealed at the end of the protocol, which may increase the chance of a PNS attack by a powerful Eve. To apply the more efficient Protocol 3.2, one must consider the inherent error probability value of 0.0625, and the exchange of classical information is also more than Protocol 3.1. We want to stress that the Protocol 3.2 is more robust against PNS attack because Alice and Bob do not reveal the basis information; instead, two non-orthogonal state information values are announced for the sifting process (M value). Our two protocols are more efficient than the SARG04 protocol $^2(\eta = 0.125)$. It is worth noting that for both protocols, the amount of classical information disclosed during the classical sifting phase is lower than that of the SARG04 protocol. This reduction decreases the probability of

¹The classical bit which is used for detecting eavesdropping is neglected here.

²The values of essential parameters for SARG04 protocol are $b_s = 0.25$, $q_t = 1$ and $b_t = 1$, resulting in an efficiency of $\eta = 0.125$.

an information gain by Eve using the announced classical information. One can use either of our two protocols as needed for the necessary task.

CHAPTER 4

CONTROLLED QUANTUM KEY AGREEMENT WITHOUT USING QUANTUM MEMORY

4.1 INTRODUCTION

Key agreement is a vital cryptographic domain, essential for achieving perfect forward secrecy. It enables two or more parties to collaboratively generate a shared key, ensuring all legitimate participants influence the outcome while preventing any subset or eavesdropper from dictating the key. A stronger KA definition, commonly adopted in QKA, mandates equal influence from all legitimate users. The foundational two-party KA protocol was introduced by Diffie and Hellman in 1976 [22], with later extensions to multiparty settings for enhanced efficiency [174, 175, 176, 177]. This stronger definition enforces "fairness", ensuring no individual or group can manipulate the final key [178, 179]. Classical KA security relies on computational complexity, but advancements in quantum computing threaten this foundation, as many underlying problems could be efficiently solved with scalable quantum computers. To counteract this, cryptographic schemes leverage quantum mechanics principles—such as collapse on measurement, the no-cloning theorem, and Heisenberg's uncertainty principle—enabling cryptographic tasks with unconditional security. QKA, the quantum counterpart of KA, benefits from these properties [180]. This work introduces two novel QKA schemes and their security proofs. Before discussing QKA and its multipartite extensions, a brief overview of quantum cryptography will highlight its unique attributes and broader applications.

QKA has emerged as a fundamental cryptographic primitive, enabling two or more parties to establish an identical key with equal contribution using quantum resources. Its significance lies in applications such as electronic auctions, multiparty secure computing, and access control [176], along with its role in ensuring forward secrecy. Due to its broad applicability, QKA has recently been recognized as a distinct domain within quantum cryptography. The first QKA

protocol, introduced by Zhou et al. in 2004 [197], employed quantum teleportation for key agreement between two users. However, Tsai and Hwang (2009) later identified a fairness issue [305], where one party could unilaterally determine the key and distribute it undetected. Subsequent research confirmed the protocol's insecurity [198]. In 2013, Shi and Zhou proposed the first MQKA scheme using entanglement swapping [199], which was later found to be insecure [200]. Meanwhile, Chong et al. (2010) developed a QKA protocol based on BB84, integrating delay measurement and authenticated classical channels [201]. Over time, various two-party QKA protocols have been extended to MQKA [200, 202, 203, 204], classified into tree-type [203], complete-graph-type [200], and circle-type [206]. The circle-type structure offers better feasibility and efficiency. Research in quantum conference key agreement and MQKA continues to grow, leveraging methods such as differential phase reference [306] and discrete variable entangled quantum states. Experimental advancements in QCKA have been demonstrated by Proietti et al. [307], while Wang et al. [308] have explored new schemes for mutually authenticated QKA.

A secure QKA protocol must ensure three key properties: *Correctness*, where all participants derive the agreed key accurately; Security, preventing unauthorized eavesdropping without detection; and Fairness, ensuring no subset of participants can solely determine the final key. Leveraging these principles, we introduce a novel CQKA protocol with a controller, Charlie, enabling key agreement between two legitimate parties without requiring quantum memory. Controlled quantum cryptography has gained significant attention, with numerous schemes proposed for controlled-QKD [207, 208], controlled-quantum dialogue [209, 210], and controlledsecure direct communication [211, 212, 213, 166]. However, to the best of our knowledge, no existing CQKA protocol achieves this without quantum memory [214]. Addressing this gap, our scheme employs Bell states and single-qubit states, using a one-way quantum channel to minimize noise, unlike two-way QKA protocols [202, 204, 214] that suffer from increased channel noise. We further analyze the impact of Markovian and non-Markovian noise on our protocol, examining fidelity as a function of the noise parameter. The security of the proposed CQKA scheme is rigorously proven, demonstrating feasibility with current quantum technologies. Additionally, we establish its efficiency over many existing schemes, with the controller mechanism providing distinct advantages in specific scenarios.

The structure of this chapter is outlined as follows: Section 4.2 introduces the fundamental concepts necessary for articulating our schemes, followed by a step-by-step explanation of our

proposed protocol. Section 4.3 presents a security evaluation, addressing both impersonation-based fraudulent attacks and broader (more generalized) threats, such as collective attacks. The influence of noise on the protocol's performance is examined in Section 4.4. A comparative analysis between our protocol and existing approaches is conducted in Section 4.5. Section 4.6 provides an in-depth discussion of the results along with the details of the experimental setup. Lastly, the conclusions of this chapter are drawn in Section 4.7.

4.2 NEW PROTOCOL FOR CQKA (PROTOCOL 4.1)

In the previous section, we highlighted the significance of correctness as a fundamental requirement for a QKA protocol. This section provides a detailed explanation of our proposed CQKA protocol, with a specific focus on ensuring "correctness". To illustrate this, we consider a particular example where Alice, Bob, and Charlie select the i^{th} key bit to prepare the corresponding i^{th} quantum state in their particle sequence for subsequent protocol steps. The first part of this section outlines the steps taken to satisfy the correctness condition, while the second part presents the protocol in a structured, step-by-step manner for a more generalized understanding.

BASIS CONCEPT OF THE PROPOSED PROTOCOL 4.1

Our proposed CQKA protocol is formulated based on core principles of quantum mechanics. To define the process, we establish the relationship between classical bit values and quantum states. Two distinct mappings are utilized: one for public announcement and another for the final key agreement between Alice and Bob [309], which remains undisclosed to uphold privacy constraints. During protocol execution, Charlie and Alice publicly declare their respective classical bit sequences, k_C and k_A , based on the quantum states they generate, as specified in Equations (4.1) and (4.2). Meanwhile, Bob determines his classical bit sequence k_B from measurement outcomes, following the mapping defined in Equation (4.3). The association between these classical sequences and their corresponding quantum states is detailed in the subsequent discussion.

0 :
$$|\phi^{+}\rangle = \frac{1}{\sqrt{2}}(|00\rangle + |11\rangle),$$

1 : $|\phi^{-}\rangle = \frac{1}{\sqrt{2}}(|00\rangle - |11\rangle).$ (4.1)

In the proposed CQKA scheme, if Charlie prepares the Bell state $|\phi^{+}\rangle$ ($|\phi^{-}\rangle$), the corresponding bit value in the sequence k_C is assigned as 0 (1). The mapping process utilized by Alice and Bob follows a similar approach, as outlined below.

$$\begin{array}{ll}
0 : |0\rangle, \\
1 : |1\rangle,
\end{array} \tag{4.2}$$

and

0:
$$|\phi^{+}\rangle = \frac{1}{\sqrt{2}}(|00\rangle + |11\rangle)$$
 or $|\psi^{-}\rangle = \frac{1}{\sqrt{2}}(|01\rangle - |10\rangle)$,
1: $|\phi^{-}\rangle = \frac{1}{\sqrt{2}}(|00\rangle - |11\rangle)$ or $|\psi^{+}\rangle = \frac{1}{\sqrt{2}}(|01\rangle + |10\rangle)$. (4.3)

Alice and Bob employ a mapping technique that associates two-bit classical information with their final measurement outcomes after performing Bell measurements. This mapping is structured as follows:

$$00: |\phi^{+}\rangle = \frac{1}{\sqrt{2}} (|00\rangle + |11\rangle),$$

$$01: |\phi^{-}\rangle = \frac{1}{\sqrt{2}} (|00\rangle - |11\rangle),$$

$$10: |\psi^{+}\rangle = \frac{1}{\sqrt{2}} (|01\rangle + |10\rangle),$$

$$11: |\psi^{-}\rangle = \frac{1}{\sqrt{2}} (|01\rangle - |10\rangle).$$
(4.4)

The first row of the mapping table indicates that if Alice's (Bob's) Bell measurement results in $|\phi^+\rangle$, they store the bit sequence 00 privately for later use in the protocol. Similar mappings apply to other cases.

Now, we outline the fundamental concept behind our CQKA protocol. Initially, Alice and Bob request Charlie to initiate the protocol. In response, Charlie generates a sequence of Bell states, choosing between $|\phi^+\rangle_{C_1C_2}$ and $|\phi^-\rangle_{C_1C_2}$. For instance, if Charlie selects $|\phi^+\rangle_{C_1C_2}$, where subscripts C_1 and C_2 denote the first and second qubits of Charlie's Bell state, he records the classical sequence k_C (in this case, 0) to store information about the prepared state. Charlie then transmits qubit C_1 to Alice and qubit C_2 to Bob while keeping k_C confidential. Upon receiving qubit C_1 (C_2) from Charlie, Alice (Bob) prepares their respective qubits in the computational basis ($Z \in \{|0\rangle, |1\rangle\}$), choosing $|0\rangle$ ($|1\rangle$) as an example. Alice records her classical sequence k_A (here, 0) and keeps it private. Alice's and Bob's prepared qubits are denoted as A and B, respectively. Next, Alice (Bob) applies a CNOT operation, where C_1 (C_2) serves as the control qubit and A (B) as the target qubit. The resulting quantum state after the CNOT operation is represented by the following equation:

$$|\psi_{2}\rangle = \frac{1}{\sqrt{2}}CNOT_{C_{1}\rightarrow A}CNOT_{C_{2}\rightarrow B}(|0\rangle_{A}|\phi^{+}\rangle_{C_{1}C_{2}}|1\rangle_{B})$$

$$= \frac{1}{\sqrt{2}}(|00\rangle_{AC_{1}}|01\rangle_{C_{2}B} + |11\rangle_{AC_{1}}|10\rangle_{C_{2}B}).$$
(4.5)

In this scenario, Alice and Bob each possess two qubits, denoted as C_1 , A for Alice and C_2 , B for Bob. Both parties perform Bell basis measurements, resulting in the following quantum state:

$$|\psi_2\rangle = \frac{1}{\sqrt{2}} (|\phi^+\rangle_{AC_1} |\psi^+\rangle_{C_2B} + |\phi^-\rangle_{AC_1} |\psi^-\rangle_{C_2B}).$$
 (4.6)

Upon obtaining their measurement outcomes, they request Charlie to disclose his bit sequence k_C (set to 0 in this case), corresponding to his initially prepared states based on the mapping in Equation (4.1). Additionally, Alice and Bob announce their respective bit sequences k_A and k_B , where k_A is determined by Alice's prepared state and k_B is derived from Bob's measurement on qubits 3 and 4 after performing a Bell measurement, as defined in Equation (4.2) and Equation (4.3), respectively. In this instance, Alice announces 0, while Bob announces either 0 or 1 with equal probability $(\frac{1}{2})$, as he may obtain the measurement outcomes $|\psi^-\rangle_{34}$ or $|\psi^+\rangle_{34}$ with equal probability (refer to Equation (4.6)). The relationship between the announced values of Charlie, Alice, and Bob, along with their undisclosed measurement outcomes and the hidden measurement results of the other party, is detailed in Table 4.1. For instance, if Charlie, Alice, and Bob announce the bit values 0, 0, and 1, respectively, Alice and Bob can infer their own two-bit classical measurement results using Equation (4.4). Based on Table 4.1, Alice deduces Bob's measurement outcome as 10, while Bob infers Alice's outcome as 00. To derive the final agreement key, Alice and Bob perform modulo-2 addition on their respective measurement results, as described in Equation (4.4). This produces a two-bit result, which is then further processed by applying modulo-2 addition between the first and second bits. In this example, the computation follows: $10 \oplus 00 = 10$ Thus, the final key is $1 \oplus 0 = 1$.

There exist eight possible state combinations resulting from the independent choices of Alice, Bob, and Charlie. These states can be represented as $|\psi_i\rangle$, where $i \in \{1, 2, \dots, 8\}$. Since $|\psi_2\rangle$ has already been discussed, the remaining state combinations are defined as follows.

$$|\psi_{1}\rangle = \frac{1}{\sqrt{2}}CNOT_{C_{1}\to A}CNOT_{C_{2}\to B}(|0\rangle_{A}|\phi^{+}\rangle_{C_{1}C_{2}}|0\rangle_{B})$$

$$= \frac{1}{\sqrt{2}}(|\phi^{+}\rangle_{AC_{1}}|\phi^{+}\rangle_{C_{2}B} + |\phi^{-}\rangle_{AC_{1}}|\phi^{-}\rangle_{C_{2}B}),$$
(4.7)

$$|\psi_{3}\rangle = \frac{1}{\sqrt{2}}CNOT_{C_{1}\to A}CNOT_{C_{2}\to B}(|1\rangle_{A}|\phi^{+}\rangle_{C_{1}C_{2}}|0\rangle_{B})$$

$$= \frac{1}{\sqrt{2}}(|\psi^{+}\rangle_{AC_{1}}|\phi^{+}\rangle_{C_{2}B} - |\psi^{-}\rangle_{AC_{1}}|\phi^{-}\rangle_{C_{2}B}),$$
(4.8)

$$|\psi_{4}\rangle = \frac{1}{\sqrt{2}}CNOT_{C_{1}\to A}CNOT_{C_{2}\to B}(|1\rangle_{A}|\phi^{+}\rangle_{C_{1}C_{2}}|1\rangle_{B})$$

$$= \frac{1}{\sqrt{2}}(|\psi^{+}\rangle_{AC_{1}}|\psi^{+}\rangle_{C_{2}B} - |\psi^{-}\rangle_{AC_{1}}|\psi^{-}\rangle_{C_{2}B}),$$
(4.9)

$$|\psi_{5}\rangle = \frac{1}{\sqrt{2}}CNOT_{C_{1}\to A}CNOT_{C_{2}\to B}(|0\rangle_{A}|\phi^{-}\rangle_{C_{1}C_{2}}|0\rangle_{B})$$

$$= \frac{1}{\sqrt{2}}(|\phi^{+}\rangle_{AC_{1}}|\phi^{-}\rangle_{C_{2}B} + |\phi^{-}\rangle_{AC_{1}}|\phi^{+}\rangle_{C_{2}B}),$$
(4.10)

$$|\psi_{6}\rangle = \frac{1}{\sqrt{2}} \text{CNOT}_{C_{1} \to A} \text{CNOT}_{C_{2} \to B} (|0\rangle_{A} |\phi^{-}\rangle_{C_{1}C_{2}} |1\rangle_{B})$$

$$= \frac{1}{\sqrt{2}} (|\phi^{+}\rangle_{AC_{1}} |\psi^{-}\rangle_{C_{2}B} + |\phi^{-}\rangle_{AC_{1}} |\psi^{+}\rangle_{C_{2}B}),$$

$$(4.11)$$

$$|\psi_{7}\rangle = \frac{1}{\sqrt{2}}CNOT_{C_{1}\to A}CNOT_{C_{2}\to B}(|1\rangle_{A}|\phi^{-}\rangle_{C_{1}C_{2}}|0\rangle_{B})$$

$$= \frac{1}{\sqrt{2}}(|\psi^{+}\rangle_{AC_{1}}|\phi^{-}\rangle_{C_{2}B} - |\psi^{-}\rangle_{AC_{1}}|\phi^{+}\rangle_{C_{2}B}),$$
(4.12)

$$|\psi_{8}\rangle = \frac{1}{\sqrt{2}}CNOT_{C_{1}\to A}CNOT_{C_{2}\to B}(|1\rangle_{A}|\phi^{-}\rangle_{C_{1}C_{2}}|1\rangle_{B})$$

$$= \frac{1}{\sqrt{2}}(|\psi^{+}\rangle_{AC_{1}}|\psi^{-}\rangle_{C_{2}B} - |\psi^{-}\rangle_{AC_{1}}|\psi^{+}\rangle_{C_{2}B}).$$
(4.13)

DESCRIPTION OF PROPOSED PROTOCOL 4.1

The new CQKA protocol is outlined in a stepwise manner:

Step 1 Charlie generates a sequence of n Bell states, denoted as $\{S_{C_1C_2}\}$, and partitions it into two sequences: S_{C_1} , containing the first qubits, and S_{C_2} , containing the second qubits of the Bell states.

$$S_{C_1} = \left\{ |s\rangle_{C_1}^1, |s\rangle_{C_1}^2, |s\rangle_{C_1}^3, \cdots, |s\rangle_{C_1}^i, \cdots, |s\rangle_{C_1}^n \right\},$$

$$S_{C_2} = \left\{ |s\rangle_{C_2}^1, |s\rangle_{C_2}^2, |s\rangle_{C_2}^3, \cdots, |s\rangle_{C_2}^i, \cdots, |s\rangle_{C_2}^n \right\}.$$

The subscripts C_1 and C_2 denote the first and second qubits of Charlie's Bell state sequence $S_{C_1C_2}$. Each Bell state in this sequence is either $|\phi^+\rangle$ or $|\phi^-\rangle$, while the superscript (e.g., $\{1,2,3,\cdots,i,\cdots,n\}$) represents the positional index of the qubits in S_{C_1} and S_{C_2} .

Step 2 Charlie randomly generates 2p decoy qubits using either the computational basis (Z-basis: $\{|0\rangle, |1\rangle\}$) or the diagonal basis (X-basis: $\{|+\rangle, |-\rangle\}$). He inserts p decoy qubits at arbitrary positions within S_{C_1} and another p within S_{C_2} , expanding the sequences to S'_{C_1}

Table 4.1: The table below illustrates the relationship between the announcements made by Charlie, Alice, and Bob, and the final key.

Announced	Alice's	Bob's An-	Bob's guess	Alice's guess	Value	Final
bit by	An-	nounced	of Alice's	of Bob's	of	key
Charlie	nounced	bit (k_B)	measurement	measurement	$r_A \oplus r_B$	after
(k_C)	bit (k_A)		outcome	outcome		QKA
			(r_A)	(r_B)		(K)
0	0	0	00	00	00	0
	0	1	01	01	00	0
	0	1	00	10	10	1
	0	0	01	11	10	1
	1	0	10	00	10	1
	1	1	11	01	10	1
	1	1	10	10	00	0
	1	0	11	11	00	0
1	0	1	00	01	01	1
	0	0	01	00	01	1
	0	0	00	11	11	0
	0	1	01	10	11	0
	1	1	10	01	11	0
	1	0	11	00	11	0
	1	0	10	11	01	1
	1	1	11	10	01	1

and S'_{C_2} , respectively. Charlie then transmits S'_{C_1} to Alice and S'_{C_2} to Bob while retaining a classical bit sequence k_C , which encodes the original Bell states in $S_{C_1C_2}$.

The correlation between k_C and $S_{C_1C_2}$ adheres to a predefined mathematical relation (Equation (4.1)).

Step 3 Upon receiving sequences S'_{C_1} and S'_{C_2} from Charlie, Alice, and Bob conduct security verification using the decoy qubits, extracting S_{C_1} and S_{C_2} .

Charlie then publicly discloses the positions and encoding basis of the decoy states, enabling Alice and Bob to assess channel security by evaluating the error rate. If the observed error rate remains within the acceptable threshold, they proceed.

Step 4 Alice and Bob prepare their respective single-qubit sequences, S_A and S_B , each of length n, using the Z-basis. Alice records the classical bit sequence k_A , which determines S_A based on a predefined relation (Equation (4.2)). The sequences S_A and S_B can be visualized as follows:

$$S_A = \{|s\rangle_A^1, |s\rangle_A^2, |s\rangle_A^3, \cdots, |s\rangle_A^i, \cdots, |s\rangle_A^n\},$$

$$S_B = \{|s\rangle_B^1, |s\rangle_B^2, |s\rangle_B^3, \cdots, |s\rangle_B^i, \cdots, |s\rangle_B^n\}.$$

- **Step 5** Alice and Bob each apply a CNOT operation, where the qubits in S_A and S_B act as target qubits, while the corresponding qubits in S_{C_1} and S_{C_2} serve as control qubits, respectively. This operation establishes a correlated two-qubit system, forming the pairs (C_1, A) for Alice and (C_2, B) for Bob.
- **Step 6** Both Alice and Bob conduct Bell-state measurements on their respective two-qubit systems, obtaining results r_A and r_B , as determined by Equation (4.4). These results remain private. Additionally, Bob generates a classical bit sequence k_B

based on his measurement outcomes, utilizing the correlation rule specified in Equation (4.3).

- **Step 7** Alice and Bob then request Charlie to disclose his classical bit sequence k_C publicly.
- **Step 8** Following Charlie's announcement, Alice and Bob reveal their respective classical bit sequences k_A and k_B publicly.
- **Step 9** Using the mapping outlined in Table 4.1, Alice predicts Bob's bit sequence r_B , while Bob predicts Alice's bit sequence r_A . They then compute the modulo-2 addition of the corresponding elements in r_A and r_B . If the result is either 00 or 11, the final key bit is $K_i = 0$; if it is 01 or 10, then $K_i = 1$.

To verify key consistency, Alice and Bob compare a subset of the final key K_i . If the mismatch probability or error rate exceeds the acceptable threshold, the protocol is aborted. Otherwise, the final key is accepted for secure communication after post-processing steps, including error correction and privacy amplification. A flowchart representation of the CQKA protocol is provided in Figure 4.1.

In this section, we introduce an alternative approach to our CQKA protocol by removing the controller's role, thereby transforming it into a two-party QKA protocol. This modification enhances feasibility and reduces noise compared to the original scheme. A detailed comparison of these two protocols, analyzing their advantages and limitations alongside previously proposed schemes, is provided in Section 4.5. The choice between these protocols depends on the specific requirements of different scenarios. To simplify the description, the modified two-party QKA protocol is outlined in the following steps without incorporating the decoy state. The mapping of Alice and Bob's announcements and the final outcome are presented in Table 4.2.

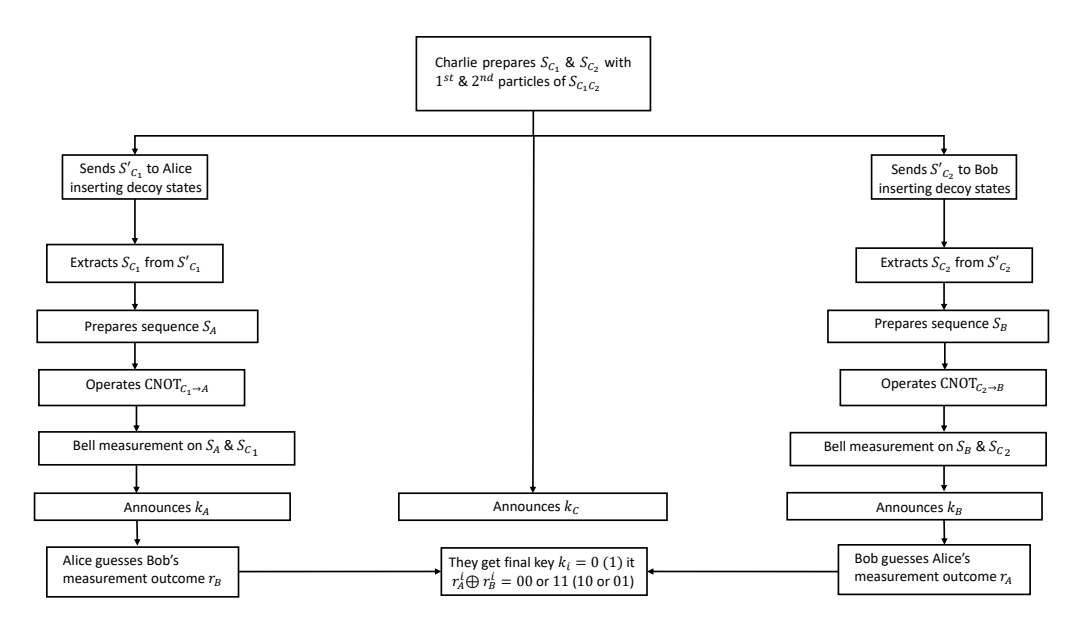


Figure 4.1: The flowchart illustrates the operational framework of the proposed CQKA protocol.

DESCRIPTION OF PROPOSED QKA PROTOCOL (PROTOCOL 4.2)

Step 1 Alice begins by generating n Bell states, denoted as $\{S_{C_1C_2}\}$, and divides them into two sequences: S_{C_1} , containing the first qubits of the Bell states, and S_{C_2} , containing the second qubits. Additionally, she prepares a sequence of n single qubits, S_A), in the Z-basis, ensuring that the bit values correspond to k_C and k_A , maintaining their equivalence 1. The sequences prepared by Alice are as follows:

$$S_{C_{1}} = \left\{ |s\rangle_{C_{1}}^{1}, |s\rangle_{C_{1}}^{2}, |s\rangle_{C_{1}}^{3}, \cdots, |s\rangle_{C_{1}}^{i}, \cdots, |s\rangle_{C_{1}}^{n} \right\},$$

$$S_{C_{2}} = \left\{ |s\rangle_{C_{2}}^{1}, |s\rangle_{C_{2}}^{2}, |s\rangle_{C_{2}}^{3}, \cdots, |s\rangle_{C_{2}}^{i}, \cdots, |s\rangle_{C_{2}}^{n} \right\},$$

$$S_{A} = \left\{ |s\rangle_{A}^{1}, |s\rangle_{A}^{2}, |s\rangle_{A}^{3}, \cdots, |s\rangle_{A}^{i}, \cdots, |s\rangle_{A}^{n} \right\}.$$

Step 2 Alice retains the S_{C_1} sequence and transmits S_{C_2} to Bob.

Step 3 Simultaneously, Bob independently generates a sequence of n single qubits, S_B , in the Z-basis, represented as:

$$S_B = \{|s\rangle_R^1, |s\rangle_R^2, |s\rangle_R^3, \cdots, |s\rangle_R^i, \cdots, |s\rangle_R^n\}.$$

Step 4 This step follows Step 5 of CQKA protocol.

¹The relations established in Equations (4.1,4.2 and 4.3) are also applicable to proposed QKA protocol.

Table 4.2: The table below illustrates the relationship between the announcements made by Alice, Bob, and the final key.

Alice's	Bob's	Bob's guess	Alice's guess	Value of	Final key
Announced bit	Announced bit	of Alice's	of Bob's	$r_A \oplus r_B$	after
(k_A)	(k_B)	measurement	measurement		QKA(K)
		outcome	outcome		
		(r_A)	(r_B)		
0	0	00	00	00	0
0	1	01	01	00	0
0	1	00	10	10	1
0	0	01	11	10	1
1	1	10	01	11	0
1	0	11	00	11	0
1	0	10	11	01	1
1	1	11	10	01	1

Step 5 This step follows Step 6 of CQKA protocol.

Step 6 Since k_A and k_C are identical, Alice and Bob publicly disclose their respective sequences, k_A and k_B .

Step 7 This step follows Step 9 of CQKA protocol.

4.3 SECURITY ANALYSIS OF THE PROPOSED PROTOCOLS

Security plays a crucial role not only in QKA protocols but in all quantum communication protocols. This section examines the security of the proposed CQKA protocol against impersonation attacks and general collective attacks. The same security analysis is also applicable to the proposed QKA protocol. Additionally, we demonstrate that our protocols remain secure even with a relatively small final agreement key length (n = 6).

4.3.1 SECURITY ANALYSIS AGAINST IMPERSONATION FRAUDULENT ATTACK

To evaluate the resilience of our protocol against impersonation attempts, we consider a scenario where an adversary, Eve, attempts to pose as Charlie by employing a generalized two-qubit system. For simplicity, we disregard the security enhancements provided by decoy qubits. In Step 2 of our protocol, an impersonating Eve transmits the first and second qubits of her generated

two-qubit system to Alice and Bob, mimicking Charlie's role. We first analyze the case where Alice and Bob select the same state $|0\rangle$ as an element of their respective sequences, S_A and S_B , and proceed with the subsequent protocol steps. After both parties perform the CNOT operation, the resulting quantum state can be expressed as follows:

$$\begin{split} |\Phi_{1}\rangle &= CNOT_{C_{1}\to A}CNOT_{C_{2}\to B} \left(|0\rangle_{A} \left(a|00\rangle + b|01\rangle + c|10\rangle + d|11\rangle \right)_{C_{1}C_{2}} |0\rangle_{B} \right) \\ &= \left(a|0\rangle|00\rangle|0\rangle + b|0\rangle|01\rangle|1\rangle + c|1\rangle|10\rangle|0\rangle + d|1\rangle|11\rangle|1\rangle)_{AC_{1}C_{2}B} \,. \end{split} \tag{4.14}$$

Let a,b,c, and d be the probability amplitudes associated with the states $|00\rangle, |01\rangle, |10\rangle$, and $|11\rangle$ in Eve's two-qubit system¹, constrained by the normalization condition $|a|^2 + |b|^2 + |c|^2 + |d|^2 = 1$. Alice and Bob perform measurements on their respective two-qubit subsystems, A, C_1 and C_2, B in the Bell basis. To facilitate the analysis of post-measurement outcomes, the above expression can be rewritten in the Bell basis as follows:

$$|\Phi_{1}\rangle = \frac{1}{2} [a(|\phi^{+}\rangle|\phi^{+}\rangle + |\phi^{+}\rangle|\phi^{-}\rangle + |\phi^{-}\rangle|\phi^{+}\rangle + |\phi^{-}\rangle|\phi^{-}\rangle) + b(|\phi^{+}\rangle|\phi^{+}\rangle - |\phi^{+}\rangle|\phi^{-}\rangle + |\phi^{-}\rangle|\phi^{+}\rangle - |\phi^{-}\rangle|\phi^{-}\rangle) + c(|\phi^{+}\rangle|\phi^{+}\rangle + |\phi^{+}\rangle|\phi^{-}\rangle - |\phi^{-}\rangle|\phi^{+}\rangle - |\phi^{-}\rangle|\phi^{-}\rangle) + d(|\phi^{+}\rangle|\phi^{+}\rangle - |\phi^{+}\rangle|\phi^{-}\rangle - |\phi^{-}\rangle|\phi^{+}\rangle + |\phi^{-}\rangle|\phi^{-}\rangle)]_{AC,C_{2}B}$$

$$(4.15)$$

Equation (4.15) represents the composite quantum system involving Alice, Bob, and Eve, following an impersonation attack where Eve generates a two-qubit state. The probability of detecting Eve's presence can be determined by comparing with Equation (4.7), which describes the expected results for Alice and Bob. After performing the necessary calculations, the detection probability of Eve is derived as:

$$P_{|0\rangle|\phi^{+}\rangle|0\rangle} = \frac{1}{2} \left[\left(|a|^{2} + |b|^{2} + |c|^{2} + |d|^{2} \right) - \left(a^{*}b + b^{*}c + c^{*}b + d^{*}a \right) \right]$$

$$= \frac{1}{2} \left[1 - \left(a^{*}b + b^{*}c + c^{*}b + d^{*}a \right) \right],$$
(4.16)

and similarly,

$$\begin{array}{ll} P_{|0\rangle|\phi^{-}\rangle|0\rangle} & = & \frac{1}{2} \left[\left(|a|^2 + |b|^2 + |c|^2 + |d|^2 \right) + \left(a^*b + b^*c + c^*b + d^*a \right) \right] \\ & = & \frac{1}{2} \left[1 + \left(a^*b + b^*c + c^*b + d^*a \right) \right]. \end{array} \tag{4.17}$$

¹One can examine the well-established two-qubit states generated by Eve and assess their resilience against an impersonation attack by assigning specific values to the nonzero parameters a, b, c, and d.

Here, the subscripts $|0\rangle, |\phi^+\rangle$, and $|0\rangle$ correspond to quantum states prepared by Alice, Bob, and Charlie, respectively. Evaluating additional scenarios—where Alice and Bob generate alternative state combinations such as $|0\rangle_A, |1\rangle_B; |1\rangle_A, |0\rangle_B;$ and $|1\rangle_A, |1\rangle_B$ —yields the corresponding detection probabilities:

$$P_{|0\rangle|\phi^{-}\rangle|0\rangle} = P_{|0\rangle|\phi^{+}\rangle|1\rangle} = P_{|1\rangle|\phi^{+}\rangle|0\rangle} = P_{|1\rangle|\phi^{+}\rangle|1\rangle},$$

$$P_{|0\rangle|\phi^{-}\rangle|0\rangle} = P_{|0\rangle|\phi^{-}\rangle|1\rangle} = P_{|1\rangle|\phi^{-}\rangle|0\rangle} = P_{|1\rangle|\phi^{-}\rangle|1\rangle}.$$
(4.18)

Thus, the probability of detecting Eve's intervention for each transmission instance is given by:

$$P_{d} = \frac{1}{8} \left[P_{|0\rangle|\phi^{+}\rangle|0\rangle} + P_{|0\rangle|\phi^{+}\rangle|1\rangle} + P_{|1\rangle|\phi^{+}\rangle|0\rangle} + P_{|1\rangle|\phi^{+}\rangle|1\rangle}$$

$$+ P_{|0\rangle|\phi^{-}\rangle|0\rangle} + P_{|0\rangle|\phi^{-}\rangle|1\rangle} + P_{|1\rangle|\phi^{-}\rangle|0\rangle} + P_{|1\rangle|\phi^{-}\rangle|1\rangle} \right]$$

$$= \frac{1}{2} \left(|a|^{2} + |b|^{2} + |c|^{2} + |d|^{2} \right)$$

$$= \frac{1}{2}.$$

$$(4.19)$$

A detection probability of $\frac{1}{2}$ signifies the highest level of statistical randomness attainable for identifying an adversary, thereby ensuring protocol security. Mathematically, this means that in each message transmission, there is a 0.5 probability of detecting an attacker (Eve) attempting to manipulate or forge a message. As established by Simmons' theorem [275], a secure protocol ensures that an adversary cannot decrease the detection probability below the randomness threshold of $\frac{1}{2}$ without being noticed. This threshold corresponds to the maximum entropy in a binary detection scenario (i.e., detected or undetected), preventing Eve from deterministically avoiding detection. If Eve engages in n independent tampering attempts across n transmissions, the probability of evading detection is $\left(\frac{1}{2}\right)^n$, which declines exponentially as n grows, making detection almost inevitable with repeated attempts. Consequently, the inherent randomness of a $\frac{1}{2}$ detection probability ensures unpredictability for the adversary and satisfies Simmons's security criteria, providing a strong defense against message tampering and forgery. Utilizing Simmons's theory [275], the proposed protocol achieves unconditional security against impersonation-based fraudulent attacks, as demonstrated in Equation (4.19).

4.3.2 SECURITY ANALYSIS AGAINST COLLECTIVE ATTACK STRATEGIES IN TWO-WAY CHANNEL

Secure quantum communication schemes are susceptible to three primary classes of attacks by an eavesdropper: (i) Individual attacks, (ii) Collective attacks, and (iii) Coherent attacks. Among these, individual attacks are the least effective. In this scenario, Eve interacts separately with each of Alice's signal systems by coupling them with an auxiliary system and applying a fixed unitary transformation. She then measures each system independently immediately after the sifting step, before Alice and Bob engage in classical post-processing. Collective attacks [310, 311] share similarities with individual attacks but allow Eve to postpone her measurement until the protocol concludes. In this case, Eve's measurement strategy can be influenced by the messages exchanged during error correction and privacy amplification, and she can conduct joint measurements on all auxiliary systems. This capability grants her greater power compared to an eavesdropper restricted to individual attacks. Assessing a protocol's resilience against collective attacks is a crucial step toward proving security against coherent attacks, which represent the most general and advanced adversarial strategy. This section examines the protocol's security under collective attacks to determine the tolerable error threshold within the security bounds. We first outline Eve's attack methodology in a two-way quantum channel, incorporating non-orthogonal ancilla states, and computing the probability of detecting her presence. Additionally, we evaluate Eve's probability of gaining information by considering key parameters such as her detection probability and the final key information. To establish a secure bound, we employ the asymptotic secret key rate formulated by Devetak and Winter [312] for collective attacks, referencing secure bounds from [299].

In the proposed CQKA protocol, two quantum channels are established: the Charlie-Alice (CA) channel and the Charlie-Bob (CB) channel. Suppose an adversary, Eve, attempts to exploit these channels to extract the final key information while minimizing the probability of detection. To execute this attack, Eve prepares two ancillary qubits, denoted as $|\zeta\rangle$ and $|\eta\rangle$, which together form a two-qubit system specifically designed to target the CA and CB channels. Eve begins by intercepting a qubit, C_1 , from the CA channel and applies an entangling operation, E_{C_1} , which entangles C_1 with the "ancillary" qubit $|\zeta\rangle$. After completing this operation, she forwards the qubit to Alice. Similarly, she intercepts another qubit, C_2 , from the CB channel and applies a corresponding entangling operation, E_{C_2} , to entangle C_2 with $|\eta\rangle$, before sending the qubit

onward. By analyzing the measurement outcomes of $|\zeta\rangle$ and $|\eta\rangle$, Eve aims to reconstruct the final key. The entangling operation E_{C_1} applied to the qubit in the CA channel can be represented by a general mathematical formulation,

$$|0_{C_1}\zeta\rangle \xrightarrow{E_{C_1}} A_{\zeta}|0_{C_1}\zeta_{00}\rangle + B_{\zeta}|1_{C_1}\zeta_{01}\rangle,$$

$$|1_{C_1}\zeta\rangle \xrightarrow{E_{C_1}} B_{\zeta}|0_{C_1}\zeta_{10}\rangle + A_{\zeta}|1_{C_1}\zeta_{11}\rangle.$$

$$(4.20)$$

Here, subscripts C_1 and C_2 denote the respective qubits in the CA and CB channels. Similarly, the entangling operation E_{C_2} on the CB channel follows a comparable expression.

$$\begin{array}{ccc}
|0_{C_{2}}\eta\rangle & \xrightarrow{E_{C_{2}}} & A_{\eta}|0_{C_{2}}\eta_{00}\rangle + B_{\eta}|1_{C_{2}}\eta_{01}\rangle, \\
|1_{C_{2}}\eta\rangle & \xrightarrow{E_{C_{2}}} & B_{\eta}|0_{C_{2}}\eta_{10}\rangle + A_{\eta}|1_{C_{2}}\eta_{11}\rangle.
\end{array} (4.21)$$

The unitary nature of operators E_{C_1} and E_{C_2} imposes the constraints $A_\zeta^2 + B_\zeta^2 = 1$ and $A_\eta^2 + B_\eta^2 = 1$, along with the conditions $\langle \zeta_{00} | \zeta_{10} \rangle + \langle \zeta_{01} | \zeta_{11} \rangle = 0$ and $\langle \eta_{00} | \eta_{10} \rangle + \langle \eta_{01} | \eta_{11} \rangle = 0$. To simplify the analysis, a set of assumptions is introduced: $\langle \zeta_{00} | \zeta_{01} \rangle = \langle \zeta_{00} | \zeta_{10} \rangle = \langle \zeta_{10} | \zeta_{11} \rangle = \langle \zeta_{01} | \zeta_{11} \rangle = 0$ and $\langle \eta_{00} | \eta_{01} \rangle = \langle \eta_{00} | \eta_{10} \rangle = \langle \eta_{10} | \eta_{11} \rangle = \langle \eta_{01} | \eta_{11} \rangle = 0$. Although these assumptions restrict the generality of Eve's attack, they still represent a typical case following Eve's entangling operations [41]. To characterize Eve's non-orthogonal states, the relations can be expressed as $\langle \zeta_{00} | \zeta_{11} \rangle = \cos \alpha_\zeta, \langle \zeta_{01} | \zeta_{10} \rangle = \cos \beta_\zeta, \langle \eta_{00} | \eta_{11} \rangle = \cos \alpha_\eta, \langle \eta_{01} | \eta_{10} \rangle = \cos \beta_\eta$. By applying these expressions to the condition represented in Equation (4.6), the probability of Eve's undetected presence can be determined. The resulting composite system after Eve's interference is then analyzed accordingly.

$$\begin{split} |\psi_{2}^{e'}\rangle &= E_{C_{2}}[E_{C_{1}}(|0\rangle_{A}|\phi^{+}\rangle_{C_{1}C_{2}}|1\rangle_{B})|\zeta\rangle]|\eta\rangle \\ &= E_{C_{2}}\left[E_{C_{1}}\frac{1}{\sqrt{2}}(|0\rangle|00\rangle|1\rangle + |0\rangle|11\rangle|1\rangle)_{AC_{1}C_{2}B}|\zeta\rangle\right]|\eta\rangle \\ &= \frac{1}{\sqrt{2}}\left[\left(A_{\zeta}A_{\eta}|0\rangle|00\rangle|1\rangle|\zeta_{00}\rangle|\eta_{00}\rangle + A_{\zeta}B_{\eta}|0\rangle|01\rangle|0\rangle|\zeta_{00}\rangle|\eta_{01}\rangle \\ &+ B_{\zeta}A_{\eta}|1\rangle|10\rangle|1\rangle|\zeta_{01}\rangle|\eta_{00}\rangle + B_{\zeta}B_{\eta}|1\rangle|11\rangle|0\rangle|\zeta_{01}\rangle|\eta_{01}\rangle) \\ &+ \left(A_{\zeta}A_{\eta}|1\rangle|11\rangle|0\rangle|\zeta_{11}\rangle|\eta_{11}\rangle + A_{\zeta}B_{\eta}|1\rangle|10\rangle|1\rangle|\zeta_{11}\rangle|\eta_{10}\rangle \\ &+ B_{\zeta}A_{\eta}|0\rangle|01\rangle|0\rangle|\zeta_{10}\rangle|\eta_{11}\rangle + B_{\zeta}B_{\eta}|0\rangle|00\rangle|1\rangle|\zeta_{10}\rangle|\eta_{10}\rangle)_{AC_{1}C_{2}B}\right]. \end{split} \tag{4.22}$$

Alice and Bob receive their respective qubits from Charlie after Eve interacts with the channel particle and her *ancillary* particle. Following the protocol, they execute the CNOT operation and subsequently perform Bell measurements on their two-particle system. The operations

performed and the possible measurement results obtained by Alice and Bob can be described by the following equation.

$$\begin{split} |\psi_{2}^{e}\rangle &= CNOT_{C_{1}\rightarrow A}CNOT_{C_{2}\rightarrow B}|\psi_{2}^{e'}\rangle \\ &= \frac{1}{2\sqrt{2}}\left[\left\{A_{\zeta}A_{\eta}\left(|\phi^{+}\rangle|\psi^{+}\rangle + |\phi^{+}\rangle|\psi^{-}\rangle + |\phi^{-}\rangle|\psi^{+}\rangle + |\phi^{-}\rangle|\psi^{-}\rangle\right)_{AC_{1}C_{2}B}|\zeta_{00}\rangle|\eta_{00}\rangle \\ &+ A_{\zeta}B_{\eta}\left(|\phi^{+}\rangle|\psi^{+}\rangle - |\phi^{+}\rangle|\psi^{-}\rangle + |\phi^{-}\rangle|\psi^{+}\rangle - |\phi^{-}\rangle|\psi^{-}\rangle\right)_{AC_{1}C_{2}B}|\zeta_{00}\rangle|\eta_{01}\rangle \\ &+ B_{\zeta}A_{\eta}\left(|\phi^{+}\rangle|\psi^{+}\rangle + |\phi^{+}\rangle|\psi^{-}\rangle - |\phi^{-}\rangle|\psi^{+}\rangle - |\phi^{-}\rangle|\psi^{-}\rangle\right)_{AC_{1}C_{2}B}|\zeta_{01}\rangle|\eta_{00}\rangle \\ &+ B_{\zeta}B_{\eta}\left(|\phi^{+}\rangle|\psi^{+}\rangle - |\phi^{+}\rangle|\psi^{-}\rangle - |\phi^{-}\rangle|\psi^{+}\rangle + |\phi^{-}\rangle|\psi^{-}\rangle\right)_{AC_{1}C_{2}B}|\zeta_{01}\rangle|\eta_{01}\rangle \right\} \\ &+ \left\{A_{\zeta}A_{\eta}\left(|\phi^{+}\rangle|\psi^{+}\rangle - |\phi^{+}\rangle|\psi^{-}\rangle - |\phi^{-}\rangle|\psi^{+}\rangle + |\phi^{-}\rangle|\psi^{-}\rangle\right)_{AC_{1}C_{2}B}|\zeta_{11}\rangle|\eta_{11}\rangle \\ &+ A_{\zeta}B_{\eta}\left(|\phi^{+}\rangle|\psi^{+}\rangle + |\phi^{+}\rangle|\psi^{-}\rangle - |\phi^{-}\rangle|\psi^{+}\rangle - |\phi^{-}\rangle|\psi^{-}\rangle\right)_{AC_{1}C_{2}B}|\zeta_{10}\rangle|\eta_{11}\rangle \\ &+ B_{\zeta}A_{\eta}\left(|\phi^{+}\rangle|\psi^{+}\rangle + |\phi^{+}\rangle|\psi^{-}\rangle + |\phi^{-}\rangle|\psi^{+}\rangle - |\phi^{-}\rangle|\psi^{-}\rangle\right)_{AC_{1}C_{2}B}|\zeta_{10}\rangle|\eta_{10}\rangle \right\} \right]. \\ (4.23) \end{split}$$

Eve's presence can be detected when Alice and Bob obtain the measurement results $|\phi^+\rangle$ and $|\psi^-\rangle$ or $|\phi^-\rangle$ and $|\psi^+\rangle$ after conducting Bell measurements. The probability of detecting Eve in such cases is given by:

$$P_{d}^{2} = \frac{1}{2} \left[A_{\zeta}^{2} A_{\eta}^{2} \left(1 + \cos \alpha_{\zeta} \cos \alpha_{\eta} \right) + A_{\zeta}^{2} B_{\eta}^{2} \left(1 + \cos \alpha_{\zeta} \cos \beta_{\eta} \right) + B_{\zeta}^{2} A_{\eta}^{2} \left(1 + \cos \beta_{\zeta} \cos \alpha_{\eta} \right) + B_{\zeta}^{2} B_{\eta}^{2} \left(1 + \cos \beta_{\zeta} \cos \beta_{\eta} \right) \right].$$

$$(4.24)$$

Here, P_d^2 represents the probability of detecting Eve's interference for a specific expected outcome, as defined by Equation (4.6). The superscript i (in this case, 2) denotes the i^{th} (here, second) configuration among the various possible state choices made by Alice, Bob, and Charlie, with an associated probability P_d^i , where $i \in \{1, 2, \dots, 8\}$. The detection probability for Eve remains the same across different measurement outcomes, such that $P_d^1 = P_d^2 = \dots = P_d^8$. Using these results, one can determine the average probability of detecting Eve's presence as follows:

$$P_{d} = \frac{1}{8} \sum_{i} P_{d}^{i}$$

$$= \frac{1}{2} \left[A_{\zeta}^{2} A_{\eta}^{2} \left(1 + \cos \alpha_{\zeta} \cos \alpha_{\eta} \right) + A_{\zeta}^{2} B_{\eta}^{2} \left(1 + \cos \alpha_{\zeta} \cos \beta_{\eta} \right) + B_{\zeta}^{2} A_{\eta}^{2} \left(1 + \cos \beta_{\zeta} \cos \alpha_{\eta} \right) + B_{\zeta}^{2} B_{\eta}^{2} \left(1 + \cos \beta_{\zeta} \cos \beta_{\eta} \right) \right].$$
(4.25)

Now, considering that Eve aims to minimize the probability of being detected, she must employ a strategy to lower her detection probability as much as possible. The optimal scenario for Eve is achieved when the condition $A_{\zeta} = A_{\eta} = 1$ holds. Additionally, an optimal incoherent attack by Eve is assumed to be balanced, satisfying $\alpha_{\zeta} = \alpha_{\eta} = \alpha$ [88]. The "minimal probability of detecting" Eve is denoted as d, expressed as:

$$d \equiv \min(P_d) = \frac{1}{2} \left(1 + \cos^2 \alpha \right) \tag{4.26}$$

The relationship described by Equation (4.26) is illustrated in Figure 4.2 demonstrating that the "minimal detection probability" of Eve reaches zero if she utilizes an orthogonal state¹.

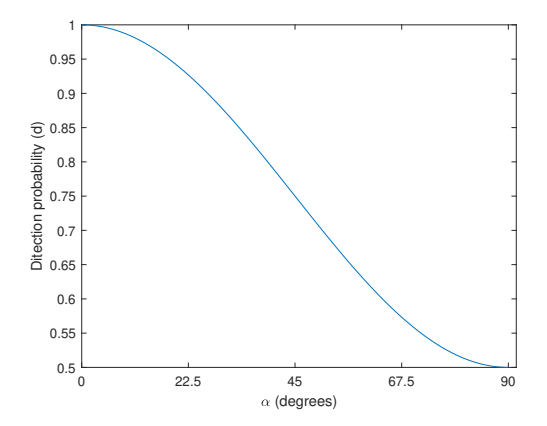


Figure 4.2: The correlation between Eve's detection probability (d) and the parameter α , which characterizes non-orthogonality.

Next, we analyze the information Eve obtains about the final one-bit key. Eve's attack operations denoted as E_{C_1} and E_{C_2} , target the qubits transmitted through the CA and CB channels, respectively, following an attack strategy \mathcal{E} . Consequently, the mutual information between Eve's attack strategy \mathcal{E} and the key \mathcal{K} is given by:

$$I(\mathcal{K}:\mathcal{E}) = H(\mathcal{E}) - H(\mathcal{E}|\mathcal{K}), \tag{4.27}$$

where $H(\mathcal{E})$ represents the entropy associated with Eve's attack strategy, while $H(\mathcal{E}|\mathcal{K})$ denotes the conditional entropy given the key. Under Eve's optimal attack conditions, as previously discussed, the Equation (4.23) can be further simplified.

 $^{^1}$ To simplify the analysis, we consider the optimal conditions that Eve must satisfy to avoid complex calculations. A more generalized assumption can be adopted, where $A_\zeta^2 + B_\zeta^2 = 1$, $A_\eta^2 + B_\eta^2 = 1$, $\alpha_\zeta \neq \alpha_\eta$ and $\beta_\zeta \neq \beta_\eta$. This allows us to further investigate how the minimal detection probability (d) of Eve is influenced by the non-orthogonality of her quantum state.

$$|\psi_{2}^{e}\rangle = \frac{1}{2\sqrt{2}} [\{(|\phi^{+}\rangle|\psi^{+}\rangle + |\phi^{+}\rangle|\psi^{-}\rangle + |\phi^{-}\rangle|\psi^{+}\rangle + |\phi^{-}\rangle|\psi^{-}\rangle)_{1234} |\zeta_{00}\rangle|\eta_{00}\rangle\} + \{(|\phi^{+}\rangle|\psi^{+}\rangle - |\phi^{+}\rangle|\psi^{-}\rangle - |\phi^{-}\rangle|\psi^{+}\rangle + |\phi^{-}\rangle|\psi^{-}\rangle)_{1234} |\zeta_{11}\rangle|\eta_{11}\rangle\}].$$
(4.28)

From this formulation, it follows that Eve's measurement outcome will be either $|\zeta_{00}\rangle|\eta_{00}\rangle$ or $|\zeta_{11}\rangle|\eta_{11}\rangle$, each occurring with equal probability, i.e., $\frac{1}{2}$. Considering various state preparations by Charlie, Alice, and Bob (such as $|\psi_1^e\rangle, |\psi_3^e\rangle, \cdots, |\psi_8^e\rangle$), Eve's measurement outcomes under attack strategy \mathcal{E} will still have a probability of $\frac{1}{2}$. The Shannon entropy of \mathcal{E} is given by $H(\mathcal{E})=1$, while the conditional entropy given \mathcal{K} is expressed as $H(\mathcal{E}|\mathcal{K})=h_2(Q_{\mathcal{E}\mathcal{K}})$, where h_2 represents the binary entropy function, and $Q_{\mathcal{E}\mathcal{K}}$ denotes the QBER introduced by Eve's attack in an attempt to infer the one-bit key. Thus, we need to derive an expression for $Q_{\mathcal{E}\mathcal{K}}$. The probability of correctly distinguishing between two quantum states with scalar product $\cos\alpha$ is given by $\frac{1}{2}(1+\sin\alpha)$ [313, 164]. Eve's ability to infer the final key depends on her capability to differentiate between the quantum states ζ and η . However, errors in distinguishing these states could occur—either misidentifying ζ or η . A single error leads to an incorrect key interpretation, but if two errors occur in a compensatory manner, Eve may still reconstruct the correct key. The general expression for $Q_{\mathcal{E}\mathcal{K}}$, incorporating α_{ζ} and α_{η} , is derived accordingly.

$$Q_{\mathcal{EK}} = 1 - \left[\left(\frac{1 + \sin \alpha_{\zeta}}{2} \right) \left(\frac{1 + \sin \alpha_{\eta}}{2} \right) + \left(\frac{1 - \sin \alpha_{\zeta}}{2} \right) \left(\frac{1 - \sin \alpha_{\eta}}{2} \right) \right]$$

$$= \frac{1 - \sin \alpha_{\zeta} \sin \alpha_{\eta}}{2}. \tag{4.29}$$

Assuming the optimal case for Eve, where $\alpha_{\zeta} = \alpha_{\eta} = \alpha$, and utilizing Equation (4.27) along with Equation (4.26), we obtain:

$$I(\mathcal{K}:\mathcal{E}) = \frac{1}{2} \left[1 - h_2 \left(\frac{1 - \sin^2 \alpha}{2} \right) \right]. \tag{4.30}$$

Here, the factor $\frac{1}{2}$ arises from the fact that in Equation (4.28), Alice and Bob's outcomes remain identical and occur with equal probability, regardless of Eve's measurement results.

Figure 4.3 illustrates the relationship between I and α under optimal conditions for Eve. As observed in the figure, when Eve employs orthogonal states ($\alpha = \frac{\pi}{2}$), the maximum extractable information is limited to 0.5 bits. In this scenario, Eve's detection probability is zero. However,

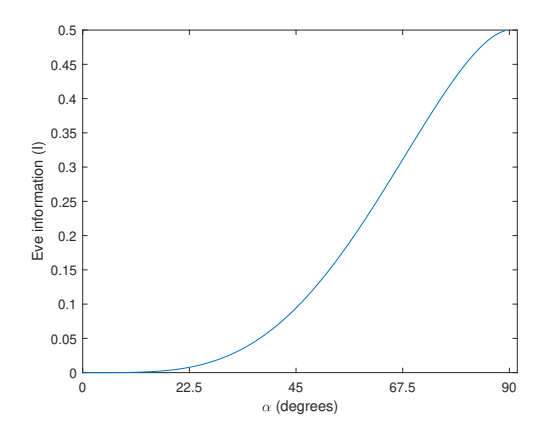


Figure 4.3: The dependence of Eve's accessible information (I) on the angle α , representing non-orthogonality.

if she utilizes non-orthogonal states, her information gain remains suboptimal in all cases¹. In practical quantum communication settings, noise may be introduced when Eve applies a unitary transformation involving the ancilla state, denoted by A_{η} and $A_{\zeta} < 1$. This factor complicates Eve's ability to execute an attack under ideal conditions. Consequently, Eve's presence becomes detectable, even when leveraging an orthogonal basis. Furthermore, the use of decoy states in legitimate quantum transmissions is a well-established method for improving channel security (refer to the stepwise breakdown of the CQKA protocol). However, for simplicity, our security analysis does not incorporate decoy states. If decoy states were considered, Eve's detection probability would increase compared to the scenario without them. In the next section, we compute the tolerable error bound, demonstrating the resilience of our protocol against collective attacks.

From Table4.1, it follows that after executing CQKA protocol, the final key agreement exhibits maximum entropy due to classical announcements within our framework. Additionally, our security analysis assumes a simplified model, leading to a symmetric measurement output for Alice and Bob (refer to Equation (4.28)) relative to Eve's ancillary state measurement. Despite this assumption, we evaluate Eve's probability of successfully estimating the final key in a generalized manner².

Based on Eve's measurement results $|\zeta_{ij}\rangle|\eta_{kl}\rangle$ for $i,j,k,l\in\{0,1\}$, along with Charlie's announcement, Eve attempts to infer the final one-bit key. To generalize, let us assume Eve

¹It is important to note that this conclusion would differ if we did not assume $B_{\eta} = B_{\zeta} = 0$ and $A_{\eta} = A_{\zeta} = 1$. A more generalized analysis could be conducted under these generalized assumptions.

²Depending on the specific protocol and the nature of Eve's collective attack, her success in estimating the final key can be described in terms of detection probability rather than being treated as a fixed value. Therefore, we adopt a more generalized analytical approach.

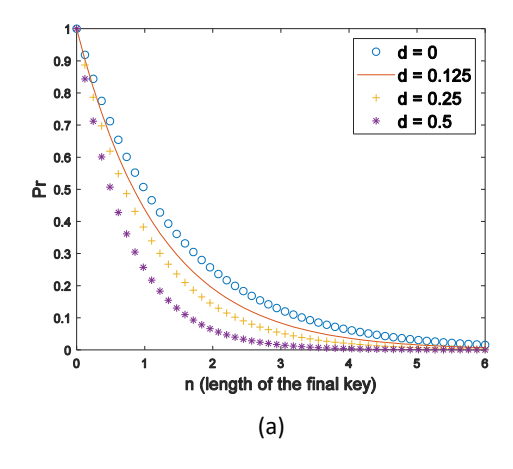
assigns the key as 0 with probability e and as 1 with probability 1 - e. Our objective is to determine the total probability of Eve correctly estimating the final key.

$$Pr_{s} = \left(\frac{1+\sin\alpha}{2}\right)^{2} \left\{\frac{1}{2}e + \frac{1}{2}(1-e)\right\} + \left(\frac{1-\sin\alpha}{2}\right)^{2} \left\{\frac{1}{2}e + \frac{1}{2}(1-e)\right\} + \frac{(1+\sin\alpha)(1-\sin\alpha)}{2} \left\{\frac{1}{2}e + \frac{1}{2}(1-e)\right\} = \frac{1}{2}.$$

$$(4.31)$$

By employing Equation (4.26) and Eq. (4.31), the probability of Eve successfully acquiring the final key denoted as n (representing the number of final key bits), can be determined,

$$Pr = [Pr_s (1-d)]^n = [\frac{1}{2} (1-d)]^n.$$
 (4.32)



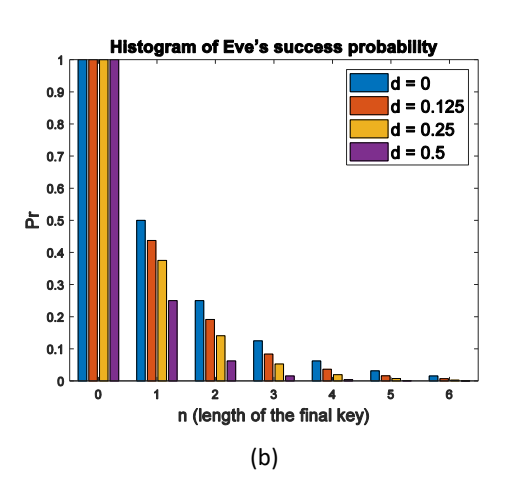


Figure 4.4: The interrelation between Pr, d and n is depicted as follows. (a) The dependence of Pr on n is examined for varying values of d. In particular, the "circle" line corresponds to d=0%, the "continuous" line represents d=12.5%, the "plus sign" line denotes d=25%, and the "asterisk" line signifies d=50%. (b) A histogram illustrates Eve's probability of success for n=6 across different values of d.

The correlation between Pr and n for varying values of d is depicted in Figure 4.4. The plotted results indicate that when n = 6, Pr is approximately zero. For instance, if Eve's detection probability (d) is set at 25%, the probability of her successfully obtaining the final key is 2.629×10^{-3} , which is negligible. Figure 4.4.a provides insight into the value of n at which Pr converges to zero. Since n is inherently discrete, Figure 4.4.b presents a histogram illustrating Pr for integer values of n. Clearly, as n increases sufficiently, the information gained by Eve through an impersonation-based fraudulent attack becomes effectively nullified.

Bound for tolerable error under collective attack scenario: Due to the inherent symmetry in the

 $^{^{1}}$ In our protocol, the final key distribution remains symmetric with respect to Charlie's announcement, making the role of e particularly significant in our analysis.

composite system's outcomes, we assume that the shared quantum state $|\psi_2^e\rangle$, involving Alice, Bob, and Eve, follows the form given in Equation (4.28). In the scenario of a collective attack [314, 312], the asymptotic lower bound for the secret key rate is governed by the Devetak-Winter rate equation. This equation quantifies the difference between the mutual information shared between Alice and Bob and the Holevo quantity describing Eve's accessible information about Bob's data¹,

$$r \ge r_{\text{DW}} = I(A:B) - \chi(B:E)$$
. (4.33)

The secret key rate in the asymptotic limit, denoted as r, has a lower bound r_{DW} , given by the Devetak-Winter rate equation. In this context, the mutual information measure [314] is expressed as: I(A:B) = H(B) - H(B|A) whereas the Holevo quantity is given by, $\chi(B:E) = S(\rho_E) - \sum_{k_B=0,1} p_{k_B} S\left(\rho_{E|k_B}\right)$. Here, S represents the von Neumann entropy, $\rho_E = \text{Tr}_{AB}|\psi_2^e\rangle\langle\psi_2^e|$ denotes Eve's quantum state after tracing out Alice's and Bob's subsystems, and $\rho_{E|k_B}$ is Eve's conditional quantum state given Bob's measurement outcome k_B . Due to symmetry considerations, the probabilities of Bob's final measurement outcomes are equal, i.e., $p_0 = p_1 = \frac{1}{2}$, when incorporating errors. Assuming uniform error rates across Alice's and Bob's measurement processes, we define this shared error rate as ε . Consequently, the mutual information simplifies to $I(A:B) = 1 - h(\varepsilon)$, where $h(\varepsilon)$ denotes the binary entropy function. By utilizing Equations (4.6) and (4.28) can be generalized² while accounting for the error probability ε , which encapsulates the combined impact of quantum channel imperfections and potential eavesdropping [315].

$$|\psi_{2}^{e}\rangle = \sqrt{\frac{1-\varepsilon}{4}}|\phi^{+}\rangle_{AC_{1}}|\psi^{+}\rangle_{C_{2}B}(|\zeta_{00}\rangle + |\zeta_{11}\rangle) + \sqrt{\frac{\varepsilon}{4}}|\phi^{+}\rangle_{AC_{1}}|\psi^{-}\rangle_{C_{2}B}(|\zeta_{00}\rangle - |\zeta_{11}\rangle) + \sqrt{\frac{\varepsilon}{4}}|\phi^{-}\rangle_{AC_{1}}|\psi^{-}\rangle_{C_{2}B}(|\zeta_{00}\rangle + |\zeta_{11}\rangle) + \sqrt{\frac{1-\varepsilon}{4}}|\phi^{-}\rangle_{AC_{1}}|\psi^{-}\rangle_{C_{2}B}(|\zeta_{00}\rangle + |\zeta_{11}\rangle)$$

$$(4.34)$$

By performing Bell basis measurements on the systems linked to Alice and Bob, one can directly ascertain the state of Eve's system, which can be represented as $|\theta^{\phi^{\pm},k_B}\rangle$, where ϕ^{\pm} and k_B denote Alice and Bob's respective outcomes. The explicit form of Eve's state is given as

¹In this framework, we evaluate the Holevo bound concerning Eve's information on Bob's measurements. Classical one-way post-processing is performed from Bob to Alice, directly influenced by his measurement outcome after the Bell-state analysis.

²The contribution of ancillary states (η) is omitted, as they do not provide additional information under the optimal conditions $B_{\eta} = B_{\zeta} = 0$ and $A_{\eta} = A_{\zeta} = 1$, maximizing Eve's limitations in extracting key information.

follows:

$$|\theta^{\phi^{+},1}\rangle = \sqrt{\frac{1-\varepsilon}{4}}(|\zeta_{00}\rangle + |\zeta_{11}\rangle)$$

$$|\theta^{\phi^{+},0}\rangle = \sqrt{\frac{\varepsilon}{4}}(|\zeta_{00}\rangle - |\zeta_{11}\rangle)$$

$$|\theta^{\phi^{-},1}\rangle = \sqrt{\frac{\varepsilon}{4}}(|\zeta_{00}\rangle - |\zeta_{11}\rangle)$$

$$|\theta^{\phi^{-},0}\rangle = \sqrt{\frac{1-\varepsilon}{4}}(|\zeta_{00}\rangle + |\zeta_{11}\rangle)$$

$$(4.35)$$

Eve's system is formulated within the density operator framework, with a conditional dependency on Bob's output,

$$\begin{split} \sigma_E^0 &= \rho_{E|0} &= \varepsilon |\theta^{\phi^+,0}\rangle \langle \theta^{\phi^+,0}| + (1-\varepsilon) |\theta^{\phi^-,0}\rangle \langle \theta^{\phi^-,0}| \\ &= \left(\frac{\varepsilon^2}{4} + \frac{(1-\varepsilon)^2}{4}\right) [|\zeta_{00}\rangle \langle \zeta_{00}| + |\zeta_{11}\rangle \langle \zeta_{11}|] + \left(-\frac{\varepsilon^2}{4} + \frac{(1-\varepsilon)^2}{4}\right) [|\zeta_{00}\rangle \langle \zeta_{11}| + |\zeta_{11}\rangle \langle \zeta_{00}|] \end{split}$$

$$\sigma_{E}^{1} = \rho_{E|1} = (1 - \varepsilon) |\theta^{\phi^{+},1}\rangle \langle \theta^{\phi^{+},1}| + \varepsilon |\theta^{\phi^{-},1}\rangle \langle \theta^{\phi^{-},1}|
= \left(\frac{\varepsilon^{2}}{4} + \frac{(1 - \varepsilon)^{2}}{4}\right) [|\zeta_{00}\rangle \langle \zeta_{00}| + |\zeta_{11}\rangle \langle \zeta_{11}|] + \left(-\frac{\varepsilon^{2}}{4} + \frac{(1 - \varepsilon)^{2}}{4}\right) [|\zeta_{00}\rangle \langle \zeta_{11}| + |\zeta_{11}\rangle \langle \zeta_{00}|]
(4.36)$$

By tracing out Alice's and Bob's systems, the resulting density matrix of Eve's system is obtained,

$$\rho_E = \frac{1}{2} \left[(|\zeta_{00}\rangle \langle \zeta_{00}| + |\zeta_{11}\rangle \langle \zeta_{11}|) + (1 - 2\varepsilon) \left(|\zeta_{00}\rangle \langle \zeta_{11}| + |\zeta_{11}\rangle \langle \zeta_{00}| \right) \right]. \tag{4.37}$$

The secret key rate is subsequently expressed using Equations (4.33), (4.36), and (4.37),

$$r \ge r_{\text{DW}} = 1 - h(\varepsilon) - \left[S(\rho_E) - \left(\frac{1}{2} S(\sigma_E^0) + \frac{1}{2} S(\sigma_E^1) \right) \right] . \tag{4.38}$$

To compute r_{DW} , we begin by defining an orthogonal basis $\{|E_{00}\rangle, |E_{01}\rangle, |E_{10}\rangle, |E_{11}\rangle\}$ within the Hilbert space \mathscr{H}^E . This allows consideration of the states in the orthogonal basis, specifically $|\zeta_{00}\rangle = \sum_{ij} a_{ij} E_{ij}$ and $|\zeta_{11}\rangle = \sum_{ij} f_{ij} E_{ij}$, where $i, j \in \{0, 1\}$. These states satisfy the constraints $|a_{00}|^2 + |a_{01}|^2 + |a_{10}|^2 + |a_{11}|^2 = 1$, $|f_{00}|^2 + |f_{01}|^2 + |f_{10}|^2 + |f_{11}|^2 = 1$, and $a_{00}^* f_{00} + a_{01}^* f_{01} + a_{10}^* f_{10} + a_{11}^* f_{11} = \cos \alpha$. Through extensive calculations, the eigenvalues of ρ_E are derived as $\lambda_{1,2}^{\rho_E} = 0,0$,

$$\lambda_3^{\rho_E} = \frac{1}{2} \left(1 + \cos \alpha - 2\varepsilon \cos \alpha - \sqrt{(1 - 2\varepsilon + \cos \alpha)^2} \right),$$

and

$$\lambda_4^{
ho_E} = rac{1}{2} \left(1 + \coslpha - 2arepsilon \coslpha + \sqrt{\left(1 - 2arepsilon + \coslpha
ight)^2}
ight).$$

Similarly, the eigenvalues for σ_E^1 or σ_E^0 are determined as $\lambda_{1,2}^{\sigma_E^\pm}=0,0,$

$$\lambda_{3}^{\sigma_{E}^{\pm}} = \frac{1}{4} \left(1 - 2\varepsilon + 2\varepsilon^{2} + \cos\alpha - 2\varepsilon\cos\alpha - \sqrt{\left(1 - 2\varepsilon + \left(1 - 2\varepsilon + 2\varepsilon^{2}\right)\cos\alpha\right)^{2}} \right),$$

and

$$\lambda_4^{\sigma_E^{\pm}} = \frac{1}{4} \left(1 - 2\varepsilon + 2\varepsilon^2 + \cos\alpha - 2\varepsilon\cos\alpha + \sqrt{(1 - 2\varepsilon + (1 - 2\varepsilon + 2\varepsilon^2)\cos\alpha)^2} \right).$$

Subsequently, the entropy expressions are utilized as $S(\rho_E) = -\sum_i \lambda_i^{\rho_E} \log_2 \lambda_i^{\rho_E}$ and $S(\sigma_E^{\pm}) = -\sum_i \lambda_i^{\sigma_E^{\pm}} \log_2 \lambda_i^{\sigma_E^{\pm}}$ to derive the explicit form of Equation (4.38).

To ascertain the tolerable error limit under secure conditions, referred to as the tolerable QBER, we solve Equation (4.38) in terms of α . A graphical representation is produced, showcasing the tolerable error probability ε as a function of the angle α , which signifies non-orthogonality (cf. Figure 4.5). The plot demonstrates that increasing non-orthogonality in Eve's ancilla state leads to a higher ε . Specifically, when Eve employs an orthogonal ancilla state ($\alpha = \frac{\pi}{2}$), the permissible error threshold is identified as 27%. This threshold acts as a crucial security benchmark in the context of collective attacks. Notably, at the 27% threshold, r equals zero. However, for the same α value, as illustrated in Figure 4.3, the error probability reaches 0.5, arising from the potential of obtaining a nonzero r value.

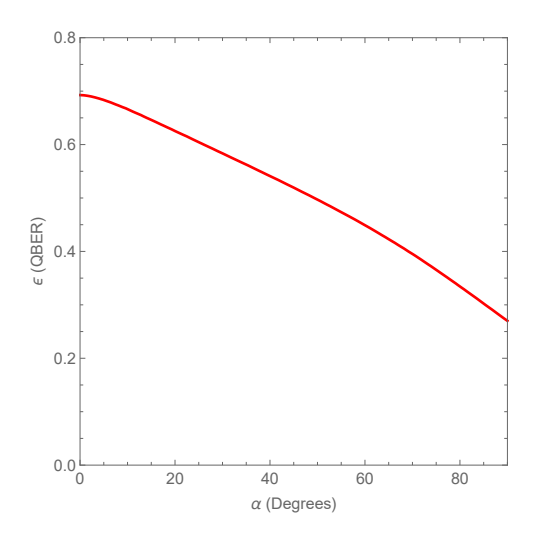


Figure 4.5: The plot illustrates the relationship between tolerable QBER (ε) and the angle characterizing non-orthogonality (α).

4.4 INFLUENCE OF NOISE ON THE PROPOSED CQKA PROTOCOL

Decoherence induced by environmental factors [316, 317, 318] is a well-documented constraint on the effectiveness of quantum-enhanced protocols [319, 320]. This issue presents a major hurdle in realizing quantum communication schemes, as qubit interactions with their surroundings can degrade accuracy, even in the absence of an adversarial entity. Such interference may lead to erroneous outputs, making any practical implementation inherently vulnerable to noise from external sources [321]. To ensure feasibility, a protocol must retain its reliability despite the presence of a controlled level of noise. Additionally, if an eavesdropper (Eve) attempts to manipulate the channel, she could mask her intrusion as environmental noise [318, 322, 323, 324]. However, distinguishing between natural noise and intentional interference is feasible through established detection methodologies [325, 326], preserving protocol security even under adversarial conditions [327].

In this study, we explore the effects of noise on the quantum communication protocols under investigation. Specifically, we evaluate amplitude damping and phase damping within a Markovian framework, alongside dephasing and depolarization in a non-Markovian reservoir context [328, 329]. Interestingly, while non-Markovian dephasing can extend entanglement longevity, dissipative interactions may also lead to entanglement revival. The quantum system's behavior is represented using the Kraus formalism, providing essential insights into the characteristics of these noise channels, which are integral to quantum information and communication implementations.

The Kraus operators governing amplitude damping (AD) are given as follows [330, 331]:

$$\mathcal{F}_0^{AD} = \begin{pmatrix} 1 & 0 \\ 0 & \sqrt{1 - \eta_a} \end{pmatrix} \quad \text{and} \quad \mathcal{F}_1^{AD} = \begin{pmatrix} 1 & \sqrt{\eta_a} \\ 0 & 0 \end{pmatrix}. \tag{4.39}$$

Similarly, the Kraus operators for phase damping (PD) are:

$$\mathcal{F}_0^{\text{PD}} = \begin{pmatrix} 1 & 0 \\ 0 & \sqrt{1 - \eta_p} \end{pmatrix} \quad \text{and} \quad \mathcal{F}_1^{\text{PD}} = \begin{pmatrix} 1 & 0 \\ 0 & \sqrt{\eta_p} \end{pmatrix}. \tag{4.40}$$

Here, η_j , $j \in \{a, p\}$ represents the damping parameter. Likewise, the evolution of non-Markovian dephasing (NMDPH) is determined by the Kraus operators outlined below [332]:

$$\mathcal{N}_{0}^{\text{NMDPH}} = \sqrt{(1-\alpha p)(1-p)}\mathbb{I},$$

$$\mathcal{N}_{0}^{\text{NMDPH}} = \sqrt{p\left[1+\alpha\left(1-p\right)\right]}\sigma_{Z}.$$
(4.41)

For the non-Markovian depolarizing (NMDPO) channel [333],

$$\mathcal{N}_{\mathbb{I}}^{\text{NMDPO}} = \sqrt{(1 - 3\alpha p)(1 - p)} \mathbb{I},$$

$$\mathcal{N}_{X}^{\text{NMDPO}} = \sqrt{[1 + 3\alpha(1 - p)]\frac{p}{3}} \sigma_{X},$$

$$\mathcal{N}_{Y}^{\text{NMDPO}} = \sqrt{[1 + 3\alpha(1 - p)]\frac{p}{3}} \sigma_{Y},$$

$$\mathcal{N}_{Z}^{\text{NMDPO}} = \sqrt{[1 + 3\alpha(1 - p)]\frac{p}{3}} \sigma_{Z}.$$

$$(4.42)$$

The parameter α $(0 \le \alpha \le 1)$ quantifies the extent of non-Markovianity. Specifically, when $\alpha = 0$, the channel exhibits standard dephasing, whereas larger values of α signify a heightened degree of non-Markovian behavior. Additionally, p serves as a time-dependent parameter constrained within $0 \le p \le \frac{1}{2}$ [332], evolving monotonically over time. Here, \mathbb{I} denotes the identity matrix in a two-dimensional Hilbert space, while σ_X , σ_Y and σ_Z correspond to the Pauli matrices.

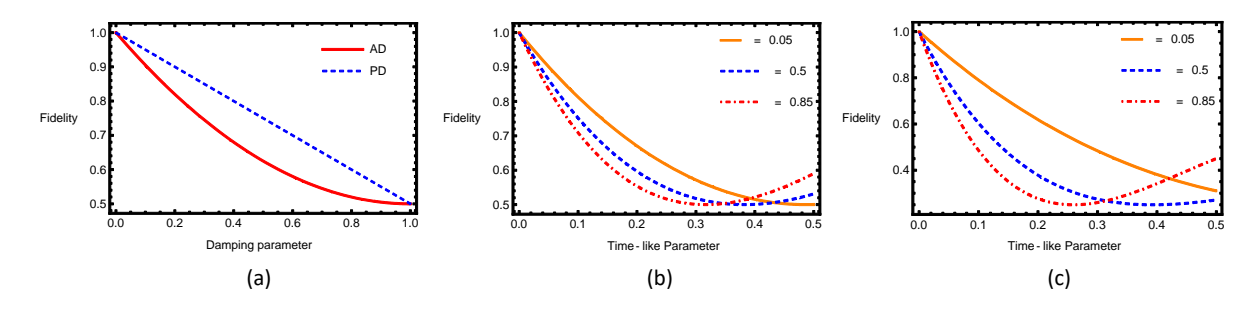


Figure 4.6: The variation of average fidelity under a noisy quantum channel is analyzed. (a) Depicts the dependence of average fidelity on the channel parameter η_j for the CQKA scheme within the Markovian framework for AD and PD channels, as described by Equations (4.39) and (4.40). (b) and (c) illustrate the variation in average fidelity for NMDPH and NMDPO channels within the non-Markovian regime, plotted against the time-like parameter p for various values of α , respectively (refer to Equations (4.41) and (4.42)).

Prior to evaluating the impact of noisy channels on the proposed scheme, it is essential to establish the initial configuration. When a p-qubit composite state, $\rho_i = |\Phi\rangle\langle\Phi|$, serves as the initial resource for executing the protocol—where p home qubits and p-q travel qubits are

represented by h and t, respectively—the general form of the final state before measurement can be expressed as:

$$ho_f^k = \sum_j \left\{ I_h^{\otimes p} \otimes \left(\mathcal{F}_1^k \otimes \ldots \otimes \mathcal{F}_j^k \otimes \ldots \otimes \mathcal{F}_{p-q}^k \right)_t \right\}
ho_i \left\{ I_h^{\otimes p} \otimes \left(\mathcal{F}_1^k \otimes \ldots \otimes \mathcal{F}_j^k \otimes \ldots \otimes \mathcal{F}_{p-q}^k \right)_t \right\}^\dagger.$$

The Kraus operators \mathcal{F}_{j}^{k} characterize the various noise channels, where $k \in \{\text{AD}, \text{PD}, \text{NMDPH}, \text{NMDPO}\}$. The degradation in protocol performance due to noise can be quantitatively assessed using a fidelity-based metric, specifically the squared fidelity (commonly referred to as average fidelity) [330], which is defined as:

$$F^k = \langle \Phi^f | \rho_f^k | \Phi^f \rangle.$$

Here, $|\Phi^f\rangle$ denotes the ideal final state that the initial pure state $|\Phi\rangle$ would achieve in the absence of decoherence, assuming perfect encoding operations performed by each participant.

The performance of the proposed scheme is analyzed by modeling the quantum channel as a noisy medium. Particles C_1 and C_2 propagate through this environment, where we initially examine the Markovian regime, considering both AD and PD channels. To assess the average fidelity [330] between the noiseless state and the state affected by noise, we plot its variation as a function of the damping parameter η_j in Figure 4.6.a. The fidelity in the AD channel exhibits a more rapid decline with increasing η_a compared to the PD channel. The fidelity expressions for these channels are given by $1 - \frac{1}{2}(\eta - 2)\eta$ for AD and $1 - \frac{\eta}{2}$ for PD. It is noteworthy that the fidelity decay in the AD channel follows a nonlinear trend, whereas a linear decline is observed in the PD channel. At $\eta_j = 1$, fidelity reaches a minimum value of 0.5 in both cases, representing the lower bound in a highly damped environment.

For the non-Markovian regime, the temporal parameter p is defined as $p = \frac{1}{2} \left(1 - e^{-\mathcal{K}t} \right)$, ranging from 0 to $\frac{1}{2}$. The average fidelity expressions for the non-Markovian dephasing and depolarizing channels are given by $\frac{1}{2} \left[1 + \left\{ 1 - 2p + 2\left(p - 1\right)p\alpha \right\} \right]$ and $1 + \frac{2}{3} \left[3\left(p - 1\right)\alpha - 1 \right] \left[6\left(p - 1\right)p\alpha - 2p + 3 \right]$, respectively. Figure 4.6.b illustrates the impact of the non-Markovian dephasing channel on the proposed scheme, revealing that fidelity decreases as p increases, with the rate of decline dependent on α . For smaller α values, fidelity remains stable for an extended period, while for larger α , a substantial revival in fidelity is observed, with the minimum value reaching 0.5. A

similar pattern is evident for the non-Markovian depolarizing channel in Figure 4.6.c, though the fidelity drop is more pronounced at higher α values compared to the dephasing channel. Conversely, for $\alpha=0.05$, the fidelity reduction is slower in the depolarizing channel than in the dephasing channel, indicating that fidelity is sustained for a longer duration in the depolarizing channel at lower α values. However, at higher α values ($\alpha=0.5,0.85$), fidelity persists for a shorter duration in the depolarizing channel than in the dephasing channel. Additionally, the non-Markovian depolarizing channel exhibits a gradual fidelity enhancement beyond a certain p value, contingent on the specific α parameter.

A crucial consideration involves examining a specific scenario: as will be demonstrated, exploiting non-Markovianity can enhance system performance (i.e., increase efficiency) in contrast to a Markovian environment. Given this, an eavesdropper (denoted as Eve) may replace a Markovian channel between Alice and Bob with a non-Markovian counterpart to reduce the probability of detection (or alternatively, swap a noisier channel with one exhibiting less noise). Therefore, legitimate communicating parties must incorporate this possibility when defining the permissible error threshold [334, 335]. Moreover, establishing this threshold may necessitate characterizing the communication channel. For example, noise in an "amplitude-damping channel" could be identified and mitigated accordingly [336].

4.5 COMPARISON OF THE PROPOSED CQKA PROTOCOL WITH EX-ISTING PROTOCOLS

This section presents a concise comparison between the proposed CQKA and QKA protocols and other recently introduced schemes of a similar nature. Notably, multiparty-based QKA protocols [206] are intentionally excluded, as the proposed scheme is specifically designed for key agreement between two parties, either with or without the involvement of a third party. Several key parameters are considered in assessing the performance of QKA schemes, including quantum resources (QR), quantum channel (QC) requirements, quantum efficiency (QE), quantum memory (QM), third-party (TP) involvement, the number of parties (NoP) required to establish the key agreement, and quantum operations executed by legitimate parties. The comparison is conducted based on these parameters to highlight the advantages and limitations of the proposed scheme relative to existing alternatives.

We adopt the initial definition of QE introduced by Cabello in his pioneering work [173].

Specifically, QE is expressed as $\eta_1 = \frac{b_s}{q_t + b_t}$, where b_s denotes the expected number of secret classical bits shared among legitimate parties, q_t represents the qubits transmitted via the quantum channel per protocol step, and b_t accounts for the classical bits required to finalize the key post-protocol execution. Since quantum resources are costlier and more challenging to preserve in a coherent state compared to classical communication, we also employ an alternative QE metric frequently utilized in literature: $\eta_2 = \frac{b_s}{q_t}$ [337]. Notably, we exclude decoy state qubits from QE computations, as their role is limited to channel security verification rather than contributing to key generation. For comparative analysis, we first consider the QKA protocol by Huang et al., which leverages quantum correlations in EPR pairs alongside single-particle measurements to establish identical key values between two participants, Alice and Bob [338]. This method represents an entanglement-based extension of the BB84 QKD protocol, differing primarily in the disclosure of basis information prior to Alice and Bob's measurements. Execution of this protocol necessitates quantum memory. However, since Bob reveals the basis information to align measurement results, the protocol becomes susceptible to a photon-number splitting attack by an eavesdropper. A comparable approach was reported by Xu et al., utilizing the GHZ state, where three participants obtain identical keys following the protocol's execution [203]. In their scheme, a three-qubit quantum state serves as the QR, and a subset of the initial sequence, prepared by party A_1 , is used to ensure security. To enhance QE, the legitimate users perform single-qubit measurements exclusively in the computational basis (B_Z) once channel security is established. The protocol's efficiency is given by $\eta_1 = \frac{n-ns}{2n+ns}$, where s represents the fraction of qubits from the initial sequence allocated for channel security verification. Like the previous scheme, this protocol also necessitates quantum memory.

In the same year, Shukla et al. introduced a QKA scheme based on EPR pairs and a bidirectional quantum channel [202]. However, this protocol is vulnerable to noise and demands quantum memory. Additionally, Pauli operations are required at Bob's end. The structure of this scheme closely resembles a modified version of the ping-pong protocol [244]. He et al. later proposed a more efficient protocol ($\eta = 0.5$), incorporating a four-qubit cluster state that demands additional quantum resources [204]. Nevertheless, maintaining coherence in a four-qubit cluster state presents significant challenges, and the protocol also relies on Pauli operations. Furthermore, its implementation requires a two-way quantum channel and quantum memory, posing

¹For this protocol, the key parameter values are defined as follows: $b_s = n - ns$, $q_t = 2n$, $b_t = ns$, and efficiency is bounded within $0.5 \ge \eta \ge 0$, with $s \in [0,1]$. Security improves as s increases.

limitations given the current state of quantum communication technology. A related protocol was introduced by Yang et al., employing a four-qubit cluster state and cluster basis measurement [339]. The authors integrated a classical permutation operation in a complex manner to enhance security against adversarial attacks by Eve. However, this approach inherently relies on quantum memory and Pauli operations¹.

We now examine the advantages and limitations of our two-party QKA schemes compared to previous approaches. For the proposed QKA protocol, we employ EPR pairs and single-photon states, which align well with current technological capabilities. Notably, it does not require quantum memory for implementation and utilizes a one-way quantum channel to mitigate unnecessary channel noise, unlike earlier protocols. Additionally, our scheme does not rely on Pauli operations and achieves quantum efficiencies of $\eta_1 = 0.33$ and $\eta_2 = 1$. Certain scenarios necessitate the involvement of an untrusted third party in QKA between two legitimate participants; our CQKA protocol is designed to accommodate this requirement. In contrast, Tang et al. proposed a CQKA protocol that utilizes GHZ states, Hadamard gates, and Pauli operations [214]. Their approach depends on a two-way quantum channel between Alice and Bob and requires quantum memory, both of which are key drawbacks. Our proposed CQKA scheme simplifies implementation by only requiring EPR pairs and CNOT operations, making it feasible with current technology. This is particularly advantageous when an untrusted third party is involved in facilitating QKA. Furthermore, our scheme eliminates the need for quantum memory and a two-way quantum channel, setting it apart from existing protocols. A comparative analysis of these aspects is presented in Table 4.3.

4.6 DISCUSSION

Key conditions that a QKA protocol must fulfill are examined in Section 4.2. In that section, we have demonstrated that the proposed schemes meet the *correctness* criterion. Here, we provide a concise discussion on the fairness condition by considering a specific scenario within our protocol, as outlined in Tables 4.1 and 4.2. As previously stated, the *fairness* condition ensures that no individual participant can unilaterally manipulate or exert control over the final agreement key. Specifically, if Alice (Bob) attempts to influence the final key by selecting all qubits in her (his) sequence $S_A(S_B)$ to be either $|0\rangle$ or $|1\rangle$, it does not introduce any bias in the

The efficiency of this scheme is expressed as $\eta_1 = \frac{4n-nC}{4n+4n+nC} < 0.5$, where $C \in [0,1]$ represents the checking set, which does not function as a decoy state.

Table 4.3: Explicit comparison with earlier protocols. Y - required, N - not required, QC - quantum channel, QR - quantum resources, TR - third party, QM - quantum memory, NoP - number of parties, QE - quantum efficiency.

Protocol	NoP	QR	QC	QM	TR	$QE(\eta_1)$	$QE(\eta_2)$
Huang et	2	EPR pair	one-way	Y	N	$\frac{n}{2n} = 0.5$	$\frac{n}{n}=1$
al. [338]							
Xu et al.	3	GHZ state	one-way	Y	N	$\frac{n-ns}{2n+ns} < 0.5$	$\frac{n-s}{2n} < 0.5$
[203]							
Shukla et	2	EPR pair	two-way	Y	N	$\frac{n}{2n+n} = 0.33$	$\frac{n}{2n} = 0.5$
al. [202]							
He et al.	2	four-qubit	two-way	Y	N	$\frac{4n}{4n+4n} = 0.5$	$\frac{4n}{4n} = 1$
[204]		cluster state					
Yang et	2	four-qubit	one-way	Y	N	$\frac{4n-nC}{4n+4n+nC}$	$\frac{4n-C}{4n} < 1$
al. [339]		cluster state				0.5	172
Tang et al.	2	GHZ state	two-way	Y	Y	$\frac{2n}{6n+n} = 0.285$	$\frac{2n}{6n} = 0.33$
[214]						on + n	On .
Our	2	EPR pair,	one-way	N	Y	$\frac{n}{2n+3n} = 0.2$	$\frac{n}{2n} = 0.5$
Protocol 1		single qubit				211 311	
Our	2	EPR pair,	one-way	N	N	$\frac{n}{n+2n} = 0.33$	$\frac{n}{n}=1$
Protocol 2		single qubit				70 270	
		state					

final key. This requirement can be validated by analyzing a particular example from Table 4.1 and Equations (4.6)-(4.13). Without loss of generality, let us assume that Alice selects all qubits in the $|0\rangle$ state, while Bob generates his sequence randomly¹. Subsequently, both Alice and Bob execute the CNOT operation on their respective qubits using those received from Charlie. As derived from Equations (4.6)-(4.13), the final agreement keys exhibit an equal probability distribution of 0s and 1s, ensuring no bias is introduced. Additionally, *fairness* mandates that all legitimate parties contribute equally to the final agreement key. In Step 4 of the CQKA protocol, Alice and Bob independently generate n-qubit sequences S_A and S_B in the Z basis, with each qubit randomly chosen as $|0\rangle$ or $|1\rangle$. In Step 5, they perform the CNOT operation, followed by a Bell measurement on their two-qubit systems. The final key is determined based on their measurement results and subsequent announcements in Steps 7 and 8, as detailed in Tables 4.1 and 4.2. This process confirms that both Alice and Bob contribute equally to the final agreement key, satisfying the fairness condition. Another crucial requirement is *security*, which is thoroughly discussed in Section 4.3.

Recent experimental realizations of quantum communication have been carried out using both free-space channels [343, 344] and fiber-optic links [345]. Within quantum networks, trajec-

¹Charlie's state is randomly chosen between $|\phi^+\rangle$ and $|\phi^-\rangle$, with bit values of 0 and 1, respectively.

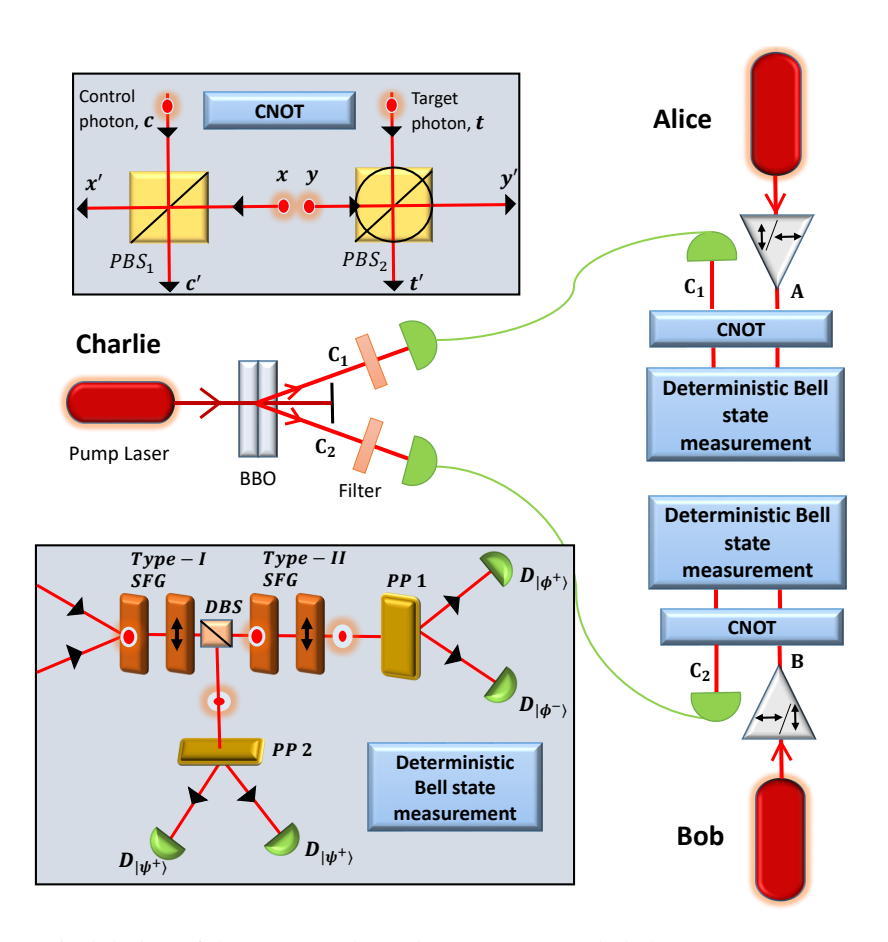


Figure 4.7: The optical design of the CQKA scheme integrates entangled photons, a CNOT operation, and a full Bell state measurement. The entangled photon pairs (Bell states) are generated using two thick β-barium borate (BBO) nonlinear crystals arranged in a cross-configuration [340]. Bell state measurement is performed via nonlinear interactions, specifically sum-frequency generation (SFG) of type-I and type-II. A dichroic beam splitter (DBS) is incorporated, along with two 45° projectors (PP1 and PP2) [341]. The system further utilizes polarizing beam splitter(s) (PBS₁ and PBS₂), each configured at a 45° orientation with half-wave plate (HWP) integrated at the input and output [342].

tories serve as conduits for transmitting quantum systems [346]. Effective phase synchronization and robust reference signals are crucial for these networks, prompting extensive research to develop efficient solutions [347]]. Single-photon quantum communication experiments are fundamental for the advancement of future quantum technologies [347]. In this work, we propose an experimental implementation of our quantum communication protocol. The setup consists of three main components (refer to Figure 4.7): an entangled photon source operated by Charlie, state preparation stations managed by Alice and Bob, and a Bell-state measurement system. Charlie generates a Bell state $\left(|\phi^{\pm}\rangle=\frac{1}{\sqrt{2}}(|00\rangle\pm|11\rangle)\right)$ using a nonlinear crystal via spontaneous parametric down-conversion (SPDC) [340], distributing one photon to Alice and the other to Bob through fiber or free-space links equipped with polarization stabilization. Alice and Bob independently prepare single-photon states in the Z basis ($|0\rangle$ or $|0\rangle$) using heralded single-photon sources and polarization control elements, such as waveplate and polarizer. Each station employs a linear-optics-based CNOT gate [342], where Charlie's entangled photon serves as the control qubit while their locally prepared photon acts as the target qubit. The CNOT gate is implemented using polarizing beam splitter (PBS₁ and PBS₂), waveplate, and postselection techniques. Bell-state measurement is deterministically conducted through nonlinear interactions via sum-frequency generation (SFG) in type-I and type-II processes [341]. The generated sum-frequency photons are separated by a dichroic beam splitter (DBS), and two 45° polarization projectors (PP1 and PP2) analyze the output states, ensuring reliable Bell-state identification with high fidelity. High-efficiency single-photon detectors and a synchronized timing system facilitate precise detection and data acquisition, thereby validating the protocol's successful execution and confirming entanglement correlations.

4.7 CONCLUSION

In certain instances, establishing a key agreement between two parties may necessitate the involvement of an untrusted third party. The quantum analogue of such scenarios demands a QKA protocol incorporating a semi-trusted third-party controller. Our proposed protocol is structured to fulfill the requirements of a controller within a QKA framework. Section 4.2 provides a detailed step-by-step exposition of our protocol, elucidating how quantum particle behavior can be harnessed to construct such protocols for practical implementations. However, specific conditions must be met for the successful execution of a QKA protocol, as outlined in Section 4.2.

The necessary security proofs addressing potential attack scenarios are detailed in Section 4.3, where we discuss critical aspects of security analysis. To implement the CQKA protocol, a Bell state—generated by an untrusted third party, Charlie—is required and subsequently distributed to the legitimate participants. Once Alice and Bob receive the first and second qubits of the Bell state prepared by Charlie, they execute the CNOT operation as prescribed by our protocol. Notably, if an eavesdropper (Eve) attempts an intercept-and-resend attack, she can only infer the Bell state originally generated by Charlie, as the channel particles are no longer entangled due to Alice and Bob's operations at that stage. Furthermore, Charlie publicly discloses this Bell state information (k_C) at the conclusion of the protocol, ensuring that Eve gains no advantage from such an attack. Additionally, we analyze the scenario where Eve attempts to impersonate the third party, referred to as an "impersonated fraudulent attack".

Our protocol is demonstrated to be resilient against this attack, with corresponding analytical proof supporting its security. Additionally, a crucial security evaluation is performed against the collective attack, establishing that our protocol remains secure even under more generalized attack scenarios¹. We further determine that the probability of Eve successfully extracting the final two-bit key is negligibly small (approaching elimination) when n = 6 (refer to Figure 4.4). Moreover, our security analysis can be extended by treating the inner product of Eve's ancillary state as a complex variable, wherein each ancilla system is represented using a complete orthogonal basis in the Hilbert space $\mathcal{H}^{\mathcal{E}}$ [315]. Furthermore, we estimate the tolerable error bound of our scheme by incorporating this approach and determine the acceptable QBER as a function of α . We evaluate our scheme under different noisy channel conditions and analyze the fidelity variation in relation to the channel parameter. Our findings indicate that the fidelity remains largely unaffected, even at higher values of the noise parameter. In Section 4.5, we further compare the advantages and limitations of our protocol with other recently proposed protocols of the same category. The results highlight that our protocol is not only more practical for implementation using current technological capabilities but also exhibits greater efficiency compared to many existing schemes discussed earlier (see Section 4.5). Notably, it introduces a novel and desirable feature involving the participation of a third party.

¹The proposed QKA protocol represents a specific instance of the CQKA protocol. Consequently, the security analysis conducted for the CQKA protocol is directly applicable to the QKA protocol as well.

CHAPTER 5

"GAMING THE QUANTUM" TO GET SECURE BOUND FOR A QUANTUM COMMUNICATION PROTOCOL

5.1 INTRODUCTION

Game theory analyzes strategic decision-making, modeling how individuals interact in competitive and cooperative settings. It plays a vital role in optimizing choices across business, economics [215], political science [216], biology [217, 218], and military strategy [219, 220]. Each participant selects from a set of strategies, with preferences represented in a payoff matrix. A key concept is the Nash equilibrium, where no player gains by unilaterally changing their strategy [221, 222], ensuring stability in decision-making. Quantum mechanics is among the most impactful theories in history. Despite early controversies, its predictions have been consistently validated through experiments [223]. Quantum game theory explores interactive decision-making involving quantum technology, serving as a quantum communication protocol and a more efficient means of randomizing strategies compared to classical games [224]. Introduced in 1999 by David [225], along with Jens, Martin, and Maciej [226], this field examines games leveraging quantum information, revealing advantages for quantum players over classical ones. Numerous quantum games, expanding on these foundational works, have since been extensively studied [227]. Experimentally, researchers have implemented the quantum Prisoners' Dilemma using an NMR quantum computer [228]. Vaidman [229] also demonstrated a game where players always win when sharing a GHZ state, unlike classical counterparts who rely on probability. Quantum strategies have further contributed to fairness in remote gambling [230] and the development of secure quantum auction algorithms [231]. Flitney and Abbott [232] have investigated quantum variations of Parrondo's games, highlighting their role in enhancing network security and inspiring novel quantum algorithms. These studies also introduce a new perspective on defining games and protocols [162, 233, 234]. Additionally, eavesdropping [32, 235] and optimal cloning [236] can be interpreted as strategic interactions among participants, further reinforcing the link between game theory and quantum mechanics. This interconnection follows two main approaches: (1) leveraging quantum resources to play classical games with enhanced advantages, referred to as "quantized game", and (2) applying game-theoretic principles to quantum scenarios, termed "gaming the quantum". A "quantized game" is mathematically described as a unitary function mapping quantum superpositions of players' pure strategies onto the game's Hilbert space while preserving its core properties under certain conditions. Conversely, "gaming the quantum" [237] involves utilizing game theory within quantum mechanics to derive strategic solutions. In this chapter, we adopt the "gaming the quantum" approach by applying non-cooperative game theory to a quantum communication protocol, demonstrating how Nash equilibrium can function as an effective solution concept. Building on these insights, Nash equilibrium points can be utilized to define secure bounds for various quantum information parameters. This approach involves modeling quantum schemes as game-theoretic scenarios and analyzing their Nash equilibria, which provide stable conditions and rational probability distributions for decision-making in a mixed-strategy framework. These probabilities help establish a stable gaming environment, enabling the evaluation of cryptographic parameters such as the threshold QBER. In practical scenarios where decisions are made autonomously, achieving stability is challenging and may lead to increased uncertainty. Therefore, identifying the minimum QBER from a stable game setting defines a secure threshold for implementing quantum communication protocols. This work specifically examines the secure threshold bound for QBER within the DL04 protocol [238], a direct secure quantum communication scheme. Such protocols generally fall into two broad categories [239]. Secure quantum communication protocols can be categorized into two types. The first category, DSQC protocols [240, 241, 165, 166], requires the receiver to decode the message only after receiving at least one bit of additional classical information per qubit. The second category, QSDC protocols [242, 243, 244, 245, 238, 246, 247, 248, 249], eliminates the need for classical information exchange. Beige et al. [242] proposed a QSDC scheme where message retrieval depends on additional classical information per qubit. Boström and Felbinger introduced the ping-pong QSDC protocol [244], offering secure key distribution and quasi-secure direct communication over an ideal quantum channel. In 2004, Deng and Long [238] developed the DL04 QSDC protocol, which operates without entangled states. Notably, secure transmission via the two-photon component was observed, consistent with two-way QKD findings [250, 88, 251].

This chapter primarily focuses on evaluating the secure threshold bound of QBER within the DL04 protocol, chosen for its experimental viability and feasibility in secure implementations [252, 253, 254, 255, 256, 257, 258].

The subsequent sections of this chapter are organized as follows. Section 5.2 introduces game theory within the specific scope of this study, as it forms the analytical foundation of our work. Additionally, this section conceptualizes the DL04 protocol as a game-like scenario. Section 5.3 delves into the computation of information-theoretic parameters essential for deriving payoff functions across various attack scenarios. In Section 5.4, we mathematically formulate the game and utilize a graphical approach to analyze the Nash equilibrium. Furthermore, we examine equilibrium points to establish the secure threshold limit of QBER for the DL04 protocol. Lastly, Section 5.5 summarizes our results and provides a concluding discussion.

5.2 FUNDAMENTALS OF GAME THEORY

Before exploring the technical aspects of this study, it is essential to provide a concise overview of "game theory". Game theory consists of mathematical frameworks used to analyze decisionmaking scenarios that involve both competition and cooperation, where the choices made by each participant (player) depend on the decisions of others. Each player has a defined set of strategies or possible actions, which dictate their responses to various situations within the game. The central goal is to determine optimal strategies for players under these conditions and to identify equilibrium states. Game outcomes are typically expressed as payoffs, representing the utility or benefit each player gains based on the collective strategy choices of all participants. These payoffs can be quantified using numerical values, rankings, or other evaluative measures. Game theory can be formulated in multiple ways, with two primary representations: the "normal form" (strategic form) and the "extensive form" (dynamic game). The normal form represents payoffs in a matrix structure, displaying outcomes for different strategy combinations, whereas the extensive form employs a tree structure to illustrate sequential and simultaneous decision-making processes. Games are generally classified into two categories: "zero-sum games" and "non-zero-sum games". In a zero-sum game, the total available payoff remains constant, meaning one player's gain directly results in another's loss. Conversely, non-zero-sum games allow for variable total payoffs, where players' interests may be partially aligned rather than entirely conflicting. A crucial concept in game theory is Nash equilibrium,

which describes a scenario in which no player has an incentive to unilaterally alter their chosen strategy, assuming all other players maintain their strategies. This equilibrium represents a stable outcome where no player can improve their payoff by deviating from their current strategy. Another key principle is "Pareto efficient" (or "Pareto optimal"), where no alternative strategy set exists that improves one player's outcome without disadvantaging another. Additionally, a dominant strategy is one that consistently yields the best outcome for a player, regardless of the strategies selected by others. This concept plays a significant role in rational decision-making. Players may follow a pure strategy, where a single action is chosen with certainty, or a mixed strategy, where actions are selected based on assigned probabilities. In certain games, mixed strategies contribute to the formation of a Nash equilibrium when no single pure strategy is superior [226, 348, 349, 350, 351].

Quantum game In conventional games that permit mixed strategies, players formulate their strategies by utilizing real coefficients to construct convex linear combinations of their pure strategies [352]. Conversely, in quantum games [226, 353], strategic choices involve unitary transformations and quantum states, which exist within significantly expanded strategic spaces. This has led to discourse suggesting that quantum games could serve as extensions of classical game theory, potentially granting participants a quantum advantage [354]. As previously noted, any quantum protocol, such as those in quantum cryptographic scenarios, can be interpreted through a game-theoretic aspect. In such a framework, players' strategies are determined by their application of unitary operations and selection of measurement bases, with payoffs derived from measurement outcomes. The quantum advantage emerges from the optimal sequential application of quantum operations on quantum states by the players. In classical quantum game theory literature, players are typically restricted to performing coherent permutations of standard basis states or other similarly constrained unitary operations. In contrast, quantum players can leverage a broader class of unitary transformations, encompassing a more comprehensive set of operations with fewer constraints. Before advancing further, it is essential to formally define "pure quantum strategies", "mixed quantum strategies", and "positive operator-valued measure (POVM) strategies" [353] within the context of this study.

A pure quantum strategy consists of deterministic actions represented by unitary transformations applied to a player's quantum state. This approach begins with an initial quantum state $|\Psi\rangle$ within a Hilbert space \mathcal{H} . Each participant i selects a unitary operation U_i to apply to their respective portion of the quantum system. Once all players have executed their chosen unitary

operations, the resultant quantum state is expressed as

$$|\Psi_f\rangle = (U_1 \otimes U_2 \otimes \cdots \otimes U_i \otimes \cdots \otimes U_n) |\Psi\rangle,$$

where n represents the total number of participants. The final state $|\Psi_f\rangle$ is subsequently measured to determine the outcome of the game. Conversely, a mixed quantum strategy incorporates probabilistic selections of different pure strategies. Similar to the pure strategy case, the system starts in the state $|\Psi\rangle$. Each player i has a set of unitary transformations $\{U_i^1, U_i^2, \cdots, U_i^k\}$, each associated with a probability distribution $\{p_i^1, p_i^2, \cdots, p_i^k\}$, constrained by $\sum_{j=1}^k p_i^j = 1$. The selection of a unitary operator U_i follows the probability p_i^j . Consequently, the ensemble of possible final states forms a probabilistic mixture of pure states, leading to the mixed state representation:

$$\rho_f = \sum_i p_i^j \left(U_i^j \otimes \cdots \otimes U_n^j \right) |\Psi\rangle\langle\Psi| \left(U_i^j \otimes \cdots \otimes U_n^j \right)^{\dagger}.$$

This mixed state ρ_f undergoes measurement to determine the game's final outcome. A POVM-based quantum strategy employs generalized quantum measurements, defined by a set of POVM elements. Beginning with the state $|\Psi\rangle$, each player i utilizes a POVM, consisting of positive semi-definite operators $\left\{\mathcal{E}_i^1,\mathcal{E}_i^2,\cdots,\mathcal{E}_i^k\right\}$ that satisfy the completeness condition $\sum_j \mathcal{E}_i^j = 1$. The probability of outcome j is given by $p_i^j = \langle \Psi | E_i^j | \Psi \rangle$. Based on the observed measurement outcome, players may perform conditional unitary transformations or other quantum operations. The resultant state, dependent on both measurement results and subsequent operations, is represented as

$$\rho_f = \sum_{j} p_i^j \left(U_i^j \otimes \cdots \otimes U_n^j \right) |\Psi\rangle \langle \Psi| \left(U_i^j \otimes \cdots \otimes U_n^j \right)^{\dagger}.$$

The final mixed state ρ_f is then measured to determine the game's outcome. Among these strategies, POVM-based methods offer the highest degree of generality and adaptability within quantum game theory. In this chapter, we implement a mixed quantum strategy where Alice, Bob, and Eve execute their quantum operations based on specific probabilistic combinations to achieve Nash equilibrium points. The resulting mixed state determines the respective payoff values for each player.

The quantum game under consideration is a non-cooperative multiplayer scenario that does not

possess a pure strategy Nash equilibrium. This absence results from the inherent structure of the multiplayer framework and the methodology employed for computing payoffs, akin to the approach in [237]. The Nash equilibrium concept is a cornerstone in game theory, serving as a predictive tool for the behavior of independent decision-makers. The proof of Nash's theorem, which establishes the existence of an equilibrium in mixed strategies within classical game settings are relatively straightforward and fundamentally relies on Kakutani's "fixed-point theorem" [355]. In the domain of quantum games, Meyer demonstrated that Nash equilibria in mixed strategies, represented as mixed quantum states, exist by leveraging Glicksberg's extension of Kakutani's "fixed-point theorem" to topological vector spaces [356]. However, Khan et al. (2019) established that the direct application of Kakutani's theorem is not feasible for quantum games utilizing pure quantum strategies [357]. Nonetheless, under specific conditions, Nash's embedding theorem, which maps compact Riemannian manifolds into Euclidean space [358], enables an indirect application of Kakutani's theorem, thereby ensuring the existence of Nash equilibrium in pure quantum strategies. Their work offers a rigorous mathematical exploration of non-cooperative game theory and fixed-point theorems, as detailed in [357]. Our contribution In our game, several critical aspects must be considered since it operates as a "mixed quantum strategic game". When players select quantum strategies according to a probability distribution—thus employing mixed quantum strategies—Meyer utilized Glicksberg's fixed-point theorem [356] to establish the guaranteed existence of a Nash equilibrium. His research also provides valuable insights into equilibrium behavior within quantum computational frameworks. The identification of quantum advantage as a Nash equilibrium in quantum games, as proposed by Meyer, remains an area with limited exploration [359]. Furthermore, in quantum communication protocols—where quantum processes are inherently noisy and represented using density matrices or mixed quantum states—the Meyer–Glicksberg theorem ensures the presence of a Nash equilibrium [225]. Typically, in such protocols, quantum players with fewer restrictions can leverage mixed strategies to determine their best response functions by evaluating their respective payoffs. The Nash equilibrium points are obtained as solutions to these best response functions. While not all equilibrium points necessarily achieve Pareto optimality, they provide a foundation for analyzing the probability distributions governing mixed strategies. This analysis facilitates the identification of "Pareto optimal Nash equilibria", aiding in the determination of secure bounds for various quantum information parameters, such as the secret key rate and QBER, by applying core principles from quantum information theory [360, 361, 362, 23]. In this chapter, we examine the DL04 protocol [238] through a gametheoretic lens, considering different attack strategies—including collective and IR attacks—to derive the secure threshold limit for QBER.

In the field of quantum cryptography, QSDC utilizes quantum states as information carriers to ensure secure transmission. Unlike conventional cryptographic techniques, QSDC eliminates the necessity for pre-established secret keys [242, 243, 244, 245, 238, 246, 247]. It fundamentally focuses on enabling secure and reliable communication through quantum mechanical principles. Extensive experimental research has validated the feasibility of QSDC and highlighted its potential applications [252, 363, 364, 254, 365, 256, 366, 367, 257]. Over the past two decades, persistent advancements have contributed to the maturation of QSDC, positioning it as a promising technology for next-generation secure communication, including potential military applications [368, 369]. Among various QSDC protocols introduced so far, the DL04 protocol stands out due to its prominence in recent experimental studies [252, 253, 254, 255, 256, 257, 258]. Given its significance, our research specifically focuses on the DL04 protocol while ensuring that the developed strategy maintains general applicability. We begin with a brief overview of the DL04 protocol [238], modified slightly for applicability in a gaming context. In this protocol, Bob generates quantum states (photons) at random, choosing between $|0\rangle$ and $|1\rangle$ in the computational basis (Z basis) or $|+\rangle$ and $|-\rangle$ in the diagonal basis (X basis), with probabilities p and 1-p, respectively. He then transmits this sequence to Alice. Alice operates in two distinct modes: message mode (encoding mode) and control mode (security verification mode). During control mode, Alice randomly selects a subset of the received photons to detect potential eavesdropping, utilizing a beam splitter. Each photon in this subset is measured in either the Z or X basis. Alice then informs Bob of the positions of these security check photons, the chosen measurement bases, and the corresponding outcomes. Together, they compute the initial QBER. If the QBER remains below a predefined threshold, they proceed with the next phase; otherwise, the transmission is discarded. In message mode, Alice applies a quantum operation I ($iY \equiv ZX$) on the remaining qubits to encode the bit 0 with probability q(or 1 with probability 1-q). Additionally, she designates some photons for encoding random bits (0 or 1) to verify the reliability of the second transmission before forwarding them back to Bob. Most of the photons in this second transmission contain Alice's encoded message, while a small fraction is used to estimate the second QBER. Upon receipt of the photons, Bob deciphers the classical bits encoded by Alice based on his initial preparation bases. Alice then reveals the positions of the photons used for random number encoding, enabling both parties to evaluate the QBER of the second transmission. This secondary QBER estimation ensures the integrity of the transmission. If the error rate remains below the acceptable threshold, the transmission is considered successful. A comparable protocol, LM05, introduced by Lucamarini et al. [88], follows a similar structure. In LM05, Alice's execution of the control mode mirrors that of DL04, but classical announcements are allowed at that stage. Once Bob receives the sequence from Alice, he performs projective measurements for decoding and subsequently announces the classical security-check bits. In both DL04 and LM05, the objective for legitimate users is to achieve perfect "double correlation" in measurement results for both the forward and return transmission paths.

Within the DL04 protocol, two quantum participants implement strategic methods to uphold secure communication. Our analysis is centered on establishing the secure threshold for the QBER while considering the interference of an eavesdropper, Eve, who may employ either quantum or classical attack methodologies. Specifically, we examine quantum Eve's utilization of three attack approaches: Wójcik's original attack [370], Wójcik's symmetrized attack [370], and Pavičić's attack [371], labeled as E_1 , E_2 and E_3 , respectively. Additionally, a classical Eve executes an IR attack, denoted as E_4 . A comprehensive examination of these attack strategies is provided in the next section, whereas a concise overview is presented here to facilitate conceptual understanding (for further details, refer to Section 5.3). In the E_1 attack, Eve applies the unitary operator Q_{txy} during the B-A attack phase and its conjugate, Q_{txy}^{\dagger} ($\equiv Q_{txy}^{-1}$), during the A-B attack. This operator is represented as:

$$Q_{txy} = \text{SWAP}_{tx} \text{CPBS}_{txy} H_y \equiv \text{SWAP}_{tx} \otimes I_y \text{CPBS}_{txy} I_t \otimes I_x \otimes H_y$$

Here, A-B and B-A attacks correspond to Eve's intervention when quantum states are transmitted from Alice to Bob and vice versa. This attack induces the system into an extended Hilbert space through Eve's unitary operations, increasing randomness due to quantum superposition. Consequently, the joint probabilities of Alice's, Bob's, and Eve's measurement outcomes are altered as follows:

$$\begin{split} p_{000}^{E_1} &= q, & p_{001}^{E_1} &= p_{010}^{E_1} = p_{011}^{E_1} = 0, \\ \\ p_{100}^{E_1} &= \frac{1}{4}(1-q) \,, & p_{101}^{E_1} &= (1-q)\left(\frac{1}{4} + \frac{p}{2}\right), \\ \\ p_{110}^{E_1} &= 0, & p_{111}^{E_1} &= \frac{1}{2}(1-p)(1-q) \,. \end{split}$$

The QBER for the E_1 attack is given by $\frac{1}{2}(1-q)(1+p)$, and the probability of detecting Eve's presence is 0.1875.

The E_2 attack resembles E_1 , with the distinction that an additional unitary operation, S_{ty} , is applied with a probability of $\frac{1}{2}$ after Q_{txy}^{-1} in the A-B attack phase. The operation S_{ty} is defined as $X_t Z_t \text{CNOT}_{ty} X_t$. This leads to modified measurement probabilities:

$$\begin{split} p_{000}^{E_2} &= \frac{q}{8} \left(5 + p \right), & p_{001}^{E_2} &= \frac{q}{8} \left(1 + p \right), \\ \\ p_{010}^{E_2} &= p_{011}^{E_2} &= \frac{q}{8} \left(1 - p \right), & p_{100}^{E_2} &= \frac{1}{4} \left(1 - q \right), \\ \\ p_{101}^{E_2} &= \frac{1}{4} \left(1 - q \right) \left(1 + 2 p \right), & p_{110}^{E_2} &= 0, \\ \\ p_{111}^{E_2} &= \frac{1}{2} \left(1 - p \right) \left(1 - q \right). \end{split}$$

The QBER for the E_2 attack is $\frac{1}{4}(2+2p-q-3pq)$, with a detection probability of 0.1875. In the E_3 attack, Eve employs the unitary operation Q'_{txy} when the photon moves from Bob to Alice (B-A attack), while in the A-B attack, she applies the inverse operator Q'_{txy}^{-1} . The unitary transformation is expressed as:

$$Q'_{txy} = \text{CNOT}_{ty}\left(\text{CNOT}_{tx} \otimes I_y\right) \left(I_t \otimes \text{PBS}_{xy}\right) \text{CNOT}_{ty}\left(\text{CNOT}_{tx} \otimes I_y\right) \left(I_t \otimes H_x \otimes H_y\right).$$

This results in the following joint probabilities:

$$p_{000}^{E_3} = q,$$
 $p_{001}^{E_3} = p_{010}^{E_3} = p_{011}^{E_3} = 0,$ $p_{100}^{E_3} = p_{101}^{E_3} = p_{110}^{E_3} = 0,$ $p_{111}^{E_3} = (1 - q).$

Here, the QBER remains 0, while the probability of detecting Eve's presence is 0.1875. Lastly, the E_4 attack corresponds to an IR attack, where the measurement outcome probabilities are:

$$p_{000}^{E_4} = \frac{3}{4}q,$$
 $p_{001}^{E_4} = p_{011}^{E_4} = 0,$ $p_{010}^{E_4} = \frac{1}{4}q,$

$$p_{100}^{E_4} = p_{110}^{E_4} = 0, \qquad p_{101}^{E_4} = \tfrac{1}{4} \left(1 - q \right), \qquad p_{111}^{E_4} = \tfrac{3}{4} \left(1 - q \right).$$

For this scenario, the QBER is 0.25, and Eve's presence can be detected with a probability of 0.375.

Before introducing the conventional payoff function, it is essential to frame the DL04 protocol within a game-theoretic context, where principles of game theory are integrated into a quantum communication protocol (see Figure 5.1). To simplify the analysis, the DL04 quantum game is categorized into distinct game scenarios. However, the subsequent discussion presents a generalized mapping approach [353, 226, 372]. Consider a game 9 modeled as a "normalform game", which is mathematically defined as a function with a specified domain and range. The players' preferences are associated with elements of the range, influencing their rational strategic decisions within the domain. The strategic choices available to players in the quantum domain are now outlined. More formally, the game \mathcal{G} has an output set O as its range and a domain represented by the Cartesian product $S_1 \times S_2 \times \cdots \times S_n$, where S_i denotes the set of pure strategies available to the i^{th} player. Each element within this domain, $S_1 \times S_2 \times \cdots \times S_n$, corresponds to a "game play" or "strategy profile". The game function is expressed as ${\mathfrak G}$: $S_1 \times S_2 \times \cdots \times S_n \longrightarrow O$, where n denotes the total number of players. In this specific case, the game involves three participants: Alice, Bob, and Eve. Bob selects a quantum state, Alice determines the measurement basis, and Eve executes an attack strategy, all of which constitute elements of the domain $S_1 \times S_2 \times S_3$, where S_1, S_2 , and S_3 correspond to the strategic choices of Alice, Bob, and Eve, respectively. Thus, the game function can be specifically defined as $\mathcal{G}: S_1 \times S_2 \times S_3 \longrightarrow O$ within the context of pure strategies. In practice, Bob encodes quantum states in either the Z or X basis before transmitting them to Alice. To ensure security, Alice measures a portion of Bob's sequence and subsequently encodes a message by applying a Pauli operation before returning it. Throughout this process, Eve attempts different attack strategies via the quantum channel. The following sections elaborate on how this game framework is incorporated into the quantum communication protocol.

Alice initializes her primary sequence as a mixed quantum state, mathematically expressed as

$$\frac{p}{2}\left(|0\rangle\langle 0|+|1\rangle\langle 1|\right)+\frac{1-p}{2}\left(|+\rangle\langle +|+|-\rangle\langle -\right)$$

Alice's quantum states exist within a two-dimensional projective complex Hilbert space, denoted as \mathcal{H}_2 . This mixed state comprises four pure states, which collectively form a superposition within \mathcal{H}_2 . Consequently, when $|0\rangle$ undergoes a projective measurement in the X basis¹, it probabilistically collapses into either $|+\rangle$ or $|+\rangle$ with an equal probability of $\frac{1}{2}$, demonstrating quantum superposition. Eve executes quantum attacks utilizing unitary transformations and ancillary states, all operating within a projective complex Hilbert space. Specifically, the attack strategies E_1 , E_2 , and E_3 are conducted in an eight-dimensional Hilbert space \mathcal{H}_8 , whereas E_4 operates in \mathcal{H}_2 . Within different game-theoretic scenarios, Eve alternates between attack strategies E_i and E_j with probabilities r and 1-r, respectively. The interaction of Eve's unitary operations with Alice and Bob's states enhances the quantum superposition, effectively increasing the number of possible outcomes based on Alice's measurement basis. This expansion in superposition influences the measurement results for the legitimate players within the game². This also broadens the possible game outcomes O, where $O = \{o_1, o_2, o_3\}$, representing the respective outputs of Alice, Bob, and Eve. Alice encodes information using Pauli operations, which also exist within \mathcal{H}_2 . Thus, the game framework can be described as a mixed strategy game, denoted by the function \mathcal{M} . The 1-simplex Δ_1 represents the space of probability distributions over each player's pure strategies, corresponding to the set of mixed strategies. Therefore, our mixed strategy game M is formally defined over a domain that is the Cartesian product of the probability distributions over the pure strategies of all players.

$$\mathfrak{M} \quad : \quad \Delta_1 \times \Delta_1 \times \Delta_1 \longrightarrow \Delta_7$$

$$\mathcal{M} : ((p, 1-p), (q, 1-q), (r, 1-r))$$

$$\mapsto (pqr, pq(1-r), p(1-q)r, p(1-q)(1-r), (1-p)qr,$$

$$(1-p)q(1-r), (1-p)(1-q)r, (1-p)(1-q)(1-r))$$

The framework encompasses probability distributions over possible outcomes by mapping these outcomes to the vertices of the 7-simplex Δ_7 . The necessary projective complex Hilbert space

¹Quantum measurements in a two-dimensional Hilbert space are characterized by the operator set: $\{M_0, M_1: M_0 = |+\rangle\langle+|, M_1 = |-\rangle\langle-|\}$.

²A comprehensive analysis of the unitary operations performed by Alice and Bob, along with their measurement outcomes, is detailed in Section 5.3.

associated with M is specified as follows:

Bob's prepared state $\longrightarrow \mathcal{H}_2$ Alice's measuremet basis $\longrightarrow \mathcal{H}_2$ Alice's unitary operation $\longrightarrow \mathcal{H}_2$ Eve's E_1, E_2, E_3 attack $\longrightarrow \mathcal{H}_8$ Eve's E_4 attack $\longrightarrow \mathcal{H}_2$

Furthermore, the superposition states are attributed to Bob, whereas the unitary operations are performed by Alice and Eve, positioning the overall state within an extended complex Hilbert space \mathcal{H}_8 . This mechanism introduces an elevated degree of randomness through quantum superposition. Such enhanced randomness influences the outputs of legitimate participants and expands the strategic scope of the game. Consequently, these outcomes significantly impact key determinants of the players' payoff functions, including mutual information, QBER, and the detection probability of Eve's intrusion. Ultimately, the effects of these payoff functions dictate the Nash equilibrium conditions across different game settings. By utilizing quantum superposition states and unitary transformations, non-cooperative game theory is applied to the DL04 protocol, demonstrating Nash equilibrium as a viable solution concept. Thus, the work of this chapter integrates quantum mechanics into game-theoretic analysis, *gaming the quantum* [372, 359].

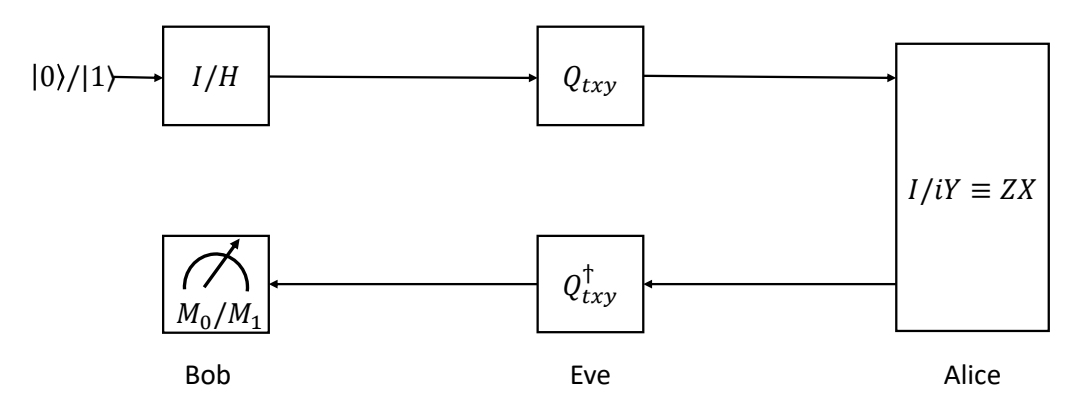


Figure 5.1: The circuit representation of DL04 quantum game.

Next, we define the payoff structure for each participant. The mutual information shared between Alice and Bob positively contributes to their respective payoffs while diminishing Eve's payoff. Conversely, any mutual information exchanged between Alice and Eve or Bob and Eve negatively impact the legitimate players' payoffs. Moreover, the legitimate parties gain

advantages from their ability to detect Eve's presence¹, which enhances their payoffs in this adversarial setting. Conversely, Eve's payoff increases with the amount of information acquired from Alice and Bob but decreases as the mutual information between Alice and Bob grows. Additionally, Eve incurs a penalty upon detection, making her payoff more favorable when the probability of remaining undetected is higher. Eve may also deploy various quantum gates to extract information from Alice and Bob, but an increased number of such operations adds to her computational overhead, ultimately reducing her payoff. Consequently, the payoff structure can be tailored to capture different strategic scenarios and player incentives under consideration. The DL04 protocol, modeled as a game, can be viewed within the framework of a zero-sum game. The payoffs for Alice, Bob, and Eve, under a general attack strategy \mathcal{E} , can thus be formulated² as follows [351].

$$P_{A}^{\mathcal{E}}(p,q) = \omega_{a}I(A,B) - \omega_{b}I(A,E) - \omega_{c}I(B,E) + \omega_{d}\left(\frac{P_{d} + QBER}{2}\right)$$

$$P_{B}^{\mathcal{E}}(p,q) = \omega_{a}I(A,B) - \omega_{c}I(A,E) - \omega_{b}I(B,E) + \omega_{d}\left(\frac{P_{d} + QBER}{2}\right)$$

$$P_{E}^{\mathcal{E}}(p,q) = -\omega_{e}I(A,B) + \omega_{f}I(A,E) + \omega_{g}I(B,E) + \omega_{h}\left(1 - \frac{P_{d} + QBER}{2}\right)$$

$$- \omega_{i}n_{1} - \omega_{i}n_{2} - \omega_{k}n_{3}$$

$$(5.1)$$

Here, ω_a , ω_b , ω_c , ω_d , ω_e , ω_f , ω_g , ω_h , ω_i , ω_j , and ω_k represent positive real-valued coefficients, serving as weighting factors for different components in the payoff function. These weights are constrained such that $\sum_{m=a}^{d} \omega_m = 1$ and $\sum_{n=e}^{k} \omega_n = 1$, where $m \in \{a,b,c,d\}$ and $n \in \{e,f,\ldots,k\}$. Additionally, I(A,B), I(A,E), and I(B,E) denote the mutual information shared between Alice and Bob, Alice and Eve, and Bob and Eve, respectively. The parameter P_d represents the probability of detecting Eve's intrusion, while n_1 , n_2 , and n_3 correspond to the number of single-qubit, two-qubit, and three-qubit gates, respectively. Notably, in the defined payoff function, P_d and QBER are treated equivalently since both provide insights into Eve's presence in a similar manner.

Under the assumption that Eve possesses unlimited quantum resources and operates with flaw-

¹The impact of both parameters is of equal importance, depending on the specific quantitative values of the QBER and the probability of detecting Eve's presence (P_d) in both the message and control modes of the DL04 protocol.

²It is assumed that the complexity of quantum state preparation and measurement operations is identical for Alice, Bob, and Eve. Consequently, this aspect is not taken into account when computing the payoffs for these parties.

less quantum gates, the weights are set such that $\omega_i = \omega_j = \omega_k = 0$. This implies that the number of quantum gates Eve employs for her attack does not impose any constraints on her payoff function. To facilitate the analysis, it is further assumed that all components contribute equally to the payoff. Therefore, in this model, the weights are uniformly distributed as $\omega_a = \omega_b = \omega_c = \omega_d = \omega_e = \omega_f = \omega_g = \omega_h = 0.25$, leading to a reformulation of Equation (5.1),

$$P_{A}^{\mathcal{E}}(p,q) = 0.25 \times \left[I(A,B) - I(A,E) - I(B,E) + \left(\frac{P_{d} + QBER}{2} \right) \right]$$

$$P_{B}^{\mathcal{E}}(p,q) = 0.25 \times \left[I(A,B) - I(A,E) - I(B,E) + \left(\frac{P_{d} + QBER}{2} \right) \right] . \tag{5.2}$$

$$P_{E}^{\mathcal{E}}(p,q) = 0.25 \times \left[-I(A,B) + I(A,E) + I(B,E) + \left(1 - \frac{P_{d} + QBER}{2} \right) \right]$$

In this scenario, it is evident that Alice and Bob receive identical payoffs, as represented by Equation (5.2). However, for our analysis, we will consider these payoffs independently. This distinction arises due to the differing probabilities—q for Alice and p for Bob—associated with choosing encoded bit values and employing the Z basis for initializing quantum states. The structured representation of the game \mathcal{M} in Table 5.1 further clarifies this concept.

Table 5.1: The payoff matrix corresponding to the \mathcal{M} game is presented, where the three values within parentheses signify the payoffs of Alice, Bob, and Eve, respectively. Here, the probabilities assigned to an eavesdropper Eve's choice of attack strategies E_i and E_j are denoted by r and 1-r, respectively.

	Bob					
		Z(p)	X(1-p)			
		$\left(rP_A^{E_i}(p,q)+(1-r)P_A^{E_j}(p,q),\right.$	$\left(rP_A^{E_i}\left(1-p,q\right)+\right.$			
	0(q)	$rP_{B}^{E_{i}}(p,q)+(1-r)P_{B}^{E_{j}}(p,q),$	$(1-r)P_A^{E_j}(1-p,q), rP_B^{E_i}(1-p,q)$			
		$P_E^{E_{i/j}}(p,q)$	$+(1-r)P_{B}^{E_{j}}(1-p,q),$			
Alice			$P_E^{E_{i/j}}(1-p,q)\Big)$			
	1(1-q)	$egin{aligned} \left(rP_A^{E_i}\left(p,1-q ight)+\ \left(1-r ight)P_A^{E_j}\left(p,1-q ight),\ rP_B^{E_i}\left(p,1-q ight)+\ \left(1-r ight)P_B^{E_j}\left(p,1-q ight),\ P_E^{E_{i/j}}\left(p,1-q ight) \end{aligned}$	$ \begin{pmatrix} rP_A^{E_i}\left(1-p,1-q\right) + \\ \left(1-r\right)P_A^{E_j}\left(1-p,1-q\right), \\ rP_B^{E_i}\left(1-p,1-q\right) + \\ \left(1-r\right)P_B^{E_j}\left(1-p,1-q\right), \\ P_E^{E_{i/j}}\left(1-p,1-q\right) \end{pmatrix} $			

5.3 INFORMATION-THEORETIC PARAMETERS IN DIFFERENT ATTACK SCENARIOS

In this section, we analyze various attack scenarios to determine the relevant information-theoretic parameters. To compute the payoffs for all parties using Equation (5.2), it is essential to obtain the mutual information between players in the game scenario, the detection probability of Eve's presence, and the QBER for each respective attack scenario. These parameters are crucial for deriving the best response function, which is discussed in the following section.

5.3.1 E_1 ATTACK STRATEGY

We adopt Wójcik's attack methodology [370] as E_1 to exploit the DL04 protocol under both message and control configurations. As outlined earlier, Bob initiates the process by randomly selecting the initial quantum state from $|0\rangle$, $|1\rangle$, $|+\rangle$, and $|-\rangle$ with respective probabilities of $\frac{p}{2}$, $\frac{p}{2}$, $\frac{1-p}{2}$, and $\frac{1-p}{2}$. Alice then encodes j (where $j \in \{0,1\}$) onto the travel photon¹ (denoted by the subscript t) received from Bob using the operation² iY_t^j . The communication channel shared between Alice and Bob is modeled as a lossy quantum channel, characterized by a single-photon transmission efficiency η . Meanwhile, Eve substitutes this lossy channel with an ideal one, where $\eta=1$. To execute her attack, Eve employs two auxiliary spatial modes, x and y, and an ancillary photon initially prepared in the state $|0\rangle$. She performs eavesdropping twice: once during the photon transmission from Bob to Alice (B-A attack) and again when it returns from Alice to Bob (A-B attack). The attack procedure (see Figure 2 in Ref. [370]) begins with Eve initializing the auxiliary modes x and y in the state $|vac\rangle_x|0\rangle_y$, where $|vac\rangle_x$ signifies an empty mode. During the B-A attack, Eve applies the unitary transformation Q_{txy} , and during the A-B attack, she utilizes its Hermitian conjugate Q_{txy}^{\dagger} (or equivalently Q_{txy}^{-1}). The transformation Q_{txy} is defined as

$$Q_{txy} = SWAP_{tx}CPBS_{txy}H_y \equiv SWAP_{tx} \otimes I_yCPBS_{txy}I_t \otimes I_x \otimes H_y$$

¹Here, t refers to the travel photon (qubit) sent by Bob (Alice) in the B-A (A-B) attack scenario.

²Alice encodes a 0 (1) using the operation $iY_t^0 \equiv I_t \left(iY_t^1 \equiv (ZX)_t^1 \right)$ with respective probabilities q (1-q).

where it consists of a Hadamard gate (a single-qubit operation), a SWAP gate (a two-qubit operation), and a controlled polarizing beam splitter (CPBS), which is a three-qubit gate¹. We will now evaluate this attack strategy under both message and control modes to determine the relevant payoff functions for Alice, Bob, and Eve.

Message mode: To begin with a straightforward approach, let us analyze cases where Alice encodes a 0. Specifically, we consider the scenario in which Bob initializes the system in the state $|0\rangle_t$. Subsequently, we examine Eve's attack strategy on the composite system, initially represented as $|0\rangle_t |\text{vac}\rangle_x |0\rangle_y$ and denoted by E_1 ,

$$\begin{split} |\mathbf{B} - \mathbf{A}\rangle_{|0\rangle E_{1}} &= Q_{txy} |0\rangle_{t} |\text{vac}\rangle_{x} |0\rangle_{y} \\ &= \mathbf{SWAP}_{tx} \mathbf{CPBS}_{txy} H_{y} \left(|0\rangle|\text{vac}\rangle|0\rangle\right)_{txy} \\ &= \mathbf{SWAP}_{tx} \mathbf{CPBS}_{txy} \frac{1}{\sqrt{2}} \left(|0\rangle|\text{vac}\rangle|0\rangle + |0\rangle|\text{vac}\rangle|1\rangle\right)_{txy} \ . \\ &= \mathbf{SWAP}_{tx} \frac{1}{\sqrt{2}} \left(|0\rangle|0\rangle|\text{vac}\rangle + |0\rangle|\text{vac}\rangle|1\rangle\right)_{txy} \\ &= \frac{1}{\sqrt{2}} \left[|0\rangle|0\rangle|\text{vac}\rangle + |\text{vac}\rangle|0\rangle|1\rangle\right]_{txy} \end{split}$$

When Alice applies the operation iY_t^0 (corresponding to encoding 0) on the t-state, the composite system, denoted as $|\mathbf{B} - \mathbf{A}\rangle_{|0\rangle E_1}$, remains unchanged. This is symbolically expressed as $|\mathbf{B} - \mathbf{A}\rangle_{|0\rangle E_1}^0$, where the superscript indicates the bit Alice encodes. The resulting system after Eve's A-B attack, denoted by (Q_{txy}^{-1}) , is given by:

$$|A - B\rangle_{|0\rangle E_{1}}^{0} = Q_{txy}^{-1} |B - A\rangle_{|0\rangle E_{1}}^{0}$$

$$= Q_{txy}^{-1} \frac{1}{\sqrt{2}} [|0\rangle|0\rangle|vac\rangle + |vac\rangle|0\rangle|1\rangle]_{txy}$$

$$= H_{y} CPBS_{txy} SWAP_{tx} \frac{1}{\sqrt{2}} [|0\rangle|0\rangle|vac\rangle + |vac\rangle|0\rangle|1\rangle]_{txy}$$

$$= H_{y} CPBS_{txy} \frac{1}{\sqrt{2}} [|0\rangle|0\rangle|vac\rangle + |0\rangle|vac\rangle|1\rangle]_{txy}$$

$$= H_{y} \frac{1}{\sqrt{2}} [|0\rangle|vac\rangle|0\rangle + |0\rangle|vac\rangle|1\rangle]_{txy}$$

$$= |0\rangle_{t} |vac\rangle_{x} |0\rangle_{y}$$
(5.3)

This final state is consistent with the original composite system, which is expected, as Alice's encoding operation acts as an identity transformation for encoding 0. Meanwhile, Eve implements a unitary A-B attack operation (Q_{txy}) and subsequently its inverse, the unitary B-A attack operation (Q_{txy}^{-1}) . Similarly, analogous composite systems can be described for cases where Alice encodes 0 while Bob prepares the initial states $|1\rangle_t$, $|+\rangle_t$, and $|-\rangle_t$.

¹The polarizing beam splitter (PBS) is assumed to allow the transmission of photons in the $|0\rangle$ state while reflecting those in the $|1\rangle$ state.

$$|\mathbf{A} - \mathbf{B}\rangle_{|1\rangle E_1}^0 = |1\rangle_t |\operatorname{vac}\rangle_x |0\rangle_y , \qquad (5.4)$$

$$|A - B\rangle_{|+\rangle E_1}^0 = |+\rangle_t |vac\rangle_x |0\rangle_y ,$$
 (5.5)

and

$$|A - B\rangle_{|-\rangle E_1}^0 = |-\rangle_t |vac\rangle_x |0\rangle_y ,$$
 (5.6)

respectively.

Now, let us explore the scenario where Alice encodes a 1 by applying the operation iY_t^1 on the t-state. First, we analyze the system when Bob's initial state is $|0\rangle_t$. Previously, we established that the composite system is represented as

$$|\mathbf{B} - \mathbf{A}\rangle_{|0\rangle} = \frac{1}{\sqrt{2}} [|0\rangle|0\rangle|\mathrm{vac}\rangle + |\mathrm{vac}\rangle|0\rangle|1\rangle]_{txy}$$

Following Alice's encoding operation, Eve subsequently applies Q_{txy}^{-1} , resulting in the composite system:

$$|A - B\rangle_{|0\rangle E_{1}}^{1} = Q_{txy}^{-1} i Y_{t}^{1} \frac{1}{\sqrt{2}} [|0\rangle|0\rangle|vac\rangle + |vac\rangle|0\rangle|1\rangle]_{txy}$$

$$= Q_{txy}^{-1} \frac{1}{\sqrt{2}} [-|1\rangle|0\rangle|vac\rangle + |vac\rangle|0\rangle|1\rangle]_{txy}$$

$$= H_{y} CPBS_{txy} SWAP_{tx} \frac{1}{\sqrt{2}} [-|1\rangle|0\rangle|vac\rangle + |vac\rangle|0\rangle|1\rangle]_{txy}$$

$$= H_{y} CPBS_{txy} \frac{1}{\sqrt{2}} [-|0\rangle|1\rangle|vac\rangle + |0\rangle|vac\rangle|1\rangle]_{txy}$$

$$= H_{y} \frac{1}{\sqrt{2}} [-|0\rangle|1\rangle|vac\rangle + |0\rangle|vac\rangle|1\rangle]_{txy}$$

$$= \left[-\frac{1}{\sqrt{2}} |0\rangle|1\rangle|vac\rangle + \frac{1}{2} |0\rangle|vac\rangle|0\rangle - \frac{1}{2} |0\rangle|vac\rangle|1\rangle \right]_{txy}$$

For the sake of brevity, we will omit explicit derivations of similar cases and instead focus on presenting the key results. Next, we analyze the transformation of the composite system when Bob's initial state is $|1\rangle_t$ following Eve's B-A attack.

$$|\mathbf{B} - \mathbf{A}\rangle_{|1\rangle E_{1}} = Q_{txy} |1\rangle_{t} |\mathbf{vac}\rangle_{x} |0\rangle_{y}$$

$$= \frac{1}{\sqrt{2}} [|\mathbf{vac}\rangle|1\rangle|0\rangle\rangle + |1\rangle|1\rangle|\mathbf{vac}\rangle]_{txy}.$$

The composite system that emerges from Alice's operation combined with Eve's A-B attack can be expressed as follows:

$$|A - B\rangle_{|1\rangle E_{1}}^{1} = Q_{txy}^{-1} iY_{t}^{1} \frac{1}{\sqrt{2}} [|vac\rangle|1\rangle|0\rangle\rangle + |1\rangle|1\rangle|vac\rangle]_{txy}$$

$$= \left[\frac{1}{\sqrt{2}}|1\rangle|0\rangle|vac\rangle + \frac{1}{2}|1\rangle|vac\rangle|0\rangle + \frac{1}{2}|1\rangle|vac\rangle|1\rangle\right]_{txy}.$$
(5.8)

The outcomes corresponding to Bob's initial states, $|+\rangle$ and $|-\rangle$, are as follows:

$$|\mathbf{B} - \mathbf{A}\rangle_{|+\rangle E_1} = \frac{1}{2} \left[|0\rangle|0\rangle|\mathrm{vac}\rangle + |\mathrm{vac}\rangle|0\rangle|1\rangle + |\mathrm{vac}\rangle|1\rangle|0\rangle + |1\rangle|1\rangle|\mathrm{vac}\rangle \right]_{txy} ,$$

$$|\mathbf{A} - \mathbf{B}\rangle_{|+\rangle E_{1}}^{1} = \left[\frac{1}{2}\{|+\rangle|\operatorname{vac}\rangle|0\rangle - |-\rangle|\operatorname{vac}\rangle|1\rangle\} + \frac{1}{2\sqrt{2}}\{-|+\rangle|1\rangle|\operatorname{vac}\rangle - |-\rangle|1\rangle|\operatorname{vac}\rangle + |+\rangle|0\rangle|\operatorname{vac}\rangle - |-\rangle|0\rangle|\operatorname{vac}\rangle\}_{txy}^{1}$$
(5.9)

and

$$|\mathbf{B} - \mathbf{A}\rangle_{|-\rangle E_1} = \frac{1}{2} [|0\rangle|0\rangle|vac\rangle + |vac\rangle|0\rangle|1\rangle - |vac\rangle|1\rangle|0\rangle - |1\rangle|1\rangle|vac\rangle_{txv}$$

$$|A - B\rangle_{|-\rangle E_{1}}^{1} = \left[\frac{1}{2}\{|-\rangle|\operatorname{vac}\rangle|0\rangle - |+\rangle|\operatorname{vac}\rangle|1\rangle\} + \frac{1}{2\sqrt{2}}\{-|+\rangle|1\rangle|\operatorname{vac}\rangle - |-\rangle|1\rangle|\operatorname{vac}\rangle - |+\rangle|0\rangle|\operatorname{vac}\rangle + |-\rangle|0\rangle|\operatorname{vac}\rangle\}_{txy}^{1}$$

$$(5.10)$$

In the primary discussion, we previously established that Bob can deterministically decode Alice's message (j) by measuring the qubit on the same basis on which it was initially prepared. This process does not require a classical announcement. The information obtained by Bob upon decoding is denoted as m. Given the aforementioned results, we can directly determine Eve's optimal approach to infer Alice's encoded information based on her measurement outcomes from her auxiliary modes, x and y. Eve's decoded information is represented as k.

Eve's optimal strategy Eve correctly deciphers k=0 if her ancillary spatial mode x is in an empty state while mode y is in state $|0\rangle$, mathematically expressed as $|\text{vac}\rangle_x|0\rangle_y$. Conversely, Eve decodes k=1 when her x mode is in a nonempty state, or if it is empty while her y mode is in state $|1\rangle$, described as $|0\rangle_x|\text{vac}\rangle_y$, $|1\rangle_x|\text{vac}\rangle_y$, or $|\text{vac}\rangle_x|1\rangle_y$. Now, considering the parameter $p_{jmk}^{E_1}$, which defines the joint probability distribution where j, m, and k correspond to Alice's encoding, Bob's decoding, and Eve's inferred information, respectively, we can express these probabilities using Equations (5.3) - (5.10) as follows:

$$p_{000}^{E_1} = q$$

$$p_{001}^{E_1} = p_{010}^{E_1} = p_{011}^{E_1} = 0$$

$$p_{100}^{E_1} = \frac{1}{4}(1-q)$$

$$p_{101}^{E_1} = (1-q)(\frac{1}{4} + \frac{p}{2})$$

$$p_{110}^{E_1} = 0$$

$$(5.11)$$

To evaluate the mutual information shared among Alice, Bob, and Eve, we employ Equation (5.11). To further simplify the resulting expressions, we utilize Shannon entropy, defined as $\mathbf{H}[x] = -x \log_2 x$, where x represents the probability of a particular event occurring.

$$H(B|A)_{E_{1}} = (1-q) \left(\mathbf{H} \left[\frac{1}{2} (1-p) \right] + \mathbf{H} \left[\frac{1}{2} (1+p) \right] \right)$$

$$H(B)_{E_{1}} = \mathbf{H} \left[q + \frac{1}{2} (1-q) (1+p) \right] + \mathbf{H} \left[\frac{1}{2} (1-p) (1-q) \right] , \qquad (5.12)$$

$$I(A,B)_{E_{1}} = H(B)_{E_{1}} - H(B|A)_{E_{1}}$$

$$H(A|E)_{E_{1}} = \frac{1}{4} (1+3q) \left(\mathbf{H} \left[\frac{4q}{1+3q} \right] + \mathbf{H} \left[\frac{1-q}{1+3q} \right] \right)$$

$$H(A)_{E_{1}} = \mathbf{H}[q] + \mathbf{H}[1-q] , \qquad (5.13)$$

$$I(A,E)_{E_{1}} = H(A)_{E_{1}} - H(A|E)_{E_{1}}$$

and

$$H(\mathbf{B}|\mathbf{E})_{E_{1}} = \frac{3}{4}(1-q)\left(\mathbf{H}\left[\frac{1}{3}(1+2p)\right] + \mathbf{H}\left[\frac{2}{3}(1-p)\right]\right)$$

$$H(\mathbf{B})_{E_{1}} = \mathbf{H}\left[\frac{1}{2}(p+q-pq+1)\right] + \mathbf{H}\left[\frac{1}{2}(1-p)(1-q)\right].$$

$$I(\mathbf{B},\mathbf{E})_{E_{1}} = H(\mathbf{B})_{E_{1}} - H(\mathbf{B}|\mathbf{E})_{E_{1}}$$
(5.14)

Additionally, it is evident that eavesdropping introduces a QBER,

QBER_{E₁} =
$$\sum_{j \neq m} p_{jmk}^{E_1}$$

= $\frac{1}{2} (1 - q) (1 + p)$ (5.15)

Control mode: As described in [238], the previously mentioned "double" control mode comprises two independent tests conducted on the quantum channel, each analogous to the single test performed in the one-way BB84 protocol [15, 164]. Following Eve's B-A attack, when Bob initializes the state as $|0\rangle_t$, the resulting composite system can be expressed as:

$$|\mathbf{B} - \mathbf{A}\rangle_{|0\rangle E_1} = \frac{1}{\sqrt{2}} [|0\rangle|0\rangle|vac\rangle + |vac\rangle|0\rangle|1\rangle]_{txy}$$
.

Within the control mode, Alice performs a random measurement on the traveling qubit using both the computational (Z basis) and diagonal (X basis) bases before sending the projected qubit back to Bob. Bob then measures the qubit using the same basis he initially selected (in this case, the Z basis). Consequently, only scenarios where Alice measures the state t in the Z basis are considered. The expression $|B - A\rangle_{|0\rangle E_1}$ signifies that there is a $\frac{1}{2}$ probability that Alice will not detect any photon. However, if a photon is detected, its state remains identical to Bob's initial state. This suggests that in the Z basis, Eve's B-A attack does not lead to a detectable probability of eavesdropping. Nevertheless, eavesdropping may still be inferred by monitoring transmission losses, provided that the channel transmittance between Alice and Bob remains below 0.5. In this setting, Eve executes an A-B attack, denoted as Q_{txy}^{-1} , on the photon detected by Alice. Bob subsequently measures the state t in the Z basis and sends the projected qubit back to Alice. The composite system following Eve's A-B attack on Alice and Bob is:

$$Q_{txy}^{-1}|0\rangle_{t}|0\rangle_{x}|vac\rangle_{y} = H_{y}CPBS_{txy}SWAP_{tx}|0\rangle_{t}|0\rangle_{x}|vac\rangle_{y} = \frac{1}{\sqrt{2}}[|0\rangle|vac\rangle|0\rangle + |0\rangle|vac\rangle|1\rangle]_{txy}$$
(5.16)

When Bob's initial state is $|1\rangle_t$, Alice has an equal probability of detecting or not detecting a photon. Bob then measures the state t in the Z basis and transmits the projected qubit back to Alice. The composite system after Eve's A-B attack is:

$$Q_{txy}^{-1}|1\rangle_t|1\rangle_x|\text{vac}\rangle_y = \frac{1}{\sqrt{2}}[|1\rangle|\text{vac}\rangle|0\rangle - |1\rangle|\text{vac}\rangle|1\rangle]_{txy}.$$
 (5.17)

The scenario undergoes a significant shift if Bob initializes the state in the X basis rather than the Z basis. Specifically, if Bob's initial state is $|+\rangle_t$, then following Eve's B-A attack, the resulting composite system is given by:

$$\begin{split} |\mathbf{B}-\mathbf{A}\rangle_{|+\rangle E_1} &= \frac{1}{2} \left[|0\rangle|0\rangle|\mathrm{vac}\rangle + |\mathrm{vac}\rangle|0\rangle|1\rangle + |\mathrm{vac}\rangle|1\rangle|0\rangle + |1\rangle|1\rangle|\mathrm{vac}\rangle \right]_{txy} \\ &= \frac{1}{2} \left[\frac{1}{\sqrt{2}} \left\{ (|+\rangle + |-\rangle) \, |0\rangle|\mathrm{vac}\rangle + (|+\rangle - |-\rangle) \, |1\rangle|\mathrm{vac}\rangle \right\} + |\mathrm{vac}\rangle|0\rangle|1\rangle \\ &+ |\mathrm{vac}\rangle|1\rangle|0\rangle]_{txy} \end{split}$$

Alice, similar to the Z basis case, has a probability of $\frac{1}{2}$ of not detecting a photon. However, in instances where detection occurs, the photon is never found in Bob's original state $|+\rangle_t$. This indicates that in the B-A attack, (Q_{txy}) , Eve's detection process is relevant to the X basis configuration, unlike the Z basis case. Next, we rigorously evaluate Eve's A-B attack (Q_{txy}^{-1}) by considering all four possible measurement outcomes from Alice. The final composite system upon which Bob performs his measurement, after Alice's measurement collapses the state, is given by $|+\rangle_t |0\rangle_x |\text{vac}\rangle_y$,

$$Q_{txy}^{-1}|+\rangle_{t}|0\rangle_{x}|\text{vac}\rangle_{y} = Q_{txy}^{-1}\frac{1}{\sqrt{2}}[|0\rangle|0\rangle|\text{vac}\rangle + |1\rangle|0\rangle|\text{vac}\rangle]_{txy}$$

$$= \frac{1}{\sqrt{2}}|0\rangle_{t}\left[\frac{1}{\sqrt{2}}|\text{vac}\rangle(|0\rangle + |1\rangle) + |1\rangle|\text{vac}\rangle\right]_{xy} . \qquad (5.18)$$

$$= \frac{1}{2}(|+\rangle + |-\rangle)_{t}\left[\frac{1}{\sqrt{2}}|\text{vac}\rangle(|0\rangle + |1\rangle) + |1\rangle|\text{vac}\rangle\right]_{xy}$$

Similarly, the remaining three composite states following Alice's measurement are $|+\rangle_t |1\rangle_x |vac\rangle_y$, $|-\rangle_t |0\rangle_x |vac\rangle_y$, and $|-\rangle_t |1\rangle_x |vac\rangle_y$. As a result, the final composite systems take the form:

$$Q_{txy}^{-1}|+\rangle_t|1\rangle_x|\text{vac}\rangle_y = \frac{1}{2}(|+\rangle - |-\rangle)_t \left[\frac{1}{\sqrt{2}}|\text{vac}\rangle(|0\rangle - |1\rangle) + |0\rangle|\text{vac}\rangle\right]_{xy}, \qquad (5.19)$$

$$Q_{txy}^{-1}|-\rangle_t|0\rangle_x|\text{vac}\rangle_y = \frac{1}{2}(|+\rangle+|-\rangle)_t\left[\frac{1}{\sqrt{2}}|\text{vac}\rangle(|0\rangle+|1\rangle)-|1\rangle|\text{vac}\rangle\right]_{xy}, \qquad (5.20)$$

and

$$Q_{txy}^{-1}|-\rangle_t|1\rangle_x|\text{vac}\rangle_y = \frac{1}{2}(|+\rangle-|-\rangle)_t\left[-\frac{1}{\sqrt{2}}|\text{vac}\rangle(|0\rangle-|1\rangle)+|0\rangle|\text{vac}\rangle\right]_{xy}. \tag{5.21}$$

In cases where Bob's initial state is $|-\rangle_t$, the composite state after Eve's B-A attack becomes:

$$\begin{split} |\mathbf{B} - \mathbf{A}\rangle_{|-\rangle E_1} &= \frac{1}{2} \left[|0\rangle |0\rangle |\mathrm{vac}\rangle + |\mathrm{vac}\rangle |0\rangle |1\rangle - |\mathrm{vac}\rangle |1\rangle |0\rangle - |1\rangle |1\rangle |\mathrm{vac}\rangle \right]_{txy} \\ &= \frac{1}{2} \left[\frac{1}{\sqrt{2}} \left\{ (|+\rangle + |-\rangle) |0\rangle |\mathrm{vac}\rangle - (|+\rangle - |-\rangle) |1\rangle |\mathrm{vac}\rangle \right\} + |\mathrm{vac}\rangle |0\rangle |1\rangle \\ &- |\mathrm{vac}\rangle |1\rangle |0\rangle \right]_{txy} \end{split}$$

From a conceptual standpoint, it is evident that the overall scenario remains fundamentally equivalent whether Bob's initial state is $|-\rangle_t$ or $|+\rangle_t$. Consequently, Eve's A-B attack affects all four possible outcomes of Alice's measurement in the same manner, yielding identical results as expressed in Equations (5.18) - (5.21).

If we disregard the possibility of photon non-detection—favoring an optimal eavesdropping strategy for Eve—the probability of Eve remaining undetected in the E_1 attack scenario can be determined using Equations (5.16) - (5.21),

$$P_{nd}^{E_1} = \frac{1}{4} \left(1 + 1 + \frac{1}{4} + \frac{1}{4} \right) = \frac{5}{8}$$
.

The mean probability of detecting Eve's presence in the E_1 attack scenario is as follows:

$$P_d^{E_1} = \frac{1}{2} \left(1 - \frac{5}{8} \right) = \frac{3}{16} = 0.1875$$
 (5.22)

The upper limit of Alice and Bob's tolerance for the probability of detecting Eve in the control mode within the E_1 attack scenario is 0.1875. This implies that the threshold probability for Eve's detection is 18.75%.

5.3.2 E_2 ATTACK STRATEGY

Message mode: Wójcik proposed an alternative approach for symmetry-based attacks, designated as E_2 , where an additional unitary operation, S_{ty} , is applied with a probability of $\frac{1}{2}$

¹Eve employs two attack strategies—B-A attack and A-B attack. Additionally, there exists a "double" control mode for Eve's detection, as described in [238], leading to the emergence of the $\frac{1}{2}$ factor.

immediately after executing Q_{txy}^{-1} during the A-B attack [370]. The S_{ty} operation is characterized as $X_t Z_t \text{CNOT}_{ty} X_t$, integrating the Pauli-Z operation, Pauli-X, and the controlled-NOT (CNOT) gate. In this scenario, the B-A attack remains identical to that in E_1 , with modifications exclusively affecting the A-B attack. The notation conventions remain unchanged, apart from substituting E_1 with E_2 . The final state of the composite system, following the application of the S_{ty} operation in an A-B attack—where Alice encodes a 0 and Bob's initial state is $|0\rangle_t$ —is determined as follows:

$$|A - B\rangle_{|0\rangle E_{2}}^{0} = S_{ty} |A - B\rangle_{|0\rangle E_{1}}^{0}$$

$$= X_{t} Z_{t} CNOT_{ty} X_{t} |0\rangle_{t} |vac\rangle_{x} |0\rangle_{y}$$

$$= X_{t} Z_{t} CNOT_{ty} |1\rangle_{t} |vac\rangle_{x} |0\rangle_{y}$$

$$= X_{t} Z_{t} |1\rangle_{t} |vac\rangle_{x} |0\rangle_{y}$$

$$= X_{t} (-|1\rangle_{t} |vac\rangle_{x} |0\rangle_{y}$$

$$= - |0\rangle_{t} |vac\rangle_{x} |0\rangle_{y}$$

$$= - |0\rangle_{t} |vac\rangle_{x} |0\rangle_{y}$$

$$= - |0\rangle_{t} |vac\rangle_{x} |0\rangle_{y}$$
(5.23)

Similarly, the resulting composite system states can be obtained for cases where Alice encodes 0 while Bob's initial states are $|1\rangle$, $|+\rangle$, and $|-\rangle$.

$$|\mathbf{A} - \mathbf{B}\rangle_{|1\rangle E_2}^0 = |1\rangle_t |\operatorname{vac}\rangle_x |0\rangle_y , \qquad (5.24)$$

$$|\mathbf{A} - \mathbf{B}\rangle_{|+\rangle E_2}^0 = \frac{1}{2} [-|+\rangle |\mathbf{vac}\rangle |1\rangle - |-\rangle |\mathbf{vac}\rangle |1\rangle + |+\rangle |\mathbf{vac}\rangle |0\rangle - |-\rangle |\mathbf{vac}\rangle |0\rangle]_{txy} , \quad (5.25)$$

and

$$|\mathbf{A} - \mathbf{B}\rangle_{|-\rangle E_2}^0 = \frac{1}{2} \left[-|+\rangle |\mathbf{vac}\rangle |1\rangle - |-\rangle |\mathbf{vac}\rangle |1\rangle - |+\rangle |\mathbf{vac}\rangle |0\rangle + |-\rangle |\mathbf{vac}\rangle |0\rangle \right]_{txy}, \quad (5.26)$$

respectively.

The final state of the composite system, after executing the S_{ty} operation in an A-B attack where Alice encodes 1 and Bob's initial state is $|0\rangle_t$, is given as follows:

$$|A - B\rangle_{|0\rangle E_{2}}^{1} = S_{ty} |A - B\rangle_{|0\rangle E_{1}}^{1}$$

$$= X_{t} Z_{t} CNOT_{ty} X_{t} \left[-\frac{1}{\sqrt{2}} |0\rangle |1\rangle |vac\rangle + \frac{1}{2} |0\rangle |vac\rangle |0\rangle - \frac{1}{2} |0\rangle |vac\rangle |1\rangle \right]_{txy}$$

$$= X_{t} Z_{t} CNOT_{ty} \left[-\frac{1}{\sqrt{2}} |1\rangle |1\rangle |vac\rangle + \frac{1}{2} |1\rangle |vac\rangle |0\rangle - \frac{1}{2} |1\rangle |vac\rangle |1\rangle \right]_{txy}$$

$$= X_{t} Z_{t} \left[-\frac{1}{\sqrt{2}} |1\rangle |1\rangle |vac\rangle + \frac{1}{2} |1\rangle |vac\rangle |1\rangle - \frac{1}{2} |1\rangle |vac\rangle |0\rangle \right]_{txy}$$

$$= X_{t} \left[\frac{1}{\sqrt{2}} |1\rangle |1\rangle |vac\rangle - \frac{1}{2} |1\rangle |vac\rangle |1\rangle + \frac{1}{2} |1\rangle |vac\rangle |0\rangle \right]_{txy}$$

$$= \left[\frac{1}{\sqrt{2}} |0\rangle |1\rangle |vac\rangle - \frac{1}{2} |0\rangle |vac\rangle |1\rangle + \frac{1}{2} |0\rangle |vac\rangle |0\rangle \right]_{txy}$$

$$(5.27)$$

Similarly, we can characterize the remaining composite systems in which Alice encodes the bit 1 when Bob's initial states are $|1\rangle$, $|+\rangle$, and $|-\rangle$.

$$|A - B\rangle_{|1\rangle E_2}^1 = \left[\frac{1}{\sqrt{2}} |1\rangle |0\rangle |vac\rangle + \frac{1}{2} |1\rangle |vac\rangle |0\rangle + \frac{1}{2} |1\rangle |vac\rangle |1\rangle \right], \qquad (5.28)$$

$$|A - B\rangle_{|+\rangle E_{2}}^{1} = \frac{1}{2} [-|-\rangle|vac\rangle|1\rangle + |+\rangle|vac\rangle|0\rangle]_{txy} + \frac{1}{2\sqrt{2}} [|-\rangle|1\rangle|vac\rangle + |+\rangle|1\rangle|vac\rangle - |-\rangle|0\rangle|vac\rangle + |+\rangle|0\rangle|vac\rangle]_{txy}$$
(5.29)

and

$$|\mathbf{A} - \mathbf{B}\rangle_{|-\rangle E_{2}}^{1} = \frac{1}{2} [-|+\rangle |\operatorname{vac}\rangle |1\rangle + |-\rangle |\operatorname{vac}\rangle |0\rangle]_{txy} + \frac{1}{2\sqrt{2}} [|-\rangle |1\rangle |\operatorname{vac}\rangle + |+\rangle |1\rangle |\operatorname{vac}\rangle + |-\rangle |0\rangle |\operatorname{vac}\rangle - |+\rangle |0\rangle |\operatorname{vac}\rangle]_{txy}$$
(5.30)

respectively.

Eve's optimal strategy Eve's optimal strategy for extracting Alice's encoded information, after measuring the ancillary spatial modes x and y, corresponds to the E_1 attack scenario. As previously mentioned, there exists a $\frac{1}{2}$ probability that an additional unitary transformation S_{ty} is applied. Consequently, Equation (5.11) remains valid for calculating joint probabilities in half of all possible cases. These joint probabilities, expressed as $p_{jmk}^{E_2}$, where j, m, and k respectively denote Alice's encoding, Bob's decoding, and Eve's inference can be determined using Equations (5.11) and (5.23) - (5.30).

$$p_{000}^{E_2} = \frac{1}{2} \left[\frac{q}{4} (1+p) + q \right] = \frac{q}{8} (5+p)$$

$$p_{001}^{E_2} = \frac{q}{8} (1+p)$$

$$p_{010}^{E_2} = p_{011}^{E_2} = \frac{q}{8} (1-p)$$

$$p_{100}^{E_2} = \frac{1}{4} (1-q) \qquad . \tag{5.31}$$

$$p_{101}^{E_2} = \frac{1}{4} (1-q) (1+2p)$$

$$p_{111}^{E_2} = 0$$

By employing Equation (5.31), the mutual information shared among Alice, Bob, and Eve can be formulated as follows:

$$H(\mathbf{B}|\mathbf{A})_{E_{2}} = q\left(\mathbf{H}\left[\frac{1}{4}(3+p)\right] + \mathbf{H}\left[\frac{1}{4}(1-p)\right]\right) + (1-q)\left(\mathbf{H}\left[\frac{1}{2}(1+p)\right] + \mathbf{H}\left[\frac{1}{2}(1-p)\right]\right)$$

$$H(\mathbf{B})_{E_{2}} = \mathbf{H}\left[\frac{1}{4}(2+2p+q-pq+2)\right] + \mathbf{H}\left[\frac{1}{4}(1-p)(2-q)\right] ,$$

$$I(\mathbf{A},\mathbf{B})_{E_{2}} = H(\mathbf{B})_{E_{2}} - H(\mathbf{B}|\mathbf{A})_{E_{2}}$$

$$H(\mathbf{E}|\mathbf{A})_{E_{2}} = 0.811278$$

$$H(\mathbf{E})_{E_{2}} = \mathbf{H}\left[\frac{1}{4}(1+2q)\right] + \mathbf{H}\left[\frac{1}{4}(3-2q)\right] ,$$

$$I(\mathbf{A},\mathbf{E})_{E_{2}} = H(\mathbf{E})_{E_{2}} - H(\mathbf{E}|\mathbf{A})_{E_{2}}$$

$$(5.33)$$

and

$$\begin{split} H\left(\mathbf{E}|\mathbf{B}\right)_{E_{2}} &= \frac{1}{4}\left(2+2p+q-pq\right)\left(\mathbf{H}\left[\frac{1}{2}\left(\frac{2+3q+pq}{2+2p+q-pq}\right)\right]+\mathbf{H}\left[\frac{1}{2}\left(\frac{2+4p-q-3pq}{2+2p+q-pq}\right)\right]\right) \\ &+ \frac{1}{4}\left(1-p\right)\left(2-q\right)\left(\mathbf{H}\left[\frac{1}{2}\left(\frac{q}{2-q}\right)\right]+\mathbf{H}\left[\frac{1}{2}\left(\frac{4-3q}{2-q}\right)\right]\right) \\ H\left(\mathbf{E}\right)_{E_{2}} &= \mathbf{H}\left[\frac{1}{4}\left(1+2q\right)\right]+\mathbf{H}\left[\frac{1}{4}\left(3-2q\right)\right] \end{split} \tag{5.34}$$

$$I\left(\mathbf{B},\mathbf{E}\right)_{E_{2}} &= H\left(\mathbf{E}\right)_{E_{2}}-H\left(\mathbf{E}|\mathbf{B}\right)_{E_{2}} \end{split}$$

Additionally, it is evident that eavesdropping contributes to the QBER.

QBER_{E2} =
$$\sum_{j \neq m} p_{jmk}^{E_2}$$
 (5.35)
= $\frac{1}{4} (2 + 2p - q - 3pq)$

Control mode: The fundamental idea for the control mode has been previously illustrated in the context of the E_1 attack. The primary distinction arises from Eve's action of applying the S_{ty} operator with a $\frac{1}{2}$ probability after executing Q_{txy}^{-1} in the A-B attack scenario. Consider the case where Bob prepares the state $|0\rangle_t$ and Alice performs a measurement in the Z basis. In this situation, the composite system $|B-A\rangle_{|0\rangle E_1}$ collapses to the state $|0\rangle_t |0\rangle_x |vac\rangle_y$ with a $\frac{1}{2}$ probability when Alice detects a photon. Following Eve's E_2 attack, the resulting composite system transforms into:

$$S_{ty}Q_{txy}^{-1}|0\rangle_{t}|0\rangle_{x}|vac\rangle_{y} = S_{ty}H_{y}CPBS_{txy}SWAP_{tx}|0\rangle_{t}|0\rangle_{x}|vac\rangle_{y}$$

$$= S_{ty}\frac{1}{\sqrt{2}}[|0\rangle|vac\rangle|0\rangle + |0\rangle|vac\rangle|1\rangle]_{txy}$$

$$= X_{t}Z_{t}CNOT_{ty}X_{t}\frac{1}{\sqrt{2}}[|0\rangle|vac\rangle|0\rangle + |0\rangle|vac\rangle|1\rangle]_{txy}$$

$$= X_{t}Z_{t}CNOT_{ty}\frac{1}{\sqrt{2}}[|1\rangle|vac\rangle|0\rangle + |1\rangle|vac\rangle|1\rangle]_{txy} . (5.36)$$

$$= X_{t}Z_{t}\frac{1}{\sqrt{2}}[|1\rangle|vac\rangle|1\rangle + |1\rangle|vac\rangle|0\rangle]_{txy}$$

$$= X_{t}\frac{1}{\sqrt{2}}[-|1\rangle|vac\rangle|1\rangle - |1\rangle|vac\rangle|0\rangle]_{txy}$$

$$= \frac{1}{\sqrt{2}}[-|0\rangle|vac\rangle|1\rangle - |0\rangle|vac\rangle|0\rangle]_{txy}$$

If Bob's initial state is $|1\rangle_t$, Alice experiences an equal probability of detecting or not detecting a photon. She then measures the state t in the Z basis and subsequently transmits the projected qubit back to Bob. After Eve's A-B attack, the composite system is given by:

$$S_{ty}Q_{txy}^{-1}|1\rangle_t|1\rangle_x|vac\rangle_y = \frac{1}{\sqrt{2}}[|1\rangle|vac\rangle|0\rangle - |1\rangle|vac\rangle|1\rangle]_{txy}$$
 (5.37)

Consider Bob's initial state, represented as $|+\rangle_t$. Following Eve's B-A attack, the composite system remains in the state $|B-A\rangle_{|+\rangle E_1}$. When Alice performs a collapse on measurement in the X basis, four possible composite states emerge: $|+\rangle_t |0\rangle_x |vac\rangle_y$, $|+\rangle_t |1\rangle_x |vac\rangle_y$, and $|-\rangle_t |1\rangle_x |vac\rangle_y$, as expressed in Equations (5.18) - (5.21).

$$S_{ty}Q_{txy}^{-1}|+\rangle_{t}|0\rangle_{x}|vac\rangle_{y} = S_{ty}\frac{1}{2}(|+\rangle+|-\rangle)_{t}\left[\frac{1}{\sqrt{2}}|vac\rangle(|0\rangle+|1\rangle)+|1\rangle|vac\rangle\right]_{xy}$$

$$= X_{t}Z_{t}CNOT_{ty}X_{t}\left[\frac{1}{2}(|0\rangle|vac\rangle|0\rangle+|0\rangle|vac\rangle|1\rangle)+\frac{1}{\sqrt{2}}|0\rangle|1\rangle|vac\rangle\right]_{txy}$$

$$= X_{t}Z_{t}\left[\frac{1}{2}(|1\rangle|vac\rangle|1\rangle+|1\rangle|vac\rangle|0\rangle)+\frac{1}{\sqrt{2}}|1\rangle|1\rangle|vac\rangle\right]_{txy}$$

$$= \left[\frac{1}{2}(-|0\rangle|vac\rangle|1\rangle-|0\rangle|vac\rangle|0\rangle)-\frac{1}{\sqrt{2}}|0\rangle|1\rangle|vac\rangle\right]_{txy}$$

$$= \left[\frac{1}{2\sqrt{2}}(-|+\rangle|vac\rangle|1\rangle-|-\rangle|vac\rangle|1\rangle-|+\rangle|vac\rangle|0\rangle-|-\rangle|vac\rangle|0\rangle)$$

$$- \frac{1}{2}(|+\rangle|1\rangle|vac\rangle+|-\rangle|1\rangle|vac\rangle)\right]_{txy}$$

$$(5.38)$$

$$S_{ty}Q_{txy}^{-1}|+\rangle_{t}|1\rangle_{x}|vac\rangle_{y} = S_{ty}\frac{1}{2}(|+\rangle-|-\rangle)_{t}\left[\frac{1}{\sqrt{2}}|vac\rangle(|0\rangle-|1\rangle)+|0\rangle|vac\rangle\right]_{xy}$$

$$= X_{t}Z_{t}CNOT_{ty}X_{t}\left[\frac{1}{2}(|1\rangle|vac\rangle|0\rangle+|1\rangle|vac\rangle|1\rangle)+\frac{1}{\sqrt{2}}|1\rangle|0\rangle|vac\rangle\right]_{txy}$$

$$= X_{t}Z_{t}\left[\frac{1}{2}(|0\rangle|vac\rangle|0\rangle+|0\rangle|vac\rangle|1\rangle)+\frac{1}{\sqrt{2}}|0\rangle|0\rangle|vac\rangle\right]_{txy}$$

$$= \left[\frac{1}{2}(|1\rangle|vac\rangle|0\rangle+|1\rangle|vac\rangle|1\rangle)+\frac{1}{\sqrt{2}}|1\rangle|0\rangle|vac\rangle\right]_{txy},$$

$$= \left[\frac{1}{2\sqrt{2}}(|+\rangle|vac\rangle|0\rangle-|-\rangle|vac\rangle|0\rangle+|+\rangle|vac\rangle|1\rangle-|-\rangle|vac\rangle|1\rangle)$$

$$+ \frac{1}{2}(|+\rangle|0\rangle|vac\rangle-|-\rangle|0\rangle|vac\rangle)\right]_{txy}$$

$$(5.39)$$

$$S_{ty}Q_{txy}^{-1}|-\rangle_{t}|0\rangle_{x}|\operatorname{vac}\rangle_{y} = S_{ty}\frac{1}{2}(|+\rangle+|-\rangle)_{t}\left[\frac{1}{\sqrt{2}}|\operatorname{vac}\rangle(|0\rangle+|1\rangle)-|1\rangle|\operatorname{vac}\rangle\right]_{xy}$$

$$= \left[\frac{1}{2\sqrt{2}}(-|+\rangle|\operatorname{vac}\rangle|1\rangle-|-\rangle|\operatorname{vac}\rangle|1\rangle-|+\rangle|\operatorname{vac}\rangle|0\rangle-|-\rangle|\operatorname{vac}\rangle|0\rangle),$$

$$+ \frac{1}{2}(|+\rangle|1\rangle|\operatorname{vac}\rangle+|-\rangle|1\rangle|\operatorname{vac}\rangle)\right]_{txy}$$
(5.40)

and

$$S_{ty}Q_{txy}^{-1}|-\rangle_{t}|1\rangle_{x}|vac\rangle_{y} = S_{ty}\frac{1}{2}(|+\rangle-|-\rangle)_{t}\left[-\frac{1}{\sqrt{2}}|vac\rangle(|0\rangle-|1\rangle)+|0\rangle|vac\rangle\right]_{xy}$$

$$= \left[-\frac{1}{2\sqrt{2}}(|+\rangle|vac\rangle|0\rangle-|-\rangle|vac\rangle|0\rangle-|+\rangle|vac\rangle|1\rangle+|-\rangle|vac\rangle|1\rangle),$$

$$+ \frac{1}{2}(|+\rangle|0\rangle|vac\rangle-|-\rangle|0\rangle|vac\rangle)\right]_{txy}$$
(5.41)

respectively.

Now, let us examine the case where Bob's initial state is $|-\rangle_t$. The composite system remains in the state $|B-A\rangle_{|-\rangle E_1}$ after Eve's B-A attack. Intuitively, the scenario remains symmetric whether Bob's initial state is $|+\rangle_t$ or $|-\rangle_t$, implying that Eve's A-B attack affects all four possible measurement outcomes of Alice in the same manner. Consequently, the results are identical to those derived in Equations (5.38) - (5.41).

If we disregard cases where no photon detection occurs under the optimal eavesdropping strategy (favoring Eve), the probability of Eve remaining undetected in the E_2 attack scenario can be determined using Equations (5.36) - (5.41),

$$P_{nd}^{E_2} = \frac{1}{4} \left(1 + 1 + \frac{1}{4} + \frac{1}{4} \right) = \frac{5}{8}$$
.

The average probability of detecting Eve in the E_2 attack scenario is calculated,

$$P_d^{E_2} = \frac{1}{2} \left(1 - \frac{5}{8} \right) = \frac{3}{16} = 0.1875$$
 (5.42)

The maximum tolerable detection probability in the control mode for this scenario is 0.1875. In other words, the upper threshold for detecting Eve is 18.75%.

5.3.3 E_3 ATTACK STRATEGY

In this scenario, we employ an alternative attack method, denoted as E_3 , originally introduced by Pavičić [371]. Eve initializes two auxiliary modes, labeled x and y, each beginning with an ancilla photon in the state $|\text{vac}\rangle_x|0\rangle_y$, where $|\text{vac}\rangle$ signifies an empty mode. She then facilitates an interaction between the traveling photon and these auxiliary modes¹. Similar to the preceding two attacks, Eve applies the unitary operation Q'_{txy} when the photon is in transit from Bob to

¹The original work [371] explores the qutrit case, our focus is restricted to the qubit scenario. To simplify notation, we represent the basis states as $|0\rangle$ and $|1\rangle$ rather than $|H\rangle$ and $|V\rangle$.

Alice during a B-A attack. Conversely, in the A-B attack setting, Eve employs the inverse operation $Q_{txy}^{\prime-1}$ on the traveling photon t.

$$Q'_{txy} = \text{CNOT}_{ty}(\text{CNOT}_{tx} \otimes I_y) (I_t \otimes \text{PBS}_{xy}) \text{CNOT}_{ty}(\text{CNOT}_{tx} \otimes I_y) (I_t \otimes H_x \otimes H_y)$$

Eve's strategy consists of sequentially applying Hadamard gates to the *x* and *y* modes, followed by two CNOT gates, a PBS operation, and two additional CNOT gates. Further details on this approach can be found in [371].

Message mode: Now, consider the scenario where Alice encodes a bit value of 1. Specifically, assume Bob prepares the initial state $|0\rangle_t$. Eve then executes the B-A attack on the composite system $|0\rangle_t|\text{vac}\rangle_x|0\rangle_y$, following the E_3 attack method,

$$|B-A\rangle_{|0\rangle E_{3}} = Q'_{txy}|0\rangle_{t}|vac\rangle_{x}|0\rangle_{y}$$

$$= CNOT_{ty}(CNOT_{tx}\otimes I_{y})(I_{t}\otimes PBS_{xy})CNOT_{ty}(CNOT_{tx}\otimes I_{y})(I_{t}\otimes H_{x}\otimes H_{y})$$

$$\times (|0\rangle|vac\rangle|0\rangle)_{txy}$$

$$= CNOT_{ty}(CNOT_{tx}\otimes I_{y})(I_{t}\otimes PBS_{xy})CNOT_{ty}(CNOT_{tx}\otimes I_{y})$$

$$\times \frac{1}{\sqrt{2}}[|0\rangle|vac\rangle(|0\rangle+|1\rangle)]_{txy}$$

$$= CNOT_{ty}(CNOT_{tx}\otimes I_{y})(I_{t}\otimes PBS_{xy})CNOT_{ty}\frac{1}{\sqrt{2}}[|0\rangle|vac\rangle(|0\rangle+|1\rangle)]_{txy}$$

$$= CNOT_{ty}(CNOT_{tx}\otimes I_{y})(I_{t}\otimes PBS_{xy})\frac{1}{\sqrt{2}}[|0\rangle|vac\rangle(|0\rangle+|1\rangle)]_{txy}$$

$$= CNOT_{ty}(CNOT_{tx}\otimes I_{y})\frac{1}{\sqrt{2}}[|0\rangle|0\rangle|vac\rangle+|0\rangle|vac\rangle|1\rangle]_{txy}$$

$$= CNOT_{ty}\frac{1}{\sqrt{2}}[|0\rangle|0\rangle|vac\rangle+|0\rangle|vac\rangle|1\rangle]_{txy}$$

$$= \frac{1}{\sqrt{2}}[|0\rangle|0\rangle|vac\rangle+|0\rangle|vac\rangle|1\rangle]_{txy}$$

As Alice applies the operation iY_t^1 to encode the bit value 1 in state t, the composite system undergoes a transformation, leading to a new state $|B - A\rangle_{|0\rangle E_3}$. The superscript 1 indicates that Alice's encoding has been incorporated. Subsequently, after Eve's interference using $Q_{txy}^{\prime-1}$, the system is modified accordingly,

$$|A - B\rangle_{|0\rangle E_{3}}^{1} = Q_{txy}^{\prime - 1} \frac{1}{\sqrt{2}} [|1\rangle|0\rangle|vac\rangle + |1\rangle|vac\rangle|1\rangle]_{txy}$$

$$= (I_{t} \otimes H_{x} \otimes H_{y}) (CNOT_{tx} \otimes I_{y}) CNOT_{ty} (I_{t} \otimes PBS_{xy})$$

$$\times (CNOT_{tx} \otimes I_{y}) CNOT_{ty} \frac{-1}{\sqrt{2}} [|1\rangle|0\rangle|vac\rangle + |1\rangle|vac\rangle|1\rangle]_{txy}$$

$$= (I_{t} \otimes H_{x} \otimes H_{y}) (CNOT_{tx} \otimes I_{y}) CNOT_{ty} (I_{t} \otimes PBS_{xy})$$

$$\times (CNOT_{tx} \otimes I_{y}) \frac{-1}{\sqrt{2}} [|1\rangle|0\rangle|vac\rangle + |1\rangle|vac\rangle|0\rangle]_{txy}$$

$$= (I_{t} \otimes H_{x} \otimes H_{y}) (CNOT_{tx} \otimes I_{y}) CNOT_{ty} (I_{t} \otimes PBS_{xy})$$

$$\times \frac{-1}{\sqrt{2}} [|1\rangle|1\rangle|vac\rangle + |1\rangle|vac\rangle|0\rangle]_{txy}$$

$$= (I_{t} \otimes H_{x} \otimes H_{y}) (CNOT_{tx} \otimes I_{y}) CNOT_{ty} \frac{-1}{\sqrt{2}} [|1\rangle|1\rangle|vac\rangle + |1\rangle|0\rangle|vac\rangle]_{txy}$$

$$= (I_{t} \otimes H_{x} \otimes H_{y}) (CNOT_{tx} \otimes I_{y}) \frac{-1}{\sqrt{2}} [|1\rangle|1\rangle|vac\rangle + |1\rangle|0\rangle|vac\rangle]_{txy}$$

$$= (I_{t} \otimes H_{x} \otimes H_{y}) \frac{-1}{\sqrt{2}} [|1\rangle|0\rangle|vac\rangle + |1\rangle|1\rangle|vac\rangle]_{txy}$$

$$= \frac{-1}{2} [|1\rangle (|0\rangle + |1\rangle)|vac\rangle + |1\rangle (|0\rangle - |1\rangle)|vac\rangle]_{txy}$$

$$= -|1\rangle_{t} |0\rangle_{x} |vac\rangle_{y}$$
(5.43)

For brevity, we present only the key results. Consider the cases where Bob initializes the states as $|1\rangle_t$, $|+\rangle_t$, and $|-\rangle_t$. After undergoing the B-A attack, the composite system evolves into a transformed state as a consequence of Eve's intervention.

$$|\mathbf{B} - \mathbf{A}\rangle_{|1\rangle E_3} = \frac{1}{\sqrt{2}} [|1\rangle |\mathbf{vac}\rangle |0\rangle + |1\rangle |1\rangle |\mathbf{vac}\rangle]_{txy}$$

$$|\mathbf{B}-\mathbf{A}\rangle_{|+\rangle E_3} \ = \ \tfrac{1}{2} \left[|0\rangle|0\rangle|\mathrm{vac}\rangle + |0\rangle|\mathrm{vac}\rangle|1\rangle + |1\rangle|\mathrm{vac}\rangle|0\rangle + |1\rangle|1\rangle|\mathrm{vac}\rangle\right]_{txy} \ ,$$

and

$$|\mathbf{B} - \mathbf{A}\rangle_{|-\rangle E_3} = \frac{1}{2} [|0\rangle|0\rangle|\mathrm{vac}\rangle + |0\rangle|\mathrm{vac}\rangle|1\rangle - |1\rangle|\mathrm{vac}\rangle|0\rangle - |1\rangle|1\rangle|\mathrm{vac}\rangle_{lxy} ,$$

respectively.

Following Eve's attack operation, Q'_{txy}^{-1} (A-B attack), the composite system evolves as follows: When Alice encodes a bit value of 1, she applies the operation iY_t^1 to Bob's initial states $|1\rangle_t$, $|+\rangle_t$, and $|-\rangle_t$,

$$|A - B\rangle_{|1\rangle E_3}^1 = |0\rangle_t |0\rangle_x |vac\rangle_y , \qquad (5.44)$$

$$|A - B\rangle_{|+\rangle E_3}^1 = |-\rangle_t |0\rangle_x |vac\rangle_y , \qquad (5.45)$$

and

$$|A - B\rangle_{|-\rangle E_3}^1 = -|+\rangle_t |0\rangle_x |vac\rangle_y , \qquad (5.46)$$

respectively.

The final composite states resulting from Eve's bidirectional attacks (B-A and A-B attacks) are obtained when Alice encodes a 0 using the operation I_t , with Bob's initial states being $|0\rangle_t$, $|1\rangle_t$, $|+\rangle_t$, and $|-\rangle_t$.

$$|\mathbf{A} - \mathbf{B}\rangle_{|0\rangle E_3}^0 = |0\rangle_t |\operatorname{vac}\rangle_x |0\rangle_y , \qquad (5.47)$$

$$|\mathbf{A} - \mathbf{B}\rangle_{|1\rangle E_3}^0 = |1\rangle_t |\operatorname{vac}\rangle_x |0\rangle_y , \qquad (5.48)$$

$$|A - B\rangle_{|+\rangle E_3}^0 = |+\rangle_t |vac\rangle_x |0\rangle_y ,$$
 (5.49)

and

$$|A - B\rangle_{|-\rangle E_3}^0 = |-\rangle_t |vac\rangle_x |0\rangle_y ,$$
 (5.50)

respectively.

Eve's optimal strategy Eve's optimal strategy for decoding is characterized by two distinct cases: (1) she deciphers k=0 when her ancillary spatial modes x and y are in the vacuum state and $|0\rangle$ state, respectively, i.e., $|\text{vac}\rangle_x|0\rangle_y$, and (2) she deciphers k=1 when the x mode is in the $|0\rangle$ state and the y mode is in the vacuum state, i.e., $|0\rangle_x|\text{vac}\rangle_y$. These scenarios are quantified by the parameter $p_{jmk}^{E_3}$, which represents the joint probability, where j, m, and k correspond to Alice's encoding, Bob's decoding, and Eve's decoding outcomes, respectively. The joint probabilities are derived from Equations (5.43) - (5.50).

$$p_{000}^{E_3} = q$$

$$p_{001}^{E_3} = p_{010}^{E_3} = p_{011}^{E_3} = 0$$

$$p_{100}^{E_3} = p_{101}^{E_3} = p_{110}^{E_3} = 0$$

$$p_{111}^{E_3} = (1-q)$$

$$(5.51)$$

Using Equation (5.51), the mutual information shared among Alice, Bob, and Eve can be formulated,

$$H(B|A)_{E_3} = 0$$
 $H(B)_{E_3} = \mathbf{H}[q] + \mathbf{H}[1-q],$ (5.52)

 $I(A,B)_{E_3} = \mathbf{H}[q] + \mathbf{H}[1-q]$
 $H(E|A)_{E_3} = 0$
 $H(E)_{E_3} = \mathbf{H}[q] + \mathbf{H}[1-q],$ (5.53)

 $I(A,E)_{E_3} = \mathbf{H}[q] + \mathbf{H}[1-q]$

and

$$H(E|B)_{E_3} = 0$$

$$H(E)_{E_3} = \mathbf{H}[q] + \mathbf{H}[1-q] . \tag{5.54}$$

$$I(B,E)_{E_3} = \mathbf{H}[q] + \mathbf{H}[1-q]$$

Furthermore, it is evident that Eve's eavesdropping introduces QBER, thereby affecting the

overall security of the system.

QBER_{E₃} =
$$\sum_{j \neq m} p_{jmk}^{E_3}$$
= 0 (5.55)

Control mode: In the given scenario, if Bob initializes the system in state $|0\rangle_t$ and Alice subsequently measures it using the Z basis, the composite system $|B-A\rangle_{|0\rangle E_3}$ probabilistically collapses into one of two possible states with equal probability: $|0\rangle_t |0\rangle_x |vac\rangle_y$ or $|0\rangle_t |vac\rangle_x |1\rangle_y$. Following Eve's Q_{txy}^{t-1} (A-B) attack, the composite system undergoes further evolution,

$$Q_{txy}^{\prime-1}|0\rangle_{t}|0\rangle_{x}|\text{vac}\rangle_{y} = \frac{1}{\sqrt{2}}\left[|0\rangle|\text{vac}\rangle|0\rangle + |0\rangle|\text{vac}\rangle|1\rangle\right]_{txy}$$

$$. \qquad (5.56)$$

$$Q_{txy}^{\prime-1}|0\rangle_{t}|\text{vac}\rangle_{x}|1\rangle_{y} = \frac{1}{\sqrt{2}}\left[|0\rangle|\text{vac}\rangle|0\rangle - |0\rangle|\text{vac}\rangle|1\rangle\right]_{txy}$$

When Bob initializes the system in state $|1\rangle_t$ and Alice performs a Z-basis measurement, the composite state $|B-A\rangle_{|1\rangle E_3}$ collapses into either $|1\rangle_t |\text{vac}\rangle_x |0\rangle_y$ and $|1\rangle_t |1\rangle_x |\text{vac}\rangle_y$, each occurring with equal probability. The application of Eve's $Q_{txy}^{\prime-1}$ (A-B) attack subsequently modifies the composite system,

$$Q_{txy}^{\prime-1}|1\rangle_{t}|\text{vac}\rangle_{x}|0\rangle_{y} = \frac{1}{\sqrt{2}}[|1\rangle|\text{vac}\rangle|0\rangle + |1\rangle|\text{vac}\rangle|1\rangle]_{txy}$$

$$. \qquad (5.57)$$

$$Q_{txy}^{\prime-1}|1\rangle_{t}|1\rangle_{x}|\text{vac}\rangle_{y} = \frac{1}{\sqrt{2}}[|1\rangle|\text{vac}\rangle|0\rangle - |1\rangle|\text{vac}\rangle|1\rangle]_{txy}$$

Similarly, if Bob prepares the system in the state $|+\rangle_t$ and Alice measures using the X basis, the composite system $|B-A\rangle_{|+\rangle E_3}$ collapses into one of the following states with equal probability: $|+\rangle_t |0\rangle_x |\text{vac}\rangle_y$, $|-\rangle_t |0\rangle_x |\text{vac}\rangle_y$, $|+\rangle_t |\text{vac}\rangle_x |1\rangle_y$, $|-\rangle_t |\text{vac}\rangle_x |1\rangle_y$, $|+\rangle_t |\text{vac}\rangle_x |0\rangle_y$, $|+\rangle_t |1\rangle_x |\text{vac}\rangle_y$, or $|-\rangle_t |1\rangle_x |\text{vac}\rangle_y$. Following Eve's $Q_{txy}^{\prime-1}$ (A-B) attack, the composite system undergoes further transformations,

$$Q_{txy}^{\prime-1}|+\rangle_{t}|0\rangle_{x}|\text{vac}\rangle_{y} = \frac{1}{2\sqrt{2}}\left[(|+\rangle+|-\rangle)_{t}|\text{vac}\rangle_{x}(|0\rangle+|1\rangle)_{y}+(|+\rangle-|-\rangle)_{t}(|0\rangle+|1\rangle)_{x}|\text{vac}\rangle_{y}\right]$$

$$Q_{txy}^{\prime-1}|+\rangle_{t}|\text{vac}\rangle_{x}|1\rangle_{y} = \frac{1}{2\sqrt{2}}\left[(|+\rangle+|-\rangle)_{t}|\text{vac}\rangle_{x}(|0\rangle-|1\rangle)_{y}+(|+\rangle-|-\rangle)_{t}(|0\rangle-|1\rangle)_{x}|\text{vac}\rangle_{y}\right]$$

$$Q_{txy}^{\prime-1}|+\rangle_{t}|\text{vac}\rangle_{x}|0\rangle_{y} = \frac{1}{2\sqrt{2}}\left[(|+\rangle+|-\rangle)_{t}(|0\rangle+|1\rangle)_{x}|\text{vac}\rangle_{y}+(|+\rangle-|-\rangle)_{t}|\text{vac}\rangle_{x}(|0\rangle+|1\rangle)_{y}\right]$$

$$Q_{txy}^{\prime-1}|+\rangle_{t}|1\rangle_{x}|\text{vac}\rangle_{y} = \frac{1}{2\sqrt{2}}\left[(|+\rangle+|-\rangle)_{t}(|0\rangle-|1\rangle)_{x}|\text{vac}\rangle_{y}+(|+\rangle-|-\rangle)_{t}|\text{vac}\rangle_{x}(|0\rangle-|1\rangle)_{y}\right]$$

$$Q_{txy}^{\prime-1}|-\rangle_{t}|0\rangle_{x}|\text{vac}\rangle_{y} = \frac{1}{2\sqrt{2}}\left[(|+\rangle+|-\rangle)_{t}|\text{vac}\rangle_{x}(|0\rangle+|1\rangle)_{y}-(|+\rangle-|-\rangle)_{t}(|0\rangle+|1\rangle)_{x}|\text{vac}\rangle_{y}\right]$$

$$Q_{txy}^{\prime-1}|-\rangle_{t}|\text{vac}\rangle_{x}|1\rangle_{y} = \frac{1}{2\sqrt{2}}\left[(|+\rangle+|-\rangle)_{t}|\text{vac}\rangle_{x}(|0\rangle-|1\rangle)_{y}-(|+\rangle-|-\rangle)_{t}(|0\rangle-|1\rangle)_{x}|\text{vac}\rangle_{y}\right]$$

$$Q_{txy}^{\prime-1}|-\rangle_{t}|\text{vac}\rangle_{x}|0\rangle_{y} = \frac{1}{2\sqrt{2}}\left[(|+\rangle+|-\rangle)_{t}(|0\rangle+|1\rangle)_{x}|\text{vac}\rangle_{y}-(|+\rangle-|-\rangle)_{t}|\text{vac}\rangle_{x}(|0\rangle+|1\rangle)_{y}\right]$$

$$Q_{txy}^{\prime-1}|-\rangle_{t}|\text{vac}\rangle_{x}|0\rangle_{y} = \frac{1}{2\sqrt{2}}\left[(|+\rangle+|-\rangle)_{t}(|0\rangle+|1\rangle)_{x}|\text{vac}\rangle_{y}-(|+\rangle-|-\rangle)_{t}|\text{vac}\rangle_{x}(|0\rangle+|1\rangle)_{y}\right]$$

For the case where Bob prepares the state $|-\rangle_t$, the corresponding composite state post Eve's B-A attack is determined accordingly.

$$\begin{split} |\mathbf{B}-\mathbf{A}\rangle_{|-\rangle E_3} &= \frac{1}{2} \left[|0\rangle|0\rangle|\mathrm{vac}\rangle + |0\rangle|\mathrm{vac}\rangle|1\rangle - |1\rangle|\mathrm{vac}\rangle|0\rangle - |1\rangle|1\rangle|\mathrm{vac}\rangle \right]_{txy} \\ &= \frac{1}{2\sqrt{2}} \left[\left(|+\rangle + |-\rangle \right) \left(|0\rangle|\mathrm{vac}\rangle + |\mathrm{vac}\rangle|1\rangle \right) - \left(|+\rangle - |-\rangle \right) \left(|\mathrm{vac}\rangle|0\rangle - |1\rangle|\mathrm{vac}\rangle \right) \right]_{txy} \end{split}$$

From an intuitive standpoint, it is apparent that the overall scenario remains equivalent regardless of whether Bob's initial state is $|-\rangle_t$ or $|+\rangle_t$. Consequently, Eve's A-B attack influences all four possible outcomes of Alice's measurement in an identical manner, yielding the same results as given in Equation (5.58). The probability of Eve remaining undetected in the E_3 attack scenario can be determined using Equations (5.56) - (5.58),

$$P_{nd}^{E_3} = \frac{1}{4} \left(1 + 1 + \frac{1}{4} + \frac{1}{4} \right) = \frac{5}{8}$$
.

The average probability of detecting Eve in the E_3 attack scenario is calculated as follows:

$$P_d^{E_3} = \frac{1}{2} \left(1 - \frac{5}{8} \right) = \frac{3}{16} = 0.1875$$
 (5.59)

Alice and Bob can tolerate a maximum detection probability of 0.1875 for Eve's presence in control mode under the E_3 attack scenario. This establishes an upper bound of 18.75% for the probability of detecting Eve's intervention.

5.3.4 E_4 ATTACK STRATEGY

Next, we define Eve's IR (E_4) attack and subsequently compute the mutual information among Alice, Bob, and Eve. Similar to the B-A attack, Eve performs a uniform (random) measurement in both the Z and X bases on Bob's qubit before forwarding the projected qubit to Alice. Depending on the mode of operation—either encoding (message mode) or measurement (control mode)—Eve then acts on the received qubit and sends it back to Bob. In the A-B attack, she applies the same measurement operation that was previously executed in the B-A attack.

Message mode: Through an extensive calculation, the joint probability p_{jmk} is obtained, where j, m, and k correspond to Alice's encoding, Bob's decoding, and Eve's decoding information, respectively.

$$p_{000}^{E_4} = \frac{3}{4}q$$

$$p_{001}^{E_4} = p_{011}^{E_4} = 0$$

$$p_{010}^{E_4} = \frac{1}{4}q$$

$$p_{100}^{E_4} = p_{110}^{E_4} = 0$$

$$p_{101}^{E_4} = \frac{1}{4}(1-q)$$

$$p_{111}^{E_4} = \frac{3}{4}(1-q)$$
(5.60)

By employing Equation (5.60), the expression for mutual information among Alice, Bob, and Eve can be derived as follows:

$$H(B|A)_{E_4} = 0.811278$$

$$H(B)_{E_4} = \mathbf{H} \left[\frac{1}{4} (1+2q) \right] + \mathbf{H} \left[\frac{1}{4} (3-2q) \right] , \qquad (5.61)$$

$$I(A,B)_{E_4} = H(B)_{E_4} - H(B|A)_{E_4}$$

$$H(E|A)_{E_4} = 0$$

$$H(E)_{E_4} = \mathbf{H} [q] + \mathbf{H} [(1-q)] , \qquad (5.62)$$

and

$$H(B|E)_{E_4} = 0.811278$$

$$H(B)_{E_4} = \mathbf{H} \left[\frac{1}{4} (1+2q) \right] + \mathbf{H} \left[\frac{1}{4} (3-2q) \right] . \tag{5.63}$$

$$I(B,E)_{E_4} = H(B)_{E_4} - H(B|E)_{E_4}$$

Eavesdropping is a contributing factor to QBER,

QBER_{E4} =
$$\sum_{j \neq m} p_{jmk}^{E_4}$$

= $\frac{1}{4}q + \frac{1}{4}(1-q)$ (5.64)
= 0.25

Control mode: In a bidirectional BB84-type security framework, the probability of Eve remaining undetected throughout both transmission directions is given by:

 $I(\mathbf{A}, \mathbf{E})_{E_4} = \mathbf{H}[q] + \mathbf{H}[(1-q)]$

$$P_{nd}^{E_4} = \frac{1}{2} \times \frac{1}{2} = \frac{1}{4}$$
.

Consequently, the mean probability of detecting Eve's presence in the E_4 attack scenario is:

$$P_d^{E_4} = \frac{1}{2} \left(1 - \frac{1}{4} \right) = \frac{3}{8} = 0.375$$
 (5.65)

Alice and Bob can tolerate a maximum detection probability of 0.375 in control mode under the E_4 attack scenario. This implies that the threshold for detecting Eve's presence is 37.5%.

5.4 ANALYZING THE QBER THRESHOLD BOUND OF USING NASH EQUILIBRIUM

A Nash equilibrium represents a strategic scenario in which no player can enhance their expected payoff by unilaterally changing their strategy, provided that other participants maintain their respective choices. In its generalized form, Nash equilibrium characterizes a stochastic steady-state condition in strategic interactions, wherein players are permitted to choose a probability distribution over their available strategies rather than being restricted to a single deterministic choice. This probabilistic approach is known as a mixed strategy. In a well-structured game, it is typically assumed that all players act rationally, striving to optimize (maximize, in this context) their expected payoffs. To simplify the analysis, we evaluate the "mixed-strategy Nash equilibrium" by examining three different game scenarios: E_1 - E_2 , E_1 - E_3 , and E_2 - E_3 . Each player aims to adopt a mixed quantum strategy² that renders their opponent indifferent between pure quantum strategies. Utilizing this principle, we compare the equilibrium points to establish a secure bound for the QBER (refer to Section 5.3).

¹A "mixed strategy Nash equilibrium" in a "normal-form game" consists of a set of mixed strategies where no player has an incentive to unilaterally deviate, given the strategies adopted by others, ensuring mutual optimality.

²All payoff elements for each player under the attack scenarios E_1 , E_2 , E_3 , and E_4 are computed in Appendices A, B, C, and D, respectively.

³Here, r and 1-r represent the probabilities that an eavesdropper, Eve, assigns to selecting attacks E_i and E_j , respectively.

$$B_A(p,r) := rP_A^{E_i}(p,1) + (1-r)P_A^{E_j}(p,1) > rP_A^{E_i}(p,0) + (1-r)P_A^{E_j}(p,0).$$

and

$$B_A(p,r) := rP_A^{E_i}(p,1) + (1-r)P_A^{E_j}(p,1) < rP_A^{E_i}(p,0) + (1-r)P_A^{E_j}(p,0),$$

respectively. For Alice's mixed strategy best response function, we define:

$$B_A(p,r) := r P_A^{E_i}(p,1) + (1-r) P_A^{E_j}(p,1) = r P_A^{E_i}(p,0) + (1-r) P_A^{E_j}(p,0).$$

By extending the definition of the best response function, we similarly define Bob's and Eve's best response functions as $B_B(q, r)$ and $B_E(p, q)$, where Bob and Eve assign their probabilities p and r while optimizing their responses based on q, r and p, q, respectively.

 E_1 - E_2 game scenario: The previously defined probabilities p and q apply here as well. Suppose Eve selects the $E_1(E_2)$ attack with probability r (1-r). Alice's "best response function", denoted as $B_A(p,r)$, represents the set of probabilities she assigns to choosing the Z basis as her optimal response to p and r [373]. Similarly, the best response functions for Bob and Eve are given by $B_B(q,r)$ and $B_E(p,q)$, respectively. We get as following:

$$B_{A}(p,r) = \begin{cases} \{q=1\} & \text{if } rP_{A}^{E_{1}}(p,1) + (1-r)P_{A}^{E_{2}}(p,1) \\ > rP_{A}^{E_{1}}(p,0) + (1-r)P_{A}^{E_{2}}(p,0) \\ \{q:0 \leq q \leq 1\} & \text{if } rP_{A}^{E_{1}}(p,1) + (1-r)P_{A}^{E_{2}}(p,1) \\ = rP_{A}^{E_{1}}(p,0) + (1-r)P_{A}^{E_{2}}(p,0) \\ \{q=0\} & \text{if } rP_{A}^{E_{1}}(p,1) + (1-r)P_{A}^{E_{2}}(p,1) \\ < rP_{A}^{E_{1}}(p,0) + (1-r)P_{A}^{E_{2}}(p,0) \end{cases}$$

$$B_{B}(q,r) = \begin{cases} \{p=1\} & \text{if } rP_{B}^{E_{1}}(1,q) + (1-r)P_{B}^{E_{2}}(1,q) \\ > rP_{B}^{E_{1}}(0,q) + (1-r)P_{B}^{E_{2}}(0,q) \end{cases} . \tag{5.66}$$

$$\{p:0 \leq p \leq 1\} & \text{if } rP_{B}^{E_{1}}(1,q) + (1-r)P_{B}^{E_{2}}(1,q) \\ = rP_{B}^{E_{1}}(0,q) + (1-r)P_{B}^{E_{2}}(0,q) \end{cases}$$

$$\{p=0\} & \text{if } rP_{B}^{E_{1}}(1,q) + (1-r)P_{B}^{E_{2}}(1,q) \\ < rP_{B}^{E_{1}}(0,q) + (1-r)P_{B}^{E_{2}}(0,q) \end{cases}$$

$$B_{E}(p,q) = \begin{cases} \{r = 1\} & \text{if } P_{E}^{E_{1}}(p,q) > P_{E}^{E_{2}}(p,q) \\ \{r : 0 \le r \le 1\} & \text{if } P_{E}^{E_{1}}(p,q) = P_{E}^{E_{2}}(p,q) \\ \{r = 0\} & \text{if } P_{E}^{E_{1}}(p,q) < P_{E}^{E_{2}}(p,q) \end{cases}$$

The best response functions corresponding to Alice, Bob, and Eve in the game scenarios E_1 - E_3 and E_2 - E_3 are defined as follows:

$$B_{A}(p,r) = \begin{cases} \{q=1\} & \text{if } rP_{A}^{E_{1}}(p,1) + (1-r)P_{A}^{E_{3}}(p,1) \\ > rP_{A}^{E_{1}}(p,0) + (1-r)P_{A}^{E_{3}}(p,0) \\ \{q:0 \leq q \leq 1\} & \text{if } rP_{A}^{E_{1}}(p,1) + (1-r)P_{A}^{E_{3}}(p,1) \\ = rP_{A}^{E_{1}}(p,0) + (1-r)P_{A}^{E_{3}}(p,0) \\ \{q=0\} & \text{if } rP_{A}^{E_{1}}(p,1) + (1-r)P_{A}^{E_{3}}(p,1) \\ < rP_{A}^{E_{1}}(p,0) + (1-r)P_{A}^{E_{3}}(p,0) \end{cases}$$

$$B_{B}(q,r) = \begin{cases} \{p = 1\} & \text{if } rP_{B}^{E_{1}}(1,q) + (1-r)P_{B}^{E_{3}}(1,q) \\ > rP_{B}^{E_{1}}(0,q) + (1-r)P_{B}^{E_{3}}(0,q) \end{cases}$$

$$= \begin{cases} \{p : 0 \le p \le 1\} & \text{if } rP_{B}^{E_{1}}(1,q) + (1-r)P_{B}^{E_{3}}(1,q) \\ = rP_{B}^{E_{1}}(0,q) + (1-r)P_{B}^{E_{3}}(0,q) \end{cases}$$

$$= rP_{B}^{E_{1}}(0,q) + (1-r)P_{B}^{E_{3}}(0,q)$$

$$< rP_{B}^{E_{1}}(0,q) + (1-r)P_{B}^{E_{3}}(0,q)$$

$$B_{E}(p,q) = \begin{cases} \{r=1\} & \text{if } P_{E}^{E_{1}}(p,q) > P_{E}^{E_{3}}(p,q) \\ \{r:0 \leq r \leq 1\} & \text{if } P_{E}^{E_{1}}(p,q) = P_{E}^{E_{3}}(p,q) \\ \{r=0\} & \text{if } P_{E}^{E_{1}}(p,q) < P_{E}^{E_{3}}(p,q) \end{cases}$$

and

$$B_{A}(p,r) = \begin{cases} \{q=1\} & \text{if } rP_{A}^{E_{2}}(p,1) + (1-r)P_{A}^{E_{3}}(p,1) \\ > rP_{A}^{E_{2}}(p,0) + (1-r)P_{A}^{E_{3}}(p,0) \\ \{q:0 \leq q \leq 1\} & \text{if } rP_{A}^{E_{2}}(p,1) + (1-r)P_{A}^{E_{3}}(p,1) \\ = rP_{A}^{E_{2}}(p,0) + (1-r)P_{A}^{E_{3}}(p,0) \\ \{q=0\} & \text{if } rP_{A}^{E_{2}}(p,1) + (1-r)P_{A}^{E_{3}}(p,1) \\ < rP_{A}^{E_{2}}(p,0) + (1-r)P_{A}^{E_{3}}(p,0) \end{cases}$$

$$B_{B}(q,r) = \begin{cases} \{p=1\} & \text{if } rP_{B}^{E_{2}}(1,q) + (1-r)P_{B}^{E_{3}}(1,q) \\ > rP_{B}^{E_{2}}(0,q) + (1-r)P_{B}^{E_{3}}(0,q) \end{cases} . \tag{5.68}$$

$$\begin{cases} \{p:0 \leq p \leq 1\} & \text{if } rP_{B}^{E_{2}}(1,q) + (1-r)P_{B}^{E_{3}}(1,q) \\ = rP_{B}^{E_{2}}(0,q) + (1-r)P_{B}^{E_{3}}(0,q) \end{cases}$$

$$\{p=0\} & \text{if } rP_{B}^{E_{2}}(1,q) + (1-r)P_{B}^{E_{3}}(1,q) \\ < rP_{B}^{E_{2}}(0,q) + (1-r)P_{B}^{E_{3}}(0,q) \end{cases}$$

$$B_{E}(p,q) = \begin{cases} \{r=1\} & \text{if } P_{E}^{E_{2}}(p,q) > P_{E}^{E_{3}}(p,q) \\ \{r:0 \le r \le 1\} & \text{if } P_{E}^{E_{2}}(p,q) = P_{E}^{E_{3}}(p,q) \\ \{r=0\} & \text{if } P_{E}^{E_{2}}(p,q) < P_{E}^{E_{3}}(p,q) \end{cases}$$

Within the framework of a quantum game, Figure 5.2 illustrates the best response functions corresponding to various game scenarios. These functions characterize the optimal strategic choices for each player, contingent on the strategies adopted by the other participants. The "mixed-strategy Nash equilibrium" is identified at the intersection points of these best response functions, signifying that each player's strategy is optimal given the strategies of the others. Notably, multiple intersection points may arise, each corresponding to distinct game scenarios. These intersections denote the Nash equilibrium states for the players within the specified game scenarios. Subfigures (a), (b), (c), and (d) of Figure 5.2 explicitly highlight the Nash equilibrium points for the E_1 - E_2 , E_1 - E_3 , E_2 - E_3 , and E_1 - E_4 game scenarios, respectively. Each subfigure comprises three distinct curves, each representing the best response function of an

individual player within the mixed quantum strategy framework. These curves delineate the optimal strategies (by considering the best response) of each player in reaction to the strategic choices of their counterparts. The intersections of these curves indicate the most stable strategic configurations within each game scenario. From these intersection points, the most stable probability distributions in the mixed quantum strategy game can be inferred, ensuring optimality for all participating players.

A comprehensive summary of the data, including each player's payoffs, is presented in Table 5.2. This summary evaluates the mixed-strategy Nash equilibrium points across different game scenarios and examines the secure QBER bound. Referring to Equation (5.2), it becomes apparent that the payoff functions for the three entities are influenced by the variables p and q, which dictate Eve's attack strategies E_1 , E_2 (or E_3 , E_4). Additionally, the game can be categorized as a normal-form (strategic-form) game, as players lack prior knowledge of their opponents' choices at the moment of decision-making. Under this framework, all participants independently determine their strategies: Bob opts for the Z basis with probability p, Eve selects an attack strategy with probability r, and Alice, when operating in message mode, encodes bit 0 with probability q. Both Alice and Bob share identical payoff functions as defined in Equation (5.2). In the E_1 - E_2 scenario, the expected payoffs for Alice/Bob and Eve are represented as $rP_{A/B}^{E_1}(p,q) + (1-r)P_{A/B}^{E_2}(p,q)$ and $rP_E^{E_1}(p,q) + (1-r)P_E^{E_2}(p,q)$, respectively. A comparative analysis of the payoff differences between Eve and Alice (refer to Table 5.2) enables the identification of Nash equilibrium points where either Eve or Alice/Bob derive the greatest advantage. Specifically, in the E_1 - E_2 game scenario, Eve attains the highest individual benefit at the equilibrium point (0.45, 0.195, 0.005), whereas Alice/Bob gains the most at (0.72, 0.208, 0.225). Similarly, in the E_1 - E_3 scenario, the equilibrium points maximizing individual benefits for Eve and Alice/Bob are (0.41, 0.39, 0.412) and (0.84, 0.047, 0.525), respectively. In the E_2 - E_3 case, Eve benefits the most at (0.385, 0.215, 0.262), while Alice/Bob attain the highest payoff at (0.80, 0.115, 0.885). Ultimately, no Nash equilibrium point in these game scenarios achieves Pareto optimality, indicating that there is no scenario where all players simultaneously receive the highest possible payoffs.

We compute the QBER for all Nash equilibrium points across various game scenarios. Notably, the expected QBER for the E_i - E_j game scenario is given by $\varepsilon_{E_i-E_2} = r \operatorname{QBER}_{E_i} + (1-r) \operatorname{QBER}_{E_j}$, where r represents the probability of Eve opting for the E_i attack. In any specific game scenario, Eve's optimal strategy is dictated either by the maximum payoff disparity—measuring the dif-

ference between Eve's and Alice's payoffs—or by the minimum QBER. Our primary goal is to establish the QBER threshold. Therefore, we determine the minimum QBER values across all game scenarios presented in Table 5.2, which correspond to Nash equilibrium points where Eve is best positioned to remain undetected. The minimum QBER values at these equilibrium points are 0.610303 is for E_1 - E_2 , 0.152451 is for E_1 - E_3 , and 0.143882 is for E_2 - E_3 game scenario. A lower minimum QBER¹ (in message mode) signifies that Eve is employing a more effective attack strategy in the given scenario while maintaining the same or minimal detection probability P_d in control mode. These reduced QBER values serve as indicators of more advanced quantum attack strategies by Eve within the game-theoretic framework. Through an evaluation of the QBER threshold values, we infer that E_3 constitutes the most formidable quantum attack, followed by E_2 and then E_1 . This suggests that as Eve deploys increasingly potent attacks, she secures higher payoffs, thereby posing a greater risk to Alice and Bob. To counteract this threat within the DL04 protocol game scenario, we establish a lower minimum QBER threshold corresponding to Eve's most aggressive attack. This threshold is derived by analyzing all Nash equilibrium points encompassing the specified attacks.

As previously stated, a player with constrained access to quantum resources effectively behaves as a classical participant. In our evaluation, the E_4 attack is categorized as a classical strategy executed by Eve, indicating that she functions as a classical eavesdropper when implementing the E_4 attack. Additionally, we compare this classical E_4 attack to the simplest quantum-based attack, E_1 . Moreover, we examine the E_4 attack, also known as the IR attack, in relation to the E_1 attack within the framework of an E_1 - E_4 game scenario. Within this strategic model, the minimum QBER is determined to be 0.323478, which is lower than the minimum QBER observed in the E_1 - E_2 game scenario. Despite this, the E_4 attack is considered weaker than E_4 due to its higher detection probability (P_d), recorded at 37.5%, compared to 18.75% for E_1 in control mode.

To establish the secure upper bound of QBER, represented as ε , across all attack scenarios within the game framework, we focus on the game scenario involving the most powerful attacks, namely the E_2 - E_3 game. In this scenario, the upper bound of QBER is determined to be ε = 0.143882, as this corresponds to the lowest QBER value associated with the scenario where the strongest attack, E_3 , is active. The lower bound of QBER is 0, as an isolated E_3 attack would not

¹Since a lower QBER value maximally benefits Eve, establishing this bound ensures the highest level of security for a quantum protocol.

introduce detectable errors in message mode (refer to Section 5.3.3). Furthermore, the bounds for Eve's detection probability (P_d) in control mode are established between 0.1875 and 0.375. Consequently, it can be concluded that the DL04 protocol maintains ε -security under the set of individual and collective IR attacks, specifically E_1 , E_2 , E_3 and E_4 .

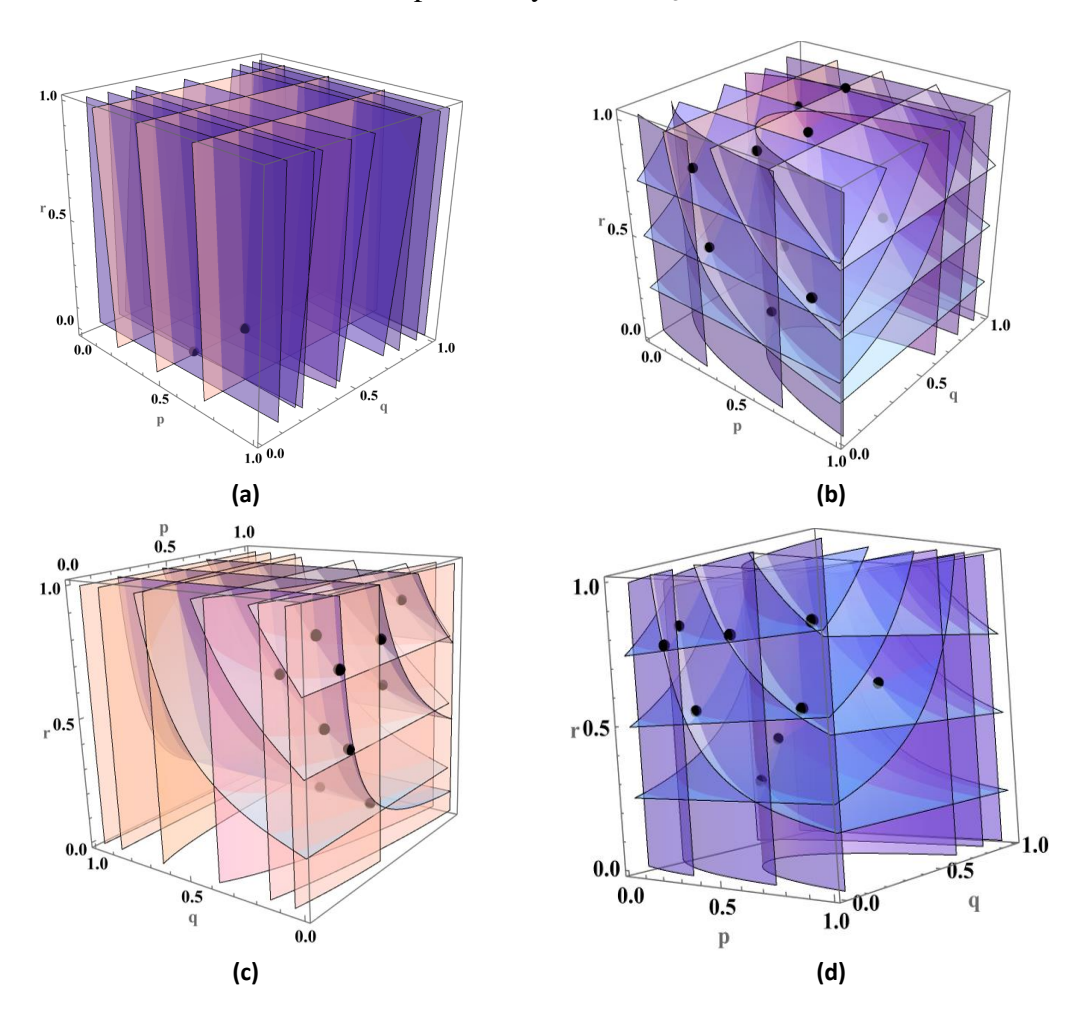


Figure 5.2: The figure illustrates the Nash equilibrium points where the optimal response functions of the three participants intersect in our mixed-strategy game framework. The response functions are represented as follows: the low-density layer for Alice, the medium-density layer for Bob, and the high-density layer for Eve. The subfigures depict different game scenarios: (a) E_1 - E_2 , (b) E_1 - E_3 , (c) E_2 - E_3 , and (d) E_1 - E_4 .

5.5 DISCUSSION

This chapter introduces a novel security framework for quantum communication protocols, specifically addressing collective attacks and IR attacks through Nash equilibrium. This approach provides an alternative perspective, framing security as a game-theoretic bound against collective attacks using Nash equilibrium principles. The Nash equilibrium points represent stable configurations that yield rational probability distributions for decision-making within a

mixed-strategy quantum game. These probabilities define an equilibrium state for all involved entities, facilitating the assessment of cryptographic parameters such as the QBER threshold. In practical implementations, where participants make decisions independently, achieving such equilibrium is improbable, potentially resulting in a more unstable system. Consequently, identifying the lowest QBER value within the stable game configuration establishes a secure boundary for practical quantum protocol deployment. Our analysis demonstrates that the security level (ε -secure) of any quantum communication protocol is contingent on the attack strategies employed by the eavesdropper, Eve. A smaller ε value signifies a stronger attack strategy by Eve. Moreover, findings suggest that a quantum-capable Eve possesses significantly greater adversarial power compared to a classical Eve¹. In our model, we assume Eve has access to unlimited quantum resources, allowing us to disregard the last three terms in Eve's payoff equation, as presented in Equation (5.1). To streamline our evaluation, we also assume uniform contributions from all payoff components for each party, assigning them equal weight $(\frac{1}{4})$. The analysis is structured into four distinct game scenarios, for which Nash equilibrium points are determined individually. We then identify the minimum QBER value corresponding to each scenario, which serves as the secure QBER bound for that specific case. Ultimately, the overall threshold QBER (ε) is established by identifying the lowest QBER within the game scenario that corresponds to the most adversarial attack. Furthermore, our study reveals that the DL04 protocol exhibits vulnerability to Pavičić attack in message mode, as the QBER in this case is zero. However, security is maintained through the control mode, which is collaboratively executed by both legitimate parties. Thus, while this attack poses a security risk in message mode, it is effectively mitigated by the control mode mechanism.

Quantum communication protocols are designed for various objectives, often balancing security against efficiency. To address these trade-offs, our analysis can be extended by introducing distinct weighting factors ω_i , ω_j , $\omega_k \neq 0$, ensuring $\omega_m \neq \omega_n$ for $m \neq n$. These weights correspond to specific payoffs, with their sum normalized to 1, thereby maintaining normalized player weight assignments. Given ω_i , ω_j , $\omega_k \neq 0$, Equation (5.1) results in $n_1 = 1$, $n_2 = 1$, $n_3 = 1$ for E_1 , $n_1 = 2$, $n_2 = 5$, $n_3 = 0$ for E_3 , $n_1 = 4$, $n_2 = 2$, $n_3 = 1$ for E_2 , and $n_1 = 2$, $n_2 = n_3 = 0$ for E_4 attack strategies. Notably, the computational cost of multi-qubit gates escalates with an increase in the number of qubits involved. Furthermore, our framework can be extended to

¹Additionally, it is crucial to ensure that Eve's choice of unitary operations and execution of measurement procedures remain synchronized within the quantum framework.

encapsulate a comprehensive game-theoretic scenario where all attack strategies coexist rather than treating them as separate cases. Under this paradigm, eavesdroppers may employ different attack strategies with varying probabilities, enabling the determination of "Pareto-optimal Nash equilibrium" under specific conditions. Consequently, the formulation of the QBER bound (ε) inherently depends on these generalized parameters.

Our methodology for determining a secure QBER threshold is applied within the DL04 protocol. This adaptable approach is compatible with both current and forthcoming quantum communication protocols, facilitating the derivation of diverse information-theoretic bounds. This flexibility accommodates multiple strategic implementations by participants, ensuring alignment with the intended applications of quantum protocols. Future research will integrate additional game-theoretic aspects tailored to different quantum communication scenarios, considering various quantum mechanical properties. This collaborative effort aims to refine the analysis of quantum information bounds for more comprehensive insights.

Table 5.2: The table presents Nash equilibrium points for different strategic interactions and provides qualitative payoff assessments for all involved entities.

	Nash equilibrium	Alice's/Bob's	Eve's	Payoff	$\varepsilon_{E_1-E_2}$
E_1 - E_2 game scenario	point (p,q,r)	payoff	payoff	difference	-1 -2
	(0.72, 0.208, 0.225)	0.055457	0.194543	0.13908	0.692404
	(0.45, 0.195, 0.005)	0.0446318	0.205368	0.16073	0.610303
	,				
E ₁ -E ₃ game scenario	Nash equilibrium	Alice's/Bob's	Eve's	Payoff	$\mathcal{E}_{E_1-E_3}$
	point (p,q,r)	payoff	payoff	difference	
	(0.22, 0.716, 0.88)	-0.110497	0.360497	0.47099	0.152451
	(0.442, 0.75, 0.999)	-0.0862188	0.336219	0.42243	0.18007
	(0.41, 0.39, 0.412)	-0.157149	0.407149	0.56429	0.177181
	(0.76, 0.577, 0.585)	-0.136264	0.386264	0.52252	0.21776
	(0.56, 0.14, 0.292)	-0.0796824	0.329682	0.40936	0.195874
	(0.325, 0.064, 0.532)	-0.0134987	0.263499	0.27699	0.329893
	(0.84, 0.047, 0.525)	0.0324084	0.217592	0.18518	0.460299
	(0.485, 0.465, 0.915)	-0.090828	0.340828	0.43165	0.363472
	(0.235, 0.096, 0.83)	-0.013356	0.263356	0.27671	0.463323
	(0.47, 0.195, 0.93)	-0.0182231	0.268223	0.28644	0.550258
E ₂ -E ₃ game scenario	Nash equilibrium	Alice's/Bob's	Eve's	Payoff	$\mathcal{E}_{E_2-E_3}$
	point (p,q,r)	payoff	payoff	difference	
	(0.385, 0.215, 0.262)	-0.111965	0.361965	0.47393	0.151087
	(0.47, 0.055, 0.205)	-0.0276507	0.277651	0.3053	0.143882
	(0.25, 0.096, 0.54)	-0.0216673	0.271667	0.29633	0.31482
	(0.24, 0.268, 0.71)	-0.0436386	0.293639	0.33727	0.35838
	(0.70, 0.138, 0.58)	-0.00442078	0.254421	0.25884	0.430969
	(0.284, 0.02, 0.472)	0.0188573	0.231143	0.21228	0.298653
	(0.235, 0.02, 0.758)	0.0320242	0.217976	0.18595	0.461603
	(0.222, 0.10, 0.865)	0.015688	0.234312	0.21862	0.492488
	(0.54, 0.048, 0.795)	0.0558727	0.194127	0.13825	0.587155
	(0.80, 0.115, 0.885)	0.0722149	0.177785	0.10557	0.709991
E ₁ -E ₄ game scenario	Nash equilibrium	Alice's/Bob's	Eve's	Payoff	$\varepsilon_{E_1-E_4}$
	point (p,q,r)	payoff	payoff	difference	
	(0.23, 0.095, 0.825)	-0.00433851	0.254339	0.25867	0.502924
	(0.245, 0.008, 0.76)	0.0492999	0.2007	0.1514	0.529315
	(0.572, 0.02, 0.765)	0.0750153	0.174985	0.0999	0.648014
	(0.928, 0.032, 0.774)	0.0997124	0.150288	0.0505	0.77876
	(0.324, 0.065, 0.535)	0.0114311	0.238569	0.22713	0.447399
	(0.85, 0.045, 0.522)	0.0603314	0.189669	0.12933	0.580622
	(0.405, 0.387, 0.415)	-0.124349	0.374349	0.49869	0.324962
	(0.54, 0.15, 0.295)	-0.0471361	0.297136	0.34427	0.369328
	(0.75, 0.57, 0.582)	-0.114078	0.364078	0.47815	0.323478

CHAPTER 6

CONCLUSION AND SCOPE OF FUTURE WORKS

The field of secure quantum communication is advancing rapidly. This thesis investigates various aspects of secure quantum communication by introducing novel protocols, extending existing frameworks, and improving the efficiency of specific quantum communication processes. The security of communication fundamentally relies on the security of the cryptographic key used. Quantum technologies enable key distribution with unconditional security by leveraging quantum resources. However, the initialization of a QKD protocol necessitates the authentication of the communicating parties. In many implementations, classical authentication methods are employed, which, due to their classical nature, lack unconditional security. This vulnerability allows an adversary (Eve) to impersonate a legitimate party, creating a significant security loophole in otherwise quantum-secure communication protocols.

To address this challenge, we analyze existing QIA schemes and propose new QIA protocols to enhance security. These protocols utilize various quantum resources, making them feasible for implementation with current technology. Once legitimate user identities are authenticated, protocols such as QKD can be executed to distribute symmetric cryptographic keys. Our analysis of prior QKD schemes reveals that information exchange typically involves a combination of quantum and classical components (e.g., BB84 and B92 protocols) or multiple quantum components (e.g., Goldenberg-Vaidman protocol). This partitioning of information fundamentally contributes to security and necessitates the exchange of both classical and quantum information for complete protocol implementation. We hypothesize that increasing the proportion of quantum information exchange while reducing reliance on classical communication may enhance both efficiency and security bounds. To evaluate this hypothesis, we propose new QKD protocols and analyze their security under various attack scenarios, determining their tolerable security thresholds. Additionally, we examine potential biases introduced by one party in the distributed symmetric key within QKD schemes. Extending QKD to multiparty settings also

presents significant challenges. To address this, we propose a novel QKA protocol that operates without the need for quantum memory, improving feasibility and scalability. Furthermore, we conceptualize quantum communication protocols as strategic games, where legitimate parties seek to secure information from Eve while increasing her probability of detection, whereas Eve aims to maximize her information gain while minimizing her detectability. Applying gametheoretic principles, we develop a method to determine the tolerable QBER based on Nash equilibrium. This approach, termed "gaming the quantum," provides a novel framework for analyzing quantum protocols. The remainder of this chapter presents a concise summary of the key findings of this thesis and outlines potential directions for future research.

6.1 SUMMARY OF THE THESIS

In this section, we provide a concise summary of the chapters in this thesis and discuss the key findings of our research. Initially, we outline the major results, followed by a chapter-wise discussion of the findings presented throughout the thesis.

- 1. The QIA schemes can be classified based on the quantum resources employed and the specific communication or computation tasks they address. These tasks can be adapted to develop QIA protocols utilizing various quantum resources. In the context of quantum communication, authentication can be incorporated into the initial phase of the primary protocol through a pre-shared authentication key. This thesis explicitly demonstrates how QSDC schemes can be utilized to design novel QIA protocols. Furthermore, we establish that existing schemes for other quantum communication and computation tasks can be systematically transformed into QIA schemes.
- 2. The proposed QIA protocols utilize single-qubit states, making them feasible for implementation with current technology. Additionally, decoy states are employed to verify the security of the quantum channel. The positioning and polarization of these decoy particles depend on the pre-shared authentication key. These assumptions contribute to the security of the proposed protocols, which are analyzed in Chapter 2.
- 3. Another set of controlled QIA protocols is designed using Bell states, permutation operations, and single-qubit state preparation by a third party acting as the controller. These schemes require a quantum register for implementation, with the controller being an un-

- trusted quantum third party. The security of these protocols is analyzed against specific attack scenarios.
- 4. Once authentication is completed, the legitimate parties aim to generate a symmetric key. To explore the benefits of increasing the quantum component and reducing classical elements in QKD protocols, we propose two new schemes incorporating classical reconciliation with BB84 and SARG04 protocols. These schemes offer improved efficiency and critical distance against PNS attack. This approach emphasizes using a higher quantum component and fewer classical elements to develop more secure quantum protocols, enhancing security against attacks performed by an eavesdropper (Eve) after classical reconciliation.
- 5. In QKD schemes, there is a possibility of one party biasing the final key, which should ideally remain symmetric. To address this issue while introducing additional security features, we propose a QKA scheme. Without requiring quantum memory or involving a trusted third party, we introduce a novel QIA scheme.
- 6. The quantum advantage is utilized to analyze the security of the QKA scheme. In our analysis, we observe that an adversary executes a collective attack using her ancilla states and unitary operations. When the information gained by Eve reaches its maximum (0.5 bits), the probability of detecting Eve's presence becomes 1. This result demonstrates that quantum technology inherently detects Eve's presence whenever she obtains useful information from the quantum channel. The trace left by Eve helps legitimate parties decide whether to continue or abort the protocol. The security analysis highlights how the fundamental properties of quantum particles enable the detection of Eve when she acquires useful information.
- 7. This QKA scheme is secure against the collective attack considered in our analysis. Additionally, we establish a specific secure error bound against this attack. However, if a different set of collective attacks is considered, this bound will change accordingly.
- 8. In this thesis, we propose a novel method to establish a secure bound for any quantum protocol. To develop this approach, we model the legitimate parties and the adversary as players in a strategic game. They formulate strategies and engage in a mixed-strategy game without direct communication (a non-cooperative game). Using Nash equilibrium

and best response functions, we demonstrate how game theory can be applied to determine a secure bound for information-theoretic parameters such as the QBER.

Thus, this thesis discusses the significance of QIA in securing quantum communication. We comprehensively review various QIA protocols proposed in previous research, analyzing their advantages and limitations. Additionally, we explore how different quantum communication schemes can be adapted into QIA protocols and propose new schemes utilizing single and entangled quantum sources. After performing an identity test for legitimate parties, they proceed with a quantum communication protocol. We propose novel QKD and QKA schemes, highlighting the benefits of incorporating additional quantum resources for QKD. In the proposed QKA scheme, we introduce an untrusted third party and implement the protocol without requiring quantum memory. Furthermore, our thesis introduces a new method that integrates game theory into quantum communication, referred to as "gaming the quantum", to establish a secure QBER for quantum protocols. The following section presents a summary of the chapters in this thesis.

Chapter 1: This chapter has examined existing protocols for QIA to explore their inherent symmetry. The analysis has demonstrated the presence of symmetry among various protocols, enabling their classification and facilitating the identification of straightforward strategies for adapting existing protocols to new QIA schemes applicable to different quantum computation and communication tasks. To substantiate this approach, two novel QIA protocols are introduced and shown to be secure against a range of potential attacks. Notably, many of the protocols discussed, including several existing ones, are not currently feasible for implementation due to technological limitations. For instance, certain protocols require a user to retain a photon until the travel photon(s) return(s), such as in the ping-pong QIA scheme described in [41] or the authentication protocols outlined in [45, 38, 40, 70, 39, 85, 43, 110]. Implementing such QIA protocols necessitates quantum memory, which remains unavailable with current technology. Additionally, most entangled-state-based QSDC protocols for QIA, as well as entangledstate-based quantum private comparison schemes and QIA protocols involving a trusted third-party (Trent) who retains a photon, encounter the same technological constraint. At present, QIA protocols that do not necessitate quantum memory should be prioritized. Notably, the protocols introduced here operate without quantum memory, making them feasible with existing technology. Although numerous approaches have been proposed for developing quantum memory, which may prove beneficial in the future, direct teleportation-based QIA schemes (such as those discussed in [70, 85]) are unlikely to have widespread applications, even in the long run. This limitation arises because teleportation is only viable for secure quantum communication under ideal, noise-free quantum channels. Moreover, any protocol reliant on shared entanglement (e.g., those outlined in [63, 64, 40, 45, 38, 70]) may require entanglement purification or concentration due to decoherence-induced degradation of shared entanglement. This, in turn, would necessitate additional and potentially insecure interactions between Alice and Bob. Despite these technical constraints, research in QIA continues to expand rapidly, driven by the fact that the purported unconditional security of quantum cryptographic schemes fundamentally depends on the security of the identity authentication mechanisms employed.

This chapter would be incomplete without acknowledging the numerous post-quantum authentication schemes proposed in recent years [296, 297]. These schemes have not been examined here, as they are fundamentally classical and only conditionally secure. A key assumption underlying these approaches is that quantum computers will be incapable of efficiently solving problems beyond the bounded-error quantum polynomial time (BQP) complexity class. However, no formal proof supports this claim, making it equivalent to assuming that if no efficient algorithm exists for a given computational problem today, none will be developed in the future. The primary content of this chapter is published on Ref. [165].

Chapter 2: In Chapter 6, we analyzed existing QIA protocols to identify their inherent symmetries, enabling their classification and adaptation for various quantum computing and communication applications, leading to novel QIA schemes. To validate this approach, four new QIA protocols were introduced and shown to be secure against specific attacks. However, many existing and proposed protocols remain impractical due to current technological limitations. For example, some require users to store photons until travel photons return, as seen in ping-pong-based QIA schemes [41] and other authentication methods [45, 38, 40, 70, 39, 85, 43, 110], which depend on quantum memory—currently unfeasible commercially. Similar challenges affect entangled-state-based QSDC protocols, quantum private comparison schemes, and third-party-assisted authentication protocols.

Prioritizing QIA protocols that do not require quantum memory is preferable, as they are compatible with current technology. The protocols proposed in this work fall into this category. While quantum memory-dependent schemes may become viable in the future, teleportation-based QIA approaches [70, 85] are unlikely to see widespread adoption due to their reliance on noise-free quantum channels. Additionally, protocols leveraging shared entanglement [63, 64, 40, 45, 38, 70] may require purification or concentration to mitigate decoherence, potentially introducing insecure interactions between Alice and Bob. Despite these limitations, QIA research is progressing rapidly, driven by the critical role of identity authentication in ensuring the purported unconditional security of quantum cryptographic protocols.

This chapter, alongside references [166, 234], explores the potential for developing diverse QIA schemes. A thorough investigation could help identify the most practical QIA approach using existing technology. The proposed entangled-state-based QIA protocol leverages Bell states, allowing Alice to securely transmit information to Bob with authorization from controller Charlie, without pre-shared keys. While it relies solely on Bell states, its implementation requires quantum memory, which is not yet commercially available—a common challenge across QIA, QSDC, DSQC, and quantum dialogue protocols. However, ongoing research and recent proposals [295] suggest imminent advancements. Until then, a delay mechanism can serve as an interim solution. Additionally, two other proposed protocols use single-photon sources as qubits, making them feasible with current technology for bi-directional identity authentication. The works presented in this chapter are published in Refs. [165, 166, 234].

Chapter 3: In this chapter, we have proposed a new protocol for QKD and a variant of it. The protocols consume more quantum resources compared to SARG04 or similar protocols but transmit less classical information over the public channel, thereby reducing the probability of some side channel attacks. Additionally, we conduct a rigorous security analysis of the proposed protocols and calculate the tolerable error limit for the upper and lower bounds of the secret key rate under a set of collective attacks. It is shown that by applying a certain type of classical pre-processing, the tolerable error limit can be increased. The same is illustrated through the graphs. Before concluding, we may emphasize some important observations of our analysis. In the seminal paper [299], the authors computed

density operators of Eve's final state in the six-state QKD protocol. Interestingly, for our protocols, we obtained the same expressions for the density operators describing Eve's final system, despite the fact that in our Protocol 2 (1), neither Alice nor Bob (Alice never) discloses the results of the measurements performed by them (her) in cases where they (she) used different bases for preparation and measurement. The reason for obtaining the same density operators for Eve's system is that the terms that appear in the density matrix in cases of basis mismatch happen, cancel each other. Additionally, we establish that for the proposed protocols, the tolerable error limit of QBER $\mathcal{E} \leq 0.124$ for the lower bound of the key rate and $\mathcal{E} \geq 0.114$ for the upper bound of the key rate if classical preprocessing is used. In our case, the tolerable error limits are expected to decrease in the absence of classical pre-processing. In the practical implementation of cryptography, various types of errors may occur during the transmission of qubits. Considering QBER > 0, Eve can attempt an attack using partial cloning machines [302, 303, 304]. Acin et al., have shown that legitimate users of SARG04 can tolerate errors up to 15% when Eve uses a best-known partial cloning machine. They also found that this tolerable error limit is higher than that for the BB84 protocol. In our case, for QBER > 0, the tolerable error limit is also computed to be 15%, which is better than the BB84 protocol and its variants. We have also performed a security-efficiency trade-off analysis for the proposed schemes and compared their efficiency with the SARG04 protocol, as detailed in Chapter 3. The result in this chapter is presented in [162].

Chapter 4: In certain cases, key agreement between two parties may require an untrusted third party. The quantum counterpart of such scenarios necessitates a QKA protocol with a semi-trusted third-party controller. Our proposed protocol is designed to meet this requirement, leveraging quantum particle behavior for practical implementation, as detailed in Chapter 4. Security proofs addressing attack scenarios are provided. For CQKA implementation, a Bell state—generated by an untrusted third party, Charlie—is distributed to Alice and Bob. Upon receiving their respective qubits, they execute the CNOT operation per protocol. If an eavesdropper (Eve) attempts an intercept-and-resend attack, she can only infer the initial Bell state, as entanglement is lost after Alice and Bob's operations. Additionally, Charlie publicly discloses the Bell state information k_C at the protocol's conclusion, preventing Eve from gaining any advantage. We also examine the case where

Eve attempts to impersonate the third party, known as an "impersonated fraudulent attack". Our proposed protocol is proven resilient against this attack, with analytical proof validating its security. Additionally, a critical evaluation of the collective attack confirms its robustness under broader attack scenarios. We show that Eve's probability of successfully extracting the final two-bit key becomes negligibly small (approaching zero) when n = 6. Our security analysis extends by modeling Eve's ancillary state as a complex variable, where each ancilla system is represented in a complete orthogonal basis within the Hilbert space $\mathcal{H}^{\mathcal{E}}$ [315]. Using this framework, we estimate the tolerable error bound and determine the acceptable QBER as a function of α . We further evaluate our scheme under varying noisy channel conditions, analyzing fidelity variations concerning the channel parameter. Results indicate that fidelity remains largely stable, even at higher noise levels. We also compare our protocol's strengths and limitations with other recent protocols in this category. Findings reveal that our scheme is not only more practical with current technology but also more efficient than many existing approaches. Notably, it introduces a novel and beneficial feature involving third-party participation. The work is published in Ref. [233].

Chapter 5: The relationship between game theory and quantum mechanics has been previously explored, revealing two primary approaches that illustrate their connection. The first approach involves using quantum resources to play a conventional game, which could also be played without any quantum resources; however, incorporating quantum elements offers certain advantages. The second approach applies game theory concepts to describe a quantum mechanical scenario. For clarity, we refer to the first approach as "quantized game" and the second as "gaming the quantum". A quantized game is defined as a unitary function that maps the Cartesian product of quantum superpositions of players' pure strategies to the entire Hilbert space of the game. This approach preserves the characteristics of the original classical game under certain conditions. In contrast, "gaming the quantum" involves applying game theory principles to quantum mechanical problems to derive solutions based on game-theoretic analysis. In Chapter 5, we utilize the gaming the quantum approach by applying non-cooperative game theory to a quantum communication protocol, demonstrating how Nash equilibrium can be employed as an effective solution concept.

The Nash equilibrium framework is utilized to determine a robust, game-theoretic security bound on the QBER for the DL04 protocol, a recently implemented scheme for quantum secure direct communication. The analysis in Chapter 5 considers the sender, receiver, and eavesdropper (Eve) as quantum players, capable of executing quantum operations. Notably, Eve is assumed to possess the ability to perform various quantum attacks, such as Wójcik's original attack, its symmetrized variant, and Pavičić's attack, as well as a classical intercept-and-resend strategy. A game-theoretic evaluation of the DL04 protocol's security under these conditions is conducted by examining multiple game scenarios. The findings indicate the absence of a Pareto optimal Nash equilibrium in these cases. Therefore, mixed strategy Nash equilibrium points are identified and employed to derive upper and lower bounds for QBER. Additionally, the analysis highlights the susceptibility of the DL04 protocol to Pavičić's attack in the message transmission mode. It is also observed that the quantum attacks by Eve are more effective than the classical attacks, as they result in lower QBER values and a decreased probability of detecting Eve's intrusion. The results reported in this chapter are published in Ref. [259].

6.2 LIMITATIONS AND FUTURE SCOPE

The limitations of any research work serve as a motivation for future advancements toward more feasible and effective results. In this study, we identified the inherent symmetry in previously proposed QIA schemes and introduced new QIA protocols utilizing QSDC/DSQC. Furthermore, we have demonstrated that various communication and computational tasks can be utilized to design novel QIA schemes. While we have not explicitly outlined all possible protocols, future research could focus on systematically constructing and analyzing these protocols in terms of security and feasibility. A comparative study may be conducted to identify the most optimal QIA scheme for specific secure quantum communication tasks. Moreover, integrating blind quantum computation (BQC) presents a promising avenue for advancing QIA protocols. Additionally, the incorporation of QIA schemes into fundamental quantum protocols may enhance resource efficiency and overall performance. In this thesis, we propose a new QKD scheme that increases quantum resource usage while reducing classical information exchange. Our protocol can be further refined, maintaining its core motivation, to enhance efficiency and extend tolerable communication distances. A similar approach can be applied to QKA proto-

cols. Furthermore, while our proposed schemes are based on DV protocols, they can be adapted into CV frameworks, with future work focusing on performance analysis. Noise analysis is only briefly addressed in this work, with a focus on specific regimes. A more comprehensive analysis across diverse environmental conditions would provide deeper insights into the performance of these schemes. As our proposed schemes align with current technological capabilities, they can be experimentally implemented in the near future. Finally, we explore the concept of "gaming the quantum", which provides a means to determine the QBER bound of a quantum protocol. This approach can be further generalized to derive other information-theoretic parameters in future research. In conclusion, it is important to acknowledge that the work presented in this thesis is primarily constrained by its entirely theoretical nature. However, we anticipate that some of the proposed schemes, either in their original form or with suitable modifications, will be experimentally realized in the near future. Additionally, during the course of this study, we have observed that certain QKD protocols are frequently implemented due to their practical feasibility, despite the lack of rigorous security proofs against coherent and collective attacks. In the future, the security analysis framework developed in this work, including the gametheoretic approach, may be utilized to assess the security of such protocols. Furthermore, all the schemes proposed and analyzed in this thesis fall within the domain of discrete-variable protocols. An interesting direction for future research would be to explore the feasibility of developing continuous-variable counterparts for these schemes.

REFERENCES

- [1] Liao S.-K., Cai W.-Q., Handsteiner J., Liu B., Yin J., Zhang L., Rauch D., Fink M., Ren J.-G., Liu W.-Y. *et al.*, "*Satellite-relayed intercontinental quantum network*," Physical Review Letters, vol. 120, no. 3, p. 030501, 2018.
- [2] Liu Y., Zhang W.-J., Jiang C., Chen J.-P., Zhang C., Pan W.-X., Ma D., Dong H., Xiong J.-M., Zhang C.-J. et al., "Experimental twin-field quantum key distribution over 1000 km fiber distance," Physical Review Letters, vol. 130, no. 21, p. 210801, 2023.
- [3] Zeydan E., Turk Y., Aksoy B., and Ozturk S. B., "Recent advances in post-quantum cryptography for networks: A survey," in 2022 Seventh International Conference On Mobile And Secure Services (MobiSecServ). IEEE, 2022, pp. 1–8.
- [4] Senapati B. and Rawal B. S., "Quantum communication with RLP quantum resistant cryptography in industrial manufacturing," Cyber Security and Applications, vol. 1, p. 100019, 2023.
- [5] Lee W.-K., Seo H., Hwang S. O., Achar R., Karmakar A., and Mera J. M. B., "DPCrypto: Acceleration of post-quantum cryptography using dot-product instructions on GPUs," IEEE Transactions on Circuits and Systems I: Regular Papers, vol. 69, no. 9, pp. 3591–3604, 2022.
- [6] Planck M., "On the law of distribution of energy in the normal spectrum," Annalen der Physik, vol. 4, no. 553, p. 1, 1901.
- [7] Einstein A., "Über einen die erzeugung und verwandlung des lichtes betreffenden heuristischen gesichtspunkt," Annalen der Physik, vol. 322, no. 6, pp. 132–148, 1905.
- [8] Pathak A. and Ghatak A., "Classical light vs. nonclassical light: characterizations and interesting applications," Journal of Electromagnetic Waves and Applications, vol. 32, no. 2, pp. 229–264, 2018.

- [9] Bohr N., "On the constitution of atoms and molecules," The London, Edinburgh, and Dublin Philosophical Magazine and Journal of Science, vol. 26, no. 151, pp. 1–25, 1913.
- [10] De Broglie L., "Recherches sur la théorie des quanta," Ph.D. dissertation, Migration-université en cours d'affectation, 1924.
- [11] Schrödinger E., "Quantisierung als eigenwertproblem," Annalen der physik, vol. 385, no. 13, pp. 437–490, 1926.
- [12] Heisenberg W., "Quantum-theoretical re-interpretation of kinematic and mechanical re-lations," Z. Phys, vol. 33, pp. 879–893, 1925.
- [13] Heisenberg W., "The physical content of quantum kinematics and mechanics," Quantum theory and measurement, pp. 62–84, 1927.
- [14] Einstein A., Podolsky B., and Rosen N., "Can quantum-mechanical description of physical reality be considered complete?" Physical Review, vol. 47, no. 10, p. 777, 1935.
- [15] Bennett C. H. and Brassard G., "Quantum cryptography: Public-key distribution and coin tossing, in Proc. IEEE Int. Conf. on Computers, Systems, and Signal Processing (Bangalore, India, 1984), pp. 175-179." 1984.
- [16] Bennett C. H., "Quantum cryptography using any two nonorthogonal states," Physical Review Letters, vol. 68, no. 21, p. 3121, 1992.
- [17] Bennett C. H., Brassard G., Crépeau C., Jozsa R., Peres A., and Wootters W. K., "*Tele-porting an unknown quantum state via dual classical and einstein-podolsky-rosen chan-nels*," Physical Review Letters, vol. 70, no. 13, p. 1895, 1993.
- [18] Bennett C. H. and Wiesner S. J., "Communication via one-and two-particle operators on Einstein-Podolsky-Rosen states," Physical Review Letters, vol. 69, no. 20, p. 2881, 1992.
- [19] Fan-Yuan G.-J., Lu F.-Y., Wang S., Yin Z.-Q., He D.-Y., Chen W., Zhou Z., Wang Z.-H., Teng J., Guo G.-C. et al., "Robust and adaptable quantum key distribution network without trusted nodes," Optica, vol. 9, no. 7, pp. 812–823, 2022.

- [20] Xie Y.-M., Lu Y.-S., Weng C.-X., Cao X.-Y., Jia Z.-Y., Bao Y., Wang Y., Fu Y., Yin H.-L., and Chen Z.-B., "Breaking the rate-loss bound of quantum key distribution with asynchronous two-photon interference," PRX Quantum, vol. 3, no. 2, p. 020315, 2022.
- [21] Rivest R. L., Shamir A., and Adleman L., "A method for obtaining digital signatures and public-key cryptosystems," Communications of the ACM, vol. 21, no. 2, pp. 120–126, 1978.
- [22] Diffie W. and Hellman M., "New directions in cryptography," IEEE Transactions on Information Theory, vol. 22, no. 6, pp. 644–654, 1976.
- [23] Pathak A., *Elements of quantum computation and quantum communication*. CRC Press Boca Raton, 2013.
- [24] Shor P. W., "Algorithms for quantum computation: discrete logarithms and factoring," in Proceedings 35th Annual Symposium on Foundations of Computer Science. IEEE, 1994, pp. 124–134.
- [25] Wootters W. K. and Zurek W. H., "A single quantum cannot be cloned," Nature, vol. 299, no. 5886, pp. 802–803, 1982.
- [26] Landauer R., "Irreversibility and heat generation in the computing process," IBM journal of research and development, vol. 5, no. 3, pp. 183–191, 1961.
- [27] Tsarev D., Osipov S., Lee R.-K., Kulik S., and Alodjants A., "Quantum sensor network metrology with bright solitons," Physical Review A, vol. 108, no. 6, p. 062612, 2023.
- [28] Kulik S. P., "*Quantum computing: Predictions and challenges*," Bulletin of the Lebedev Physics Institute, vol. 50, no. Suppl 12, pp. S1330–S1340, 2023.
- [29] DiVincenzo D. P. and Loss D., "Quantum computers and quantum coherence," Journal of Magnetism and Magnetic Materials, vol. 200, no. 1-3, pp. 202–218, 1999.
- [30] Wiesner S., "Conjugate coding," ACM Sigact News, vol. 15, no. 1, pp. 78–88, 1983.
- [31] Brassard G., "Brief history of quantum cryptography: A personal perspective," in IEEE Information Theory Workshop on Theory and Practice in Information-Theoretic Security, 2005. IEEE, 2005, pp. 19–23.

- [32] Ekert A. K., "Quantum cryptography based on Bell's theorem," Physical Review Letters, vol. 67, no. 6, p. 661, 1991.
- [33] Wegman M. N. and Carter J. L., "New hash functions and their use in authentication and set equality," Journal of Computer and System Sciences, vol. 22, no. 3, pp. 265–279, 1981.
- [34] Tretiakov V., Kravtsov K., Klimov A., and Kulik S., "A multi-mode free-space delay interferometer with no refractive compensation elements for phase-encoded QKD protocols," Laser Physics Letters, vol. 21, no. 6, p. 065206, 2024.
- [35] Crépeau C. and Salvail L., "Quantum oblivious mutual identification," in International Conference on the Theory and Applications of Cryptographic Techniques. Springer, 1995, pp. 133–146.
- [36] Zeng G. and Wang X., "Quantum key distribution with authentication," arXiv preprint quant-ph/9812022, 1998.
- [37] Dušek M., Haderka O., Hendrych M., and Myška R., "Quantum identification system," Physical Review A, vol. 60, no. 1, p. 149, 1999.
- [38] Li X. and Barnum H., "Quantum authentication using entangled states," International Journal of Foundations of Computer Science, vol. 15, no. 04, pp. 609–617, 2004.
- [39] WANG J., ZHANG Q., and TANG C.-J., "Multiparty simultaneous quantum identity authentication based on entanglement swapping," Chinese Physics Letters, vol. 23, no. 9, pp. 2360–2363, 2006.
- [40] Zhang Y.-S., Li C.-F., and Guo G.-C., "Quantum authentication using entangled state," arXiv preprint quant-ph/0008044, 2000.
- [41] Zhang Z., Zeng G., Zhou N., and Xiong J., "Quantum identity authentication based on ping-pong technique for photons," Physics Letters A, vol. 356, no. 3, pp. 199–205, 2006.
- [42] Zhang S., Chen Z.-K., Shi R.-H., and Liang F.-Y., "A novel quantum identity authentication based on Bell states," International Journal of Theoretical Physics, vol. 59, no. 1, pp. 236–249, 2020.

- [43] Kang M.-S., Heo J., Hong C.-H., Yang H.-J., Han S.-W., and Moon S., "Controlled mutual quantum entity authentication with an untrusted third party," Quantum Information Processing, vol. 17, no. 7, p. 159, 2018.
- [44] Chang Y., Xu C., Zhang S., and Yan L., "Controlled quantum secure direct communication and authentication protocol based on five-particle cluster state and quantum one-time pad," Chinese Science Bulletin, vol. 59, no. 21, pp. 2541–2546, 2014.
- [45] Mihara T., "Quantum identification schemes with entanglements," Physical Review A, vol. 65, no. 5, p. 052326, 2002.
- [46] Brassard G., "Quantum communication complexity," Foundations of Physics, vol. 33, no. 11, pp. 1593–1616, 2003.
- [47] Yao A. C.-C., "Quantum circuit complexity," in Proceedings of 1993 IEEE 34th Annual Foundations of Computer Science. IEEE, 1993, pp. 352–361.
- [48] Cleve R. and Buhrman H., "Substituting quantum entanglement for communication," Physical Review A, vol. 56, no. 2, p. 1201, 1997.
- [49] Guedes E. B. and Assis F. M. de, "Quantum communication complexity of quantum authentication protocols," arXiv preprint arXiv:1105.5370, 2011.
- [50] Ghilen A., Belmabrouk H., and Bouallegue R., "Classification of quantum authentication protocols and calculation of their complexity," in 2014 15th International Conference on Sciences and Techniques of Automatic Control and Computer Engineering (STA). IEEE, 2014, pp. 169–173.
- [51] Yadav P., Srikanth R., and Pathak A., "Two-step orthogonal-state-based protocol of quantum secure direct communication with the help of order-rearrangement technique," Quantum Information Processing, vol. 13, no. 12, pp. 2731–2743, 2014.
- [52] Nayana D. and Paul G. K., "Quantum secure direct communication with mutual authentication via rotation of an arbitrary basis," Nov. 16 2023, uS Patent App. 17/894,801.
- [53] Shukla C., Kothari V., Banerjee A., and Pathak A., "On the group-theoretic structure of a class of quantum dialogue protocols," Physics Letters A, vol. 377, no. 7, pp. 518–527, 2013.

- [54] Shukla C. and Pathak A., "Orthogonal-state-based deterministic secure quantum communication without actual transmission of the message qubits," Quantum Information Processing, vol. 13, no. 9, pp. 2099–2113, 2014.
- [55] Lo H.-K. and Chau H. F., "Is quantum bit commitment really possible?" Physical Review Letters, vol. 78, no. 17, p. 3410, 1997.
- [56] Barnum H. N., "Quantum secure identification using entanglement and catalysis," arXiv preprint quant-ph/9910072, 1999.
- [57] Majumdar R. and Das S., "Sok: An evaluation of quantum authentication through systematic literature review," in Proceedings of the Workshop on Usable Security and Privacy (USEC), 2021.
- [58] Ljunggren D., Bourennane M., and Karlsson A., "Authority-based user authentication in quantum key distribution," Physical Review A, vol. 62, no. 2, p. 022305, 2000.
- [59] Zeng G. and Guo G., "Quantum authentication protocol," arXiv preprint quantph/0001046, 2000.
- [60] Jensen J. G. and Schack R., "Quantum authentication and key distribution using catalysis," arXiv preprint quant-ph/0003104, 2000.
- [61] Srinatha N., Omkar S., Srikanth R., Banerjee S., and Pathak A., "The quantum crypto-graphic switch," Quantum Information Processing, vol. 13, no. 1, pp. 59–70, 2014.
- [62] Thapliyal K. and Pathak A., "Applications of quantum cryptographic switch: various tasks related to controlled quantum communication can be performed using Bell states and permutation of particles," Quantum Information Processing, vol. 14, no. 7, pp. 2599–2616, 2015.
- [63] Curty M. and Santos D. J., "Quantum authentication of classical messages," Physical Review A, vol. 64, no. 6, p. 062309, 2001.
- [64] Curty M., Santos D. J., Pérez E., and García-Fernández P., "*Qubit authentication*," Physical Review A, vol. 66, no. 2, p. 022301, 2002.

- [65] Dam W. van, "Comment on "Quantum identification schemes with entanglements"," Physical Review A, vol. 68, no. 2, p. 026301, 2003.
- [66] Sharma R. D., Thapliyal K., Pathak A., Pan A. K., and De A., "Which verification qubits perform best for secure communication in noisy channel?" Quantum Information Processing, vol. 15, no. 4, pp. 1703–1718, 2016.
- [67] Zawadzki P., "Security of ping-pong protocol based on pairs of completely entangled qudits," Quantum Information Processing, vol. 11, pp. 1419–1430, 2012.
- [68] Zawadzki P., "Improving security of the ping-pong protocol," Quantum Information Processing, vol. 12, pp. 149–155, 2013.
- [69] Zawadzki P., Puchała Z., and Miszczak J. A., "Increasing the security of the ping–pong protocol by using many mutually unbiased bases," Quantum Information Processing, vol. 12, pp. 569–576, 2013.
- [70] Zhou N., Zeng G., Zeng W., and Zhu F., "Cross-center quantum identification scheme based on teleportation and entanglement swapping," Optics Communications, vol. 254, no. 4-6, pp. 380–388, 2005.
- [71] Lee H., Lim J., and Yang H., "Quantum direct communication with authentication," Physical Review A, vol. 73, no. 4, p. 042305, 2006.
- [72] Boström K. and Felbinger T., "Deterministic secure direct communication using entanglement," Physical Review Letters, vol. 89, no. 18, p. 187902, 2002.
- [73] Zhang Z.-j., Liu J., Wang D., and Shi S.-h., "Comment on "Quantum direct communication with authentication"," Physical Review A, vol. 75, no. 2, p. 026301, 2007.
- [74] Yu-Guang Y. and Qiao-Yan W., "Economical multiparty simultaneous quantum identity authentication based on Greenberger–Horne–Zeilinger states," Chinese Physics B, vol. 18, no. 8, p. 3233, 2009.
- [75] Rass S., Schartner P., and Greiler M., "*Quantum coin-flipping-based authentication*," in 2009 IEEE International Conference on Communications. IEEE, 2009, pp. 1–5.

- [76] Dan L., Chang-Xing P., Dong-Xiao Q., and Nan Z., "A new quantum secure direct communication scheme with authentication," Chinese Physics Letters, vol. 27, no. 5, p. 050306, 2010.
- [77] Huang P., Zhu J., Lu Y., and Zeng G.-H., "Quantum identity authentication using gaussian-modulated squeezed states," International Journal of Quantum Information, vol. 9, no. 02, pp. 701–721, 2011.
- [78] Gong C.-Q., Tang H., and Zhang D.-W., "Identity authentication and key distribution protocol based on quantum one-way function," Computer Engineering, vol. 38, no. 6, pp. 161–160, 2012.
- [79] Gelfond R. and Berzanskis A., "Key management and user authentication for quantum cryptography networks," Dec. 25 2012.
- [80] Pappu R., Recht B., Taylor J., and Gershenfeld N., "Physical one-way functions," Science, vol. 297, no. 5589, pp. 2026–2030, 2002.
- [81] Goorden S. A., Horstmann M., Mosk A. P., Škorić B., and Pinkse P. W., "Quantum-secure authentication of a physical unclonable key," Optica, vol. 1, no. 6, pp. 421–424, 2014.
- [82] Ziola T., Paral Z., Devadas S., Suh G. E., and Khandelwal V., "Authentication with physical unclonable functions," Jul. 15 2014.
- [83] Yang Y.-G., Tian J., Xia J., and Zhang H., "Quantum authenticated direct communication using Bell states," International Journal of Theoretical Physics, vol. 52, no. 2, pp. 336–344, 2013.
- [84] Thapliyal K., Verma A., and Pathak A., "A general method for selecting quantum channel for bidirectional controlled state teleportation and other schemes of controlled quantum communication," Quantum Information Processing, vol. 14, no. 12, pp. 4601–4614, 2015.
- [85] Tan X. and Jiang L., "Identity authentication by entanglement swapping in controlled quantum teleportation," International Journal of Embedded Systems 4, vol. 6, no. 1, pp. 3–13, 2014.

- [86] Shi W.-M., Zhou Y.-H., and Yang Y.-G., "Quantum deniable authentication protocol," Quantum Information Processing, vol. 13, no. 7, pp. 1501–1510, 2014.
- [87] Yuan H., Liu Y.-m., Pan G.-z., Zhang G., Zhou J., and Zhang Z.-j., "Quantum identity authentication based on ping-pong technique without entanglements," Quantum Information Processing, vol. 13, no. 11, pp. 2535–2549, 2014.
- [88] Lucamarini M. and Mancini S., "Secure deterministic communication without entanglement," Physical Review Letters, vol. 94, no. 14, p. 140501, 2005.
- [89] Lai H., Xiao J., Orgun M. A., Xue L., and Pieprzyk J., "Quantum direct secret sharing with efficient eavesdropping-check and authentication based on distributed fountain codes," Quantum Information Processing, vol. 13, no. 4, pp. 895–907, 2014.
- [90] Shi W.-M., Zhang J.-B., Zhou Y.-H., and Yang Y.-G., "A novel quantum deniable authentication protocol without entanglement," Quantum Information Processing, vol. 14, no. 6, pp. 2183–2193, 2015.
- [91] Pirandola S., Ottaviani C., Spedalieri G., Weedbrook C., Braunstein S. L., Lloyd S., Gehring T., Jacobsen C. S., and Andersen U. L., "High-rate measurement-device-independent quantum cryptography," Nature Photonics, vol. 9, no. 6, pp. 397–402, 2015.
- [92] Xu F., Curty M., Qi B., Qian L., and Lo H.-K., "Discrete and continuous variables for measurement-device-independent quantum cryptography," Nature Photonics, vol. 9, no. 12, pp. 772–773, 2015.
- [93] Pirandola S., Ottaviani C., Spedalieri G., Weedbrook C., Braunstein S. L., Lloyd S., Gehring T., Jacobsen C. S., and Andersen U. L., "Reply to'discrete and continuous variables for measurement-device-independent quantum cryptography"," Nature Photonics, vol. 9, no. 12, pp. 773–775, 2015.
- [94] Rass S., König S., Schauer S., and Maurhart O., "Implementation and evaluation of intrinsic authentication in quantum key distribution protocols," International Journal on Advances in Security, vol. 9, no. 1, 2016.
- [95] Škorić B., "Quantum readout of physical unclonable functions," International Journal of Quantum Information, vol. 10, no. 01, p. 1250001, 2012.

- [96] Yao Y., Gao M., Li M., and Zhang J., "Quantum cloning attacks against PUF-based quantum authentication systems," Quantum Information Processing, vol. 15, no. 8, pp. 3311–3325, 2016.
- [97] Škorić B., Mosk A. P., and Pinkse P. W., "Security of quantum-readout PUFs against quadrature-based challenge-estimation attacks," International Journal of Quantum Information, vol. 11, no. 04, p. 1350041, 2013.
- [98] Hayden P., Leung D. W., and Mayers D., "The universal composable security of quantum message authentication with key recyling," arXiv preprint arXiv:1610.09434, 2016.
- [99] Renner R., "Security of quantum key distribution," International Journal of Quantum Information, vol. 6, no. 01, pp. 1–127, 2008.
- [100] Hong C. ho, Heo J., Jang J. G., and Kwon D., "Quantum identity authentication with single photon," Quantum Information Processing, vol. 16, no. 10, p. 236, 2017.
- [101] Abulkasim H., Hamad S., Khalifa A., and El Bahnasy K., "Quantum secret sharing with identity authentication based on Bell states," International Journal of Quantum Information, vol. 15, no. 04, p. 1750023, 2017.
- [102] Nikolopoulos G. M. and Diamanti E., "Continuous-variable quantum authentication of physical unclonable keys," Scientific Reports, vol. 7, p. 46047, 2017.
- [103] Portmann C., "Quantum authentication with key recycling," in Annual International Conference on the Theory and Applications of Cryptographic Techniques. Springer, 2017, pp. 339–368.
- [104] Hughes R. J., Peterson C. G., Thrasher J. T., Nordholt J. E., Yard J. T., Newell R. T., and Somma R. D., "Multi-factor authentication using quantum communication," Feb. 6 2018.
- [105] Boyer M., Kenigsberg D., and Mor T., "Quantum key distribution with classical Bob," Physical Review Letters, vol. 99, no. 14, p. 140501, 2007.
- [106] Shukla C., Thapliyal K., and Pathak A., "Semi-quantum communication: protocols for key agreement, controlled secure direct communication and dialogue," Quantum Information Processing, vol. 16, no. 12, p. 295, 2017.

- [107] Thapliyal K., Sharma R. D., and Pathak A., "Orthogonal-state-based and semi-quantum protocols for quantum private comparison in noisy environment," International Journal of Quantum Information, vol. 16, no. 05, p. 1850047, 2018.
- [108] Mishra S., Thapliyal K., Parakh A., and Pathak A., "Quantum anonymous veto: A set of new protocols," arXiv preprint arXiv:2109.06260, 2021.
- [109] Asagodu P., Thapliyal K., and Pathak A., "Quantum and semi-quantum sealed-bid auction: Vulnerabilities and advantages," arXiv preprint arXiv:2108.06388, 2021.
- [110] Wen X.-J., Zhao X.-Q., Gong L.-H., and Zhou N.-R., "A semi-quantum authentication protocol for message and identity," Laser Physics Letters, vol. 16, no. 7, p. 075206, 2019.
- [111] Liu B., Gao Z., Xiao D., Huang W., Zhang Z., and Xu B., "Quantum identity authentication in the counterfactual quantum key distribution protocol," Entropy, vol. 21, no. 5, p. 518, 2019.
- [112] Zheng X.-y. and Long Y.-x., "Controlled quantum secure direct communication with authentication protocol based on five-particle cluster state and classical xor operation," Quantum Information Processing, vol. 18, no. 5, p. 129, 2019.
- [113] Gope P. and Hwang T., "A realistic lightweight anonymous authentication protocol for securing real-time application data access in wireless sensor networks," IEEE Transactions on Industrial Electronics, vol. 63, no. 11, pp. 7124–7132, 2016.
- [114] Yan C., Shi-Bin Z., Li-Li Y., and Gui-Hua H., "Robust quantum secure direct communication and authentication protocol against decoherence noise based on six-qubit df state," Chinese Physics B, vol. 24, no. 5, p. 050307, 2015.
- [115] Qu Z., Liu X., and Wu S., "Quantum identity authentication protocol based on three-photon quantum error avoidance code in edge computing," Transactions on Emerging Telecommunications Technologies, p. e3945, 2020.
- [116] Xiao M. and Lei S., "Quantum private query with authentication," Quantum Information Processing, vol. 20, no. 5, p. 166, 2021.
- [117] Das N., Paul G., and Majumdar R., "Quantum secure direct communication with mutual authentication using a single basis," arXiv preprint arXiv:2101.03577, 2021.

- [118] Zawadzki P., "Quantum identity authentication without entanglement," Quantum Information Processing, vol. 18, no. 1, p. 7, 2019.
- [119] González-Guillén C. E., González Vasco M. I., Johnson F., and Pozo Á. L. Pérez del, "An attack on Zawadzki's quantum authentication scheme," Entropy, vol. 23, no. 4, p. 389, 2021.
- [120] Jacinto H. S., Smith A. M., and Rafla N. I., "Utilizing a fully optical and reconfigurable PUF as a quantum authentication mechanism," OSA Continuum, vol. 4, no. 2, pp. 739–747, 2021.
- [121] Doosti M., Kumar N., Delavar M., and Kashefi E., "Client-server identification protocols with quantum PUF," ACM Transactions on Quantum Computing, vol. 2, no. 3, pp. 1–40, 2021.
- [122] Phalak K., Ash-Saki A., Alam M., Topaloglu R. O., and Ghosh S., "*Quantum PUF* for security and trust in quantum computing," IEEE Journal on Emerging and Selected Topics in Circuits and Systems, vol. 11, no. 2, pp. 333–342, 2021.
- [123] Li X., Zhang K., Zhang L., and Zhao X., "A new quantum multiparty simultaneous identity authentication protocol with the classical third-party," Entropy, vol. 24, no. 4, p. 483, 2022.
- [124] Das N. and Paul G., "Measurement device–independent quantum secure direct communication with user authentication," Quantum Information Processing, vol. 21, no. 7, p. 260, 2022.
- [125] He Y.-F., Pang Y., and Di M., "Mutual authentication quantum key agreement protocol based on Bell states," Quantum Information Processing, vol. 21, no. 8, p. 290, 2022.
- [126] Li G.-D., Cheng W.-C., Wang Q.-L., and Liu J.-C., "A measurement device independent multi-party quantum key agreement protocol with identity authentication," Quantum Information Processing, vol. 22, no. 12, p. 443, 2023.
- [127] Kulik S. and Molotkov S., "Entanglement based six-state quantum cryptography protocol: exact proof of security," Laser Physics Letters, vol. 20, no. 5, p. 055203, 2023.

- [128] Chen G., Wang Y., Jian L., Zhou Y., and Liu S., "Quantum identity authentication based on the extension of quantum rotation," EPJ Quantum Technology, vol. 10, no. 1, p. 11, 2023.
- [129] Chen G., Wang Y., Jian L., Zhou Y., Liu S., Luo J., and Yang K., "Quantum identity authentication protocol based on flexible quantum homomorphic encryption with qubit rotation," Journal of Applied Physics, vol. 133, no. 6, 2023.
- [130] Zhang Q., Du M.-M., Zhong W., Sheng Y.-B., and Zhou L., "Single-photon based three-party quantum secure direct communication with identity authentication," Annalen der Physik, vol. 536, no. 3, p. 2300407, 2024.
- [131] Mawlia P., Siwach V., Bijaranian P., and Singh D., "Quantum secret sharing with (m, n) threshold: QFT and identity authentication," Quantum Information Processing, vol. 23, no. 10, p. 348, 2024.
- [132] Zhu H., Wang L., and Zhang Y., "An efficient quantum identity authentication key agreement protocol without entanglement," Quantum Information Processing, vol. 19, no. 10, p. 381, 2020.
- [133] Sobota M., Kapczyński A., and Banasik A., "Application of quantum cryptography protocols in authentication process," in Proceedings of the 6th IEEE International Conference on Intelligent Data Acquisition and Advanced Computing Systems, vol. 2. IEEE, 2011, pp. 799–802.
- [134] Srikara S., Thapliyal K., and Pathak A., "Continuous variable direct secure quantum communication using gaussian states," Quantum Information Processing, vol. 19, no. 4, p. 132, 2020.
- [135] Banerjee A. and Pathak A., "Maximally efficient protocols for direct secure quantum communication," Physics Letters A, vol. 376, no. 45, pp. 2944–2950, 2012.
- [136] Pirandola S., Braunstein S. L., Mancini S., and Lloyd S., "*Quantum direct communication with continuous variables*," EPL (Europhysics Letters), vol. 84, no. 2, p. 20013, oct 2008. [Online]. Available: https://doi.org/10.1209/0295-5075/84/20013

- [137] Li X. and Chen L., "Quantum authentication protocol using Bell state," in The First International Symposium on Data, Privacy, and E-Commerce (ISDPE 2007). IEEE, 2007, pp. 128–132.
- [138] Lo H.-K. and Chau H. F., "Unconditional security of quantum key distribution over arbitrarily long distances," Science, vol. 283, no. 5410, pp. 2050–2056, 1999.
- [139] Lal N., Mishra S., Rani A., Banerji A., Perumangatt C., and Singh R., "Polarization—orbital angular momentum duality assisted entanglement observation for indistinguishable photons," Quantum Information Processing, vol. 22, no. 1, p. 90, 2023.
- [140] Banerji A., Singh R. P., Banerjee D., and Bandyopadhyay A., "*Entanglement propagation of a quantum optical vortex state*," Optics Communications, vol. 380, pp. 492–498, 2016.
- [141] Ma H., Huang P., Bao W., and Zeng G., "Continuous-variable quantum identity authentication based on quantum teleportation," Quantum Information Processing, vol. 15, no. 6, pp. 2605–2620, 2016.
- [142] Barnum H., Crépeau C., Gottesman D., Smith A., and Tapp A., "Authentication of quantum messages," in The 43rd Annual IEEE Symposium on Foundations of Computer Science, 2002. Proceedings. IEEE, 2002, pp. 449–458.
- [143] Basak N., Das N., Paul G., Nandi K., and Patel N., "Quantum secret sharing protocol using GHZ state: implementation on IBM qiskit," Quantum Information Processing, vol. 22, no. 11, p. 393, 2023.
- [144] Yang Y., Wen Q., and Zhang X., "Multiparty simultaneous quantum identity authentication with secret sharing," Science in China Series G: Physics, Mechanics and Astronomy, vol. 51, no. 3, pp. 321–327, 2008.
- [145] Abulkasim H., Hamad S., El Bahnasy K., and Rida S. Z., "Authenticated quantum secret sharing with quantum dialogue based on Bell states," Physica Scripta, vol. 91, no. 8, p. 085101, 2016.
- [146] Shi R.-H., "Useful equations about Bell states and their applications to quantum secret sharing," IEEE Communications Letters, vol. 24, no. 2, pp. 386–390, 2019.

- [147] Yin A. and Chen T., "Authenticated semi-quantum secret sharing based on GHZ-type states," International Journal of Theoretical Physics, vol. 60, no. 1, pp. 265–273, 2021.
- [148] Banerjee A., Shukla C., Thapliyal K., Pathak A., and Panigrahi P. K., "Asymmetric quantum dialogue in noisy environment," Quantum Information Processing, vol. 16, no. 2, p. 49, 2017.
- [149] Gao G., Wang Y., Wang D., and Ye L., "Comment on "Authenticated quantum secret sharing with quantum dialogue based on Bell states"," Physica Scripta, vol. 93, no. 2, p. 027002, 2018.
- [150] Abulkasim H., Hamad S., and Elhadad A., "Reply to comment on "Authenticated quantum secret sharing with quantum dialogue based on Bell states"," Physica Scripta, vol. 93, no. 2, p. 027001, 2018.
- [151] Childs A. M., "Secure assisted quantum computation," Quantum Information and Computation, vol. 5, no. 6, pp. 456–466, 2005.
- [152] Li Q., Li Z., Chan W. H., Zhang S., and Liu C., "Blind quantum computation with identity authentication," Physics Letters A, vol. 382, no. 14, pp. 938–941, 2018.
- [153] Quan J., Li Q., Liu C., Shi J., and Peng Y., "A simplified verifiable blind quantum computing protocol with quantum input verification," Quantum Engineering, vol. 3, no. 1, p. e58, 2021.
- [154] Shan R.-T., Chen X., and Yuan K.-G., "Multi-party blind quantum computation protocol with mutual authentication in network," Science China Information Sciences, vol. 64, no. 6, p. 162302, 2021.
- [155] Li W., Shi R., and Guo Y., "Blind quantum signature with blind quantum computation," International Journal of Theoretical Physics, vol. 56, no. 4, pp. 1108–1115, 2017.
- [156] Qu Z., Liu X., and Wu S., "Quantum identity authentication protocol based on three-photon quantum error avoidance code," in 2019 International Conference on Internet of Things (iThings) and IEEE Green Computing and Communications (GreenCom) and IEEE Cyber, Physical and Social Computing (CPSCom) and IEEE Smart Data (Smart-Data). IEEE, 2019, pp. 471–475.

- [157] Saxena A., Thapliyal K., and Pathak A., "Continuous variable controlled quantum dialogue and secure multiparty quantum computation," International Journal of Quantum Information, vol. 18, no. 04, p. 2050009, 2020.
- [158] Crépeau C., Gottesman D., and Smith A., "Secure multi-party quantum computation," in Proceedings of the thiry-fourth annual ACM symposium on Theory of computing, 2002, pp. 643–652.
- [159] Banerjee A., Thapliyal K., Shukla C., and Pathak A., "*Quantum conference*," Quantum Information Processing, vol. 17, no. 7, p. 161, 2018.
- [160] Goldenberg L. and Vaidman L., "Quantum cryptography based on orthogonal states," Physical Review Letters, vol. 75, no. 7, p. 1239, 1995.
- [161] Liu L., Xiao M., and Song X., "Authenticated semiquantum dialogue with secure delegated quantum computation over a collective noise channel," Quantum Information Processing, vol. 17, no. 12, p. 342, 2018.
- [162] Dutta A. and Pathak A., "New protocols for quantum key distribution with explicit upper and lower bound on secret key rate," The European Physical Journal D, vol. 79, no. 5, p. 48, 2025.
- [163] Shenoy-Hejamadi A., Pathak A., and Radhakrishna S., "Quantum cryptography: key distribution and beyond," Quanta, vol. 6, no. 1, pp. 1–47, 2017.
- [164] Gisin N., Ribordy G., Tittel W., and Zbinden H., "*Quantum cryptography*," Reviews of Modern Physics, vol. 74, no. 1, p. 145, 2002.
- [165] Dutta A. and Pathak A., "A short review on quantum identity authentication protocols: How would Bob know that he is talking with Alice?" Quantum Information Processing, vol. 21, p. 369, 2022.
- [166] Dutta A. and Pathak A., "Controlled secure direct quantum communication inspired scheme for quantum identity authentication," Quantum Information Processing, vol. 22, p. 13, 2023.
- [167] Lu C.-Y. and Pan J.-W., "Quantum-dot single-photon sources for the quantum internet," Nature Nanotechnology, vol. 16, no. 12, pp. 1294–1296, 2021.

- [168] Thomas S. and Senellart P., "The race for the ideal single-photon source is on," Nature Nanotechnology, vol. 16, no. 4, pp. 367–368, 2021.
- [169] Biswas A., Banerji A., Lal N., Chandravanshi P., Kumar R., and Singh R. P., "*Quantum key distribution with multiphoton pulses: an advantage*," Optics Continuum, vol. 1, no. 1, pp. 68–79, 2022.
- [170] Huttner B., Imoto N., Gisin N., and Mor T., "Quantum cryptography with coherent states," Physical Review A, vol. 51, no. 3, p. 1863, 1995.
- [171] Brassard G., Lütkenhaus N., Mor T., and Sanders B. C., "Limitations on practical quantum cryptography," Physical Review Letters, vol. 85, no. 6, p. 1330, 2000.
- [172] Scarani V., Acín A., Ribordy G., and Gisin N., "Quantum cryptography protocols robust against photon number splitting attacks for weak laser pulse implementations," Physical Review Letters, vol. 92, no. 5, p. 057901, 2004.
- [173] Cabello A., "Quantum key distribution in the holevo limit," Physical Review Letters, vol. 85, no. 26, p. 5635, 2000.
- [174] Ingemarsson I., Tang D., and Wong C., "A conference key distribution system," IEEE Transactions on Information Theory, vol. 28, no. 5, pp. 714–720, 1982.
- [175] Mitchell C. J., Ward M., Wilson P. et al., "Key control in key agreement protocols," Electronics Letters, vol. 34, no. 10, pp. 980–980, 1998.
- [176] Steiner M., Tsudik G., and Waidner M., "Key agreement in dynamic peer groups," IEEE Transactions on Parallel and Distributed Systems, vol. 11, no. 8, pp. 769–780, 2000.
- [177] Ateniese G., Steiner M., and Tsudik G., "New multiparty authentication services and key agreement protocols," IEEE Journal on Selected Areas in Communications, vol. 18, no. 4, pp. 628–639, 2000.
- [178] Huang W., Wen Q.-Y., Liu B., Su Q., and Gao F., "Cryptanalysis of a multi-party quantum key agreement protocol with single particles," Quantum Information Processing, vol. 13, no. 7, pp. 1651–1657, 2014.

- [179] Huang W., Su Q., Liu B., He Y.-H., Fan F., and Xu B.-J., "Efficient multiparty quantum key agreement with collective detection," Scientific Reports, vol. 7, no. 1, p. 15264, 2017.
- [180] Hahn F., Jong J. de, and Pappa A., "Anonymous quantum conference key agreement," PRX Quantum, vol. 1, no. 2, p. 020325, 2020.
- [181] Bennett C. H., Brassard G., and Mermin N. D., "Quantum cryptography without Bell's theorem," Physical Review Letters, vol. 68, no. 5, p. 557, 1992.
- [182] Lo H.-K., Curty M., and Qi B., "Measurement-device-independent quantum key distribution," Physical Review Letters, vol. 108, no. 13, p. 130503, 2012.
- [183] Curty M., Xu F., Cui W., Lim C. C. W., Tamaki K., and Lo H.-K., "Finite-key analysis for measurement-device-independent quantum key distribution," Nature communications, vol. 5, no. 1, p. 3732, 2014.
- [184] Scarani V., Bechmann-Pasquinucci H., Cerf N. J., Dušek M., Lütkenhaus N., and Peev M., "The security of practical quantum key distribution," Reviews of modern physics, vol. 81, no. 3, p. 1301, 2009.
- [185] Deng F.-G., Long G. L., and Liu X.-S., "Two-step quantum direct communication protocol using the einstein-podolsky-rosen pair block," Physical Review A, vol. 68, no. 4, p. 042317, 2003.
- [186] Hillery M., Bužek V., and Berthiaume A., "Quantum secret sharing," Physical Review A, vol. 59, no. 3, p. 1829, 1999.
- [187] Karlsson A., Koashi M., and Imoto N., "Quantum entanglement for secret sharing and secret splitting," Physical Review A, vol. 59, no. 1, p. 162, 1999.
- [188] Mishra S., Shukla C., Pathak A., Srikanth R., and Venugopalan A., "An integrated hierarchical dynamic quantum secret sharing protocol," International Journal of Theoretical Physics, vol. 54, pp. 3143–3154, 2015.
- [189] Liu S., Lu Z., Wang P., Tian Y., Wang X., and Li Y., "Experimental demonstration of multiparty quantum secret sharing and conference key agreement," npj Quantum Information, vol. 9, no. 1, p. 92, 2023.

- [190] Yang Y.-G. and Wen Q.-Y., "An efficient two-party quantum private comparison protocol with decoy photons and two-photon entanglement," Journal of Physics A: Mathematical and Theoretical, vol. 42, no. 5, p. 055305, 2009.
- [191] Yang Y.-G., Cao W.-F., and Wen Q.-Y., "Secure quantum private comparison," Physica Scripta, vol. 80, no. 6, p. 065002, 2009.
- [192] Chen X.-B., Xu G., Niu X.-X., Wen Q.-Y., and Yang Y.-X., "An efficient protocol for the private comparison of equal information based on the triplet entangled state and single-particle measurement," Optics Communications, vol. 283, no. 7, pp. 1561–1565, 2010.
- [193] Thapliyal K., Sharma R. D., and Pathak A., "Orthogonal-state-based and semi-quantum protocols for quantum private comparison in noisy environment," International Journal of Quantum Information, vol. 16, no. 05, p. 1850047, 2018.
- [194] Gottesman D. and Chuang I., "Quantum digital signatures," arXiv preprint quantph/0105032, 2001.
- [195] Dunjko V., Wallden P., and Andersson E., "Quantum digital signatures without quantum memory," Physical Review Letters, vol. 112, no. 4, p. 040502, 2014.
- [196] Wallden P., Dunjko V., Kent A., and Andersson E., "Quantum digital signatures with quantum-key-distribution components," Physical Review A, vol. 91, no. 4, p. 042304, 2015.
- [197] Zhou N., Zeng G., and Xiong J., "Quantum key agreement protocol," Electronics Letters, vol. 40, no. 18, p. 1, 2004.
- [198] Chong S.-K., Tsai C.-W., and Hwang T., "Improvement on "quantum key agreement protocol with maximally entangled states"," International Journal of Theoretical Physics, vol. 50, no. 6, pp. 1793–1802, 2011.
- [199] Shi R.-H. and Zhong H., "Multi-party quantum key agreement with Bell states and Bell measurements," Quantum Information Processing, vol. 12, no. 2, pp. 921–932, 2013.
- [200] Liu B., Gao F., Huang W., and Wen Q.-y., "Multiparty quantum key agreement with single particles," Quantum Information Processing, vol. 12, no. 4, pp. 1797–1805, 2013.

- [201] Chong S.-K. and Hwang T., "Quantum key agreement protocol based on bb84," Optics Communications, vol. 283, no. 6, pp. 1192–1195, 2010.
- [202] Shukla C., Alam N., and Pathak A., "Protocols of quantum key agreement solely using Bell states and Bell measurement," Quantum Information Processing, vol. 13, no. 11, pp. 2391–2405, 2014.
- [203] Xu G.-B., Wen Q.-Y., Gao F., and Qin S.-J., "Novel multiparty quantum key agreement protocol with GHZ states," Quantum Information Processing, vol. 13, no. 12, pp. 2587–2594, 2014.
- [204] He Y.-F. and Ma W.-P., "Quantum key agreement protocols with four-qubit cluster states," Quantum Information Processing, vol. 14, no. 9, pp. 3483–3498, 2015.
- [205] Liu B., Xiao D., Jia H.-Y., and Liu R.-Z., "Collusive attacks to "circle-type" multi-party quantum key agreement protocols," Quantum Information Processing, vol. 15, no. 5, pp. 2113–2124, 2016.
- [206] Lin S., Zhang X., Guo G.-D., Wang L.-L., and Liu X.-F., "Multiparty quantum key agreement," Physical Review A, vol. 104, no. 4, p. 042421, 2021.
- [207] Deng F.-G. and Long G.-L., "Controlled order rearrangement encryption for quantum key distribution," Physical Review A, vol. 68, no. 4, p. 042315, 2003.
- [208] Hugues-Salas E., Ntavou F., Gkounis D., Kanellos G. T., Nejabati R., and Simeonidou D., "Monitoring and physical-layer attack mitigation in sdn-controlled quantum key distribution networks," Journal of Optical Communications and Networking, vol. 11, no. 2, pp. A209–A218, 2019.
- [209] Dong L., Xiu X.-M., Gao Y.-J., and Chi F., "A controlled quantum dialogue protocol in the network using entanglement swapping," Optics Communications, vol. 281, no. 24, pp. 6135–6138, 2008.
- [210] Kao S.-H. and Hwang T., "Controlled quantum dialogue using cluster states," Quantum Information Processing, vol. 16, p. 139, 2017.

- [211] Wang J., Zhang Q., and Tang C.-j., "Quantum secure direct communication based on order rearrangement of single photons," Physics Letters A, vol. 358, no. 4, pp. 256–258, 2006.
- [212] Chen X.-B., Wen Q.-Y., Guo F.-Z., Sun Y., Xu G., and Zhu F.-C., "Controlled quantum secure direct communication with w state," International Journal of Quantum Information, vol. 6, no. 04, pp. 899–906, 2008.
- [213] Li Y.-h., Li X.-l., Sang M.-h., Nie Y.-y., and Wang Z.-s., "Bidirectional controlled quantum teleportation and secure direct communication using five-qubit entangled state," Quantum Information Processing, vol. 12, pp. 3835–3844, 2013.
- [214] Tang J., Shi L., and Wei J., "Controlled quantum key agreement based on maximally three-qubit entangled states," Modern Physics Letters B, vol. 34, no. 18, p. 2050201, 2020.
- [215] Gibbons R. S., *Game theory for applied economists*. Princeton University Press: Princeton, NJ, USA, 1992; ISBN 978-0-691-00395-5, 1992.
- [216] Ordeshook P. C. et al., "Game theory and political theory," Cambridge Books, 1986.
- [217] Colman A. M., *Game theory and its applications: In the social and biological sciences*. Psychology Press, 2013.
- [218] Nowak M. A. and Sigmund K., "*Phage-lift for game theory*," Nature, vol. 398, no. 6726, pp. 367–368, 1999.
- [219] Dresher M., Some military applications of the Theory of Games. Rand, 1959.
- [220] Hardin R., One for all: The logic of group conflict. Princeton University Press, 1997.
- [221] Nash Jr J. F., "Equilibrium points in n-person games," Proceedings of The National Academy of Sciences, vol. 36, no. 1, pp. 48–49, 1950.
- [222] Nash J., "Non-cooperative games," Annals of Mathematics, pp. 286–295, 1951.
- [223] Aspect A., Grangier P., and Roger G., "Experimental realization of Einstein-Podolsky-Rosen-Bohm gedankenexperiment: A new violation of Bell's inequalities," Physical Review Letters, vol. 49, no. 2, p. 91, 1982.

- [224] Landsburg S. E., *Quantum Game Theory*. John Wiley & Sons, Inc.: Hoboken, NJ, USA, 2011; ISBN 978-0-470-40053-1, 2011.
- [225] Meyer D. A., "Quantum strategies," Physical Review Letters, vol. 82, no. 5, p. 1052, 1999.
- [226] Eisert J., Wilkens M., and Lewenstein M., "Quantum games and quantum strategies," Physical Review Letters, vol. 83, no. 15, p. 3077, 1999.
- [227] Guo H., Zhang J., and Koehler G. J., "A survey of quantum games," Decision Support Systems, vol. 46, no. 1, pp. 318–332, 2008.
- [228] Du J., Li H., Xu X., Shi M., Wu J., Zhou X., and Han R., "Experimental realization of quantum games on a quantum computer," Physical Review Letters, vol. 88, no. 13, p. 137902, 2002.
- [229] Vaidman L., "Variations on the theme of the greenberger-horne-zeilinger proof," Foundations of Physics, vol. 29, no. 4, pp. 615–630, 1999.
- [230] Goldenberg L., Vaidman L., and Wiesner S., "Quantum gambling," Physical Review Letters, vol. 82, no. 16, p. 3356, 1999.
- [231] Patel N., "Quantum games: States of play," Nature, vol. 445, no. 7124, pp. 144–147, 2007.
- [232] Flitney A. and Abbott D., "Quantum models of Parrondo's games," Physica A: Statistical Mechanics and its Applications, vol. 324, no. 1-2, pp. 152–156, 2003.
- [233] Dutta A. and Pathak A., "Collective attack free controlled quantum key agreement without quantum memory," Physica Scripta, vol. 100, no. 3, p. 035101, 2025.
- [234] Dutta A. and Pathak A., "Simultaneous quantum identity authentication scheme utilizing entanglement swapping with secret key preservation," Modern Physics Letters A, p. 2450196, 2025.
- [235] Gisin N. and Huttner B., "Quantum cloning, eavesdropping and Bell's inequality," Physics Letters A, vol. 228, no. 1-2, pp. 13–21, 1997.

- [236] Werner R. F., "Optimal cloning of pure states," Physical Review A, vol. 58, no. 3, p. 1827, 1998.
- [237] Khan F. S. and Phoenix S. J., "Mini-maximizing two qubit quantum computations," Quantum information processing, vol. 12, pp. 3807–3819, 2013.
- [238] Deng F.-G. and Long G. L., "Secure direct communication with a quantum one-time pad," Physical Review A, vol. 69, no. 5, p. 052319, 2004.
- [239] Long G.-l., Deng F.-g., Wang C., Li X.-h., Wen K., and Wang W.-y., "Quantum secure direct communication and deterministic secure quantum communication," Frontiers of Physics in China, vol. 2, pp. 251–272, 2007.
- [240] Zhu A.-D., Xia Y., Fan Q.-B., and Zhang S., "Secure direct communication based on secret transmitting order of particles," Physical Review A, vol. 73, no. 2, p. 022338, 2006.
- [241] Hwang T., Hwang C., and Tsai C., "Quantum key distribution protocol using dense coding of three-qubit W state," The European Physical Journal D, vol. 61, pp. 785–790, 2011.
- [242] Beige A., Englert B., Kurtsiefer C., and Weinfurter H., "Secure communication with a publicly known key," Acta Physica Polonica A, vol. 3, no. 101, pp. 357–368, 2002.
- [243] Long G.-L. and Liu X.-S., "Theoretically efficient high-capacity quantum-key-distribution scheme," Physical Review A, vol. 65, no. 3, p. 032302, 2002.
- [244] Boström K. and Felbinger T., "Deterministic secure direct communication using entanglement," Physical Review Letters, vol. 89, no. 18, p. 187902, 2002.
- [245] Deng F.-G., Long G. L., and Liu X.-S., "Two-step quantum direct communication protocol using the einstein-podolsky-rosen pair block," Physical Review A, vol. 68, no. 4, p. 042317, 2003.
- [246] Degiovanni I., Berchera I. R., Castelletto S., Rastello M. L., Bovino F., Colla A., and Castagnoli G., "*Quantum dense key distribution*," Physical Review A, vol. 69, no. 3, p. 032310, 2004.

- [247] Wang C., Deng F.-G., Li Y.-S., Liu X.-S., and Long G. L., "Quantum secure direct communication with high-dimension quantum superdense coding," Physical Review A, vol. 71, no. 4, p. 044305, 2005.
- [248] Zhou L., Sheng Y.-B., and Long G.-L., "Device-independent quantum secure direct communication against collective attacks," Science Bulletin, vol. 65, no. 1, pp. 12–20, 2020.
- [249] Wu J., Lin Z., Yin L., and Long G.-L., "Security of quantum secure direct communication based on wyner's wiretap channel theory," Quantum Engineering, vol. 1, no. 4, p. e26, 2019.
- [250] Deng F.-G. and Long G. L., "Bidirectional quantum key distribution protocol with practical faint laser pulses," Physical Review A, vol. 70, no. 1, p. 012311, 2004.
- [251] Lu H., "Ambiguous discrimination among linearly dependent quantum states and its application to two-way deterministic quantum key distribution," JOSA B, vol. 36, no. 3, pp. B26–B30, 2019.
- [252] Hu J.-Y., Yu B., Jing M.-Y., Xiao L.-T., Jia S.-T., Qin G.-Q., and Long G.-L., "Experimental quantum secure direct communication with single photons," Light: Science & Applications, vol. 5, no. 9, pp. e16 144–e16 144, 2016.
- [253] Zhu F., Zhang W., Sheng Y., and Huang Y., "Experimental long-distance quantum secure direct communication," Science Bulletin, vol. 62, no. 22, pp. 1519–1524, 2017.
- [254] Qi R., Sun Z., Lin Z., Niu P., Hao W., Song L., Huang Q., Gao J., Yin L., and Long G.-L., "Implementation and security analysis of practical quantum secure direct communication," Light: Science & Applications, vol. 8, no. 1, p. 22, 2019.
- [255] Zhou Z., Sheng Y., Niu P., Yin L., Long G., and Hanzo L., "Measurement-device-independent quantum secure direct communication," Science China Physics, Mechanics & Astronomy, vol. 63, no. 3, p. 230362, 2020.
- [256] Pan D., Lin Z., Wu J., Zhang H., Sun Z., Ruan D., Yin L., and Long G. L., "Experimental free-space quantum secure direct communication and its security analysis," Photonics Research, vol. 8, no. 9, pp. 1522–1531, 2020.

- [257] Pan D., Song X.-T., and Long G.-L., "Free-space quantum secure direct communication: basics, progress, and outlook," Advanced Devices & Instrumentation, vol. 4, p. 0004, 2023.
- [258] Niu P.-H., Zhou Z.-R., Lin Z.-S., Sheng Y.-B., Yin L.-G., and Long G.-L., "Measurement-device-independent quantum communication without encryption," Science Bulletin, vol. 63, no. 20, pp. 1345–1350, 2018.
- [259] Dutta A. and Pathak A., "Use of nash equilibrium in finding game theoretic robust security bound on quantum bit error rate," Physica Scripta, vol. 99, no. 9, p. 095106, 2024.
- [260] Wang X.-f., Sun X.-j., Liu Y.-x., Wang W., Kan B.-x., Dong P., and Zhao L.-l., "*Transmission of photonic polarization states from geosynchronous earth orbit satellite to the ground*," Quantum Engineering, vol. 3, no. 3, p. e73, 2021.
- [261] She L.-G. and Zhang C.-M., "Reference-frame-independent quantum key distribution with modified coherent states," Quantum Information Processing, vol. 21, no. 5, p. 161, 2022.
- [262] Cao Y., Li Y.-H., Yang K.-X., Jiang Y.-F., Li S.-L., Hu X.-L., Abulizi M., Li C.-L., Zhang W., Sun Q.-C. *et al.*, "Long-distance free-space measurement-device-independent quantum key distribution," Physical Review Letters, vol. 125, no. 26, p. 260503, 2020.
- [263] Jouguet P., Kunz-Jacques S., Leverrier A., Grangier P., and Diamanti E., "Experimental demonstration of long-distance continuous-variable quantum key distribution," Nature Photonics, vol. 7, no. 5, pp. 378–381, 2013.
- [264] Hu L., Al-Amri M., Liao Z., and Zubairy M., "Continuous-variable quantum key distribution with non-gaussian operations," Physical Review A, vol. 102, no. 1, p. 012608, 2020.
- [265] Wang S., Yin Z.-Q., He D.-Y., Chen W., Wang R.-Q., Ye P., Zhou Y., Fan-Yuan G.-J., Wang F.-X., Chen W. et al., "Twin-field quantum key distribution over 830-km fibre," Nature Photonics, vol. 16, no. 2, pp. 154–161, 2022.

- [266] Jian L., Wang Y., Chen G., Zhou Y., and Liu S., "Quantum identity authentication using a Hadamard gate based on a GHZ state," Journal of Physics B: Atomic, Molecular and Optical Physics, vol. 56, no. 7, p. 075502, 2023.
- [267] Faleiro R. and Goulão M., "Device-independent quantum authorization based on the clauser-horne-shimony-holt game," Physical Review A, vol. 103, no. 2, p. 022430, 2021.
- [268] Paparelle I., Mousavi F., Scazza F., Paris M., Bassi A., and Zavatta A., "A continuous-variable quantum secure direct communication protocol with squeezed states," in European Quantum Electronics Conference. Optica Publishing Group, 2023, p. eb_5_4.
- [269] Pathak A., "Efficient protocols for unidirectional and bidirectional controlled deterministic secure quantum communication: different alternative approaches," Quantum Information Processing, vol. 14, pp. 2195–2210, 2015.
- [270] Lo H.-K., "Insecurity of quantum secure computations," Physical Review A, vol. 56, no. 2, p. 1154, 1997.
- [271] Lo H.-K. and Chau H. F., "Why quantum bit commitment and ideal quantum coin tossing are impossible," Physica D: Nonlinear Phenomena, vol. 120, no. 1-2, pp. 177–187, 1998.
- [272] Buhrman H., Christandl M., and Schaffner C., "Complete insecurity of quantum protocols for classical two-party computation," Physical Review Letters, vol. 109, no. 16, p. 160501, 2012.
- [273] Colbeck R., "Impossibility of secure two-party classical computation," Physical Review A, vol. 76, no. 6, p. 062308, 2007.
- [274] Holevo A. S., "Bounds for the quantity of information transmitted by a quantum communication channel," Problemy Peredachi Informatsii, vol. 9, no. 3, pp. 3–11, 1973.
- [275] Simmons G. J., "A survey of information authentication," Proceedings of The IEEE, vol. 76, no. 5, pp. 603–620, 1988.
- [276] Shukla C., Pathak A., and Srikanth R., "Beyond the goldenberg–vaidman protocol: secure and efficient quantum communication using arbitrary, orthogonal, multi-particle quantum states," International Journal of Quantum Information, vol. 10, no. 08, p. 1241009, 2012.

- [277] Lo H.-K., Ma X., and Chen K., "Decoy state quantum key distribution," Physical Review Letters, vol. 94, no. 23, p. 230504, 2005.
- [278] Christandl M., Renner R., and Ekert A., "A generic security proof for quantum key distribution," arXiv preprint quant-ph/0402131, 2004.
- [279] Cai B., Guo G., Lin S., Zuo H., and Yu C., "Multipartite quantum key agreement over collective noise channels," IEEE Photonics Journal, vol. 10, no. 1, pp. 1–11, 2018.
- [280] He Y.-F. and Ma W.-P., "Two-party quantum key agreement against collective noise," Quantum Information Processing, vol. 15, no. 12, pp. 5023–5035, 2016.
- [281] Huang W., Wen Q.-Y., Liu B., Gao F., and Sun Y., "Quantum key agreement with epr pairs and single-particle measurements," Quantum Information Processing, vol. 13, pp. 649–663, 2014.
- [282] Walton Z. D., Abouraddy A. F., Sergienko A. V., Saleh B. E., and Teich M. C., "Decoherence-free subspaces in quantum key distribution," Physical Review Letters, vol. 91, no. 8, p. 087901, 2003.
- [283] Su W., Qin W., Miranowicz A., Li T., and Nori F., "Heralded nonlocal quantum gates for distributed quantum computation in a decoherence-free subspace," Physical Review A, vol. 110, no. 5, p. 052612, 2024.
- [284] Qin W., Miranowicz A., and Nori F., "Exponentially improved dispersive qubit readout with squeezed light," Physical Review Letters, vol. 133, no. 23, p. 233605, 2024.
- [285] He Y. and Ma W., "Two robust quantum key agreement protocols based on logical ghz states," Modern Physics Letters B, vol. 31, no. 03, p. 1750015, 2017.
- [286] Gao H., Chen X.-G., and Qian S.-R., "Two-party quantum key agreement protocols under collective noise channel," Quantum Information Processing, vol. 17, p. 140, 2018.
- [287] Li X.-H., Deng F.-G., and Zhou H.-Y., "Efficient quantum key distribution over a collective noise channel," Physical Review A, vol. 78, no. 2, p. 022321, 2008.
- [288] Takeuchi Y., Fujii K., Ikuta R., Yamamoto T., and Imoto N., "*Blind quantum computation over a collective-noise channel*," Physical Review A, vol. 93, no. 5, p. 052307, 2016.

- [289] Wang P., Chen X., and Sun Z., "Deterministic secure quantum communication against collective noise," Physics Letters A, vol. 446, p. 128291, 2022.
- [290] Li D.-f., Wang R.-j., Zhang F.-l., Baagyere E., Qin Z., Xiong H., and Zhan H., "A noise immunity controlled quantum teleportation protocol," Quantum Information Processing, vol. 15, pp. 4819–4837, 2016.
- [291] Kang M.-S., Heo J., Hong C.-H., Yang H.-J., Moon S., and Han S.-W., "Response to "Comment on 'Controlled mutual quantum entity authentication with an untrusted third party'"," Quantum Information Processing, vol. 19, p. 24, 2020.
- [292] Jiang S., Zhou R.-G., and Hu W., "Semi-quantum mutual identity authentication using Bell states," International Journal of Theoretical Physics, vol. 60, pp. 3353–3362, 2021.
- [293] Wu Y.-T., Chang H., Guo G.-D., and Lin S., "Multi-party quantum key agreement protocol with authentication," International Journal of Theoretical Physics, pp. 4066–4077, 2021.
- [294] Sharma R. D., Thapliyal K., Pathak A., Pan A. K., and De A., "Which verification qubits perform best for secure communication in noisy channel?" Quantum Information Processing, vol. 15, no. 4, pp. 1703–1718, 2016.
- [295] Liu J.-L., Luo X.-Y., Yu Y., Wang C.-Y., Wang B., Hu Y., Li J., Zheng M.-Y., Yao B., Yan Z. et al., "Creation of memory–memory entanglement in a metropolitan quantum network," Nature, vol. 629, no. 8012, pp. 579–585, 2024.
- [296] Wang L.-J., Zhang K.-Y., Wang J.-Y., Cheng J., Yang Y.-H., Tang S.-B., Yan D., Tang Y.-L., Liu Z., Yu Y., Zhang Q., and Pan J.-W., "Experimental authentication of quantum key distribution with post-quantum cryptography," npj Quantum Information, vol. 7, no. 1, p. 67, 2021.
- [297] Mendiola M. A., Gillis J. T., Binder A. J., and Haddad R., "*Post-quantum authentication schemes*," in Proceedings of the 33rd International Technical Meeting of the Satellite Division of The Institute of Navigation (ION GNSS+ 2020), 2020, pp. 3812–3825.

- [298] Kraus B., Gisin N., and Renner R., "Lower and upper bounds on the secret-key rate for quantum key distribution protocols using one-way classical communication," Physical Review Letters, vol. 95, no. 8, p. 080501, 2005.
- [299] Renner R., Gisin N., and Kraus B., "Information-theoretic security proof for quantum-key-distribution protocols," Physical Review A, vol. 72, no. 1, p. 012332, 2005.
- [300] Acín A., Gisin N., and Scarani V., "Coherent-pulse implementations of quantum cryptography protocols resistant to photon-number-splitting attacks," Physical Review A, vol. 69, no. 1, p. 012309, 2004.
- [301] Peres A., Quantum theory: concepts and methods. Springer, 1997.
- [302] Cerf N. J. and Iblisdir S., "Optimal n-to-m cloning of conjugate quantum variables," Physical Review A, vol. 62, no. 4, p. 040301, 2000.
- [303] Niu C.-S. and Griffiths R. B., "Optimal copying of one quantum bit," Physical Review A, vol. 58, no. 6, p. 4377, 1998.
- [304] Cerf N. J., "Pauli cloning of a quantum bit," Physical Review Letters, vol. 84, no. 19, p. 4497, 2000.
- [305] Tsai C. and Hwang T., "On quantum key agreement protocol," Technical Report, C-S-I-E, NCKU, Taiwan, ROC,, 2009.
- [306] Inoue K. and Honjo T., "Quantum conference key agreement based on differential-phase-shift quantum key distribution," Quantum Information Processing, vol. 23, no. 7, p. 253, 2024.
- [307] Proietti M., Ho J., Grasselli F., Barrow P., Malik M., and Fedrizzi A., "Experimental quantum conference key agreement," Science Advances, vol. 7, no. 23, p. eabe0395, 2021.
- [308] Wang C., Zhang Q., Liang S., and Zhu H., "Secure mutual authentication quantum key agreement scheme for two-party setting with key recycling," Quantum Information Processing, vol. 23, no. 4, p. 139, 2024.

- [309] Sun Z., Huang J., and Wang P., "Efficient multiparty quantum key agreement protocol based on commutative encryption," Quantum Information Processing, vol. 15, pp. 2101–2111, 2016.
- [310] Biham E. and Mor T., "Security of quantum cryptography against collective attacks," Physical Review Letters, vol. 78, no. 11, p. 2256, 1997.
- [311] Biham E. and Mor T., "Bounds on information and the security of quantum cryptography," Physical Review Letters, vol. 79, no. 20, p. 4034, 1997.
- [312] Devetak I. and Winter A., "Distillation of secret key and entanglement from quantum states," Proceedings of the Royal Society A: Mathematical, Physical and engineering sciences, vol. 461, no. 2053, pp. 207–235, 2005.
- [313] Helstrom C. W., "Quantum detection and estimation theory," Journal of Statistical Physics, vol. 1, no. 2, pp. 231–252, 1969.
- [314] Pironio S., Acín A., Brunner N., Gisin N., Massar S., and Scarani V., "Device-independent quantum key distribution secure against collective attacks," New Journal of Physics, vol. 11, no. 4, p. 045021, 2009.
- [315] Lu H., Fung C.-H. F., Ma X., and Cai Q.-y., "Unconditional security proof of a deterministic quantum key distribution with a two-way quantum channel," Physical Review A, vol. 84, no. 4, p. 042344, 2011.
- [316] Walls D., Milburn G., Walls D., and Milburn G., "Atomic optics," Quantum Optics, pp. 315–340, 1994.
- [317] Breuer H.-P., Laine E.-M., Piilo J., and Vacchini B., "Colloquium: Non-Markovian dynamics in open quantum systems," Reviews of Modern Physics, vol. 88, no. 2, p. 021002, 2016.
- [318] Zoller P. and Gardiner C. W., "Quantum noise in quantum optics: the stochastic Schr\" odinger equation," arXiv preprint quant-ph/9702030, 1997.
- [319] Xiu X.-M., Dong L., Shen H.-Z., Gao Y.-J., and Yi X., "Construction scheme of a two-photon polarization controlled arbitrary phase gate mediated by weak cross-phase modulation," JOSA B, vol. 30, no. 3, pp. 589–597, 2013.

- [320] Thapliyal K., Pathak A., and Banerjee S., "Quantum cryptography over non-Markovian channels," Quantum Information Processing, vol. 16, pp. 1–21, 2017.
- [321] Gardiner C. W. and Collett M. J., "Input and output in damped quantum systems: Quantum stochastic differential equations and the master equation," Physical Review A, vol. 31, no. 6, p. 3761, 1985.
- [322] Rajagopal A., Usha Devi A., and Rendell R., "Kraus representation of quantum evolution and fidelity as manifestations of Markovian and non-Markovian forms," Physical Review A, vol. 82, no. 4, p. 042107, 2010.
- [323] Usha Devi A., Rajagopal A., and Sudha, "Open-system quantum dynamics with correlated initial states, not completely positive maps, and non-Markovianity," Physical Review A, vol. 83, no. 2, p. 022109, 2011.
- [324] Shen H., Wang Q., and Yi X., "Dispersive readout with non-Markovian environments," Physical Review A, vol. 105, no. 2, p. 023707, 2022.
- [325] Lai D.-G., Liao J.-Q., Miranowicz A., and Nori F., "Noise-tolerant optomechanical entanglement via synthetic magnetism," Physical Review Letters, vol. 129, no. 6, p. 063602, 2022.
- [326] Lin J.-D., Kuo P.-C., Lambert N., Miranowicz A., Nori F., and Chen Y.-N., "*Non-Markovian quantum exceptional points*," Nature Communications, vol. 16, no. 1, p. 1289, 2025.
- [327] Hathaliya J. J., Tanwar S., and Sharma P., "Adversarial learning techniques for security and privacy preservation: A comprehensive review," Security and Privacy, vol. 5, no. 3, p. e209, 2022.
- [328] Shen H., Xu S., Li H., Wu S., and Yi X., "Linear response theory for periodically driven systems with non-Markovian effects," Optics Letters, vol. 43, no. 12, pp. 2852–2855, 2018.
- [329] Abu-Nada A., Banerjee S., and Sabale V. B., "Exploring the non-Markovian dynamics in depolarizing maps," Physical Review A, vol. 110, no. 5, p. 052209, 2024.

- [330] Nielsen M. A. and Chuang I. L., *Quantum computation and quantum information*. Cambridge university press, 2010.
- [331] Mishra S., Thapliyal K., Parakh A., and Pathak A., "Quantum anonymous veto: a set of new protocols," EPJ Quantum Technology, vol. 9, no. 1, p. 14, 2022.
- [332] Naikoo J., Dutta S., and Banerjee S., "Facets of quantum information under non-Markovian evolution," Physical Review A, vol. 99, no. 4, p. 042128, 2019.
- [333] Shrikant U., Srikanth R., and Banerjee S., "Non-Markovian dephasing and depolarizing channels," Physical Review A, vol. 98, no. 3, p. 032328, 2018.
- [334] Zawadzki P., "An improved control mode for the ping-pong protocol operation in imperfect quantum channels," Quantum Information Processing, vol. 14, no. 7, pp. 2589–2598, 2015.
- [335] Zawadzki P., "Eavesdropping on quantum secure direct communication in quantum channels with arbitrarily low loss rate," Quantum Information Processing, vol. 15, no. 4, pp. 1731–1741, 2016.
- [336] Omkar S., Srikanth R., and Banerjee S., "Characterization of quantum dynamics using quantum error correction," Physical Review A, vol. 91, no. 1, p. 012324, 2015.
- [337] Tsai C., Hsieh C., and Hwang T., "Dense coding using cluster states and its application on deterministic secure quantum communication," The European Physical Journal D, vol. 61, pp. 779–783, 2011.
- [338] Huang W., Wen Q.-Y., Liu B., Gao F., and Sun Y., "Quantum key agreement with EPR pairs and single-particle measurements," Quantum information processing, vol. 13, no. 3, pp. 649–663, 2014.
- [339] Yang Y.-G., Li B.-R., Kang S.-Y., Chen X.-B., Zhou Y.-H., and Shi W.-M., "New quantum key agreement protocols based on cluster states," Quantum Information Processing, vol. 18, p. 77, 2019.
- [340] Piveteau A., Pauwels J., Håkansson E., Muhammad S., Bourennane M., and Tavakoli A., "Entanglement-assisted quantum communication with simple measurements," Nature Communications, vol. 13, no. 1, p. 7878, 2022.

- [341] Sisodia M., Thapliyal K., and Pathak A., "Optical designs for realization of a set of schemes for quantum cryptography," Optical and Quantum Electronics, vol. 53, no. 4, p. 206, 2021.
- [342] Zhao Z., Zhang A.-N., Chen Y.-A., Zhang H., Du J.-F., Yang T., and Pan J.-W., "Experimental demonstration of a nondestructive controlled-NOT quantum gate for two independent photon qubits," Physical Review Letters, vol. 94, no. 3, p. 030501, 2005.
- [343] Lu C.-Y., Cao Y., Peng C.-Z., and Pan J.-W., "Micius quantum experiments in space," Reviews of Modern Physics, vol. 94, no. 3, p. 035001, 2022.
- [344] Sidhu J. S., Joshi S. K., Gündoğan M., Brougham T., Lowndes D., Mazzarella L., Krutzik M., Mohapatra S., Dequal D., Vallone G. *et al.*, "*Advances in space quantum communications*," IET Quantum Communication, vol. 2, no. 4, pp. 182–217, 2021.
- [345] Bhaskar M. K., Riedinger R., Machielse B., Levonian D. S., Nguyen C. T., Knall E. N., Park H., Englund D., Lončar M., Sukachev D. D. *et al.*, "*Experimental demonstration of memory-enhanced quantum communication*," Nature, vol. 580, no. 7801, pp. 60–64, 2020.
- [346] Rubino G., Rozema L. A., Ebler D., Kristjánsson H., Salek S., Allard Guérin P., Abbott A. A., Branciard C., Brukner Č., Chiribella G. et al., "Experimental quantum communication enhancement by superposing trajectories," Physical Review Research, vol. 3, no. 1, p. 013093, 2021.
- [347] Zhou L., Lin J., Xie Y.-M., Lu Y.-S., Jing Y., Yin H.-L., and Yuan Z., "Experimental quantum communication overcomes the rate-loss limit without global phase tracking," Physical Review Letters, vol. 130, no. 25, p. 250801, 2023.
- [348] Piotrowski E. W. and Sładkowski J., "An invitation to quantum game theory," International Journal of Theoretical Physics, vol. 42, pp. 1089–1099, 2003.
- [349] Alonso-Sanz R., Quantum game simulation. Springer, 2019, vol. 36.
- [350] Bostanci J. and Watrous J., "Quantum game theory and the complexity of approximating quantum Nash equilibria," Quantum, vol. 6, p. 882, 2022.

- [351] Kaur H. and Kumar A., "*Game-theoretic perspective of ping-pong protocol*," Physica A: Statistical Mechanics and its Applications, vol. 490, pp. 1415–1422, 2018.
- [352] Osborne M. J. et al., An introduction to game theory. Oxford University Press New York, 2004, vol. 3, no. 3.
- [353] Eisert J. and Wilkens M., "*Quantum games*," Journal of Modern Optics, vol. 47, no. 14-15, pp. 2543–2556, 2000.
- [354] Enk S. J. van and Pike R., "Classical rules in quantum games," Physical Review A, vol. 66, no. 2, p. 024306, 2002.
- [355] Kakutani S., "A generalization of Brouwer's fixed point theorem," Duke Math. J., vol. 8, no. 3, pp. 457–459, 1941.
- [356] Glicksberg I. L., "A further generalization of the kakutani fixed theorem, with application to nash equilibrium points," Proceedings of the American Mathematical Society, vol. 3, no. 1, pp. 170–174, 1952.
- [357] Khan F. S. and Humble T. S., "Nash embedding and equilibrium in pure quantum states," in Quantum Technology and Optimization Problems: First International Workshop, QTOP 2019, Munich, Germany, March 18, 2019, Proceedings 1. Springer, 2019, pp. 51–62.
- [358] Nash J., "The imbedding problem for riemannian manifolds," Annals of mathematics, vol. 63, no. 1, pp. 20–63, 1956.
- [359] Khan F. S., Solmeyer N., Balu R., and Humble T. S., "Quantum games: a review of the history, current state, and interpretation," Quantum Information Processing, vol. 17, p. 309, 2018.
- [360] Nielsen M. A. and Chuang I. L., *Quantum computation and quantum information*. Cambridge University Press, 2010.
- [361] Wilde M. M., Quantum information theory. Cambridge University Press, 2017.
- [362] Watrous J., *The theory of quantum information*. Cambridge University Press, 2018.

- [363] Lum D. J., Howell J. C., Allman M., Gerrits T., Verma V. B., Nam S. W., Lupo C., and Lloyd S., "Quantum enigma machine: Experimentally demonstrating quantum data locking," Physical Review A, vol. 94, no. 2, p. 022315, 2016.
- [364] Zhang W., Ding D.-S., Sheng Y.-B., Zhou L., Shi B.-S., and Guo G.-C., "*Quantum secure direct communication with quantum memory*," Physical Review Letters, vol. 118, no. 22, p. 220501, 2017.
- [365] Massa F., Moqanaki A., Baumeler Ä., Del Santo F., Kettlewell J. A., Dakić B., and Walther P., "Experimental two-way communication with one photon," Advanced Quantum Technologies, vol. 2, no. 11, p. 1900050, 2019.
- [366] Zhang H., Sun Z., Qi R., Yin L., Long G.-L., and Lu J., "Realization of quantum secure direct communication over 100 km fiber with time-bin and phase quantum states," Light: Science & Applications, vol. 11, no. 1, p. 83, 2022.
- [367] Long G.-L., Pan D., Sheng Y.-B., Xue Q., Lu J., and Hanzo L., "An evolutionary pathway for the quantum internet relying on secure classical repeaters," IEEE Network, vol. 36, no. 3, pp. 82–88, 2022.
- [368] You X., Wang C.-X., Huang J., Gao X., Zhang Z., Wang M., Huang Y., Zhang C., Jiang Y., Wang J. et al., "Towards 6g wireless communication networks: Vision, enabling technologies, and new paradigm shifts," Science China Information Sciences, vol. 64, pp. 1–74, 2021.
- [369] Krelina M., "Quantum technology for military applications," EPJ Quantum Technology, vol. 8, no. 1, p. 24, 2021.
- [370] Wójcik A., "Eavesdropping on the "ping-pong" quantum communication protocol," Physical Review Letters, vol. 90, no. 15, p. 157901, 2003.
- [371] Pavičić M., "In quantum direct communication an undetectable eavesdropper can always tell ψ from φ Bell states in the message mode," Physical Review A, vol. 87, no. 4, p. 042326, 2013.
- [372] Khan F. S. and Phoenix S. J., "Gaming the quantum," Quantum Information & Computation, vol. 13, no. 3-4, pp. 231–244, 2013.

[373] Houshmand M., Houshmand M., and Mashhadi H. R., "Game theory based view to the quantum key distribution bb84 protocol," in 2010 Third International Symposium on Intelligent Information Technology and Security Informatics. IEEE, 2010, pp. 332–336.

LIST OF AUTHOR'S PUBLICATIONS

• Published in International Journals

- 1. Dutta A., and Pathak A., "A short review on quantum identity authentication protocols: How would Bob know that he is talking with Alice", Quantum Information Processing, vol. 21, pp. 369, 2022.
- 2. Dutta A., and Pathak A., "Controlled secure direct quantum communication inspired scheme for quantum identity authentication", Quantum Information Processing, vol. 22, pp. 13, 2023.
- 3. Dutta A., and Pathak A., "Use of Nash equilibrium in finding game theoretic robust security bound on quantum bit error rate", Physica Scripta, vol. 99, pp. 095106, 2024.
- 4. Dutta A., and Pathak A., "Simultaneous quantum identity authentication scheme utilizing entanglement swapping with secret key preservation", Modern Physics Letters A, pp. 2450196, 2025.
- 5. Dutta A., and Pathak A., "Collective attack free controlled quantum key agreement without quantum memory", Physica Scripta, vol. 100, pp. 035101, 2025.
- 6. Dutta A. and Pathak A., "New protocols for quantum key distribution with explicit upper and lower bound on secret key rate", The European Physical Journal D, vol. 79, no. 5, p. 48, 2025.